



National Technical University of Athens
School of Civil Engineering
Laboratory of Earthquake Engineering

**“A NEW DEFINITION OF NEAR FIELD GROUND MOTION
DURATION AND ITS EFFECT ON RC BUILDINGS”**

A Postgraduate Thesis By
Basel Jamal Abujabal

(Analysis and Design of Earthquake Resistant Structures) **ADERS** Program

Under the supervision of
Prof. M. Fragiadakis,
Dr. Taflampas Ioannis

Submitted in partial fulfillment of the requirements
For the degree of Master of Science in structural Engineering
July, 2019



Table of Contents

ABSTRACT	1
CHAPTER 1 INTRODUCTION	2
CHAPTER 2 NEAR-FAULT GROUND MOTIONS	5
Statement of Problem	5
Near-Fault effects	6
Directional effects	8
Parameterization of Near-Fault Ground Motion	10
Pulse characteristics	13
Effect of the pulse on the acceleration response spectrum	14
CHAPTER 3 BUILDING DESCRIPTION	16
Truncated time histories	16
CHAPTER 4 BUILDING DESCRIPTION	19
Building Layout	19
Modelling of the building using Seismostruct	21
Materials	23
Concrete	23
Steel Reinforcement	23
Modeling Elements	24
Beams	24
Columns	25
Loading	26
Eigenvalues Analysis	28
Dynamic Time History Analysis	29
Theory and purpose	29
Dynamic time history in seismostruct	30
CHAPTER 5 GROUND MOTIONS RECORDS	35
L’Aquila earthquake 2009:	35
Norcia earthquake 2016:	39
CHAPTER 6 DATA ANALYSIS AND RESULTS	46
Identification of damage limit states for RC buildings	46
Methodology	47
Dynamic time history Results for the original building	48
Maximum displacement of the original ground motions Data1 and DataQ.	48
Profile of Displacements ,Base Shear and Inter story and Drift	49
CHAPTER 7 CONCLUSIONS	146
Conclusions	146
REFERENCES	147



ABSTRACT

In this study the seismic risk of five storey existing reinforced concrete building in Athens is investigated.

In this study a new measure of strong ground motion duration, with special application in pulse-like dynamic time-history analysis, is proposed.

The special interest produced by near-field directivity records and their effect on structural response has given a new significance in the velocity time history, its pulse-like content and relevant parameters and indices.

According to this study the duration of the inherent pulse-like content is used in order to define the limits of the strong ground motion duration, expected to produce a structural response almost identical to that affected by the total duration of the ground motion.

Two duration levels, the total duration and a truncated one, equal to that of the inherent velocity pulse, are used as seismic excitation for a particular of medium to high rise reinforced concrete buildings.

The results for the response displacements and forces are quite close permitting the acceptance of the pulse duration as the strong ground motion time interval at least for pulse-like records.

Near-fault records have high frequency content. In addition, in the positive directivity the records may contain large amplitude velocity pulse of long duration.

These characteristics affect the response and design of both high frequency and long period structures.

The long period pulse in near-fault records may cause strong fundamental mode response of long period structures. In addition, the high frequency content of the same record may coincide with the second (or higher modes) resulting in severe overall response of the structure.

In traditional seismic design procedures, the high frequency content of near fault records has been accounted for in the development of the seismic design spectra.

Eventually, The results show fairly good agreement, showing that the truncated records can be used instead of the original ones for the calculation of the elastic and the inelastic response, reducing significantly the computational time.



CHAPTER 1 INTRODUCTION

Near-field ground motions have caused much damage in the vicinity of seismic sources during recent earthquakes.

It is found that ground shaking near a fault rupture is characterized by a short-duration impulsive motion which is clearly obvious in the velocity time history record. This impulsive motion exposes the structure to high input energy at the beginning of the record unlike what happens in ground shakings far from the fault rupture.

In the near-fault region, which is usually assumed to extend about 20 to 60 km from the seismic source, the short travel distance of the seismic waves does not allow enough time for the high frequency content to be damped out of the record as is normally observed in far field records.

The effect of this pulse type motion on the response is important in the design of structures for near-fault events.

This phenomenon requires consideration in the design process for structures that are located in the near-field region, unfortunately the seismic design codes are based on “far-fault” ground motion data only without taking into consideration the characteristics of the near fault ground motion therefore the design of structures for near-fault events is inappropriate according to the seismic design code provisions, except for the American seismic design code “ASCE” which recently this phenomenon is taken into consideration.

Since the beginnings of seismic hazard investigation, parameters associated solely with the amplitude of the ground motion have not been considered adequate for the expression of the damageability of an earthquake and in order to account for the released energy content due to the seismic excitation duration, several measures and indices have been defined. Most of these have been associated with the acceleration time history, as the bracketed and uniform durations depending on a bounding value of ground acceleration, or the significant duration introduced by Trifunac and Brady as the time interval between the 5% and 95% boundaries of the Arias Integral.

As known, the ground acceleration is considered a measure affecting low period structures.

If medium to long period structures are to be taken into account, the ground velocity time history is considered a better measure of the seismic damageability.

In that case, a duration index depending on the ground velocity is needed, which should consider the significant part of the energy flux, given as the time integral of the squared ground velocity. The energy flux is an efficient measure of the energy released by the ground motion at the examined site.

Since this energy is usually dominated by the pulse contained in the velocity time history, it is proven here in after that the pulse duration can be used for the definition of the strong motion duration. Accordingly, it is considered that the underlying velocity pulse, coupled with the relevant portion of the overlying high frequency component of the ground acceleration, can account for the structural response instead of the total record duration.



In this approach, a major matter that counts is the selection of the appropriate wavelet to use in the procedure of evaluating the underlying pulse and defining its parameters. Many wavelets have been proposed for the simulation of the predominant velocity pulses.

In many of them, however, the mother wavelet selected for the simulation procedure is handicapped by a predetermined number of half cycles which, combined with the wavelet period, define its duration. Such a handicap burdens the procedure proposed by Baker in 2007, where the selected Daubechies of the 4th order wavelet has a predetermined shape and number of cycles. Although this can be appropriate for near field directivity records it cannot fit cases of pulse like records with a large number of cycles, as in case of liquefaction or basin effects.

In the proposed procedure, a wavelet, versatile in the representation of different duration levels, has to be used. As such, the Mavroeides and Papageorgiou wavelet [3] (denoted as M&P wavelet in the ensuing) is selected, which includes a specific parameter explicitly associated with the number of cycles of the pulse. The duration of the pulse is given as the product of the number of cycles γ with the pulse period T_p . An effective procedure presented by Mimoglou et al [5] is used for the evaluation of the pulse parameters and especially for the time interval accounting for the predominant pulse and the associated proposed truncated duration.

The new definition of strong motion duration is not simply another index, since it can be used, with very good accuracy, for the definition of a truncated substitute of the original time history for the inelastic dynamic time history analyses of structural response. As a result, a significant reduction in the required runtimes can be achieved.

In this study, the proposed methodology is applied to 49 selected pulse like records.

First, the extraction of the predominant pulse inherent in each record is performed, which permits the determination of the time boundaries of the pulse content and consequently of the truncated duration.

Then, the original **Data1** and the truncated records **DataQ** are used as the seismic excitation for a particular of reinforced concrete buildings and the resulting response deformations and forces are compared.

The results show fairly good agreement, showing that the truncated records can be used instead of the original ones for the calculation of the elastic and the inelastic response, reducing significantly the computational time.

the effect of near-fault ground motions are investigated, along with other seismological parameters such as earthquake magnitude and distance from the fault, to evaluate the seismic response of five-story RC structural system building (MRF), and perform a damage assessment for that building under certain earthquake events.

Using Seismostruct software, a dynamic time-history analysis is performed, in order to calculate the displacement time histories, maximum displacement of the original ground motions **Data1** vs the displacement of pulses **DataQ** and interstorey drifts and base shears for original ground motion and Pulse.



This thesis consists of seven chapters, the first chapter is an introduction to the procedures used in the thesis, and a summary for each chapter.

In Chapter 2, identification of near fault ground motion phenomenon, characteristics, and parameters is discussed with mentioning the difference between near and far fault, followed by the pulse characteristics and its effect on the elastic response spectrum.

In Chapter 3, identification, determination of the pulse parameters and the method that has been proposed by Mimoglou et al. [5] is adopted herein for the determination of the properties of the predominant velocity pulse of a record

In Chapter 4, A description of the building, and its modeling in Seismostruct are provided, including the building layout, material characteristics, typical reinforcement detailing of the structural elements, applied loads, seismic characteristics, and additionally eigenvalue and dynamic time-history analysis are performed.

In Chapter 5, a brief description of the ground motion records used, including maps and figures showing the projection of the rupture surface, each station distance from the epicenter, and the criterion of picking up pulse like records (Pulse Indicator).

In Chapter 6, the results from subjecting the building to the near fault ground motion records are obtained, these results are the maximum top floor displacement that the building undergoes due to a certain ground motion record.

The displacement value indicates the structural damage state of the building, the results are illustrated in plots and tabulated forms for each earthquake showing the inter-storey drift (maximum roof displacement/building height) and the corresponding predefined limit damage state.

In Chapter 7, the conclusions upon reviewing the results obtained are summed up in the form of figures and tables representing the damage limit states reached by the original and strengthened buildings, and showing the improvement percentage.



CHAPTER 2 NEAR-FAULT GROUND MOTIONS

Statement of Problem

Near-field ground motions have caused much damage in the vicinity of seismic sources during recent earthquakes (Northridge 1994, Kobe 1995). There is evidence indicating that ground shaking near a fault rupture is characterized by a short-duration impulsive motion that exposes the structure to high input energy at the beginning of the record. This pulse-type motion is particularly prevalent in the "forward" direction, where the fault rupture propagates towards the site at a velocity close to the shear wave velocity.

The effect of this pulse type motion on the response is important in the design of structures for near-fault events. In the near-fault region, the short travel distance of the seismic waves does not allow enough time for the high frequency content to be damped out of the record as is normally observed in far field records.

This phenomenon requires consideration in the design process for structures that are located in the near-field region, which is usually assumed to extend about 20 to 60 km from the seismic source (1996 SEAOC Bluebook).

Near-field ground motions exhibit special response characteristics that are different from the response characteristics of "ordinary" ground motions. This is shown in Fig. 2.1, which compares velocity response spectra of near-field and ordinary ground motions. The solid line (denoted as 15-D*) represents the mean velocity spectrum of a set of ordinary ground motions whose individual spectra resemble the 97 UBC soil type SD spectrum. The other lines correspond to the velocity spectra of individual near-field ground motions from different events.

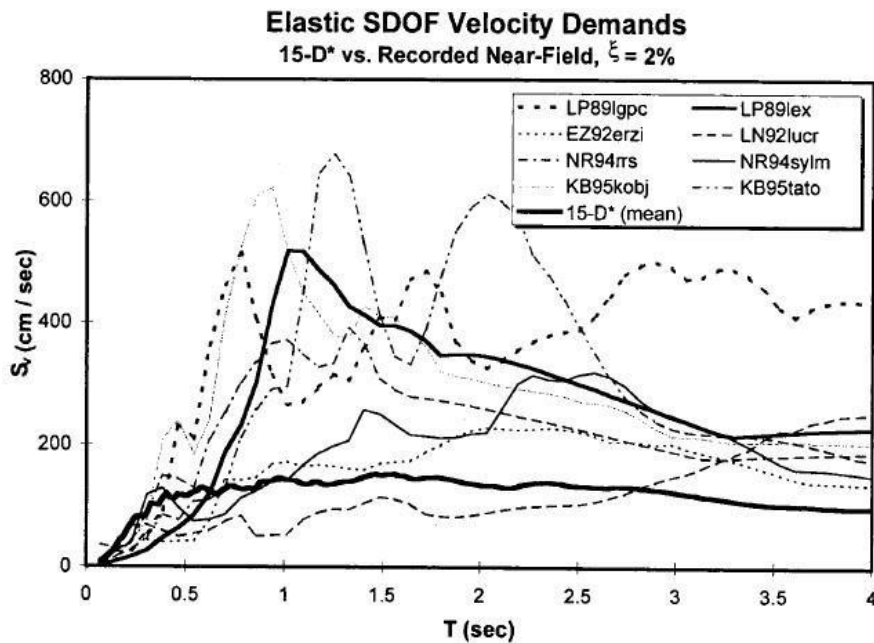


Fig. 2.1 Velocity Response Spectra of Near-Field and Ordinary Ground Motions

Near-Fault effects

Within this near-fault zone, ground motions are significantly influenced by the rupture mechanism, the direction of rupture propagation relative to the site, and possible permanent ground displacements resulting from the fault slip. These factors result in effects termed herein as “rupture-directivity” and “fling step.” The estimation of ground motions close to an active fault should account for these characteristics of near-fault ground motions.

Forward directivity occurs when the rupture propagates toward a site and the direction of slip on the fault is also toward the site. This occurs because the velocity of fault rupture is close to (generally slightly less than) the shear wave velocity of the rock near the source. As shown in Figure 2.2 for a strike-slip focal mechanism, as the rupture front propagates away from the hypocenter and toward a site, energy is accumulated near the rupture front from each successive zone of slip along the fault. The wave front arrives as a large pulse of motion (a shock wave effect) that occurs at the beginning of the record (Somerville et al. 1997a) and is polarized in the strike-normal direction. The pulse of motion is typically characterized by large amplitude at intermediate to long periods and short duration.

If a site is located near the epicenter, i.e., rupture propagates away from the site, the arrival of seismic waves is distributed in time. This condition, referred to as backward directivity, is characterized by motions with relatively long duration and low amplitude.

Neutral directivity occurs for sites located off to the side of the fault rupture surface (i.e., rupture is neither predominantly toward nor away from the site).

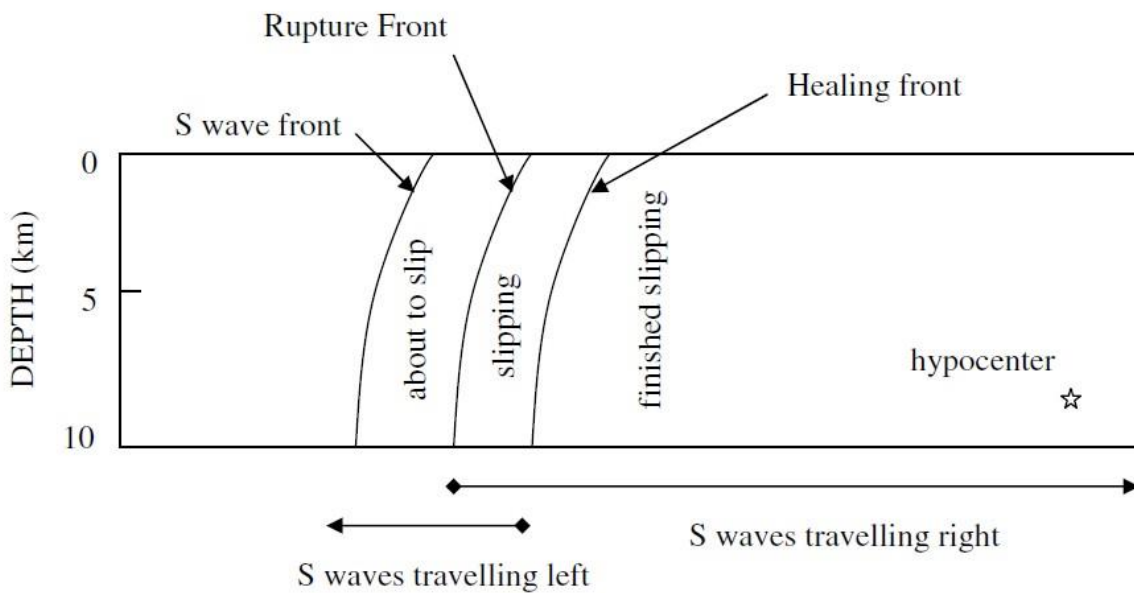


Fig. 2.2 Schematic diagram of rupture-directivity effects for a vertical strike-slip fault. The rupture begins at the hypocenter and spreads at a speed that is about 80% of the shear wave velocity. The figure shows a snapshot of the rupture front at a given instant (from Somerville et al. 1997a).



The effects of rupture-directivity on ground displacements recorded during the 1989 Loma Prieta earthquake are shown in Figure 2.3. The epicenter of the earthquake is near Corralitos and Branciforte Drive, where the horizontal ground displacements are moderate on both fault-normal and fault-parallel components. This is attributed to backward directivity.

At the ends of the fault, however, at Lexington Dam and Hollister, forward directivity causes the horizontal ground motions in the fault-normal direction to be impulsive and much larger than the fault-parallel motions, which are similar to those near the epicenter. The large impulsive motions occur only in the fault-normal direction and only away from the epicenter.

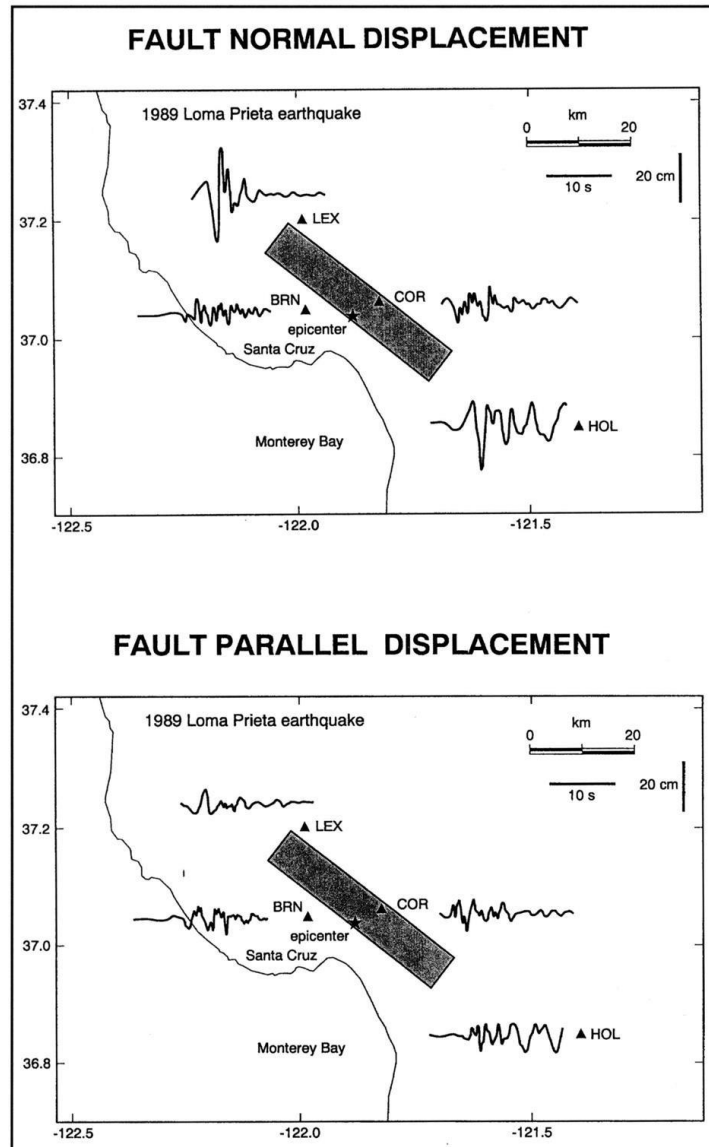


Fig. 2.3 Rupture-directivity effects in the recorded displacement time histories of the 1989 Loma Prieta earthquake, for the fault-normal (top) and fault-parallel (bottom) components. Source: EERI, 1995.

Directional effects

In the case of an earthquake, ground motion recorded at near-source sites may be subjected to rupture directivity effects which result in a low frequency full cycle velocity pulse at the beginning of the signal. The occurrence of this effect depends on the rupture process and on the geometrical configuration of the fault and the site. More specifically, according to Somerville, the seismic energy radiated from the source arrives almost in single large pulse of motion if the rupture propagates toward the site, the direction of slip on the fault is aligned with the site, and the propagation velocity of rupture is almost as large as the shear wave velocity.

Figure 2.4 (a) sketches rupture directivity effect in the simple case of a unilateral strike-slip fault. As the rupture, which may be seen as a point source moving along the fault, goes away from the epicenter, it radiates energy in seismic waves originated at different instants. Roughly speaking, the wave fronts tend to all arrive at the same time in site 2, this may be seen as constructive interference of waves.

Conversely, in site 1, with respect to which the rupture moves away, waves radiated in different instants tend also to arrive in different moments. Therefore, in the former case the energy is concentrated in a high amplitude and short duration (impulsive) motion, whereas in the latter the energy is spread over a larger amount of time and in a lower amplitude signal.

Because of the radiation pattern, in the case of strike-slip ruptures, directivity pulses are oriented in the rupture-normal (RN) direction that corresponds to the strike-normal direction, while in the rupture-parallel direction (RP), which coincides with the strike-parallel direction, minor directivity effects, if any, are expected. In dip-slip earthquakes, the rupture directivity pulse is expected in the direction normal to the fault dip, which in the horizontal plane reflects on the strike-normal direction. Hereinafter, referring to the horizontal ground-motion components, strike-normal and strike-parallel directions will be referred to as fault-normal (FN) and fault parallel (FP) (Figure 2.4 (b)).

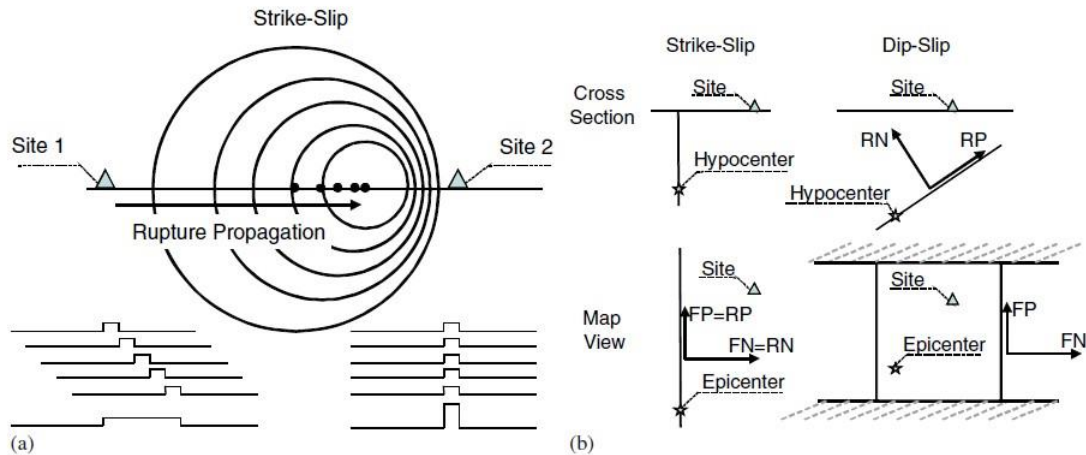


Fig. 2.4 (a) Directivity of seismic energy: snapshot of wave fronts (adapted from Singh) and (b) directions of effects' observation for strike-slip and dip-slip cases (adapted from Somerville).



Rupture-directivity effects can be present both for strike-slip and dip-slip events. In dip-slip events, forward-directivity conditions occur for sites located near the up-dip projection of the fault plane. As with strike-slip focal mechanisms.

The radiation pattern of the shear dislocation of the fault causes the pulse to be mostly oriented perpendicular to the fault, causing the fault normal component of the motion to be more severe than the fault-parallel component (Somerville, 1998).

Modern digital recordings of near-fault ground motions, for example from the 1999 Turkey and Taiwan earthquakes, contain permanent ground displacements due to the static deformation field of the earthquake.

These static displacements, termed “fling step,” occur over a discrete time interval of several seconds as the fault slip is developed. Fling step displacements occur in the direction of fault slip, and therefore are not strongly coupled with the aforementioned dynamic displacements referred to as the “rupture-directivity pulse.”

In strike-slip faulting, the directivity pulse occurs on the strike-normal component while the fling step occurs on the strike parallel component.

In dip-slip faulting, both the fling step and the directivity pulse occur on the strike-normal component. The orientations of fling step and directivity pulse for strike-slip and dip-slip faulting are shown schematically in Figure 2.5, and time histories in which these contributions are shown together and separately are shown schematically in Figure 2.6.

The available strong motion data that can be used to quantify these effects are limited, although the recent earthquakes in Turkey and Taiwan have significantly supplemented the near-fault ground motion database.

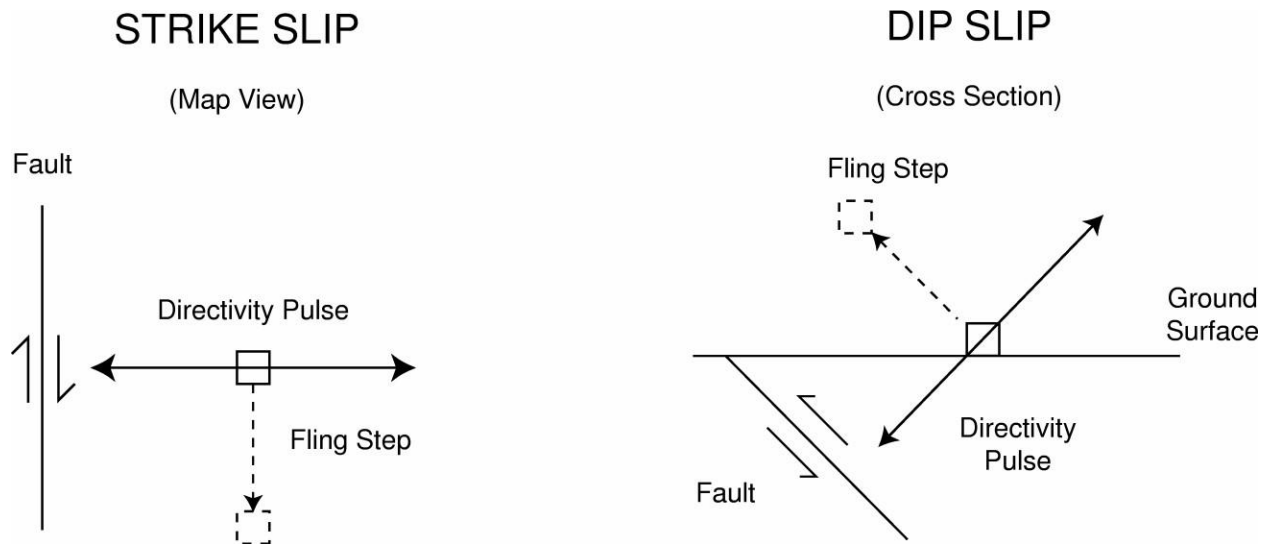


Fig. 2.5 Schematic diagram showing the orientations of fling step and directivity pulse for strike-slip and dip-slip faulting.

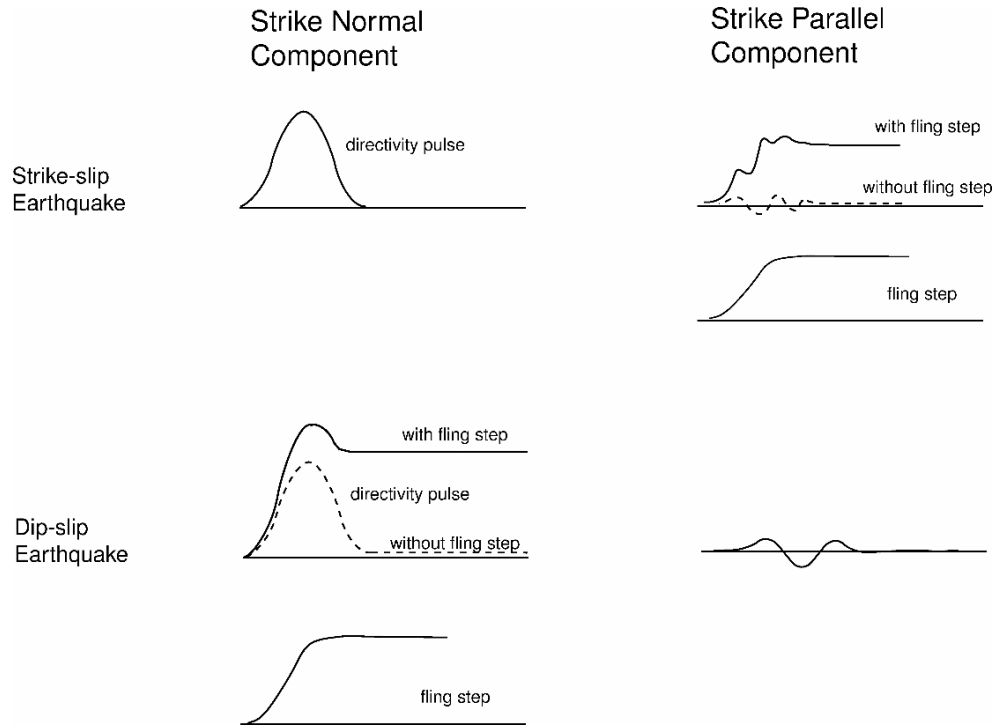


Fig. 2.6 Schematic diagram of time histories for strike-slip and dip-slip faulting in which the fling step and directivity pulse are shown together and separately.

Parameterization of Near-Fault Ground Motion

Somerville et al. (1997a) parameterized the conditions that lead to forward and backward-directivity.

As shown in Figure 2.7, the spatial variation of directivity effects depends on the angle between the direction of rupture propagation and the direction of waves traveling from the fault to the site (θ for strike-slip faults, and φ for dip-slip faults), and on the fraction of the fault rupture surface that lies between the hypocenter and the site (X for strike-slip faults and Y for dip-slip faults). More significant forward-directivity results from smaller angles between the site and fault and for larger fractions of ruptured fault between the site and hypocenter. It should be noted that even when the geometric conditions for forward directivity are satisfied, the effects of forward directivity may not occur. This could happen if a station is at the end of a fault and rupture occurs toward the station but slip is concentrated near the end of the fault where the station is located.

To account for directivity effects, Somerville et al. (1997a) correlated the residuals of response spectral ordinates (at 5% damping) to the geometric parameters defined in Figure 2.7, with the results shown in Figure 2.8. The ground motion parameters that are modified are the average horizontal response spectra and the ratios of fault-normal to fault-parallel response spectra. Details of the model are presented in Section 4.2.1. The 1997 UBC accounts for near-fault effects by means of near-source factors, N_a and N_v , applied to the low period (acceleration) and



intermediate period (velocity) parts of the acceleration response spectrum, respectively. The near-source factors are specified for distances less than 15 km and for three different fault types (Table 4.1). The near-source factors in the UBC are compatible with the average of the fault-normal and fault-parallel components in the Somerville et al. (1997a) model, and hence, the code provisions do not address the larger fault-normal component of motion (Somerville, 1998).

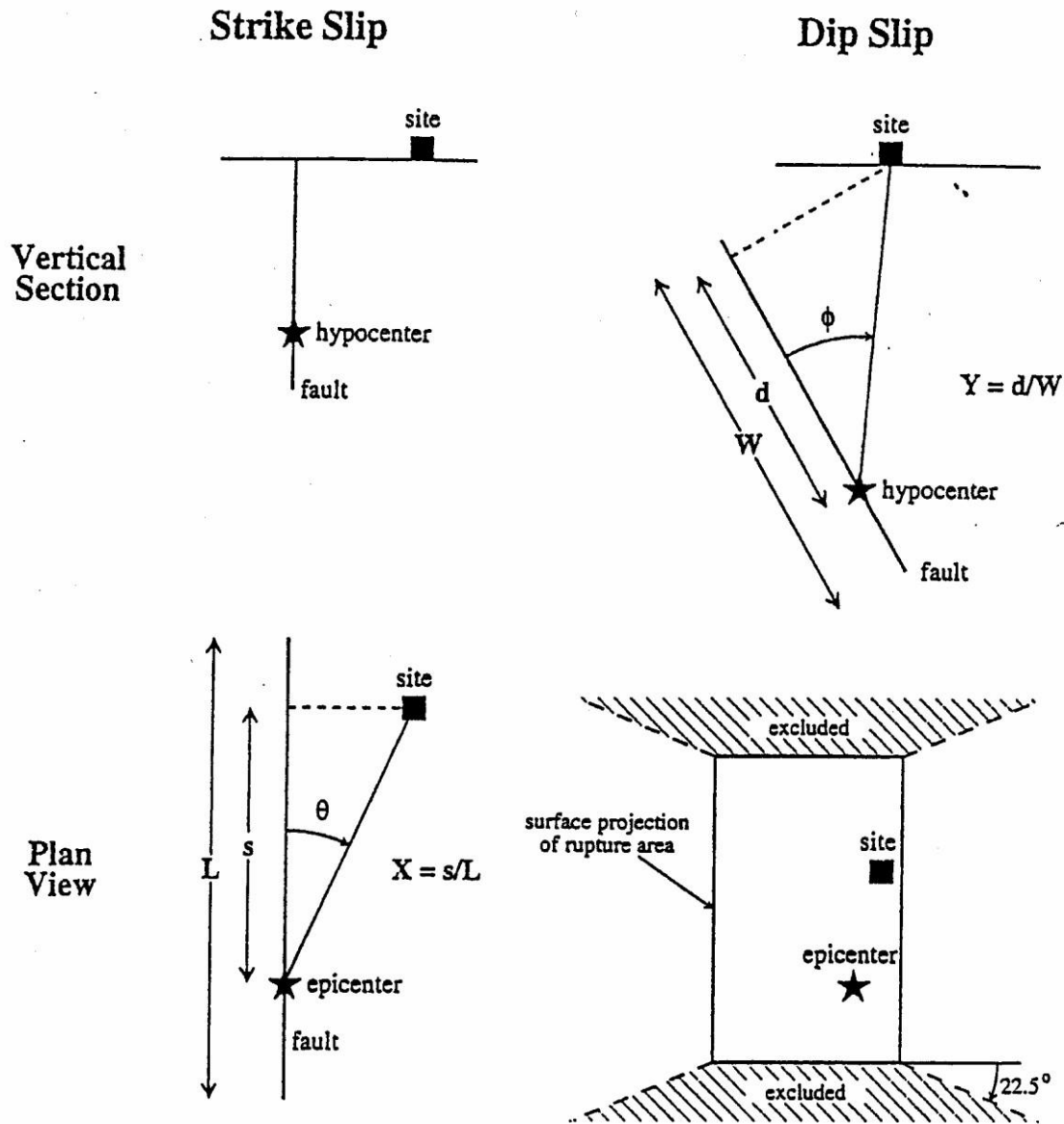
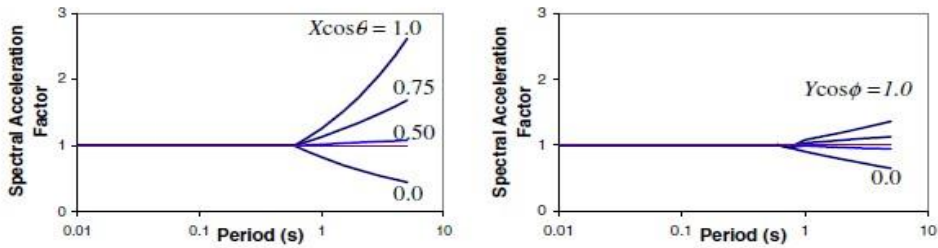
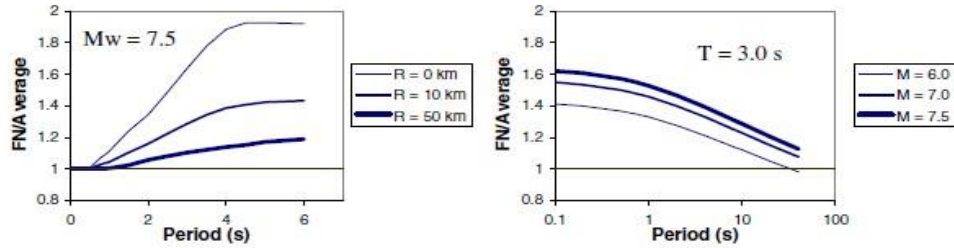


Fig. 2.7. Parameters used to define rupture-directivity conditions (adapted from Somerville et al. 1997a).



(a) Average response spectra ratio, showing dependence on period and on directivity parameters



(b) Strike-normal to average horizontal response spectral ratio for maximum forward-directivity conditions ($X\cos\theta = 1$)

Fig. 2.8. Predictions from the Somerville et al. (1997a) relationship for varying directivity conditions.

(a) Short-period factor (N_a)

Seismic Source Type	Closest Distance to Known Seismic Source ¹		
	≤ 2 km	5 km	≥ 10 km
A	1.5	1.2	1.0
B	1.3	1.0	1.0
C	1.0	1.0	1.0

(b) Intermediate-period factor (N_v)

Seismic Source Type	Closest Distance to Known Seismic Source ¹			
	≤ 2 km	5 km	10 km	≥ 15 km
A	2.0	1.6	1.2	1.0
B	1.6	1.2	1.0	1.0
C	1.0	1.0	1.0	1.0

Table 2.1. Near-source factors from the 1997 Uniform Building Code.



Pulse characteristics

Research on the response of structures to near-fault motions has found a time history representation of the motions to be preferable to a response spectrum representation (e.g. Somerville, 1998; Alavi and Krawinkler, 2000; Sasani and Bertero, 2000; Rodriguez-Marek, 2000). A time history representation is preferable because the frequency-domain characterization of ground motion (i.e. through a response spectrum) implies a stochastic process having a relatively uniform distribution of energy throughout the duration of the motion. When the energy is concentrated in a few pulses of motion, the resonance phenomenon that the response spectrum was conceived to represent may have insufficient time to build up (Somerville, 1998).

Krawinkler and Alavi (1998) identify the velocity pulse by a clear and global peak in the velocity response spectrum of the ground motion which is illustrated in Figure 2.9.

Some simplified pulses are shown in Figure 2.10. The simplified sine-pulse representations of velocity time histories are defined by the number of equivalent half-cycles, the period of each half-cycle, and the corresponding amplitudes. To represent bidirectional shaking, a sine-pulse representation of the fault-parallel component is needed along with the time lag between initiation of the fault-normal and fault-parallel components.

A simple characterization is possible with the use of peak horizontal velocity (PHV), approximate period of the dominant pulse (T_v), and the number of significant half-cycles of motion in the (larger) fault-normal direction.

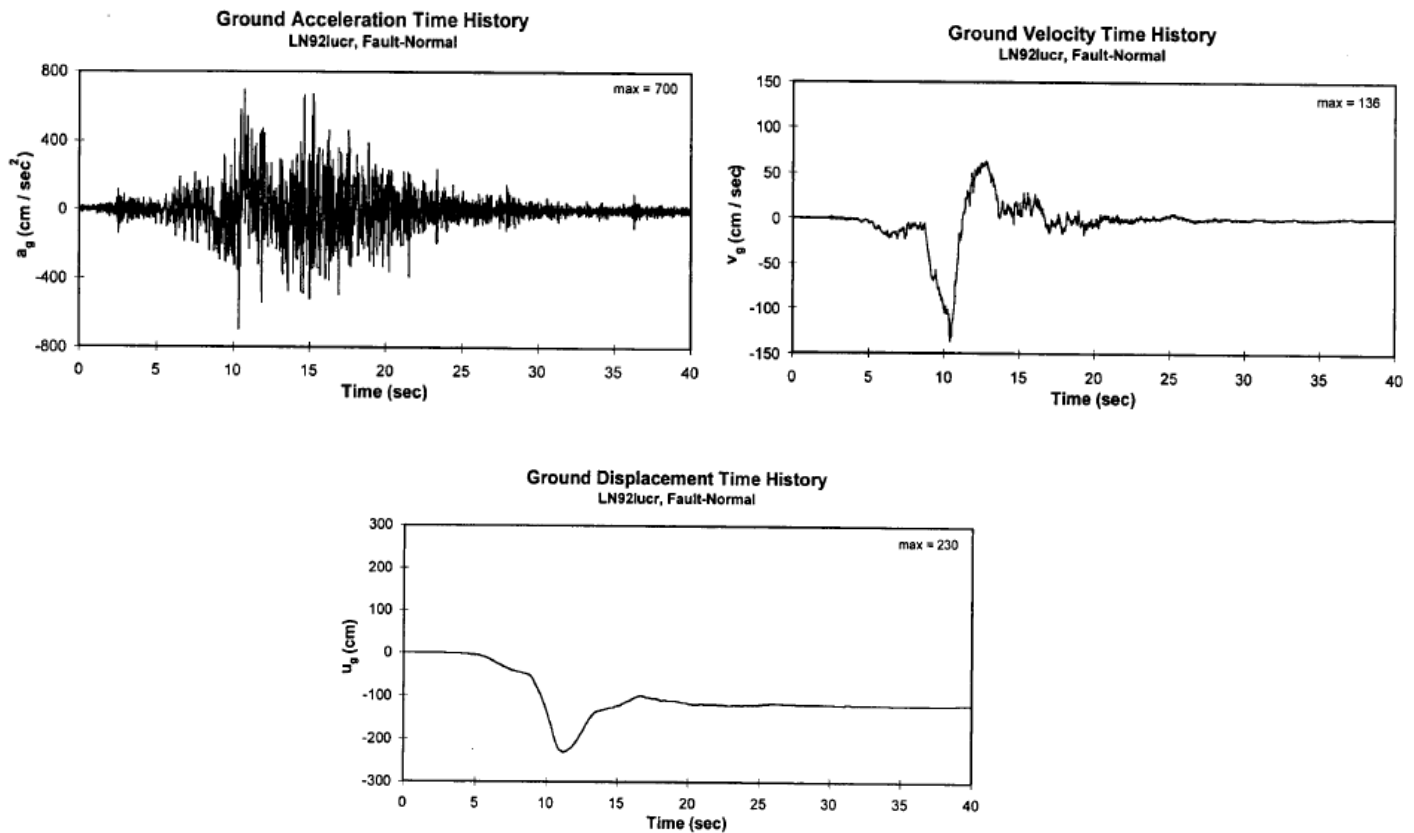


Fig. 2.9. Ground Acceleration, Velocity, and Displacement Time Histories of Fault-Normal Component of Record LN921ucr with Forward Directivity

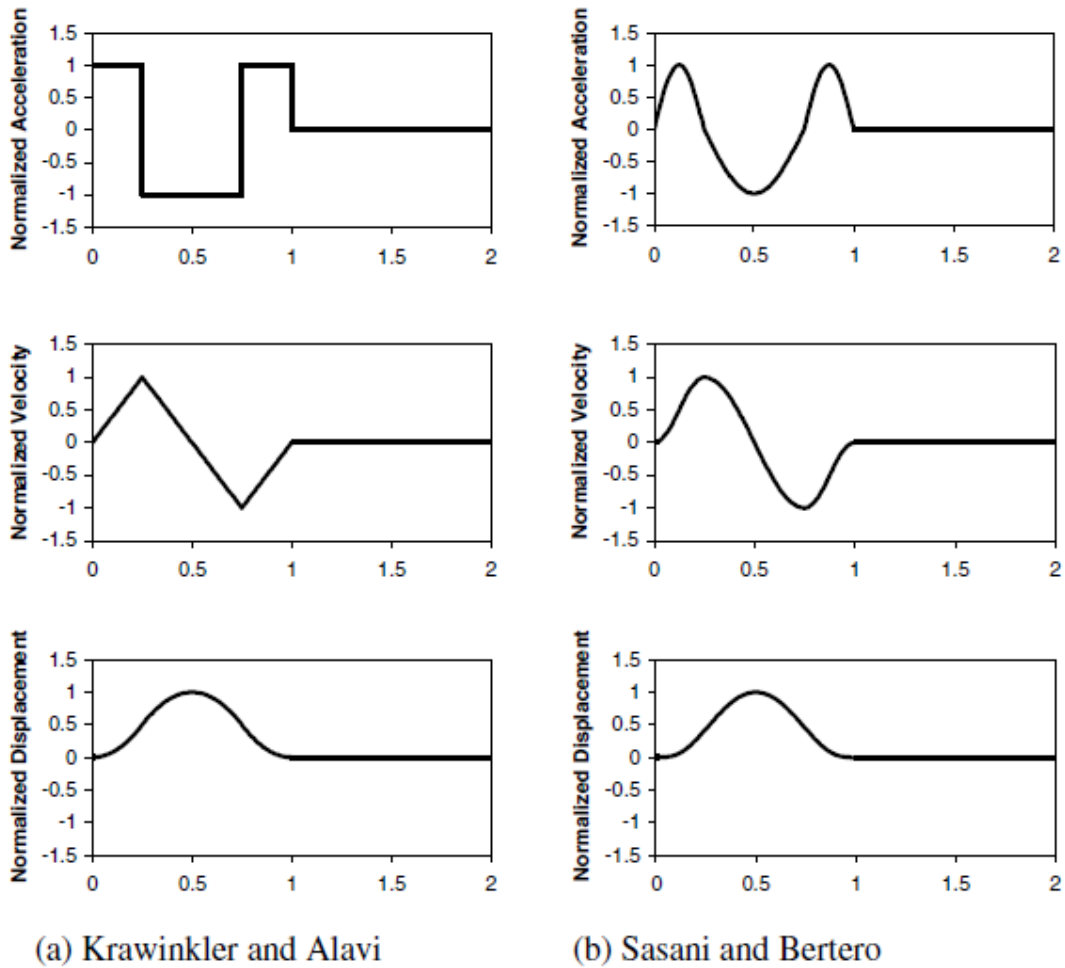


Fig 2.10. Simplified pulses that have been used by some researchers.

Effect of the pulse on the acceleration response spectrum

It is observed that in near field ground motion, there is a bell shaped curve in the declining part of the acceleration response spectrum which is due to the constructive pulse of the forward directivity as shown in figure (2.11a).

This bell shaped curve lies around the predominant period of the pulse (T_v) which affects buildings have elastic period close or equal to half the pulse period, hence it should be taken into consideration while designing such buildings in order to avoid response amplification as shown in figure (2.11b).

Usually it is taken into account in the design process that the ductility demand is equal to the behavior factor, but in reality the ductility demand is much bigger than the behavior factor due to the near fault effect (existence of a constructive pulse), and this is illustrated in figure 2.12.

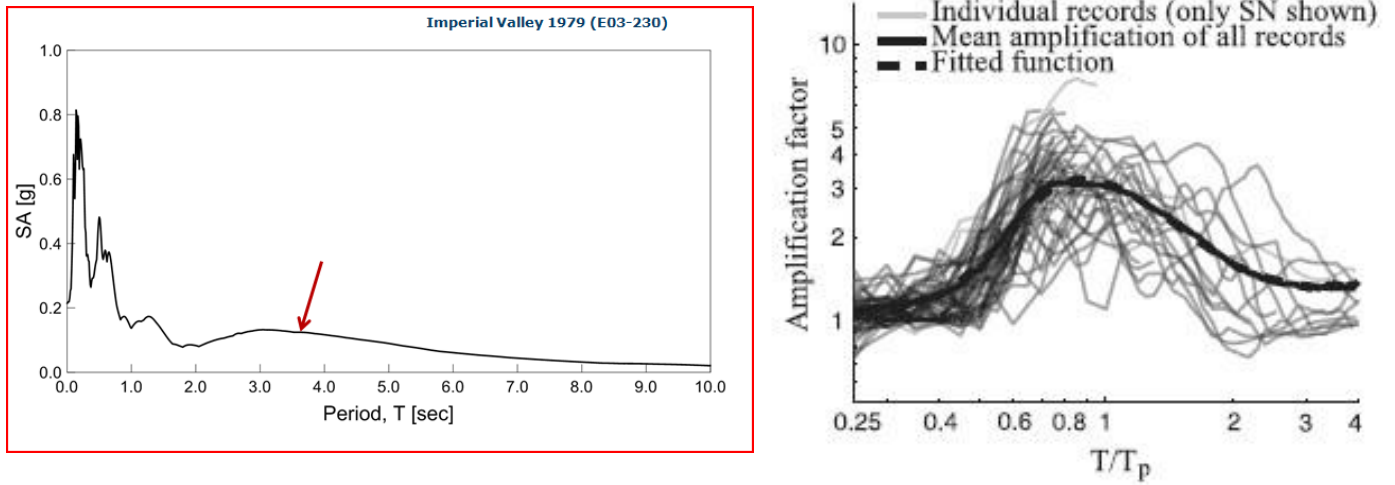


Fig. 2.11. Bell shaped amplification around T_p .

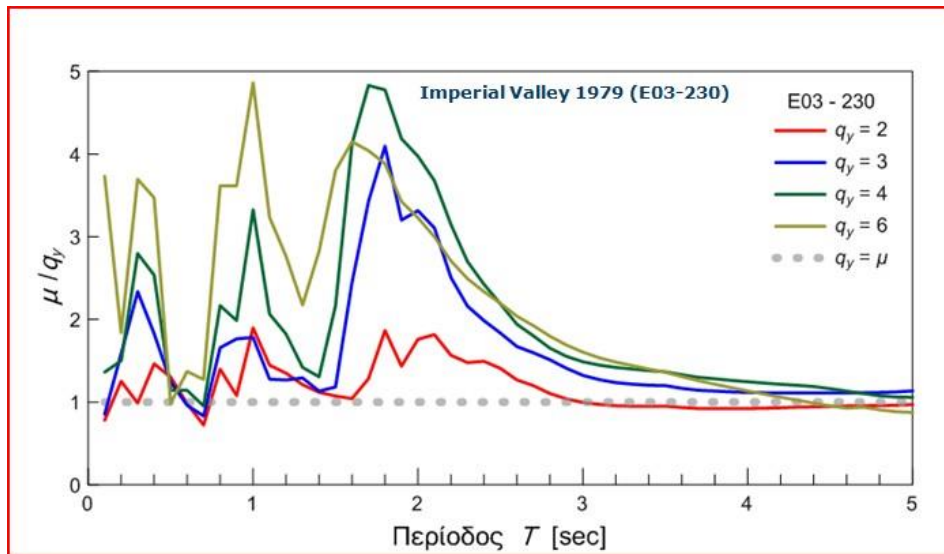


Fig. 2.12. Ductility demand to behavior factor ratio (μ/q_y) for different behavior factor (q_y) curves.



CHAPTER 3 TRUNCATED TIME HISTORIES

- METHODOLOGY
- DETERMINATION OF THE PULSE PARAMETERS

The near field pulse like records have given a boost in the use of wavelet analysis in earthquake engineering. The wavelets have been used for the simulation of the predominant pulse inherent in directivity and fling step affected records and the evaluation of the main parameters defining the shape of the predominant pulse as the pulse period, amplitude and duration.

A repetitive procedure regarding the wavelet approximation of consecutive residual time histories has permitted the extraction of further pulses, up to a certain number sufficient for an adequate approximation of the whole velocity time history, as already shown by Lu and Panayotou.

This wavelet approximation of the whole time history brings the question of whether all the evaluated wavelets are significant regarding their effect on elastic and inelastic displacement spectra.

The significance of each separate wavelet was estimated through the following procedure, At each cycle a particular wavelet is subtracted from the original time history.

The ratio between the residual and the original time history displacement spectra is produced. If the spectral ratio for the whole period range is close to unity, the omitted pulse does not affect the referred spectra and is considered as not significant.

According to the produced results, it appears that the wavelets considered to be significant are those with a duration coupling the time interval of the predominant pulse. Accordingly, it appears that the significant duration of the pulse like records coincides with the time interval of the predominant pulse.

This conclusion is enhanced by the comparison between the inelastic displacement spectra, for a reduction factor of 4, for the original records and those of time histories reduced to the time interval of the predominant pulse.

The method that has been proposed by Mimoglou et al .[5] is adopted herein for the determination of the properties of the predominant velocity pulse of a record.

According to this method, the period of the pulse, T_p , is determined first, Having realized that the common determination of T_p from the peak of the pseudo-velocity response spectrum is sometimes inadequate, and following the example of other researchers that have sought better ways to determine the period of the pulse, Mimoglou et al. .[5] proposed a new approach, in which both the velocity and the displacement response spectra for 5% damping are used and the period of the pulse is determined from the peak of the product spectrum $S_d \times S_v$.



After the pulse period T_p has been determined, the remaining parameters of the M&P wavelet, i.e. the amplitude A , the duration γ and the phase shift ν , are calculated so that the displacement response spectrum of the pulse for 5% damping best fits the corresponding spectrum of the record.

However, since the pseudo-velocity response spectrum is directly related to the displacement spectrum through the relation $PS_v = \omega \cdot S_d$, the wavelet will also fit the pseudo-velocity response spectrum. The determination of A , γ and ν is achieved with the use of the ground motion parameter CAD (Taflampas et al. [6]), which is related to the peak spectral amplitude of the pulse.

For the M&P wavelets, the value of CAD is directly associated with the amplitude A and the duration index γ , since the following relation holds:

$$CAD = \frac{\gamma A T_p}{\pi} \quad (1)$$

for the M&P wavelet the following equation also holds:

$$\frac{S_{d,\xi}(T_{res})}{CAD} = \frac{1 - e^{-2\pi\gamma\xi}}{8\gamma\xi} [1 + (\gamma - 1)\xi] \quad (2)$$

where ξ is the damping coefficient, and that $PS_v = (2\pi/T) \cdot S_d$, the following relation can be established between CAD and PS_v :

$$\frac{PS_{v,\xi,max}}{CAD} = \frac{\pi(1 - e^{-2\pi\gamma\xi})[1 + (\gamma - 1)\xi]}{4 \gamma \xi T_p} \quad (3)$$

Substituting CAD and changing $PS_{v,\xi,max}$ with $PS_{v,\xi}(T_p)$, which is the value of the pseudo-velocity response spectrum of the ground motion for period T_p and damping equal to ξ , since bestfitting of the response spectrum is desired, one gets:

$$A = \frac{4 \xi PS_{v,\xi}(T_p)}{(1 - e^{-2\pi\gamma\xi})[1 + (\gamma - 1)\xi]} \quad (4)$$

For the determination of the wavelet's amplitude A from Eq. (4), the value of the duration γ must be known. Since this is an unknown parameter, all the values in a selected range of variation of γ are examined. From this set of pairs (A, γ) , the ones that lead to amplitudes of the wavelet's acceleration, velocity or displacement larger than the corresponding peak values of the ground motion, p_{ga} , p_{gv} and p_{gd} respectively, are rejected.



For the remaining, acceptable pairs (A, γ) , and for all values of the phase ν between 0° and 360° , the corresponding wavelets are calculated. For each of these wavelets, several values of time delay d for the initiation of the pulse are examined. Thus, a set of candidate wavelets is determined, each one corresponding to a different set of parameters A, γ, ν and d . From the corresponding pulse time-histories, $v_p(A, \gamma, \nu, d, t)$, the wavelet that correlates best with the time history of the ground velocity, $v_g(t)$, is selected.

To this end, the cross correlation factor, r , is calculate for each pair of time histories (v_p, v_g) and the pulse with the largest r is selected. In this way, the cross correlation operation is used to identify not only the pulse which best fits the velocity time history of the ground motion, but also its starting time d .

It is mentioned that the time delay d , is related to the time t_0 defining the epoch of the envelope's peak of the wavelet, as $t_0 = d + \gamma T_p / 2$.

CHAPTER 4 BUILDING DESCRIPTION

The building used for the study of seismic near field response five-storey building of reinforced concrete. The building is located in the municipality of Athens, Geroulanou Street 3, Palaio Faliro. It has a total height of 16 m and the dimensions of the floor plan is 14.4x10.5 m². The ground floor and the rest of the floors have a height of 3 m. Here are the top view (Figure 4.1) and the section of the building from the seismoStruct program (Figure 4.2).

Building Layout

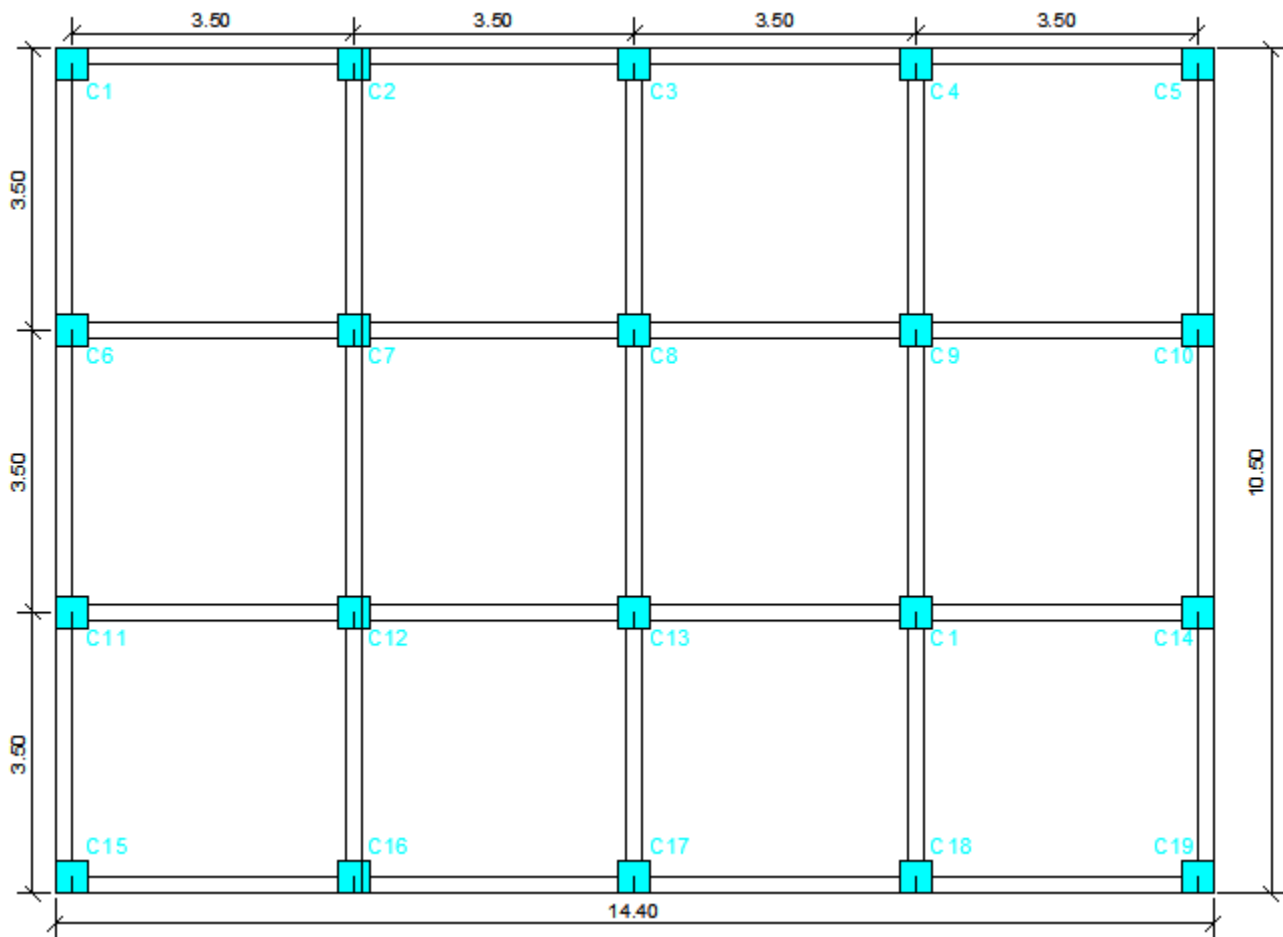


Figure 4.1. Plan View of the Building

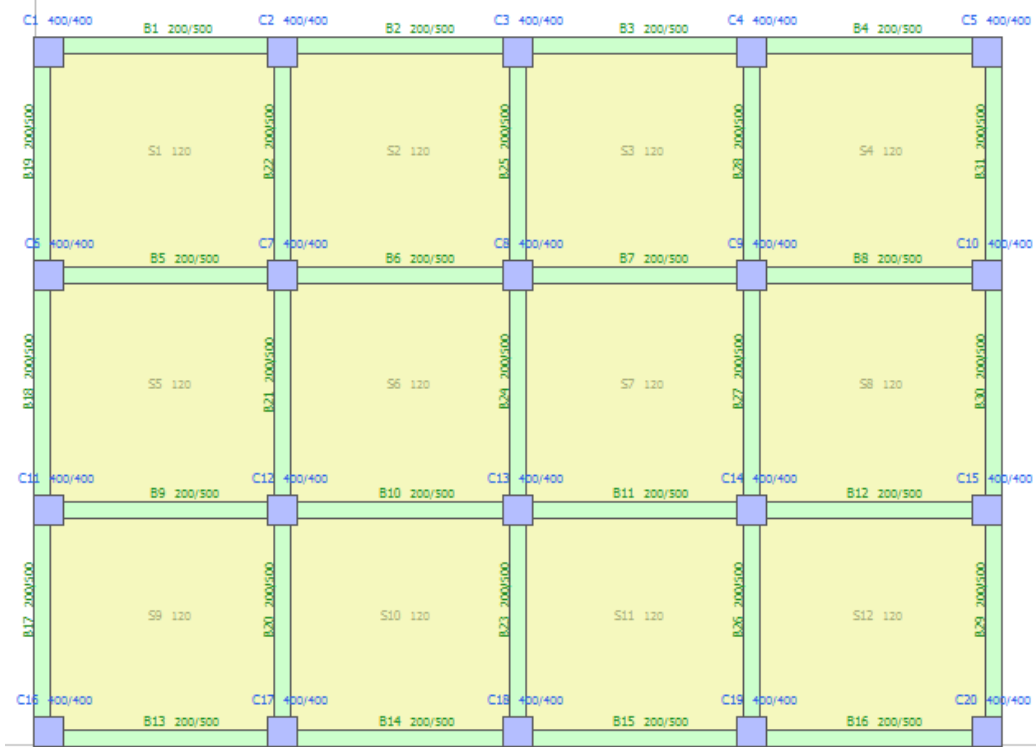


Figure 4.2. details of the Plan View of the Building from the Seismostruct

Modelling of the building using Seismostruct:

The Reinforced concrete building consists of beams which are simulated as T-sections at the interior spans while are considered as L-sections on the perimeter of the building.

Beams and Columns are modeled as inelastic forced based plastic hinge elements (infrmFBPH), while the slabs are considered as rigid diaphragms as illustrated in figures 4.4 and 4.5 respectively.

The structure was modelled using the building modeller of seismostruct program, the height of each floor was taken approximately 3m. The modeling procedures will be illustrated in the following subdivisions.

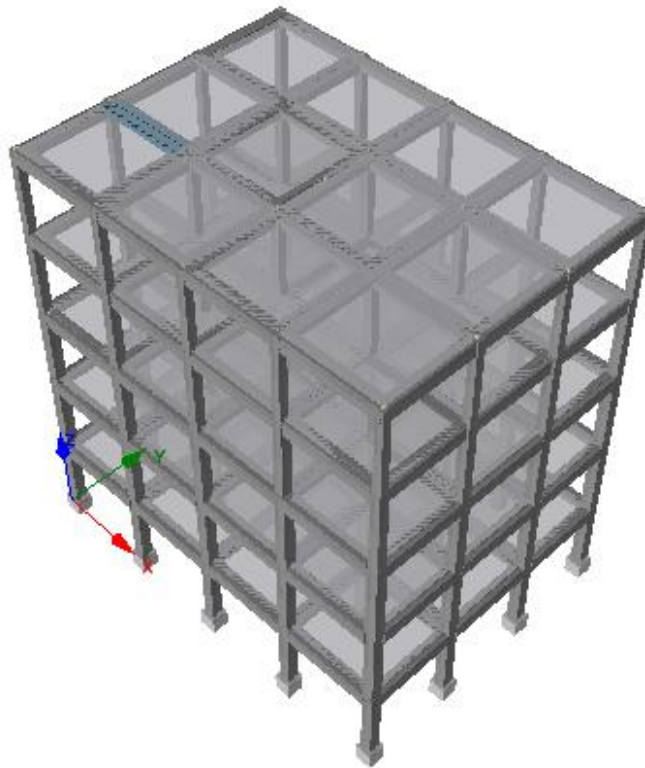


Figure 4.3. 3D Model of the Building in Seismostruct



Figure 4.4. Frame elements modelling types in Seismostruct.

Materials	Sections	Element Classes	Nodes	Element Connectivity	Constraints	Restraints	Applied Loads	Analysis Output																																																																																
<div style="display: flex; justify-content: space-between;"> <div style="width: 20%;"> <p>Add</p> <p>Edit</p> <p>Remove</p> <p>Incrementation</p> <p>Table Input ✓</p> <p>Graphical Input</p> <p><<</p> </div> <table border="1" style="width: 80%;"> <thead> <tr> <th>Constraint type</th> <th>Master Nodes</th> <th>Restrained DOFs</th> <th>Slave Node(s)</th> </tr> </thead> <tbody> <tr><td>Rigid Diaphragm</td><td>n1_C1up</td><td>X-Y plane</td><td>n1_C6up n1_C7up n1_C2up</td></tr> <tr><td>Rigid Diaphragm</td><td>n1_C2up</td><td>X-Y plane</td><td>n1_C7up n1_C8up n1_C3up</td></tr> <tr><td>Rigid Diaphragm</td><td>n1_C3up</td><td>X-Y plane</td><td>n1_C8up n1_C9up n1_C4up</td></tr> <tr><td>Rigid Diaphragm</td><td>n1_C4up</td><td>X-Y plane</td><td>n1_C9up n1_C10up n1_C5up</td></tr> <tr><td>Rigid Diaphragm</td><td>n1_C6up</td><td>X-Y plane</td><td>n1_C11up n1_C12up n1_C7up</td></tr> <tr><td>Rigid Diaphragm</td><td>n1_C7up</td><td>X-Y plane</td><td>n1_C12up n1_C13up n1_C8up</td></tr> <tr><td>Rigid Diaphragm</td><td>n1_C8up</td><td>X-Y plane</td><td>n1_C13up n1_C14up n1_C9up</td></tr> <tr><td>Rigid Diaphragm</td><td>n1_C9up</td><td>X-Y plane</td><td>n1_C14up n1_C15up n1_C10up</td></tr> <tr><td>Rigid Diaphragm</td><td>n1_C11up</td><td>X-Y plane</td><td>n1_C16up n1_C17up n1_C12up</td></tr> <tr><td>Rigid Diaphragm</td><td>n1_C12up</td><td>X-Y plane</td><td>n1_C17up n1_C18up n1_C13up</td></tr> <tr><td>Rigid Diaphragm</td><td>n1_C13up</td><td>X-Y plane</td><td>n1_C18up n1_C19up n1_C14up</td></tr> <tr><td>Rigid Diaphragm</td><td>n1_C14up</td><td>X-Y plane</td><td>n1_C19up n1_C20up n1_C15up</td></tr> <tr><td>Rigid Diaphragm</td><td>n2_C1up</td><td>X-Y plane</td><td>n2_C6up n2_C7up n2_C2up</td></tr> <tr><td>Rigid Diaphragm</td><td>n2_C2up</td><td>X-Y plane</td><td>n2_C7up n2_C8up n2_C3up</td></tr> <tr><td>Rigid Diaphragm</td><td>n2_C3up</td><td>X-Y plane</td><td>n2_C8up n2_C9up n2_C4up</td></tr> <tr><td>Rigid Diaphragm</td><td>n2_C4up</td><td>X-Y plane</td><td>n2_C9up n2_C10up n2_C5up</td></tr> <tr><td>Rigid Diaphragm</td><td>n2_C6up</td><td>X-Y plane</td><td>n2_C11up n2_C12up n2_C7up</td></tr> <tr><td>Rigid Diaphragm</td><td>n2_C7up</td><td>X-Y plane</td><td>n2_C12up n2_C13up n2_C8up</td></tr> <tr><td>Rigid Diaphragm</td><td>n2_C8up</td><td>X-Y plane</td><td>n2_C13up n2_C14up n2_C9up</td></tr> </tbody> </table> </div>									Constraint type	Master Nodes	Restrained DOFs	Slave Node(s)	Rigid Diaphragm	n1_C1up	X-Y plane	n1_C6up n1_C7up n1_C2up	Rigid Diaphragm	n1_C2up	X-Y plane	n1_C7up n1_C8up n1_C3up	Rigid Diaphragm	n1_C3up	X-Y plane	n1_C8up n1_C9up n1_C4up	Rigid Diaphragm	n1_C4up	X-Y plane	n1_C9up n1_C10up n1_C5up	Rigid Diaphragm	n1_C6up	X-Y plane	n1_C11up n1_C12up n1_C7up	Rigid Diaphragm	n1_C7up	X-Y plane	n1_C12up n1_C13up n1_C8up	Rigid Diaphragm	n1_C8up	X-Y plane	n1_C13up n1_C14up n1_C9up	Rigid Diaphragm	n1_C9up	X-Y plane	n1_C14up n1_C15up n1_C10up	Rigid Diaphragm	n1_C11up	X-Y plane	n1_C16up n1_C17up n1_C12up	Rigid Diaphragm	n1_C12up	X-Y plane	n1_C17up n1_C18up n1_C13up	Rigid Diaphragm	n1_C13up	X-Y plane	n1_C18up n1_C19up n1_C14up	Rigid Diaphragm	n1_C14up	X-Y plane	n1_C19up n1_C20up n1_C15up	Rigid Diaphragm	n2_C1up	X-Y plane	n2_C6up n2_C7up n2_C2up	Rigid Diaphragm	n2_C2up	X-Y plane	n2_C7up n2_C8up n2_C3up	Rigid Diaphragm	n2_C3up	X-Y plane	n2_C8up n2_C9up n2_C4up	Rigid Diaphragm	n2_C4up	X-Y plane	n2_C9up n2_C10up n2_C5up	Rigid Diaphragm	n2_C6up	X-Y plane	n2_C11up n2_C12up n2_C7up	Rigid Diaphragm	n2_C7up	X-Y plane	n2_C12up n2_C13up n2_C8up	Rigid Diaphragm	n2_C8up	X-Y plane	n2_C13up n2_C14up n2_C9up
Constraint type	Master Nodes	Restrained DOFs	Slave Node(s)																																																																																					
Rigid Diaphragm	n1_C1up	X-Y plane	n1_C6up n1_C7up n1_C2up																																																																																					
Rigid Diaphragm	n1_C2up	X-Y plane	n1_C7up n1_C8up n1_C3up																																																																																					
Rigid Diaphragm	n1_C3up	X-Y plane	n1_C8up n1_C9up n1_C4up																																																																																					
Rigid Diaphragm	n1_C4up	X-Y plane	n1_C9up n1_C10up n1_C5up																																																																																					
Rigid Diaphragm	n1_C6up	X-Y plane	n1_C11up n1_C12up n1_C7up																																																																																					
Rigid Diaphragm	n1_C7up	X-Y plane	n1_C12up n1_C13up n1_C8up																																																																																					
Rigid Diaphragm	n1_C8up	X-Y plane	n1_C13up n1_C14up n1_C9up																																																																																					
Rigid Diaphragm	n1_C9up	X-Y plane	n1_C14up n1_C15up n1_C10up																																																																																					
Rigid Diaphragm	n1_C11up	X-Y plane	n1_C16up n1_C17up n1_C12up																																																																																					
Rigid Diaphragm	n1_C12up	X-Y plane	n1_C17up n1_C18up n1_C13up																																																																																					
Rigid Diaphragm	n1_C13up	X-Y plane	n1_C18up n1_C19up n1_C14up																																																																																					
Rigid Diaphragm	n1_C14up	X-Y plane	n1_C19up n1_C20up n1_C15up																																																																																					
Rigid Diaphragm	n2_C1up	X-Y plane	n2_C6up n2_C7up n2_C2up																																																																																					
Rigid Diaphragm	n2_C2up	X-Y plane	n2_C7up n2_C8up n2_C3up																																																																																					
Rigid Diaphragm	n2_C3up	X-Y plane	n2_C8up n2_C9up n2_C4up																																																																																					
Rigid Diaphragm	n2_C4up	X-Y plane	n2_C9up n2_C10up n2_C5up																																																																																					
Rigid Diaphragm	n2_C6up	X-Y plane	n2_C11up n2_C12up n2_C7up																																																																																					
Rigid Diaphragm	n2_C7up	X-Y plane	n2_C12up n2_C13up n2_C8up																																																																																					
Rigid Diaphragm	n2_C8up	X-Y plane	n2_C13up n2_C14up n2_C9up																																																																																					

Figure 4.5. Rigid diaphragms modelled in Seismostruct.



Materials:

Concrete

The concrete used for construction of the building is C16/20 (with $f_{ck} = 16$ MPa).

Steel Reinforcement

The steel used in reinforcement is grade S310 ($f_{yk}=310$ Mpa).

The screenshot shows a dialog box titled "Modify existing material scheme". It contains the following fields and controls:

- Name:
- Type:
- Concrete Strength (MPa):
 - Mean Value:
 - Mean - σ :
 - Concrete Class:
- Steel Strength (MPa):
 - Mean Value:
 - Mean - σ :
 - Steel Class:
- Buttons: Help, Ok, Cancel

Figure 4.6. Material characteristics in Seismostruct

Modeling Elements

Beams

The cross section of the typical beam is shown in Figure 4.7 and the side view in Figure 3.8. In these figures the layout of the main reinforcement satisfies all the requirements of the codes, including the requirement that the compression reinforcement of a section to be at least 50 percent of the tension.

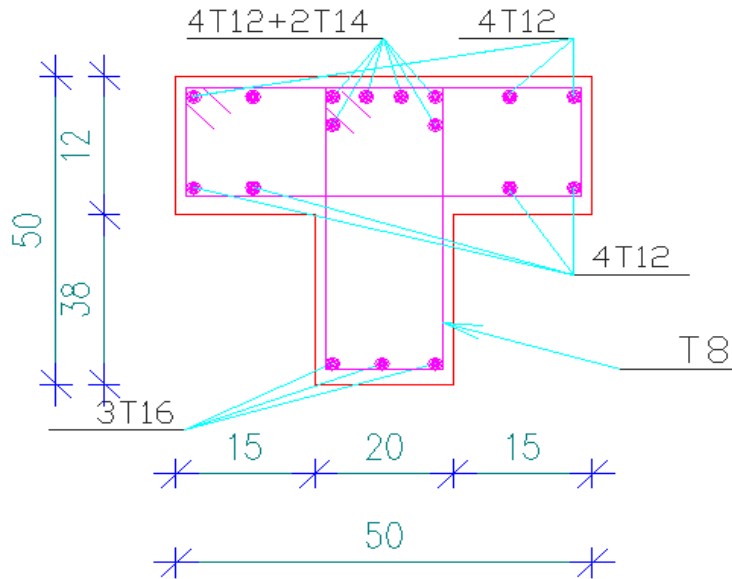


Figure 3.7. Cross section of the Beam

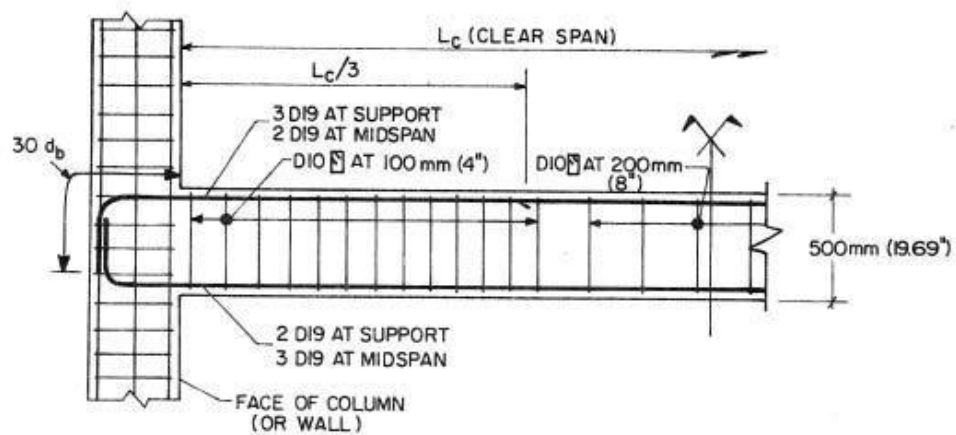


Figure 4.8. Side View of the Beam



Columns

The cross section of the typical column is shown in the figure below. This section with the exception of the stirrups is the same for all columns of the structure.

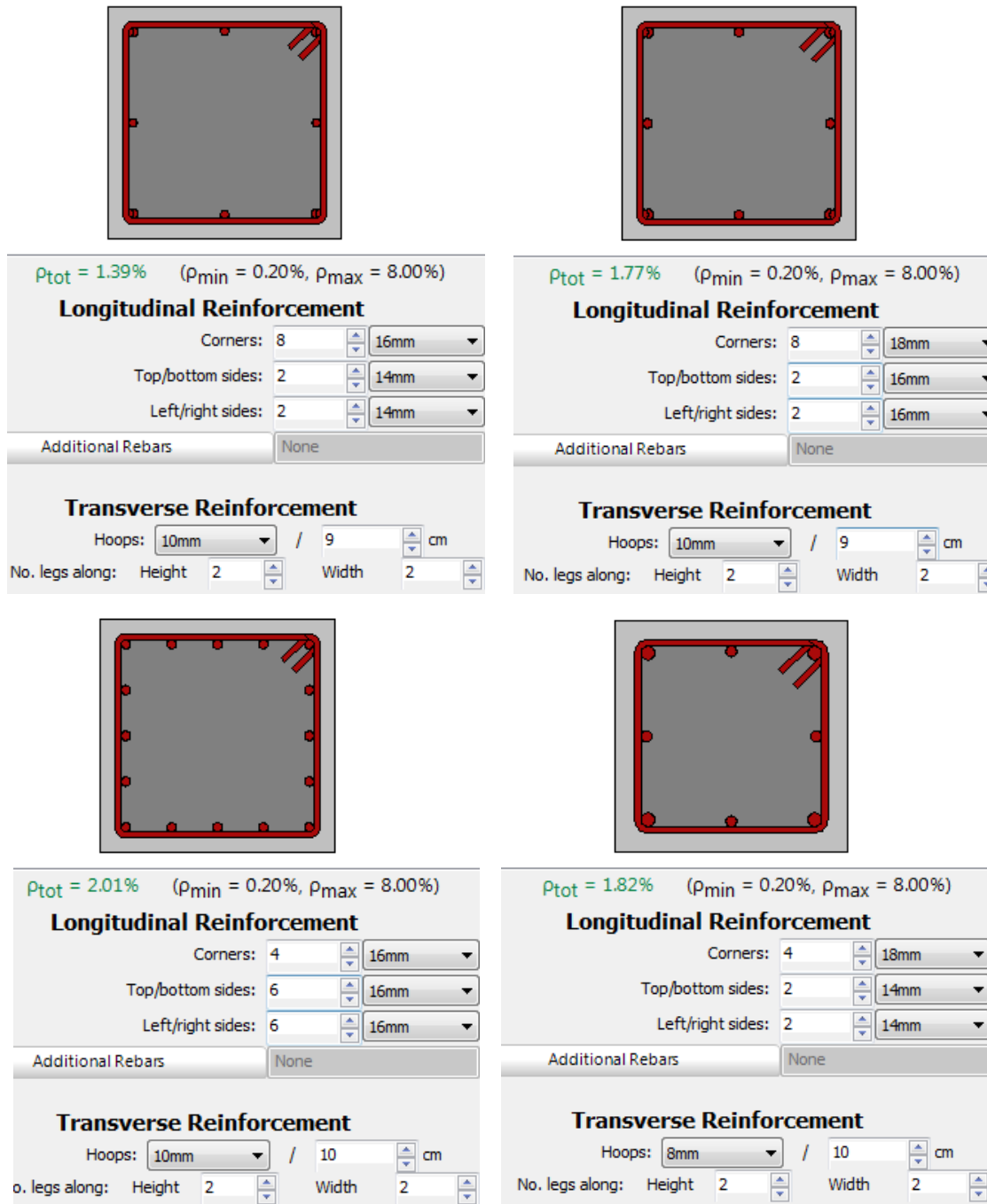


Figure 4.9. Typical column Section 400X400 mm & 35X35 mm

Loading

Loads of the building consists of live loads and dead loads. Dead loads are the own weight of the members, floor covering and wall loads. Since the walls are divided into exterior and interior walls, the interior wall loads are distributed on the slabs while the exterior wall loads are uniformly distributed on the beams. All dead and live loads are transferred to the beams as distributed loads according to the following figures.

Beam-Column Element Types

Element Class	Section Name	Section Fibres	Plastic-hinge length Lp/L(%)	Damping	Additional Mass
class_B2_1	sec_BL2_1 sec_BR2_1	60	16.67	None	1.27087
class_B3_1	sec_BL3_1 sec_BR3_1	60	16.67	None	1.27087
class_B4_1	sec_BL4_1 sec_BR4_1	61	16.67	None	1.29421
class_B1_1	sec_BL1_1 sec_BR1_1	62	16.67	None	1.29016
class_B5_1	sec_BL5_1 sec_BR5_1	69	16.67	None	0.74774429
class_B6_1	sec_BL6_1 sec_BR6_1	68	16.67	None	0.69985476
class_B7_1	sec_BL7_1 sec_BR7_1	68	16.67	None	0.65743932
class_B8_1	sec_BL8_1 sec_BR8_1	68	16.67	None	0.67528911
class_B9_1	sec_BL9_1 sec_BR9_1	69	16.67	None	0.74774429
class_B10_1	sec_BL10_1 sec_BR10_1	68	16.67	None	0.69985476
class_B11_1	sec_BL11_1 sec_BR11_1	68	16.67	None	0.65743932
class_B12_1	sec_BL12_1 sec_BR12_1	69	16.67	None	0.6622878
class_B13_1	sec_BL13_1 sec_BR13_1	62	16.67	None	1.29008
class_B14_1	sec_BL14_1 sec_BR14_1	61	16.67	None	1.26675

Figure 4.11. Loads transferred to the beams in the form of additional mass by the software.

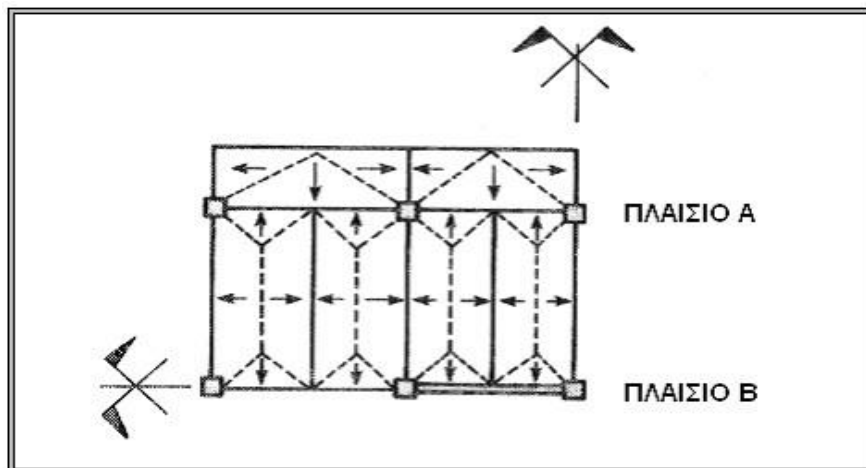


Figure 4.12. Description of how the loads are being transferred to the beams.



Loads

Permanent Loads (G, G') and Live Loads (Q) :

G (kN/m²) 2.88 Automatic Calculation

G' (kN/m²) 1.50

Q (kN/m²) 2.00

S (kN/m²) 0.00 (required only by ASCE 41-17 and TBDY)

Slab Inclination

Floor Elevation: 3000

Inclined or elevated slab (defined by 3 points)

Fig. 3.13. Uniformly distributed loads “including interior walls” on the slabs.

Loads

Additional Permanent Loads (G^m) & Live Loads (Q) :

G' (kN/m²) 2.00

Q (kN/m²) 3.50

Slab Inclination

Inclined or elevated slab (defined by 3 points)

Fig. 3.14. Uniformly distributed loads for the stairs slab.

B 2

Display/Modify Effective Width

View/Modify Geometry

Additional Permanent Load (G') :

G' (kN/m) 9.00

Fig. 4.15. Uniformly distributed wall loads on exterior beams

Loading Combination Coefficients

Gravity and Live Loads

Gravity Loads Coefficient C_g 1.00

Live Loads Coefficient C_q 0.30

Snow Loads Coefficient C_s 0.00 (used for ASCE 41_13 and TBDY only)

Fig. 4.16. Loading Combination coefficients.



Eigenvalues Analysis

In the calculation of eigenvalues analysis the efficient Lanczos algorithm [Hughes, 1987] is used for the evaluation of the structural natural frequencies and mode shapes.

The number of Eigenvalues used is 10 as shown in table 3.1.

MODAL PERIODS AND FREQUENCIES		
Mode	Period	Frequency
#	(sec)	(Hertz)
1	0.48365283	2.0676
2	0.47988535	2.08383
3	0.45248589	2.21001
4	0.18401287	5.4344
5	0.18262786	5.47562
6	0.17097673	5.84875
7	0.11358375	8.80408
8	0.11350025	8.81055
9	0.1078133	9.27529
10	0.08160214	12.25458

Table 4.1. Modal periods and frequencies.



Dynamic time-history Analysis

Theory and purpose

Dynamic time-history loads

These are dynamic loads (accelerations or forces) that vary according to different load curves in the real time domain. The product of their constant nominal value and the variable load factor obtained from its load curve (e.g. accelerogram) at any particular time gives the magnitude of the load applied to the structure. These loads can be used in dynamic time history analysis, to reproduce the response of a structure subjected to an earthquake, or in incremental dynamic analysis, to evaluate the horizontal structural capacity of a structure.

Dynamic analysis is commonly used to predict the nonlinear inelastic response of a structure subjected to earthquake loading (evidently, linear elastic dynamic response can also be modelled for as long as elastic elements and/or low levels of input excitation are considered).

The direct integration of the equations of motion is accomplished using the numerically dissipative α -integration algorithm [Hilber et al., 1977] or a special case of the former, the well-known Newmark scheme [Newmark, 1959], with automatic time-step adjustment for optimum accuracy and efficiency.

Modelling of seismic action is achieved by introducing acceleration loading curves (accelerograms) at the supports, noting that different curves can be introduced at each support, thus allowing for representation of asynchronous ground excitation.

In addition, dynamic analysis may also be employed for modelling of pulse loading cases (e.g. blast, impact, etc.), in which case instead of acceleration time-histories at the supports, force pulse functions of any given shape (rectangular, triangular, parabolic, and so on), can be employed to describe the transient loading applied to the appropriate nodes.

A plot of the total base shear versus top displacement in a structure is obtained by this analysis that would indicate any premature failure or weakness. The analysis is carried out up to failure, thus it enables determination of collapse load and ductility capacity. On a building frame, and plastic rotation is monitored, and lateral inelastic forces versus displacement response for the complete structure is analytically computed.

This type of analysis enables weakness in the structure to be identified. The decision to retrofit can be taken in such studies.



Dynamic time- history in seismostruct

Fifty records from the PEER NGA database 7 that were classified as pulse-like by Baker **Error! Reference source not found.** were applied for the inelastic time history analyses of the five structures described above. The characteristics of the selected earthquakes are shown in 4.2.

Table 4.2.Pulse-like ground motions normal to the fault component characteristics.

No	NGA No.	Event	Year	Station	T_p (sec)	A (cm/sec)	γ	ν (°)	t_d (sec)
1	150	Coyote Lake	1979	Gilroy Array #6	0.94	44.94	1.6	355	1.93
2	158	Imperial Valley-06	1979	Aeropuerto Mexicali	1.64	46.78	2.1	345	3.64
3	159	Imperial Valley-06	1979	Agrarias	1.90	44.04	2.0	25	5.87
4	161	Imperial Valley-06	1979	Brawley Airport	4.78	48.66	1.1	100	5.47
5	170	Imperial Valley-06	1979	EC County Center FF	4.17	52.27	1.5	130	3.77
6	171	Imperial Valley-06	1979	EC Meloland Overpass FF	3.01	114.85	1.4	0	2.86
7	173	Imperial Valley-06	1979	El Centro Array #10	6.08	58.79	1.1	140	3.66
8	174	Imperial Valley-06	1979	El Centro Array #11	6.39	18.55	2.9	245	0.60
9	178	Imperial Valley-06	1979	El Centro Array #3	5.55	39.65	1.2	180	5.00
10	179	Imperial Valley-06	1979	El Centro Array #4	4.32	71.39	1.9	125	2.00
11	180	Imperial Valley-06	1979	El Centro Array #5	3.79	86.02	1.8	135	3.37
12	181	Imperial Valley-06	1979	El Centro Array #6	3.94	97.47	1.9	85	2.62
13	182	Imperial Valley-06	1979	El Centro Array #7	3.44	74.50	2.2	45	2.52
14	183	Imperial Valley-06	1979	El Centro Array #8	5.08	69.50	1.1	80	3.37
15	184	Imperial Valley-06	1979	El Centro Differential Array	5.86	60.43	1.1	70	2.66
16	185	Imperial Valley-06	1979	Holtville Post Office	4.24	47.52	1.7	175	3.35
17	250	Mammoth Lakes-06	1980	Long Valley Dam (Upr L Abut)	1.14	34.99	1.4	300	4.59
18	292	Irpinia, Italy-01	1980	Sturno	2.64	23.95	5.6	110	1.13
19	316	Westmorland	1981	Parachute Test Site	3.00	25.91	2.2	300	7.54
20	407	Coalinga-05	1983	Oil City	0.56	35.39	3.4	0	2.22
21	415	Coalinga-05	1983	Transmitter Hill	0.75	44.06	3.2	310	2.00
22	418	Coalinga-07	1983	Coalinga-14th & Elm (Old CHP)	0.38	44.60	1.5	135	2.54
23	451	Morgan Hill	1984	Coyote Lake Dam (SW Abut)	0.77	42.78	4.2	300	2.30
24	459	Morgan Hill	1984	Gilroy Array #6	1.17	31.87	2.6	235	4.45
25	503	Taiwan SMART1(40)	1986	SMART1 C00	1.49	29.00	2.1	215	5.91
26	508	Taiwan SMART1(40)	1986	SMART1 M07	1.39	35.07	2.1	215	10.29
27	529	N. Palm Springs	1986	North Palm Springs	1.44	56.48	1.5	345	1.80
28	568	San Salvador	1986	GeotechInvestig Center	0.70	68.43	2.2	190	0.63
29	615	Whittier Narrows-01	1987	Downey - Co MaintBldg	0.81	27.35	2.5	260	4.36
30	645	Whittier Narrows-01	1987	LB - Orange Ave	0.78	30.64	2.4	255	5.10
31	738	Loma Prieta	1989	Alameda Naval Air Stn Hanger	2.31	48.18	2.3	1.1	10.87
32	766	Loma Prieta	1989	Gilroy Array #2	1.54	28.64	4.8	270	1.16
33	802	Loma Prieta	1989	Saratoga - Aloha Ave	6.48	36.31	1.2	180	3.10
34	821	Erzican, Turkey	1992	Erzincan	2.42	89.81	1.7	20	1.58
35	828	Cape Mendocino	1992	Petrolia	2.74	57.86	1.5	325	1.13
36	838	Landers	1992	Barstow	7.57	22.97	1.7	135	11.2
37	879	Landers	1992	Lucerne	4.57	96.72	1.6	65	7.03
38	900	Landers	1992	Yermo Fire Station	8.73	56.46	1.1	160	13.28
39	982	Northridge-01	1994	Jensen Filter Plant	2.94	60.02	3.0	285	0.00
40	983	Northridge-01	1994	Jensen Filter Plant Generator	2.94	60.02	3.0	285	0.00
41	1009	Northridge-01	1994	LA-Wadsworth VA Hospital North	2.35	41.98	1.1	110	8.16
42	1013	Northridge-01	1994	LA Dam	2.17	76.26	1.1	220	1.78
43	1045	Northridge-01	1994	Newhall - W Pico Canyon Rd.	2.39	117.85	1.2	290	3.82
44	1050	Northridge-01	1994	Pacoima Dam (downstr)	3.37	11.71	3.2	25	0.04
45	1051	Northridge-01	1994	Pacoima Dam (upper left)	0.90	100.31	1.6	255	3.26
46	1063	Northridge-01	1994	Rinaldi Receiving Station	1.11	132.51	1.9	240	1.55
47	1085	Northridge-01	1994	Sylmar - Converter Station East	3.06	89.17	1.6	175	1.15
48	1086	Northridge-01	1994	Sylmar - Olive View Med FF	2.56	61.88	3.6	355	0.37
49	1119	Kobe, Japan	1995	Takarazuka	1.23	55.97	2.3	145	3.82
50	1161	Kocaeli, Turkey	1999	Gebze	4.88	42.18	1.8	190	3.37



The dynamic time history loading type, and the performance criteria taken into consideration are illustrated in the figures below.

Loading Combination Coefficients		Performance Criteria		Code-based Checks			
Analysis Type		Frame Elements Modelling		Slabs Modelling		Structural Configuration	
Loading							
Analysis Type: Dynamic time-history analysis							
Control Node							
Define Control Node Automatic <input checked="" type="checkbox"/> Do not define control node in floors with mass less than 10% of lower floor's mass							
Automatic definition of control node at the center of mass of highest floor with mass no less than 10% of the floor right below it.							

Figure 4.17. Dynamic time history analysis and loading type.

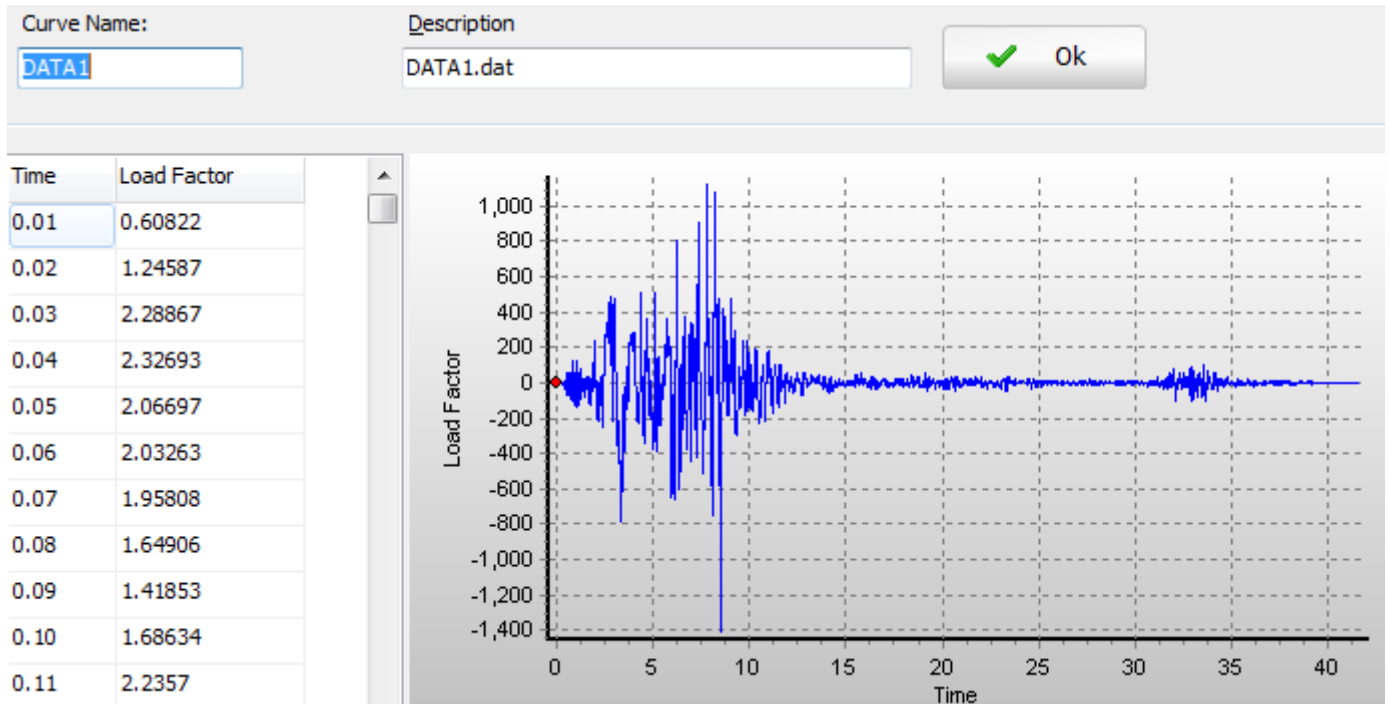


Figure 4.18. Load Curve time history value for Data1

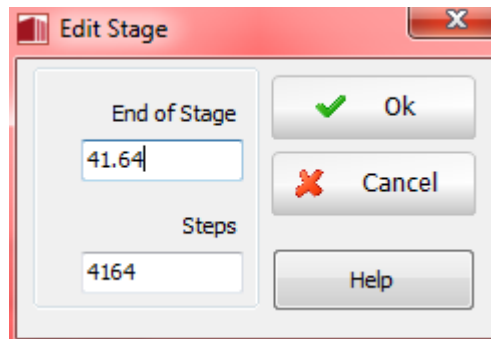


Figure 4.19. Time history stage.

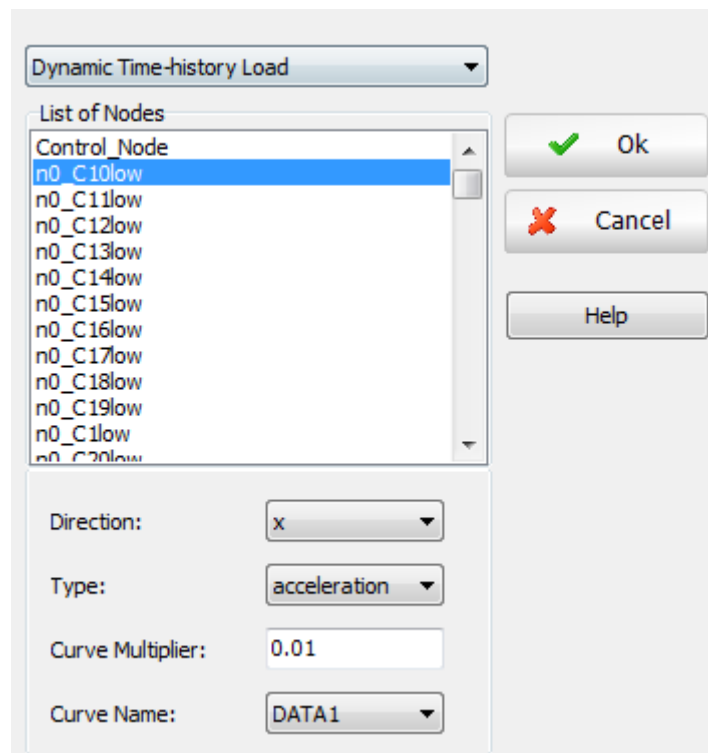


Figure 4.20. Applied Loads Module in X-direction.

Nodal Loads

Category	Node Name	Direction	Type	Value	Curve Name
Dynamic Time-hi...	n0_C10low	x	acceleration	0.01	DATA1
Dynamic Time-hi...	n0_C11low	x	acceleration	0.01	DATA1
Dynamic Time-hi...	n0_C12low	x	acceleration	0.01	DATA1
Dynamic Time-hi...	n0_C13low	x	acceleration	0.01	DATA1
Dynamic Time-hi...	n0_C14low	x	acceleration	0.01	DATA1
Dynamic Time-hi...	n0_C15low	x	acceleration	0.01	DATA1
Dynamic Time-hi...	n0_C16low	x	acceleration	0.01	DATA1
Dynamic Time-hi...	n0_C17low	x	acceleration	0.01	DATA1
Dynamic Time-hi...	n0_C18low	x	acceleration	0.01	DATA1
Dynamic Time-hi...	n0_C19low	x	acceleration	0.01	DATA1
Dynamic Time-hi...	n0_C1low	x	acceleration	0.01	DATA1
Dynamic Time-hi...	n0_C20low	x	acceleration	0.01	DATA1
Dynamic Time-hi...	n0_C2low	x	acceleration	0.01	DATA1

Figure 4.21. Applied Loads at the ground nodes nodes in X-direction .

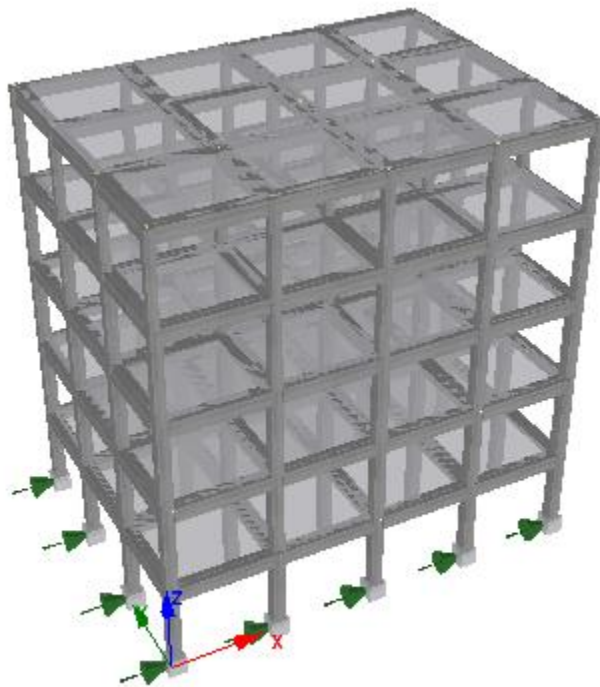


Figure 4.22. 3D the loads value at the ground nodes in X-direction .



Code Employed in Capacity Checks

EuroCode 8, Part-3 Safety Factors Knowledge Level

Advanced Member Properties

Element Name	Primary/Second...	Earthqua...	Cold-Worke...	Smooth (Plain...	Type/Length of...	Length of Lapping	Accessibility (ne
B10_1	Primary	yes	no	no	At_End_Sections	Adequate	yes
B10_2	Primary	yes	no	no	At_End_Sections	Adequate	yes
B10_3	Primary	yes	no	no	At_End_Sections	Adequate	yes
B10_4	Primary	yes	no	no	At_End_Sections	Adequate	yes
B10_5	Primary	yes	no	no	At_End_Sections	Adequate	yes
B11_1	Primary	yes	no	no	At_End_Sections	Adequate	yes
B11_2	Primary	yes	no	no	At_End_Sections	Adequate	yes
B11_3	Primary	yes	no	no	At_End_Sections	Adequate	yes

Code-based Capacity Checks

Criterion Name	Type	Elements	Strength De...	Notifica...	Parame...	Color	Display...
Chord_Rotation_Capacity	Frame Element Chord Rot...	C1_1 C2_1 ...	Keep Strength	Notify	EC8 S...	dOlive	Very_S...
Shear_Capacity	Frame Element Shear Cap...	C1_1 C2_1 ...	Keep Strength	Notify	EC8 S...	&0016...	Seriou...

Figure 4.23. Chord rotation yielding

Criterion Name	Description	Type	Value	Material	Elements	Strengt...	Notification	Parame...	Color	Display of ...
crush_conf	(Concrete Strain [RC/Composite sections]) < -0.008	Concre...	-0.008	All Con...	C1_1 C2_1 ...	Keep S...	Notify	Core_...	&00804000	Very_Seri...
yield	(Reinforcement Strain [RC/Composite sections]) > 0.0025	Reinfo...	0.0025	All Ste...	C1_1 C2_1 ...	Keep S...	Notify		&003378E4	Slight_Da...
crush_unc	(Concrete Strain [RC/Composite sections]) < -0.0035	Concre...	-0.0035	All Con...	C1_1 C2_1 ...	Keep S...	Notify		&00229138	Slight_Da...
fracture	(Reinforcement Strain [RC/Composite sections]) > 0.100	Reinfo...	0.10	All Ste...	C1_1 C2_1 ...	Keep S...	Notify		&002F2F4E	Very_Seri...

Figure 4.24. performance criterion.

CHAPTER 5 GROUND MOTIONS RECORDS

In this study, two seismic regions including near-fault phenomenon were examined which are:

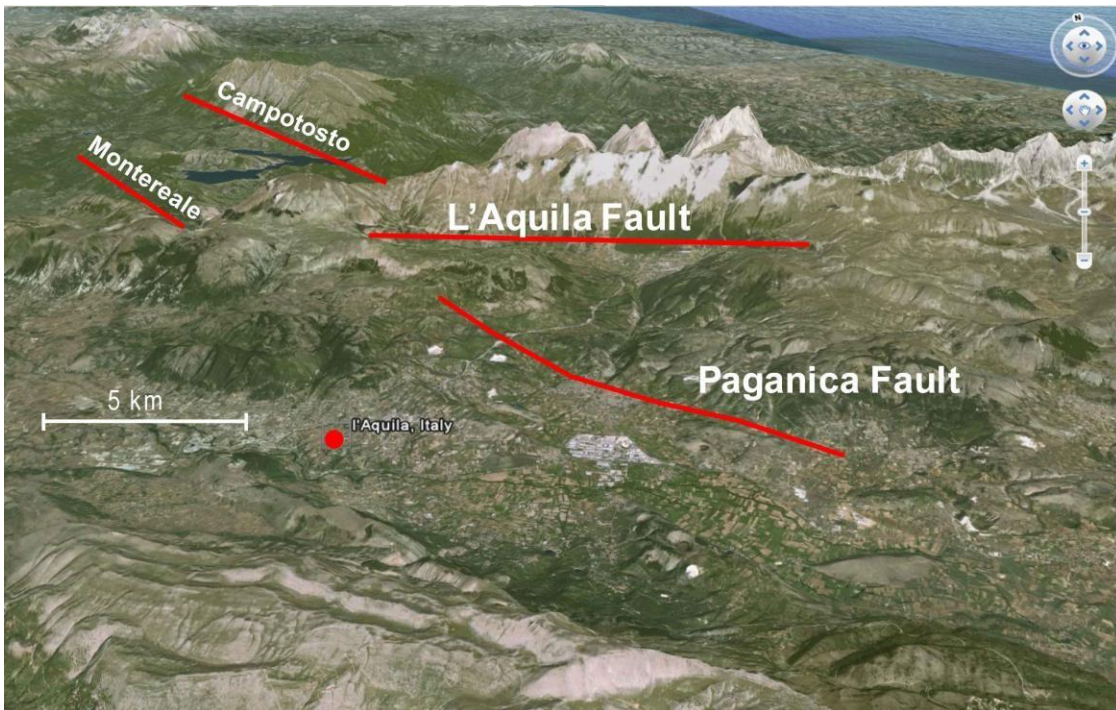
- 1) L'Aquila Earthquake 2009**
- 2) Norcia Earthquake 2016**

L'Aquila earthquake 2009:

L'Aquila earthquake of 2009, severe earthquake that occurred on April 6, 2009, near the city of L'Aquila in the Abruzzi region of central Italy.

The magnitude-6.3 on moment magnitude scale earthquake struck at 3:32 am local time, extensively damaging the 13th-century city of L'Aquila, located only about 60 miles (100 km) northeast of Rome. The earthquake resulted from normal faulting on the northwest-southeast-trending Paganica Fault. It and several neighboring faults are related to extensional tectonic forces associated with the opening of the Tyrrhenian Basin to the west. For more than three months after the main earthquake, the National Institute of Geophysics and Volcanology, using a portable network of seismometers, continued to detect thousands of aftershocks. The aftershocks from the country's worst earthquake in 30 years rippled through central Italy, fraying both public and political nerves. In all, more than 300 people died, and an estimated 60,000 were left homeless.





Pictures representing the damage after the L'Aquila earthquake and the geography of the region

Near Source Features

Results of seismological studies have shown that the Abruzzi event was a *normal* faulting earthquake (or *dip-slip*), with a rectangular rupture plane of about 17×14km² and located at a depth between 12 and 0.6 km from the surface. The rupture plan has a strike of 142°, a dip of 50° and a rake of 90°.

Coordinates of the vertices of the rupture plane and of the hypocenter are reported in Table 4.1. These data are not uniquely identified by all seismologists, but the various available estimates are not very different each other. The main shock was recorded by the stations of the National Accelerometric Network (RAN) of the Italian Civil Protection, Figure 4.1 shows the projection of rupture surface with the epicentral location, the code of RAN Stations, their Eurocode 8 (EC8) site class, and some severely damaged towns and villages.

	Fault plane vertices				Hypocenter
Longitude	13.424°	13.552°	13.465°	13.336°	13.353°
Latitude	42.405°	42.293°	42.238°	42.351°	42.340°
Depth (km)	0.600	0.600	11.800	11.800	11.800

Table 5.1. Hypocenter and rupture plane coordinates.

NEAR-SOURCE SEISMIC DEMAND AND PULSE-LIKE RECORDS

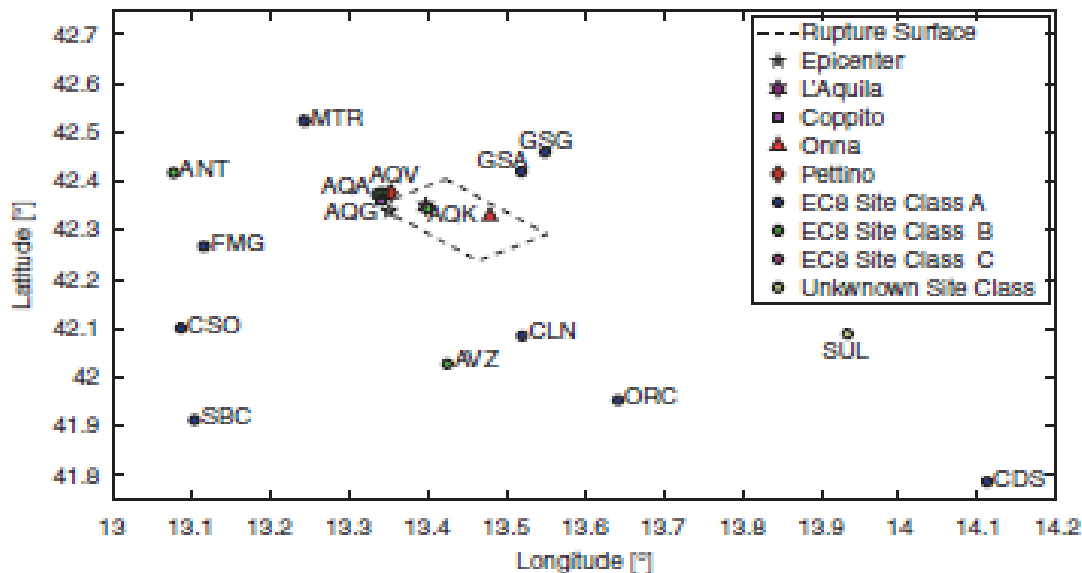


Figure 5.1. Map view of rupture surface and RAN Accelerometric stations within about 60 km from the fault projection.



The algorithm developed by Baker calculates, for each record, a score called *pulse indicator*. Records with score above 0.85 and below 0.15 are classified as pulses and non-pulses, respectively, while signals with a score between these limits are considered ambiguous. The procedure to identify pulses has been implemented by J.W. Baker was used to analyze L'Aquila records; Table VII shows the results of pulse identification for the records of Table VI; identified pulse-like records are reported in bold. Thirteen stations were analyzed and seven of them have a horizontal component classified as pulse-like: six of them in the FN direction and only one in the FP direction, AQV.

	Record	PGA (cm/s ²)	PGV (cm/s)	PGD* (cm)	A _I (cm/s)	I _D (-)	S _D (s)	B _D (s)
1	AQV_FN	725.37	37.63	5.53	228.76	5.24	7.69	25.14
	AQV_FP	474.42	31.41	7.07	253.90	10.64	7.61	66.41
2	AQG_FN	357.16	34.08	8.19	114.47	5.88	8.16	18.23
	AQG_FP	391.79	26.60	5.45	144.91	8.68	8.45	25.17
3	AQA_FN	425.86	28.67	7.11	132.60	6.79	6.91	14.78
	AQA_FP	404.55	19.91	3.32	198.89	15.50	7.72	67.33
4	AQK_FN	413.57	45.01	13.22	138.10	4.63	10.55	66.06
	AQK_FP	261.99	16.66	5.32	81.96	11.73	15.37	66.51
5	GSA_FN	153.52	10.91	3.35	37.13	13.86	9.38	25.53
	GSA_FP	197.58	6.02	1.37	46.50	24.48	8.02	24.10
6	CLN_FN	99.54	5.48	1.76	3.87	4.43	8.00	20.05
	CLN_FP	63.29	5.82	2.26	3.75	6.37	6.53	19.13
7	AVZ_FN	61.91	13.06	3.40	8.43	6.51	21.56	51.28
	AVZ_FP	63.41	9.89	3.54	9.14	9.10	18.25	49.76
8	MTR_FN	51.04	4.08	0.93	4.02	12.04	14.84	45.93
	MTR_FP	57.19	3.04	0.88	5.17	18.59	11.39	34.84
9	GSG_FN	20.31	3.66	2.14	0.81	6.81	10.65	33.28
	GSG_FP	25.52	2.31	0.71	0.69	7.33	10.97	25.59
10	FMG_FN	21.87	2.12	0.98	1.34	18.12	22.76	60.38
	FMG_FP	24.43	1.90	0.92	0.88	11.87	20.58	41.78
11	ANT_FN	26.66	2.25	0.47	1.67	17.33	21.68	54.48
	ANT_FP	19.19	1.99	0.43	0.96	15.74	22.87	64.52
12	CSO_FN	18.91	2.24	1.00	0.89	13.11	21.38	58.06
	CSO_FP	13.74	1.48	0.43	0.48	14.74	27.23	65.69
13	ORC_FN	72.64	6.88	1.11	4.77	5.97	10.24	30.10
	ORC_FP	31.85	2.86	0.99	1.83	12.60	14.00	50.95

Table 5.2. Peak and integral IMs of L'Aquila near-source records.

Component	Pulse indicator	Late pulse indicator	PGV (cm/s)	Classified as pulse	T _p (s)
AQV_FN	0.70	0.00	37.63	No	0.53
AQV_FP	0.85	0.00	31.41	Yes	1.06
AQG_FN	1.00	0.00	34.08	Yes	1.02
AQG_FP	0.71	0.00	26.60	No	1.11
AQA_FN	0.93	0.00	28.67	Yes	0.74
AQA_FP	0.00	0.00	19.91	No	0.62
AQK_FN	1.00	0.00	45.01	Yes	1.99
AQK_FP	0.00	1.00	16.66	No	1.26

Table 5.3. Results of pulse identification for horizontal components.



Norcia earthquake 2016:

Norcia Earthquake was the most powerful earthquake to hit Italy since 1980, striking a blow to the regions of Marche and Umbria just days after they were hit by two other earthquakes. It was even more powerful than the April 2009 earthquake that hit L'Aquila, killing more than 300 people, and worse than the August 2016 earthquake that killed hundreds in Amatrice. It also frightened and displaced thousands of already-jittery residents who have seen the ancient structures and walls in their towns, including the San Benedetto basilica in Norcia, which is considered a sacred site, crumble into heaps on the street. The epicenter of the latest earthquake was about 40 miles (68km) south-west of Perugia and close to the town of Norcia, which had also been hit by previous earthquakes.





Pictures representing the damage after the Norcia earthquake and the geography of the region

About 650 Accelerometric signals, manually processed using the procedure by Paolucci et al (2011), are used to evaluate the peak ground motion, acceleration and displacement spectral ordinates, integral parameters and measures of duration.

The first strong earthquake of the sequence (Mw 6.0) struck central Italy on 24-08-2016 at 01:36:32 GMT, in the vicinity of Amatrice, causing diffuse building collapse and about 300 casualties. After 2 months, on 26-10-2016 two events of moment magnitude 5.4 (17:10:36 UTC) and 5.9 (19:18:06 UTC) extended to the NW the seismogenic volume. After 4 days, on 30-10-2016 at 06:40:18 UTC an event of Mw 6.5, struck the area corresponding to the Sibillini Mountains with epicenter located in the vicinity of Norcia.

The four events have been caused by normal faulting, the prevalent style of faulting in the area, all of them having NW-SE or NNW-SSE strike and dip towards SW. The location of the three epicenters together with events having magnitude larger than 4.0 is shown in Fig 4.2.

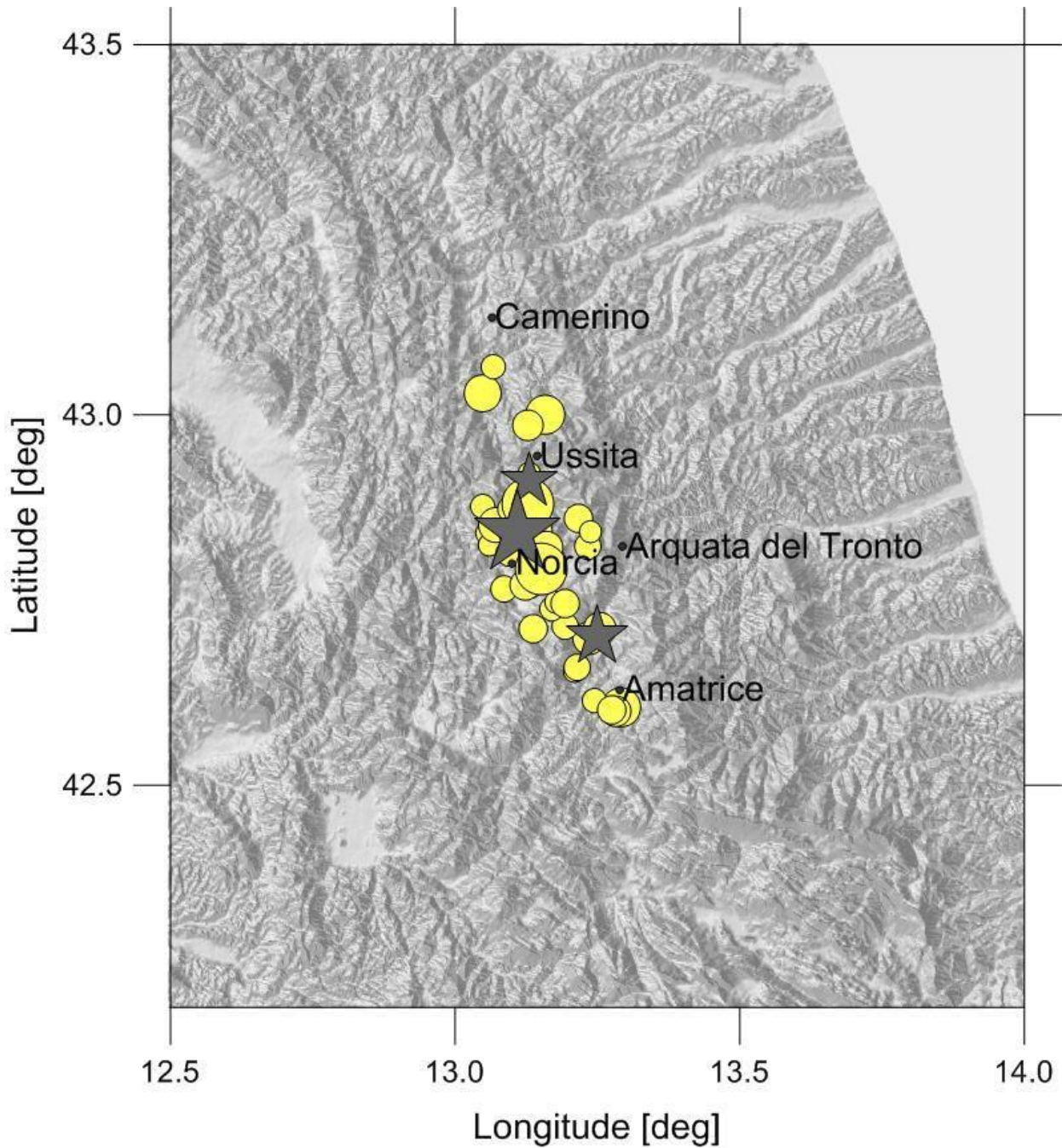


Figure 4.2: Epicenters of the events with $M \geq 4.0$ in period time from 24-08-2016 to 3-11-2016. The size of the symbols is proportional to the magnitude. The grey stars represent the three main-shocks: Amatrice, 24-08-2016, Mw 6.0; Ussita, 28-10-2016, Mw 5.9 and Norcia, 30-10-2016, Mw 6.5 (coordinates from <http://cnt.rm.ingv.it/>).

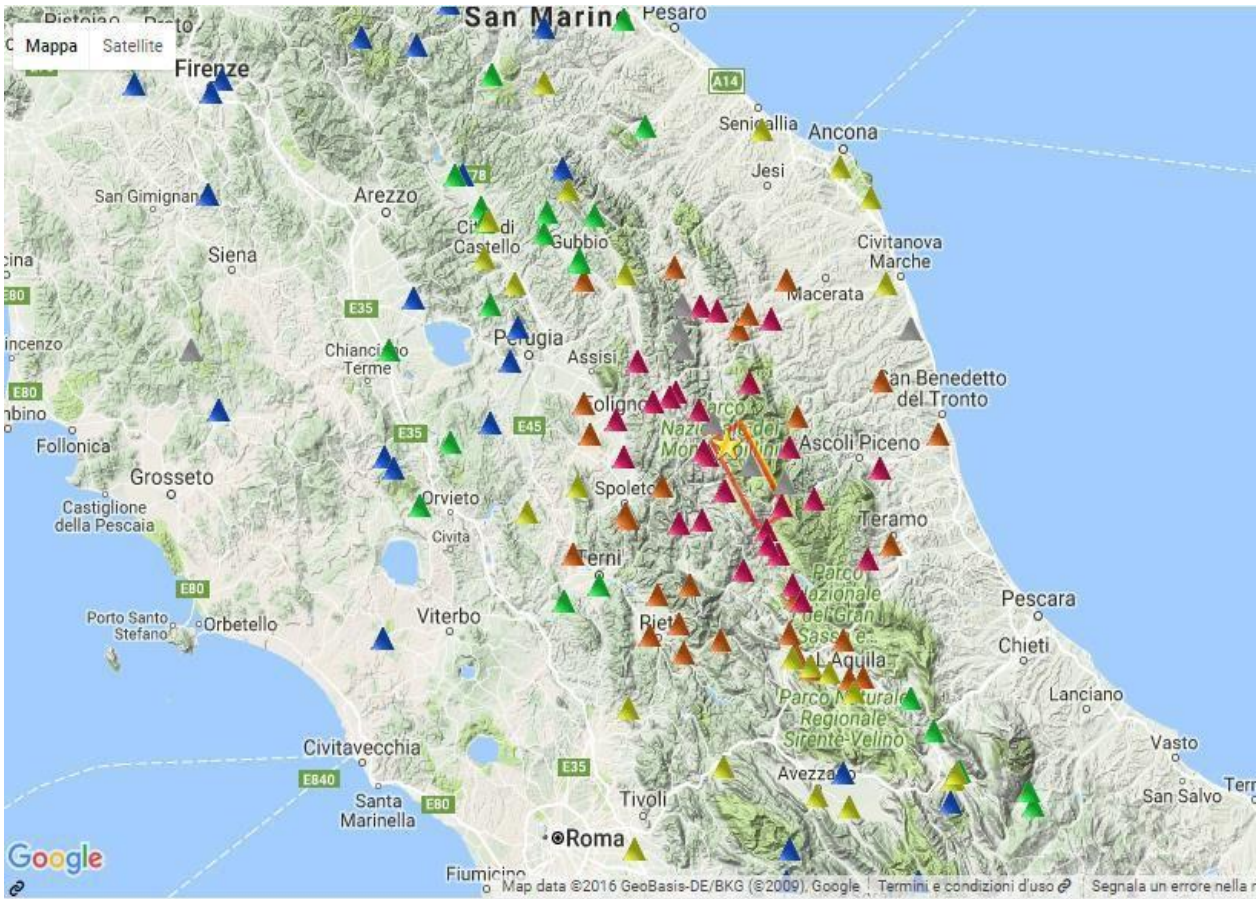


Figure 4.3. Location of the epicenters (yellow star) and strong motion stations within 150 km from the epicenter of a) 2016-08-24 Mw 6.0; b) 2016-10-26 Mw 5.9; c) 2016-10-30 Mw 6.5. The triangles indicate strong-motion stations and the colors correspond to the PGA values (gal). The red boxes are the surface fault projections: the fault geometries are preliminary for the Ussita and Norcia events.



A map of the various epicenters along with the stations for which notable pulses we detected in the strike-normal (fault-normal, FN) component, can be seen in Figure 4.4 (note that no impulsive ground motions were detected in the case of the 26/10/2016 Mw5.9 shock).

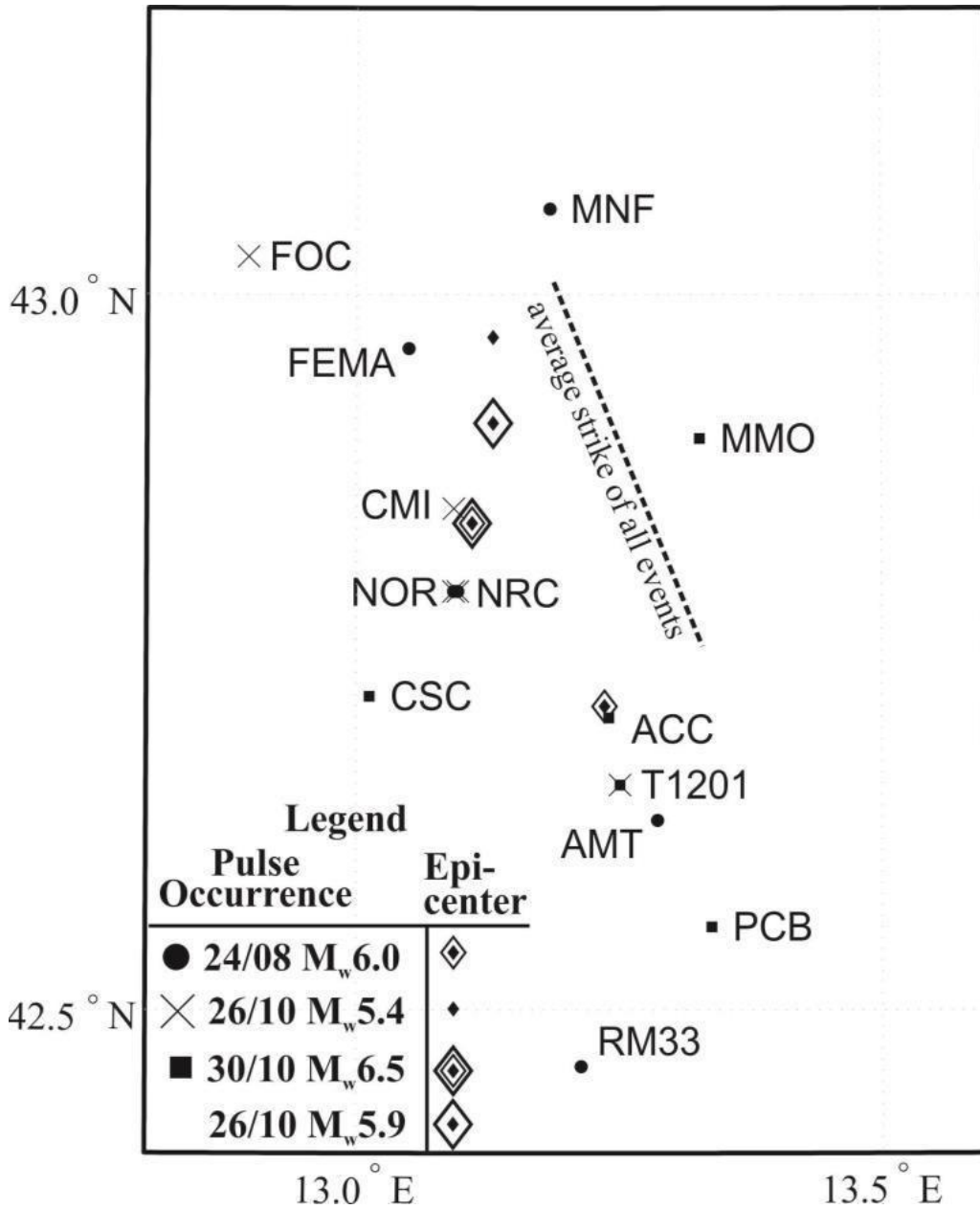


Figure 5.4. Surface projection of rupture plane; province borders and some NS stations shown on the map.

Out of all the records investigated belonging to the 24/08/2016 Mw6.0 shock, the six ground motions recorded at Amatrice (AMT), Norcia (NRC), Norcia Le Castellina (NOR), Montreal (RM33), Monte Fema (FEMA) and Fiastra (MNF) exhibited impulsive characteristics over a multitude of orientations, as expressed by a Pulse Indicator (PI) score in excess of 0.85 (see Baker, 2007). The record at Amatrice revealed two distinct pulses, one being predominant in the fault-normal (FN) and the other longer pulse in the fault-parallel (FP) direction. The FN pulse has a pulse period T_p of 0.40s while the FP 0.98s. The Norcia record on the other hand was found to contain a 2.09s period pulse mostly towards orientations that lie between the FN and FP without being decidedly prevalent in any of the perpendicular/parallel directions to the strike. Note that some deviation of directivity pulses from the strictly FN orientation is not unheard of in dip-slip faulting. Finally, the ground motions recorded at the stations of Fiastra and Montreal were found to contain pulses in the FN direction with T_p of 1.4s and 1.2s respectively, also hinting at rupture directivity effects, despite the lower velocity amplitude due to the greater distance from the fault and consequent attenuation.

In the following Figures, a polar plot is presented for each station displaying the PI score per azimuth as well as the velocity time histories at the most relevant directions (original signal and extracted pulse superimposed).

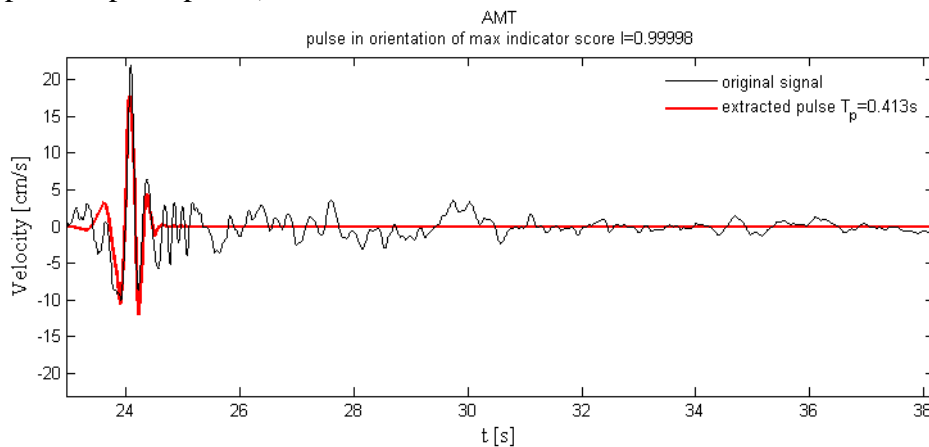


Figure 5.5 Original velocity time-history and CWT extracted pulse and residual signal for the fault-normal component of the Amatrice record - 24/08/2016 Mw6.0 event.

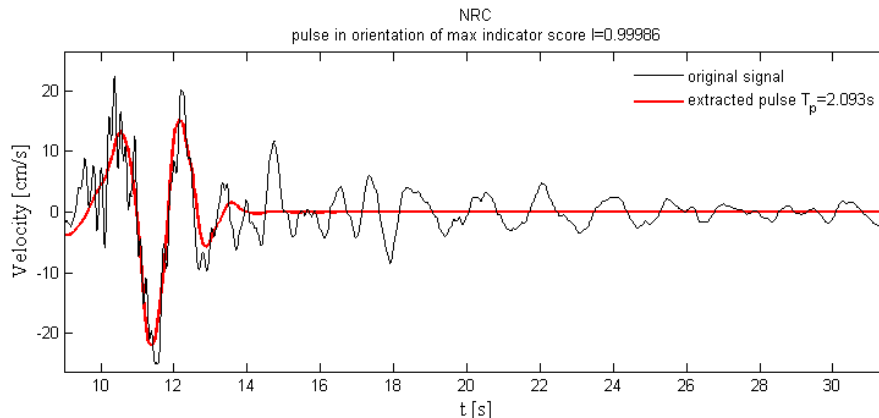


Figure 5.6 Original velocity time-history and CWT extracted pulse and residual signal for the fault-normal component of the Norcia (NRC) record - 24/08/2016 Mw6.0 event.

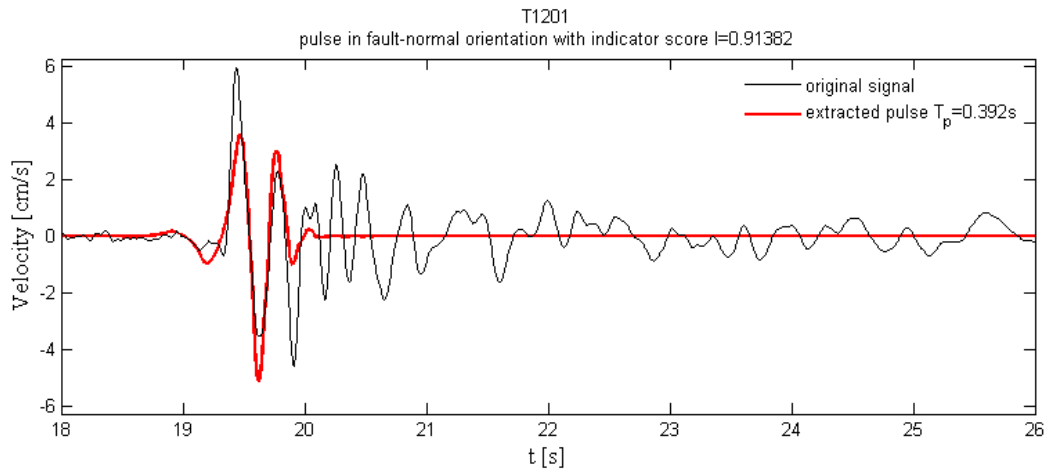


Figure 5.7 Original velocity time-history and CWT extracted pulse and residual signal for the fault-normal component of the mobile station T1201 record - 26/10/2016 Mw5.4 event.

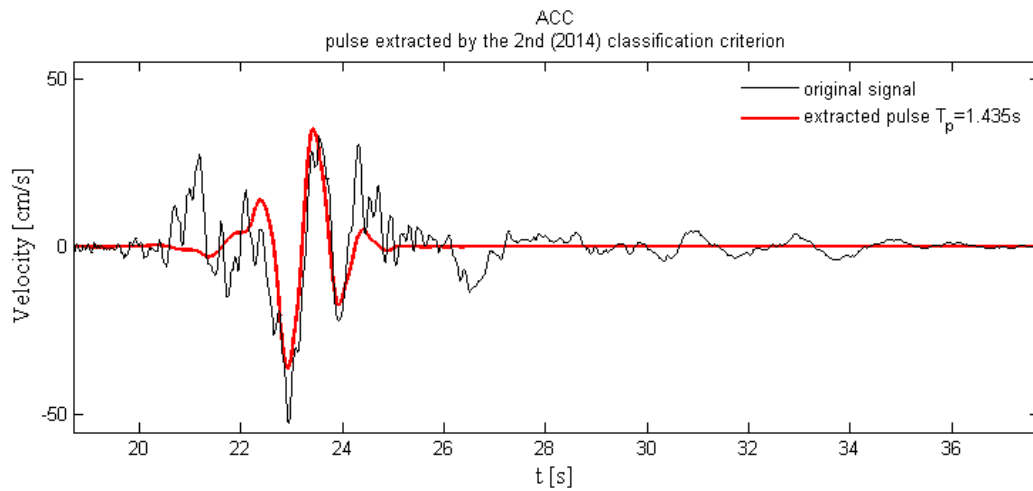


Figure 5.8 Original velocity time-history and CWT extracted pulse and residual signal for the quasi-fault-normal component of the Accumoli record - 30/10/2016 Mw6.5 event.



CHAPTER 6 DATA ANALYSIS AND RESULTS

NONLINEAR time history analyses

Fifty records from the PEER NGA database 7 that were classified as pulse-like by Baker were applied for the inelastic time history analyses of the five structures described above.

The characteristics of the selected earthquakes are shown in the table

No	NGA No.	Event	Year	Station	T_p (sec)	A (cm/sec ²)	γ	ν (°)	t_d (sec)
1	150	Coyote Lake	1979	Gilroy Array #6	0.94	44.94	1.6	355	1.93
2	158	Imperial Valley-06	1979	Aeropuerto Mexicali	1.64	46.78	2.1	345	3.64
3	159	Imperial Valley-06	1979	Agrarias	1.90	44.04	2.0	25	5.87
4	161	Imperial Valley-06	1979	Brawley Airport	4.78	48.66	1.1	100	5.47
5	170	Imperial Valley-06	1979	EC County Center FF	4.17	52.27	1.5	130	3.77
6	171	Imperial Valley-06	1979	EC Meloland Overpass FF	3.01	114.85	1.4	0	2.86
7	173	Imperial Valley-06	1979	El Centro Array #10	6.08	58.79	1.1	140	3.66
8	174	Imperial Valley-06	1979	El Centro Array #11	6.39	18.55	2.9	245	0.60
9	178	Imperial Valley-06	1979	El Centro Array #3	5.55	39.65	1.2	180	5.00
10	179	Imperial Valley-06	1979	El Centro Array #4	4.32	71.39	1.9	125	2.00
11	180	Imperial Valley-06	1979	El Centro Array #5	3.79	86.02	1.8	135	3.37
12	181	Imperial Valley-06	1979	El Centro Array #6	3.94	97.47	1.9	85	2.62
13	182	Imperial Valley-06	1979	El Centro Array #7	3.44	74.50	2.2	45	2.52
14	183	Imperial Valley-06	1979	El Centro Array #8	5.08	69.50	1.1	80	3.37
15	184	Imperial Valley-06	1979	El Centro Differential Array	5.86	60.43	1.1	70	2.66
16	185	Imperial Valley-06	1979	Holtville Post Office	4.24	47.52	1.7	175	3.35
17	250	Mammoth Lakes-06	1980	Long Valley Dam (Upr L Abut)	1.14	34.99	1.4	300	4.59
18	292	Irpinia, Italy-01	1980	Sturmo	2.64	23.95	5.6	110	1.13
19	316	Westmorland	1981	Parachute Test Site	3.00	25.91	2.2	300	7.54
20	407	Coalinga-05	1983	Oil City	0.56	35.39	3.4	0	2.22
21	415	Coalinga-05	1983	Transmitter Hill	0.75	44.06	3.2	310	2.00
22	418	Coalinga-07	1983	Coalinga-14th & Elm (Old CHP)	0.38	44.60	1.5	135	2.54
23	451	Morgan Hill	1984	Coyote Lake Dam (SW Abut)	0.77	42.78	4.2	300	2.30
24	459	Morgan Hill	1984	Gilroy Array #6	1.17	31.87	2.6	235	4.45
25	503	Taiwan SMART1(40)	1986	SMART1 C00	1.49	29.00	2.1	215	5.91
26	508	Taiwan SMART1(40)	1986	SMART1 M07	1.39	35.07	2.1	215	10.29
27	529	N. Palm Springs	1986	North Palm Springs	1.44	56.48	1.5	345	1.80
28	568	San Salvador	1986	GeotechInvestig Center	0.70	68.43	2.2	190	0.63
29	615	Whittier Narrows-01	1987	Downey - Co MaintBldg	0.81	27.35	2.5	260	4.36
30	645	Whittier Narrows-01	1987	LB - Orange Ave	0.78	30.64	2.4	255	5.10
31	738	Loma Prieta	1989	Alameda Naval Air Stn Hanger	2.31	48.18	2.3	1.1	10.87
32	766	Loma Prieta	1989	Gilroy Array #2	1.54	28.64	4.8	270	1.16
33	802	Loma Prieta	1989	Saratoga - Aloha Ave	6.48	36.31	1.2	180	3.10
34	821	Erzincan, Turkey	1992	Erzincan	2.42	89.81	1.7	20	1.58
35	828	Cape Mendocino	1992	Petrolia	2.74	57.86	1.5	325	1.13
36	838	Landers	1992	Barstow	7.57	22.97	1.7	135	11.2
37	879	Landers	1992	Lucerne	4.57	96.72	1.6	65	7.03
38	900	Landers	1992	Yermo Fire Station	8.73	56.46	1.1	160	13.28
39	982	Northridge-01	1994	Jensen Filter Plant	2.94	60.02	3.0	285	0.00
40	983	Northridge-01	1994	Jensen Filter Plant Generator	2.94	60.02	3.0	285	0.00
41	1009	Northridge-01	1994	LA-Wadsworth VA Hospital North	2.35	41.98	1.1	110	8.16
42	1013	Northridge-01	1994	LA Dam	2.17	76.26	1.1	220	1.78
43	1045	Northridge-01	1994	Newhall - W Pico Canyon Rd.	2.39	117.85	1.2	290	3.82
44	1050	Northridge-01	1994	Pacoima Dam (downstr)	3.37	11.71	3.2	25	0.04
45	1051	Northridge-01	1994	Pacoima Dam (upper left)	0.90	100.31	1.6	255	3.26
46	1063	Northridge-01	1994	Rinaldi Receiving Station	1.11	132.51	1.9	240	1.55
47	1085	Northridge-01	1994	Sylmar - Converter Station East	3.06	89.17	1.6	175	1.15
48	1086	Northridge-01	1994	Sylmar - Olive View Med FF	2.56	61.88	3.6	355	0.37
49	1119	Kobe, Japan	1995	Takarazuka	1.23	55.97	2.3	145	3.82
50	1161	Kocaeli, Turkey	1999	Gebze	4.88	42.18	1.8	190	3.37

Table 6.1. Pulse-like ground motions normal to the fault component characteristics.



Methodology

Using Seismostruct software a nonlinear time history analysis has been performed for 16 near field records to obtain the displacement time history of an existing building in Athens. These 16 records are originally obtained from 8 stations, 4 accelerograms in each of Norcia and Aquila regions, each accelerogram gives 2 components the East-west and the North-south which are illustrated below as Data1 represent the original record with long duration and DataQ represent the pulses record with short duration.

Results arising from applying these “near-fault” ground motion records to the building are obtained, these results indicates the top floor displacement that the building undergoes due to that certain ground motion record divided by the total building height representing the inter storey drift ratio.

The ground motions under investigation have an input parameter of time step size 0.01 sec, the total number of output time step ranges between 3000 to 5000 (30 sec to 50 sec) depending on the length of the accelerogram. All accelerograms are applied in positive X with a damping ratio near to 5%.

These results are represented in the form of plots followed by tables for each earthquake showing the maximum displacement of the original ground motions vs the displacement of pulses and interstorey drifts and base shears for original ground motion and pulses.

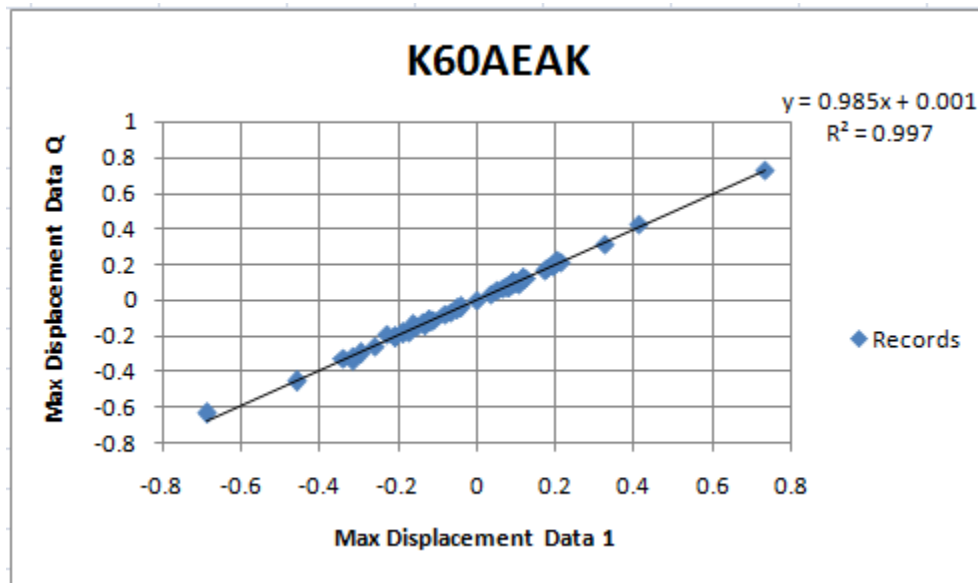


Figure 6.1 Maximum displacement of the original ground motions vs the displacement of pulses.



**Dynamic time history Results for the original building
Record 1**

Record No.(1)	Data1	DataQ
Time (Sec.)	3.89	2.09
Displacement at the top of building (m)	0.412	0.426

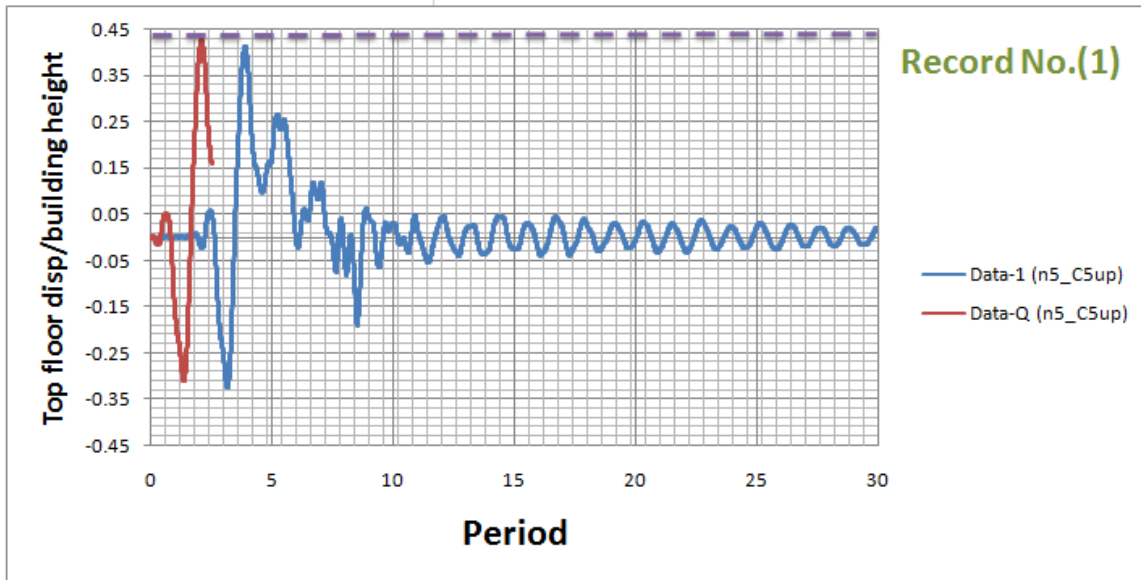


Figure 6.1. Maximum displacement of the original ground motions Data1 and the displacement of DataQ along height of the building.

Height of floor (m)	3				
Record No.(1)	Max. (Disp./height)	Drift (Disp./height)%			
Floor No.	Data1	DataQ	Data1	DataQ	
GF	0	0.000	0.000	0.000	0.000
1 st Floor	1	0.154	0.163	5.133	5.433
2 ^{sd} Floor	2	0.370	0.385	7.200	7.400
3 rd Floor	3	0.393	0.407	0.767	0.733
4 th Floor	4	0.405	0.419	0.400	0.400
5 th Floor	5	0.412	0.426	0.233	0.233

Record No.(1)	Shear Force (KN) for every floor		
Floor No.	Data1	DataQ	
GF	0	2122.294	2476.870
1 st Floor	1	2122.294	2476.870
2 ^{sd} Floor	2	1756.682	1746.714
3 rd Floor	3	1120.154	1065.686
4 th Floor	4	706.482	693.132
5 th Floor	5	262.906	232.290

Table 6.2. Table Maximum Displacement and inter storey drifts and shear force for every floor Vs along of the height of Building for recording Data1&DataQ

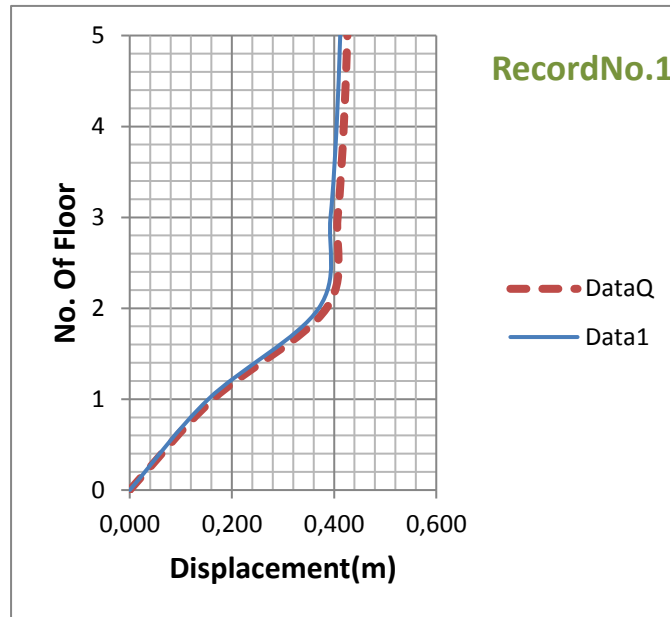


Figure 6.2. Profile of displacements for every floor along of the height of Building.

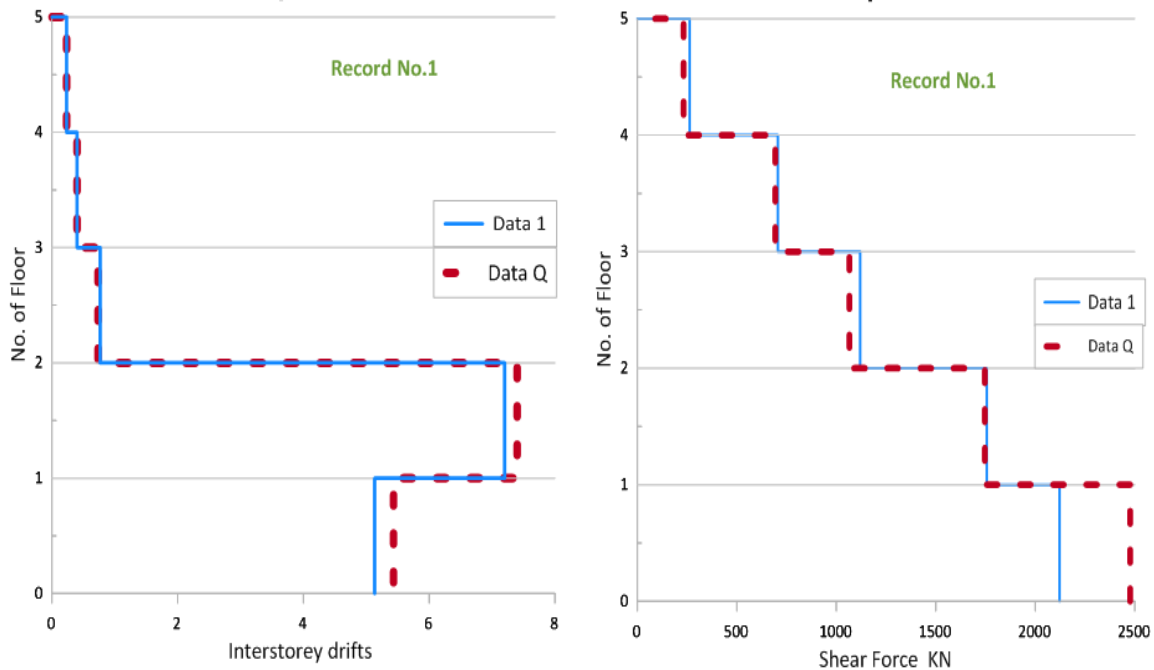


Figure 6.3. Profile of inter storey drifts and shear force for every floor Vs along of the height of Building.



Record 2

Record No.(2)	Data1	DataQ
Time (Sec.)	3.13	1.19
Displacement at the top of building (m)	0.176	0.176

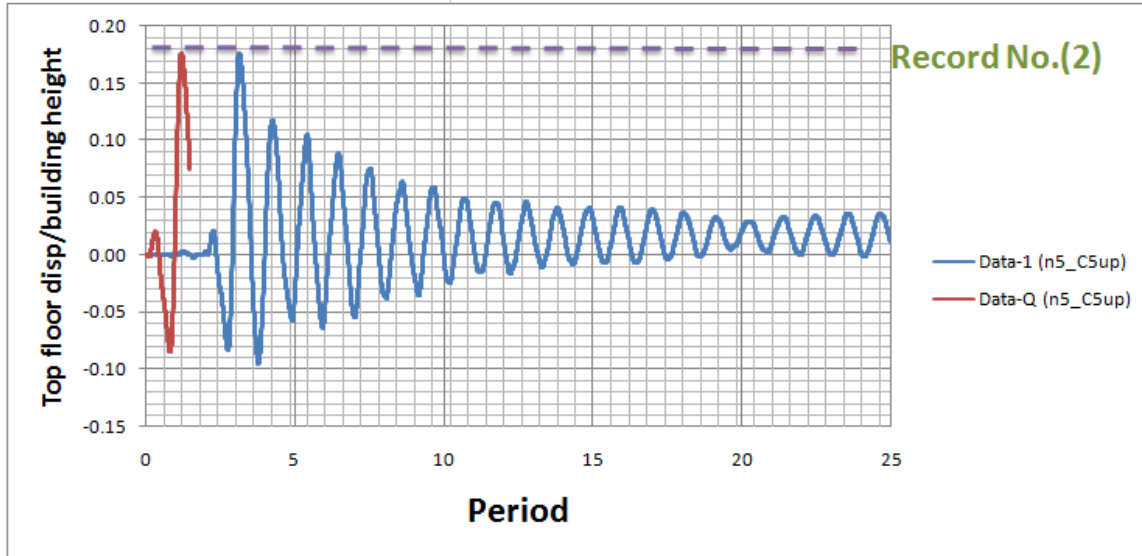


Figure 6.4. Maximum displacement of the original ground motions Data1 and the displacement of DataQ along height of the building.

Height of floor (m)		3			
Record No.(2)		Max. (Disp./height)		Drift (Disp./height)%	
Floor No.		Data1	DataQ	Data1	DataQ
GF	0	0.000	0.000	0.000	0.000
1 st Floor	1	0.032	0.032	1.067	1.067
2 ^{sd} Floor	2	0.096	0.098	2.133	2.200
3 rd Floor	3	0.139	0.140	1.433	1.400
4 th Floor	4	0.159	0.159	0.667	0.633
5 th Floor	5	0.176	0.176	0.567	0.567

Record No.(2)		Shear Force (KN) for every floor	
Floor No.		Data1	DataQ
GF	0	3194.032	3195.812
1 st Floor	1	3194.032	3195.812
2 ^{sd} Floor	2	2095.416	2100.756
3 rd Floor	3	1894.454	1899.082
4 th Floor	4	1236.388	1253.298
5 th Floor	5	542.366	554.114

Table 6.3. Table Maximum Displacement and inter storey drifts and shear force for every floor Vs along of the height of Building for recording Data1&DataQ

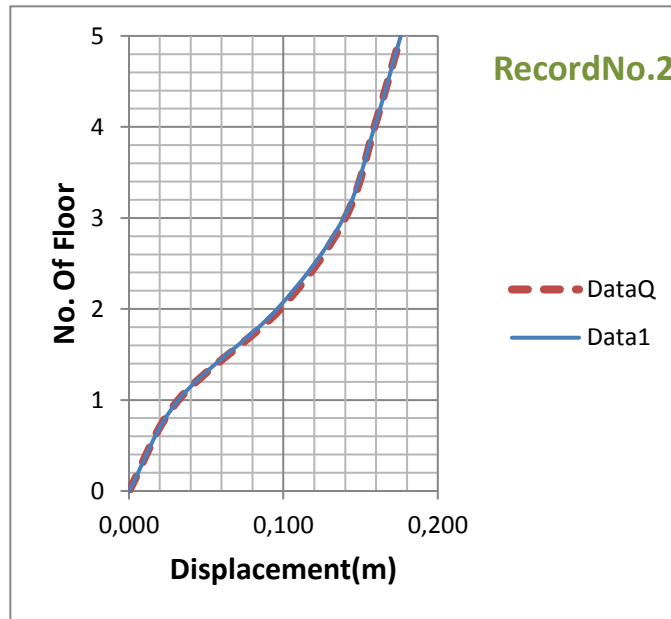


Figure 6.5. Profile of displacements for every floor along of the height of Building.

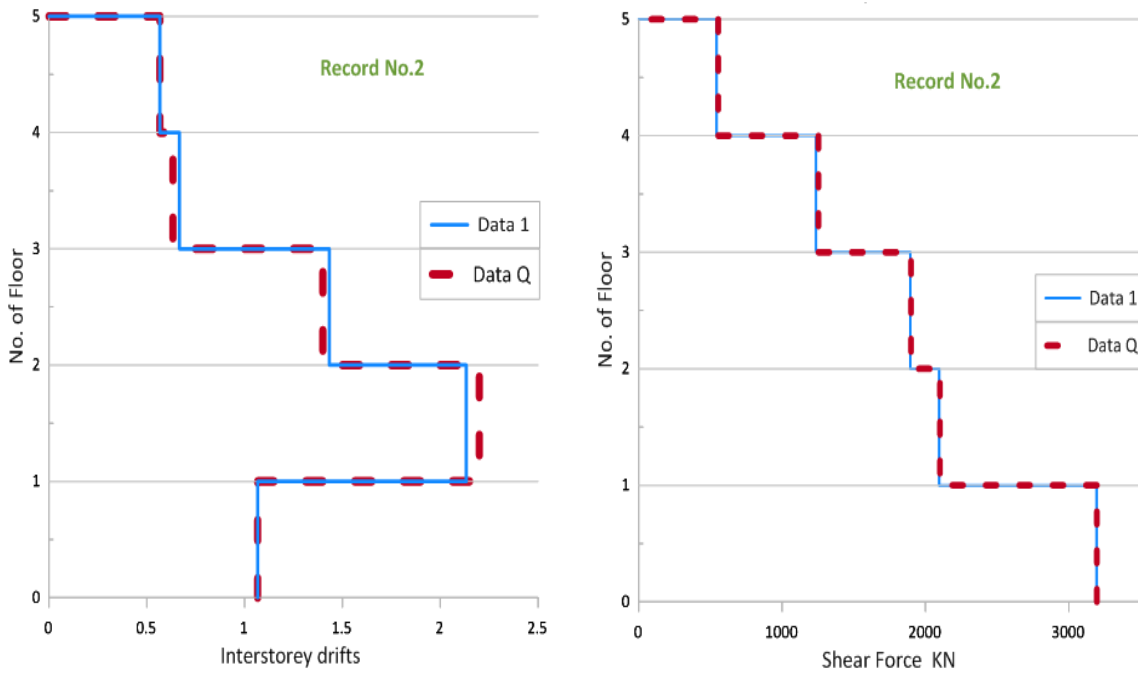


Figure 6.6. Profile of inter storey drifts and shear force for every floor Vs along of the height of Building.



Record 3

Record No.(3)	Data1	DataQ
Time (Sec.)	9.14	2.93
Displacement at the top of buliding (m)	0.105	0.091

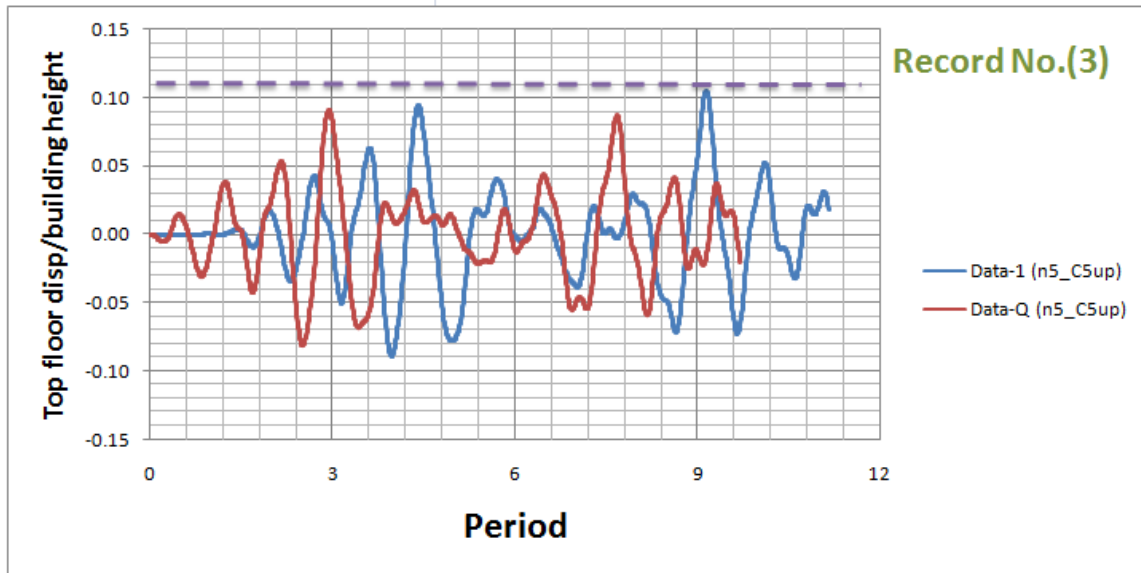


Figure 6.7. Maximum displacement of the original ground motions Data1 and the displacement of DataQ along height of the building.

Height of floor (m)	3				
Record No.(3)	Max. (Disp./height)	Drift (Disp./height)%			
Floor No.	Data1	DataQ	Data1	DataQ	
GF	0	0.000	0.000	0.000	0.000
1 st Floor	1	0.019	0.015	0.633	0.500
2 ^{sd} Floor	2	0.046	0.039	0.900	0.800
3 rd Floor	3	0.066	0.059	0.667	0.667
4 th Floor	4	0.085	0.075	0.633	0.533
5 th Floor	5	0.105	0.091	0.667	0.533

Record No.(3)	Shear Force (KN) for every floor		
Floor No.	Data1	DataQ	
GF	0	2288.546	2396.948
1 st Floor	1	2288.546	2396.948
2 ^{sd} Floor	2	1613.570	1949.812
3 rd Floor	3	1565.866	1654.866
4 th Floor	4	1318.446	1164.654
5 th Floor	5	746.532	596.122

Table 6.4. Table Maximum Displacement and inter storey drifts and shear force for every floor Vs along of the height of Building for recording Data1&DataQ

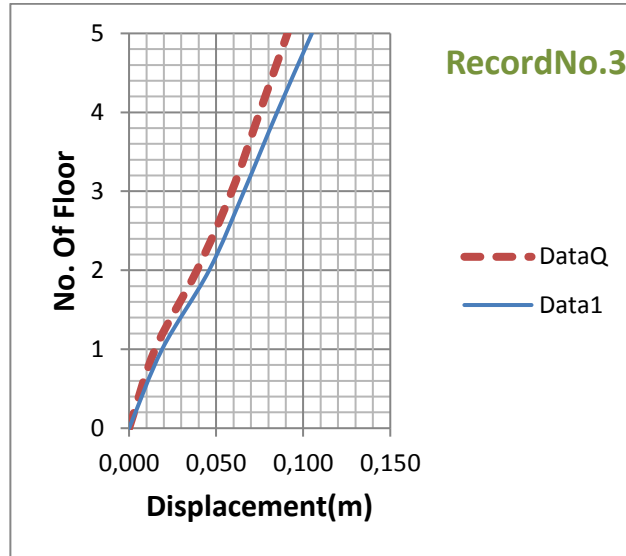


Figure 6.8. Profile of displacements for every floor along of the height of Building.

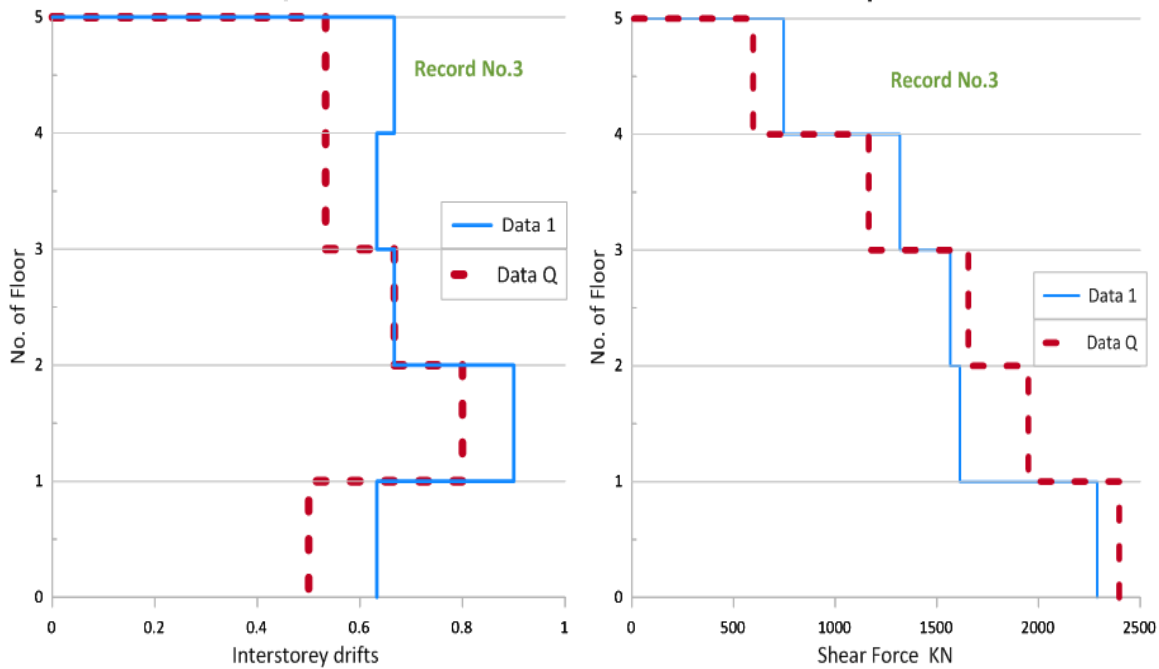


Figure 6.9. Profile of inter storey drifts and shear force for every floor Vs along of the height of Building.



Record 4

Record No.(4)	Data1	DataQ
Time (Sec.)	16.26	16.21
Displacement at the top of buliding (m)	0.033	0.033

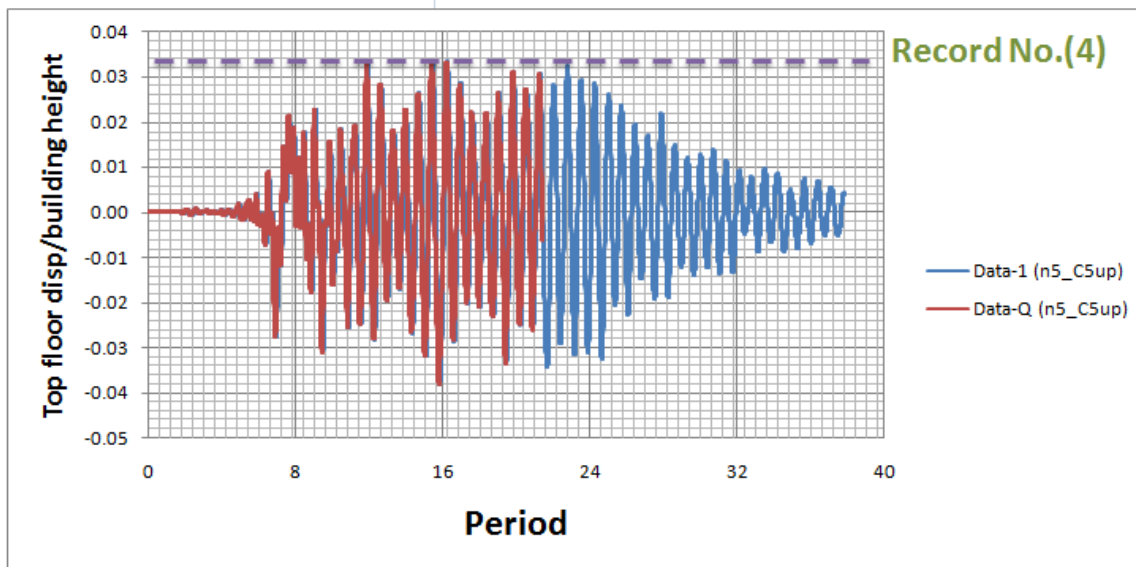


Figure 6.10. Maximum displacement of the original ground motions Data1 and the displacement of DataQ along height of the building.

Height of floor (m)		3			
Record No.(4)		Max. (Disp./height)		Drift (Disp./height)%	
Floor No.		Data1	DataQ	Data1	DataQ
GF	0	0.000	0.000	0.000	0.000
1 st Floor	1	0.005	0.005	0.167	0.167
2 ^{sd} Floor	2	0.014	0.014	0.300	0.300
3 rd Floor	3	0.021	0.021	0.233	0.233
4 th Floor	4	0.026	0.026	0.167	0.167
5 th Floor	5	0.033	0.033	0.233	0.233

Record No.(4)		Shear Force (KN) for every floor	
Floor No.		Data1	DataQ
GF	0	1033.824	1028.306
1 st Floor	1	1033.824	1028.306
2 ^{sd} Floor	2	905.486	898.544
3 rd Floor	3	728.376	729.800
4 th Floor	4	448.738	440.550
5 th Floor	5	291.920	292.454

Table 6.5 Table Maximum Displacement and inter storey drifts and shear force for every floor Vs along of the height of Building for recording Data1&DataQ

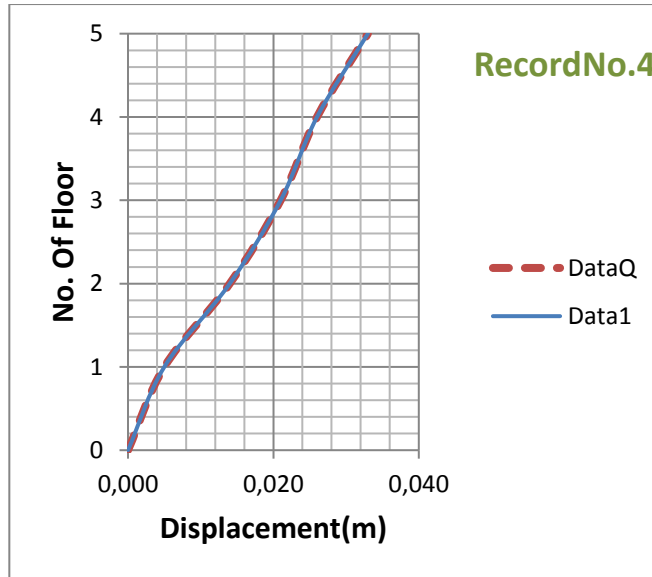


Figure 6.11. Profile of displacements for every floor along of the height of Building.

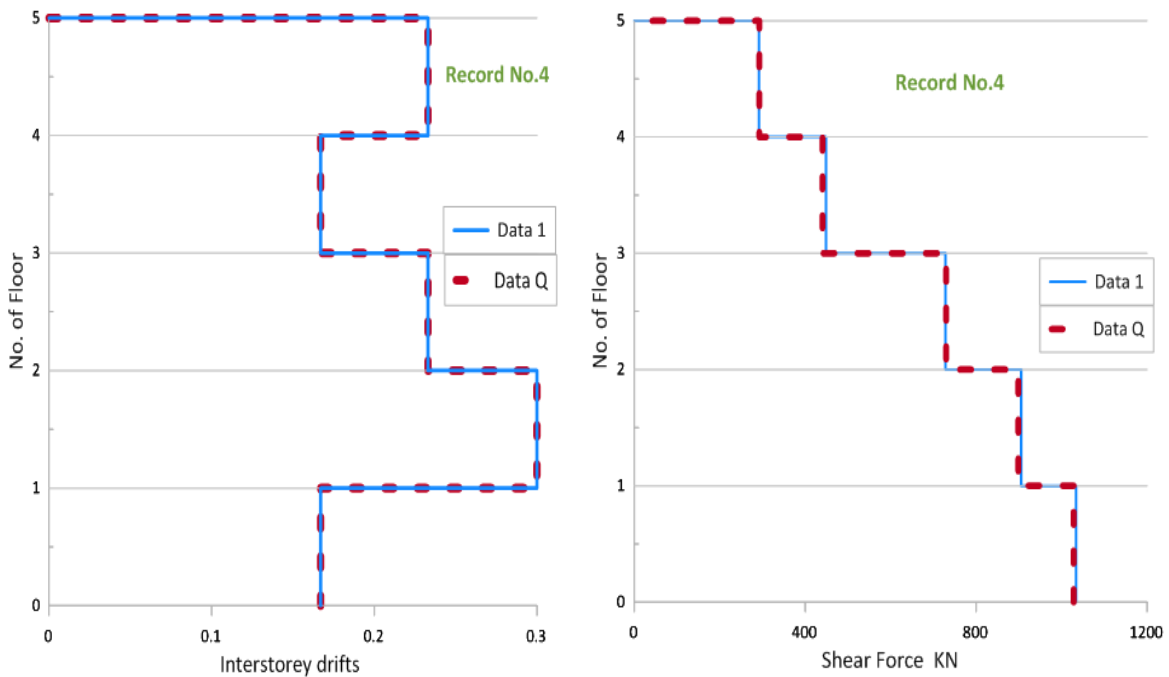


Figure 6.12. Profile of inter storey drifts and shear force for every floor Vs along of the height of Building.



Record 5

Record No.(5)	Data1	DataQ
Time (Sec.)	7.91	5.24
Displacement at the top of building (m)	-0.067	-0.068

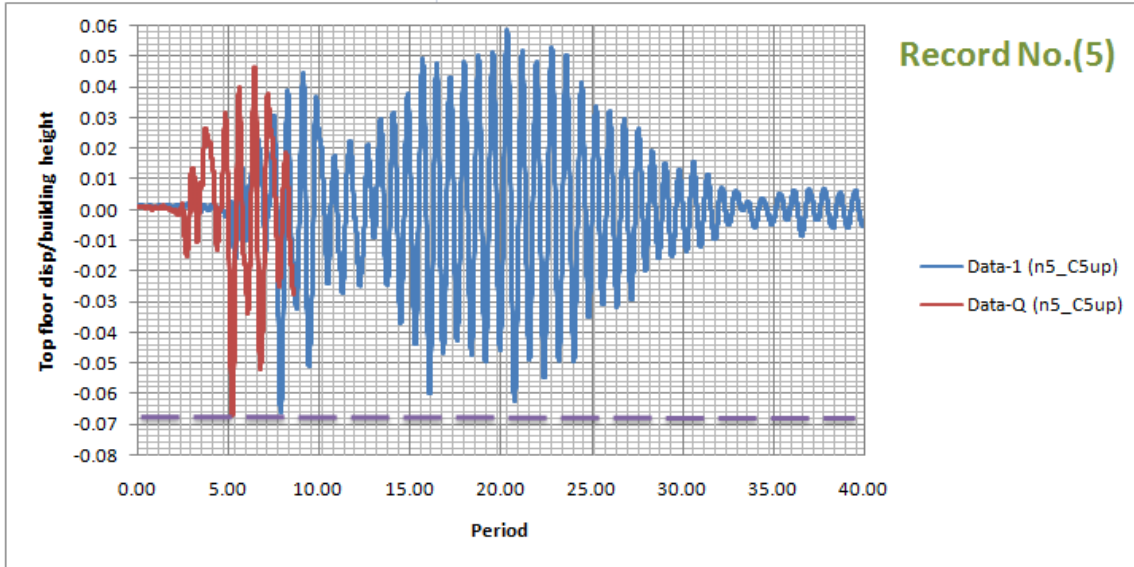


Figure 6.13. Maximum displacement of the original ground motions Data1 and the displacement of DataQ along height of the building.

Height of floor (m)		3			
Record No.(5)		Max. (Disp./height)		Drift (Disp./height)%	
Floor No.		Data1	DataQ	Data1	DataQ
GF	0	0.000	0.000	0.000	0.000
1 st Floor	1	0.011	0.011	0.367	0.367
2 ^{sd} Floor	2	0.029	0.029	0.600	0.600
3 rd Floor	3	0.046	0.046	0.567	0.567
4 th Floor	4	0.058	0.058	0.400	0.400
5 th Floor	5	0.067	0.068	0.300	0.333

Record No.(5)		Shear Force (KN) for every floor	
Floor No.		Data1	DataQ
GF	0	1865.974	1898.904
1 st Floor	1	1865.974	1898.904
2 ^{sd} Floor	2	1673.200	1674.980
3 rd Floor	3	1614.994	1623.894
4 th Floor	4	988.790	1030.620
5 th Floor	5	323.960	325.918

Table 6.6 Table Maximum Displacement and inter storey drifts and shear force for every floor Vs along of the height of Building for recording Data1&DataQ

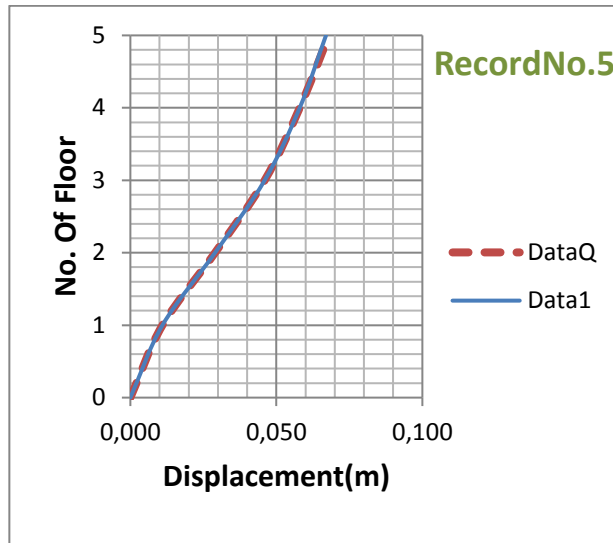


Figure 6.14. Profile of displacements for every floor along of the height of Building.

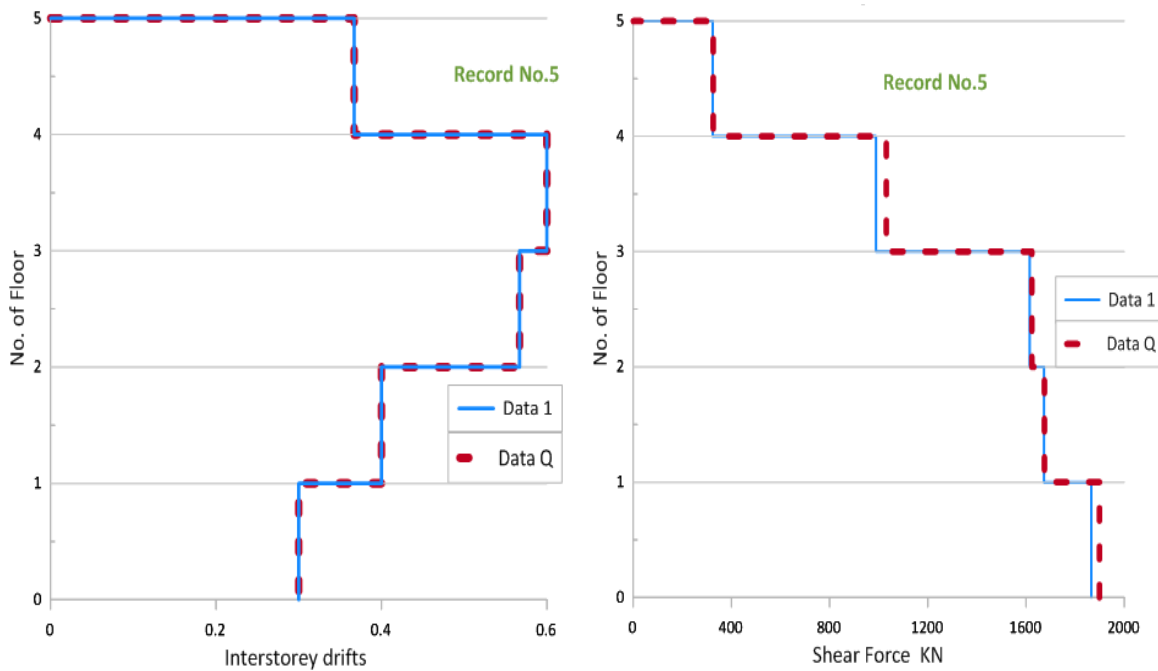


Figure 6.15. Profile of inter storey drifts and shear force for every floor Vs along of the height of Building.



Record 6

Record No.(6)	Data1	DataQ
Time (Sec.)	5.59	3.62
Displacement at the top of building (m)	0.192	0.191

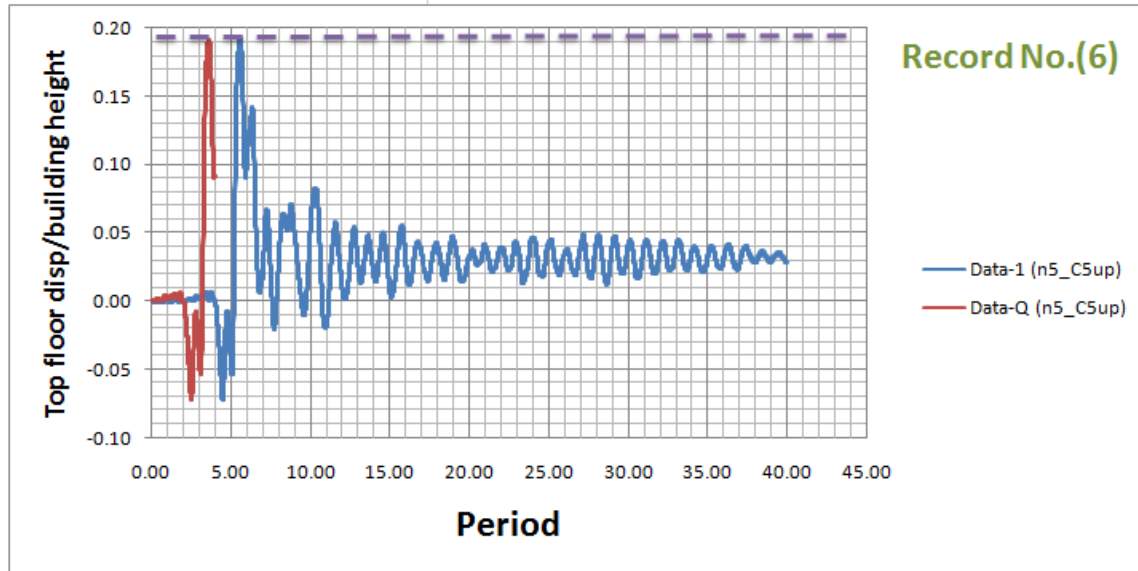


Figure 6.16. Maximum displacement of the original ground motions Data1 and the displacement of DataQ along height of the building.

Height of floor (m)	3				
Record No.(6)	Max. (Disp./height)	Drift (Disp./height)%			
Floor No.	Data1	DataQ	Data1	DataQ	
GF	0	0.000	0.000	0.000	0.000
1 st Floor	1	0.080	0.079	2.667	2.633
2 ^{sd} Floor	2	0.148	0.147	2.267	2.267
3 rd Floor	3	0.171	0.170	0.767	0.767
4 th Floor	4	0.182	0.182	0.367	0.400
5 th Floor	5	0.192	0.191	0.333	0.300

Record No.(6)	Shear Force (KN) for every floor		
Floor No.	Data1	DataQ	
GF	0	3019.770	3019.770
1 st Floor	1	3019.770	3019.770
2 ^{sd} Floor	2	1449.988	1450.522
3 rd Floor	3	919.014	917.056
4 th Floor	4	678.180	676.044
5 th Floor	5	201.496	201.140

Table 6.7 Table Maximum Displacement and inter storey drifts and shear force for every floor Vs along of the height of Building for recording Data1&DataQ

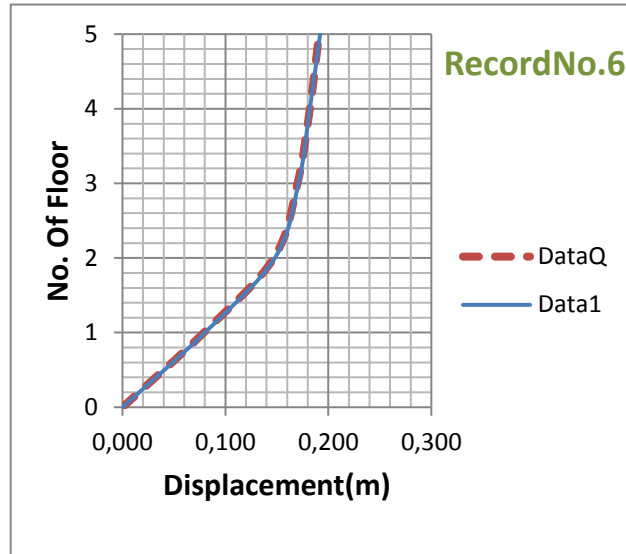


Figure 6.17. Profile of displacements for every floor along of the height of Building.

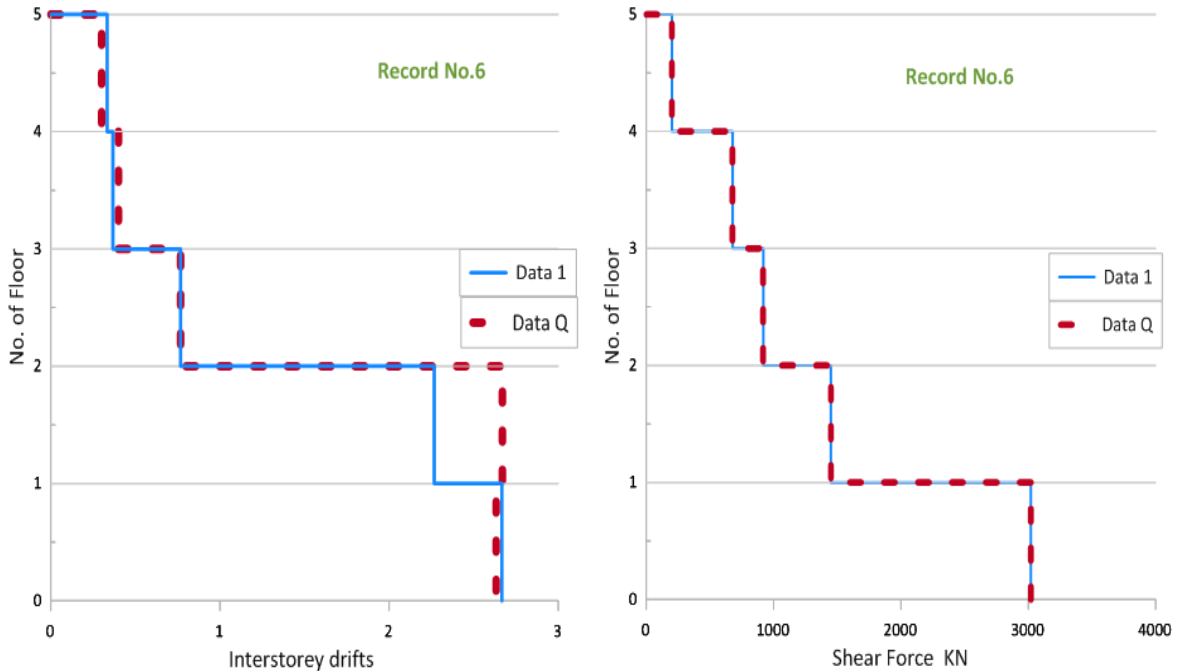


Figure 6.18. Profile of inter storey drifts and shear force for every floor Vs along of the height of Building.



Record 7

Record No.(7)	Data1	DataQ
Time (Sec.)	10.98	10.97
Displacement at the top of building (m)	-0.042	-0.042

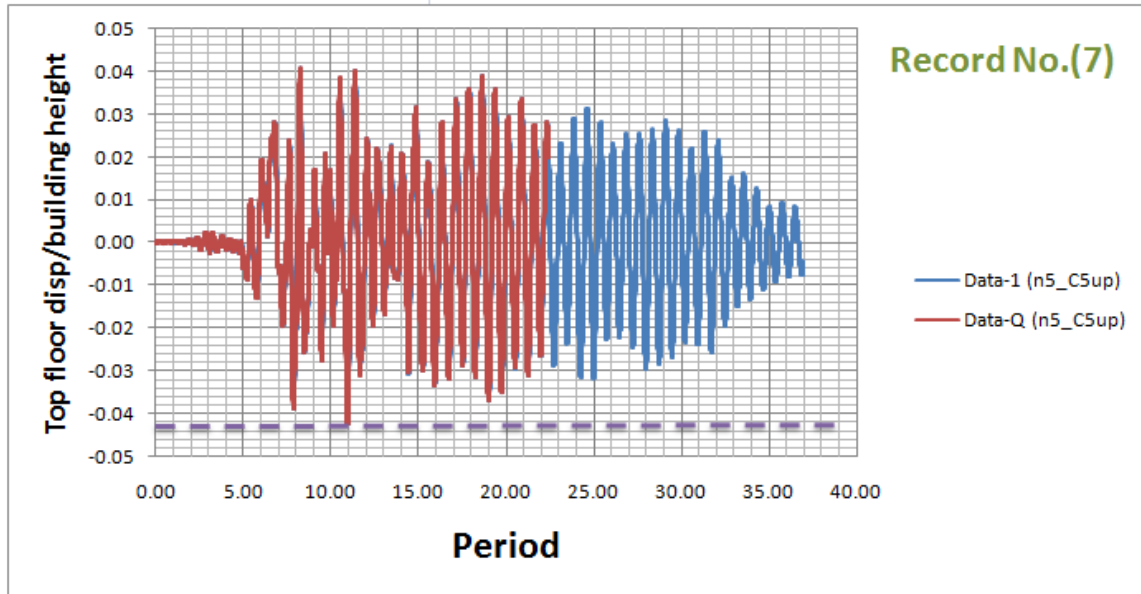


Figure 6.19. Maximum displacement of the original ground motions Data1 and the displacement of DataQ along height of the building.

Height of floor (m)		3			
Record No.(7)		Max. (Disp./height)		Drift(Disp./height)%	
Floor No.		Data1	DataQ	Data1	DataQ
GF	0	0.000	0.000	0.000	0.000
1 st Floor	1	0.002	0.002	0.067	0.067
2 ^{sd} Floor	2	0.007	0.007	0.167	0.167
3 rd Floor	3	0.016	0.015	0.300	0.267
4 th Floor	4	0.027	0.026	0.367	0.367
5 th Floor	5	0.041	0.040	0.467	0.467

Record No.(7)		Shear Force (KN) for every floor	
Floor No.		Data1	DataQ
GF	0	916.700	922.752
1 st Floor	1	916.700	922.752
2 ^{sd} Floor	2	721.078	739.768
3 rd Floor	3	633.680	631.010
4 th Floor	4	491.102	523.498
5 th Floor	5	329.300	342.650

Table 6.8 Table Maximum Displacement and inter storey drifts and shear force for every floor Vs along of the height of Building for recording Data1&DataQ

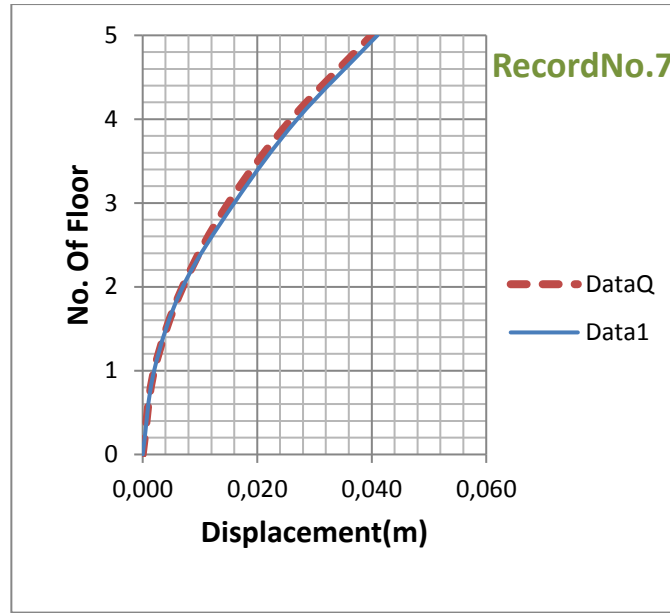


Figure 6.20. Profile of displacements for every floor along of the height of Building.

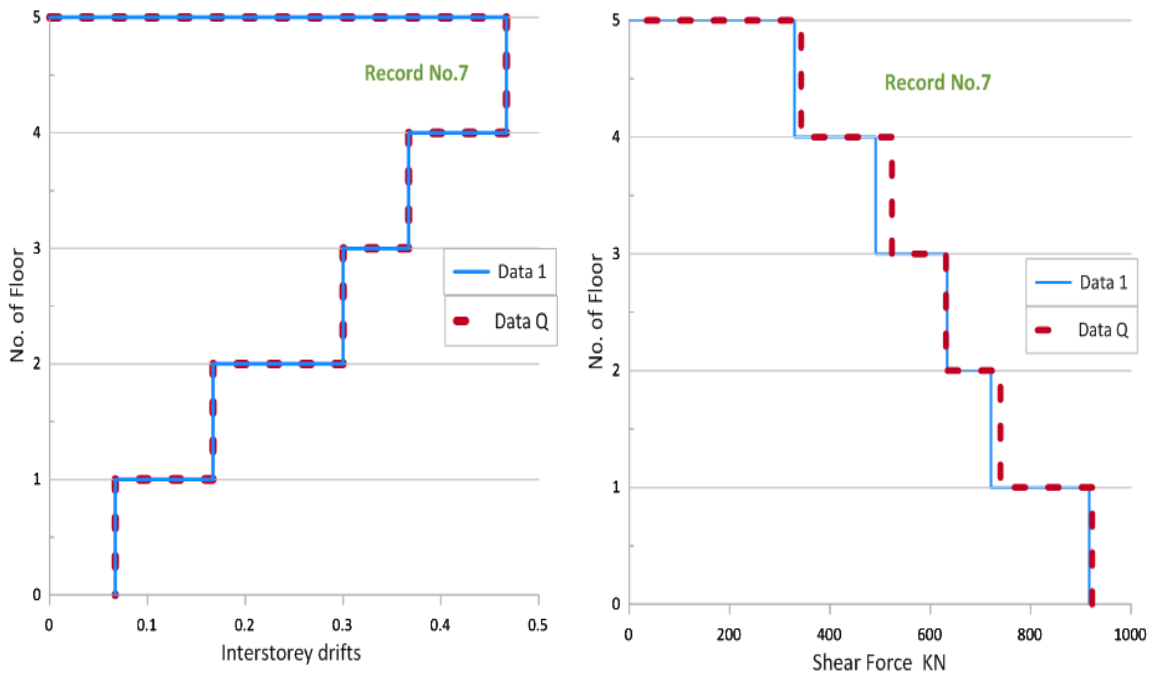


Figure 6.21. Profile of inter storey drifts and shear force for every floor Vs along of the height of Building.



Record 8

Record No.(8)	Data1	DataQ
Time (Sec.)	10.48	10.47
Displacement at the top of building (m)	-0.12	-0.12

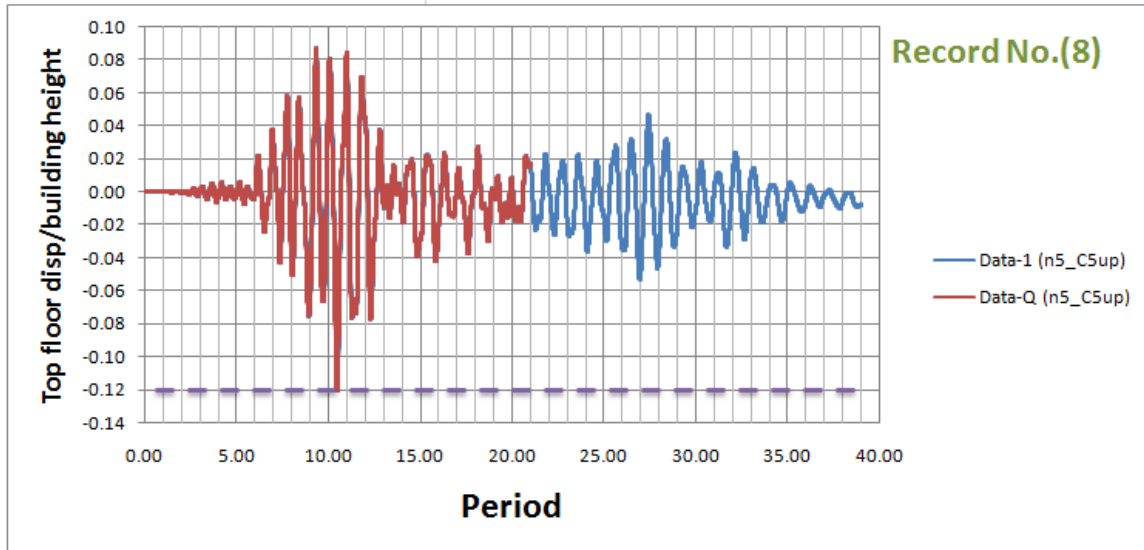


Figure 6.22. Maximum displacement of the original ground motions Data1 and the displacement of DataQ along height of the building.

Height of floor (m)		3			
Record No.(8)		Max. (Disp./height)		Drift (Disp./height)%	
Floor No.		Data1	DataQ	Data1	DataQ
GF	0	0.000	0.000	0.000	0.000
1 st Floor	1	0.018	0.018	0.600	0.600
2 ^{sd} Floor	2	0.055	0.055	1.233	1.233
3 rd Floor	3	0.075	0.075	0.667	0.667
4 th Floor	4	0.093	0.093	0.600	0.600
5 th Floor	5	0.120	0.120	0.900	0.900

Record No.(8)		Shear Force (KN) for every floor	
Floor No.		Data1	DataQ
GF	0	2210.048	2205.242
1 st Floor	1	2210.048	2205.242
2 ^{sd} Floor	2	2082.600	2082.600
3 rd Floor	3	1538.454	1537.208
4 th Floor	4	1389.646	1388.756
5 th Floor	5	839.270	839.270

Table 6.9 Table Maximum Displacement and inter storey drifts and shear force for every floor Vs along of the height of Building for recording Data1&DataQ

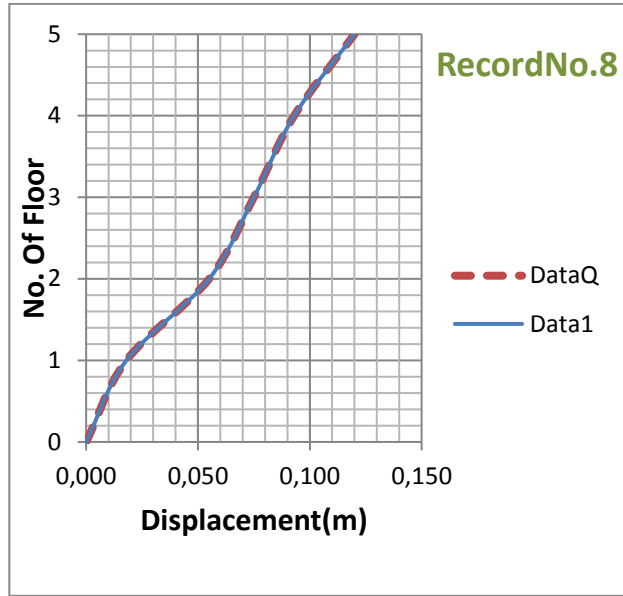


Figure 6.23. Profile of displacements for every floor along of the height of Building.

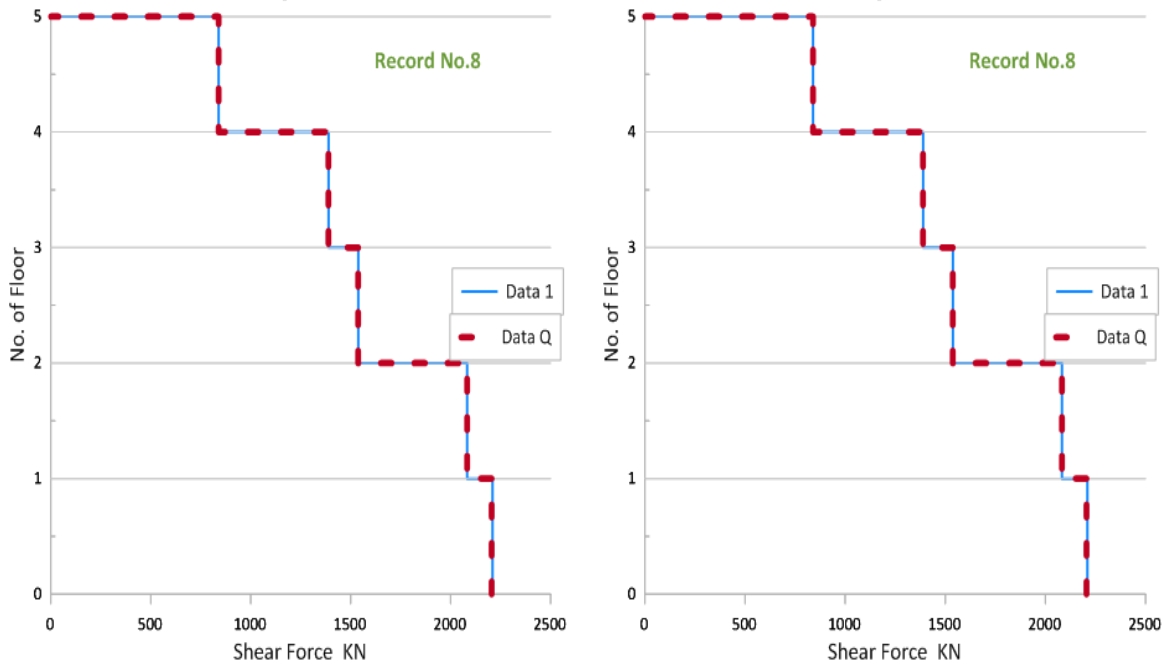


Figure 6.24 Profile of inter storey drifts and shear force for every floor Vs along of the height of Building.



Record 9

Record No.(9)	Data1	DataQ
Time (Sec.)	13.33	5.18
Displacement at the top of building (m)	0.053	0.051

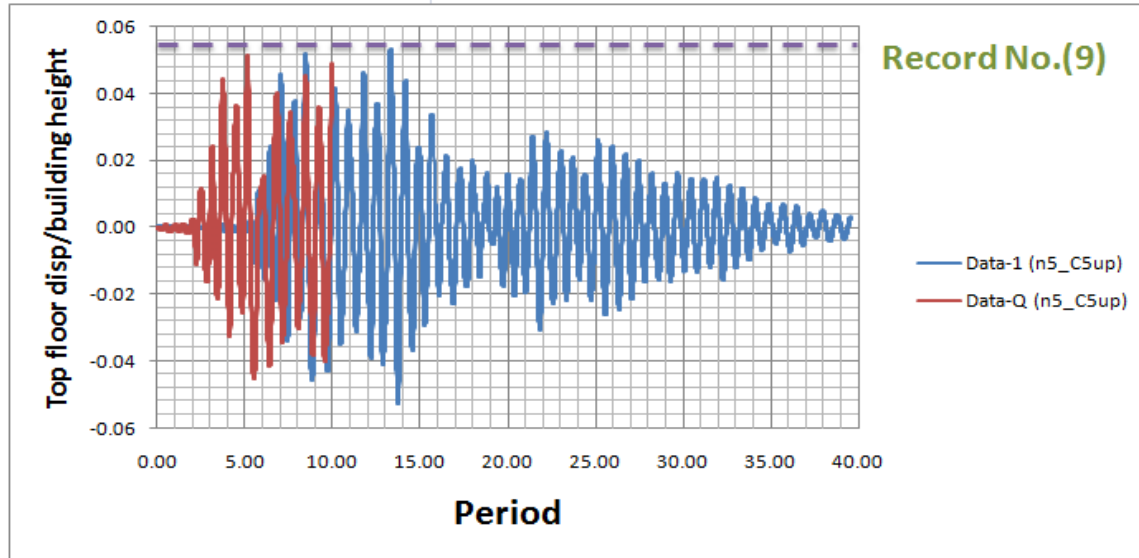


Figure 6.25. Maximum displacement of the original ground motions Data1 and the displacement of DataQ along height of the building.

Height of floor (m)		3			
Record No.(9)		Max. (Disp./height)		Drift(Disp./height)%	
Floor No.		Data1	DataQ	Data1	DataQ
GF	0	0.000	0.000	0.000	0.000
1 st Floor	1	0.007	0.006	0.233	0.200
2 ^{sd} Floor	2	0.018	0.017	0.367	0.367
3 rd Floor	3	0.029	0.024	0.367	0.233
4 th Floor	4	0.038	0.034	0.300	0.333
5 th Floor	5	0.053	0.051	0.500	0.567

Record No.(9)		Shear Force (KN) for every floor	
Floor No.		Data1	DataQ
GF	0	1224.996	1134.572
1 st Floor	1	1224.996	1134.572
2 ^{sd} Floor	2	1128.520	1051.802
3 rd Floor	3	1019.762	961.200
4 th Floor	4	669.458	748.134
5 th Floor	5	589.536	721.078

Table 6.10 Table Maximum Displacement and inter storey drifts and shear force for every floor Vs along of the height of Building for recording Data1&DataQ

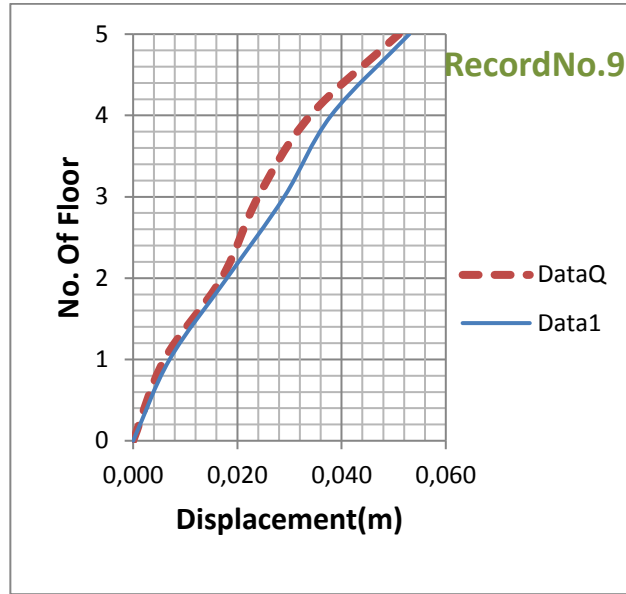


Figure 6.26. Profile of displacements for every floor along of the height of Building.

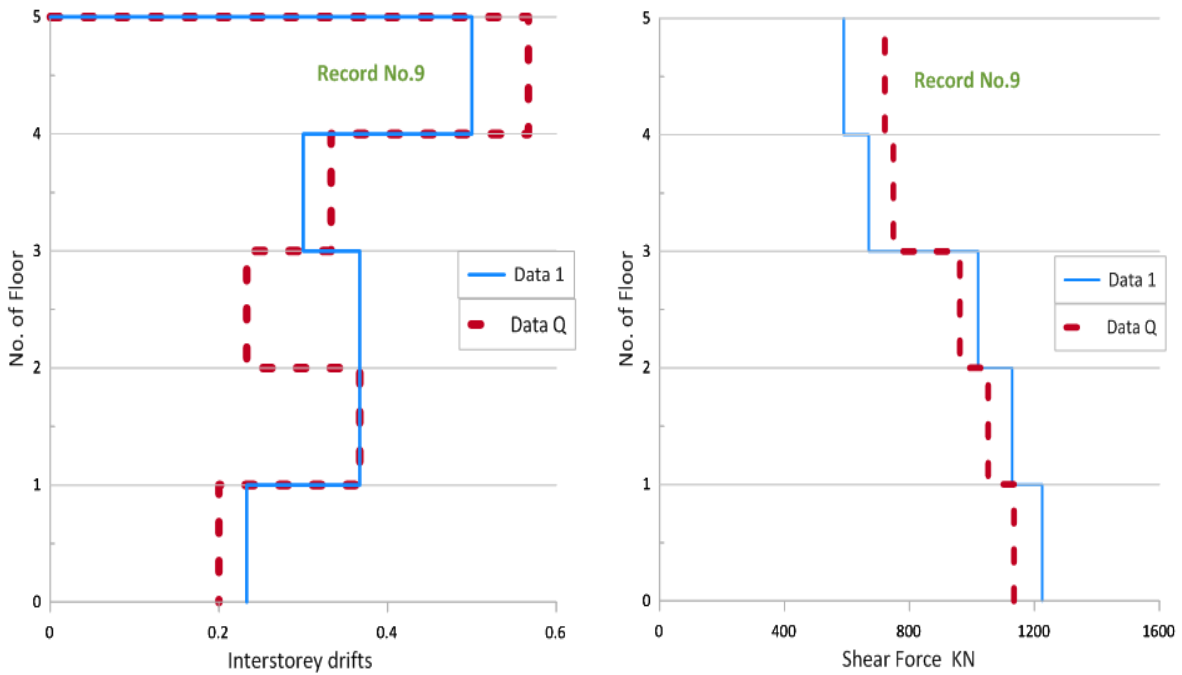


Figure 6.27 Profile of inter storey drifts and shear force for every floor Vs along of the height of Building.



Record 10

Record No.(10)	Data1	DataQ
Time (Sec.)	5.54	3.52
Displacement at the top of building (m)	0.092	0.093

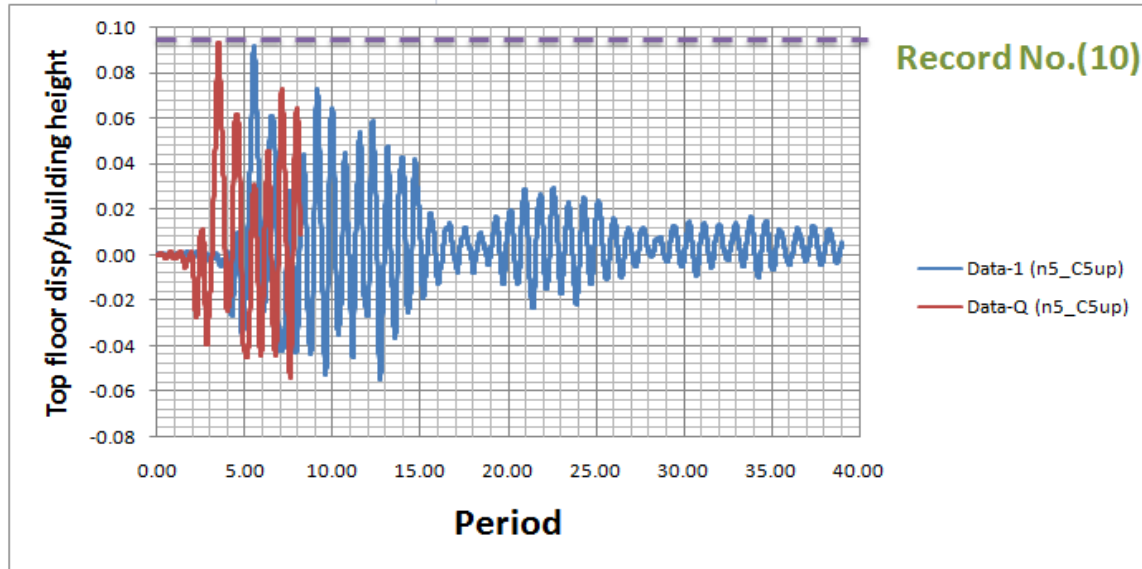


Figure 6.28. Maximum displacement of the original ground motions Data1 and the displacement of DataQ along height of the building.

Height of floor (m)		3			
Record No.(10)		Max.(Disp./height)		Drift(Disp./height)%	
Floor No.		Data1	DataQ	Data1	DataQ
GF	0	0.000	0.000	0.000	0.000
1 st Floor	1	0.022	0.023	0.733	0.767
2 ^{sd} Floor	2	0.046	0.047	0.800	0.800
3 rd Floor	3	0.063	0.064	0.567	0.567
4 th Floor	4	0.077	0.078	0.467	0.467
5 th Floor	5	0.092	0.093	0.500	0.500

Record No.(10)		Shear Force (KN) for every floor	
Floor No.		Data1	DataQ
GF	0	2743.870	2826.818
1 st Floor	1	2743.870	2826.818
2 ^{sd} Floor	2	1745.646	1727.312
3 rd Floor	3	1411.540	1381.458
4 th Floor	4	1046.462	1044.682
5 th Floor	5	579.212	577.254

Table 6.11 Table Maximum Displacement and inter storey drifts and shear force for every floor Vs along of the height of Building for recording Data1&DataQ

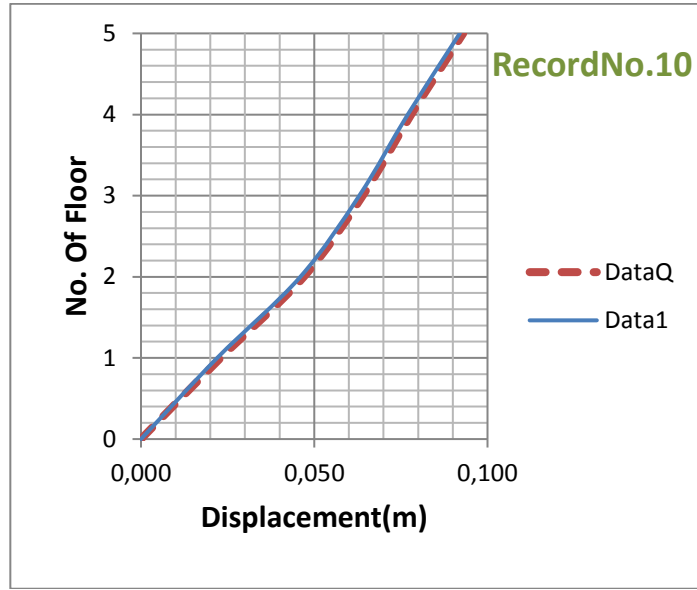


Figure 6.29. Profile of displacements for every floor along of the height of Building.

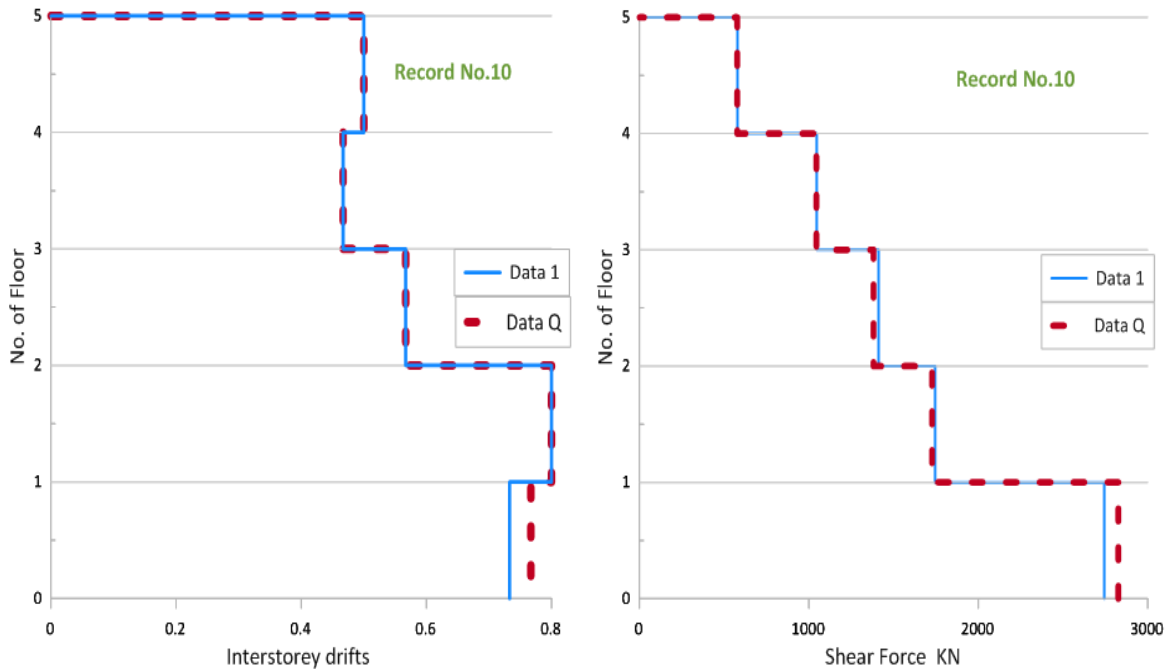


Figure 6.30. Profile of inter storey drifts and shear force for every floor Vs along of the height of Building.



Record 11

Record No.(11)	Data1	DataQ
Time (Sec.)	8.15	4.75
Displacement at the top of building (m)	-0.21	-0.21

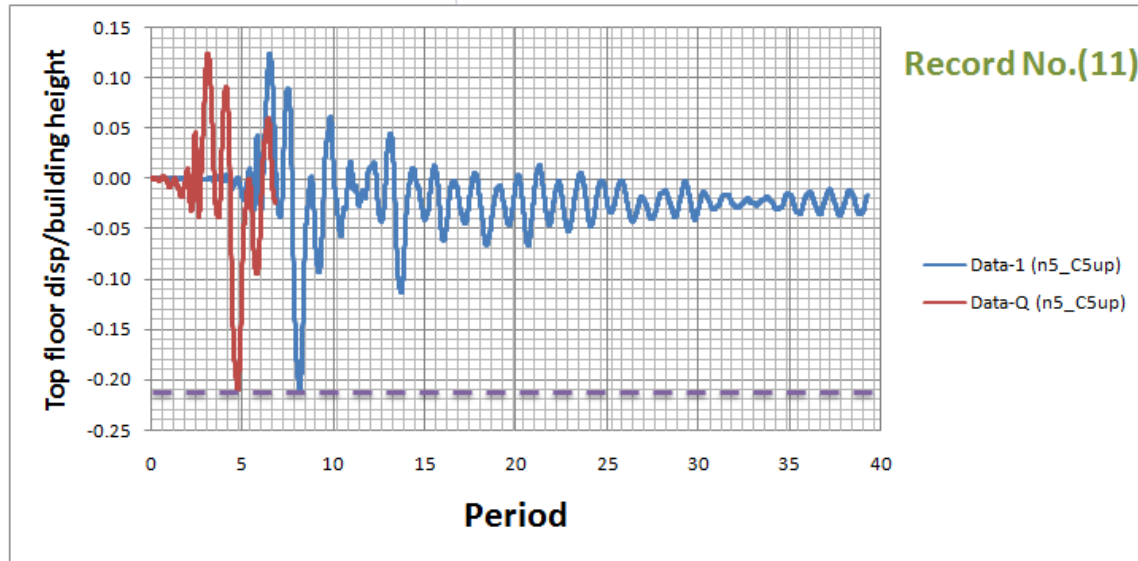


Figure 6.31. Maximum displacement of the original ground motions Data1 and the displacement of DataQ along height of the building.

Height of floor (m)		3			
Record No.(11)		Max. (Disp./height)		Drift (Disp./height)%	
Floor No.		Data1	DataQ	Data1	DataQ
GF	0	0.000	0.000	0.000	0.000
1 st Floor	1	0.089	0.090	2.967	3.000
2 ^{sd} Floor	2	0.151	0.152	2.067	2.067
3 rd Floor	3	0.187	0.188	1.200	1.200
4 th Floor	4	0.199	0.200	0.400	0.400
5 th Floor	5	0.209	0.210	0.333	0.333

Record No.(11)		Shear Force (Kn) for every floor	
Floor No.		Data1	DataQ
GF	0	2926.498	2932.372
1 st Floor	1	2920.980	2932.372
2 ^{sd} Floor	2	1598.618	1586.514
3 rd Floor	3	1139.556	1129.054
4 th Floor	4	813.104	796.372
5 th Floor	5	307.584	309.008

Table 6.12. Table Maximum Displacement and inter storey drifts and shear force for every floor Vs along of the height of Building for recording Data1&DataQ.

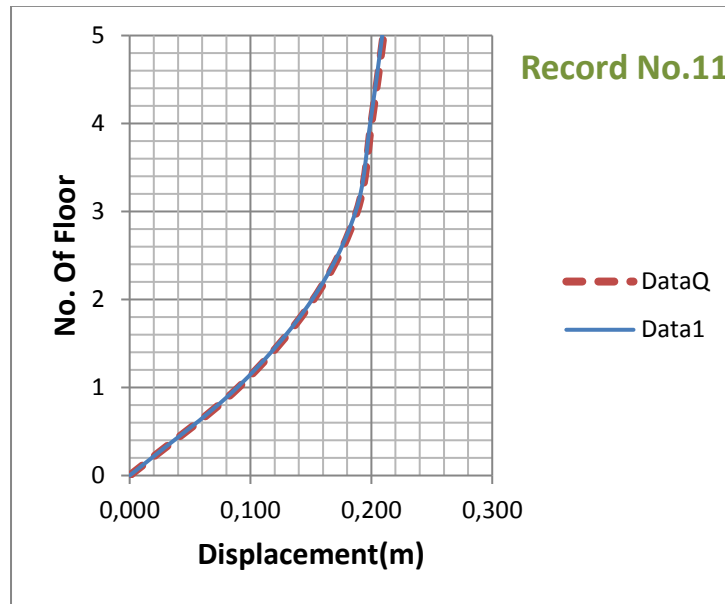


Figure 6.32. Profile of displacements for every floor along of the height of Building.

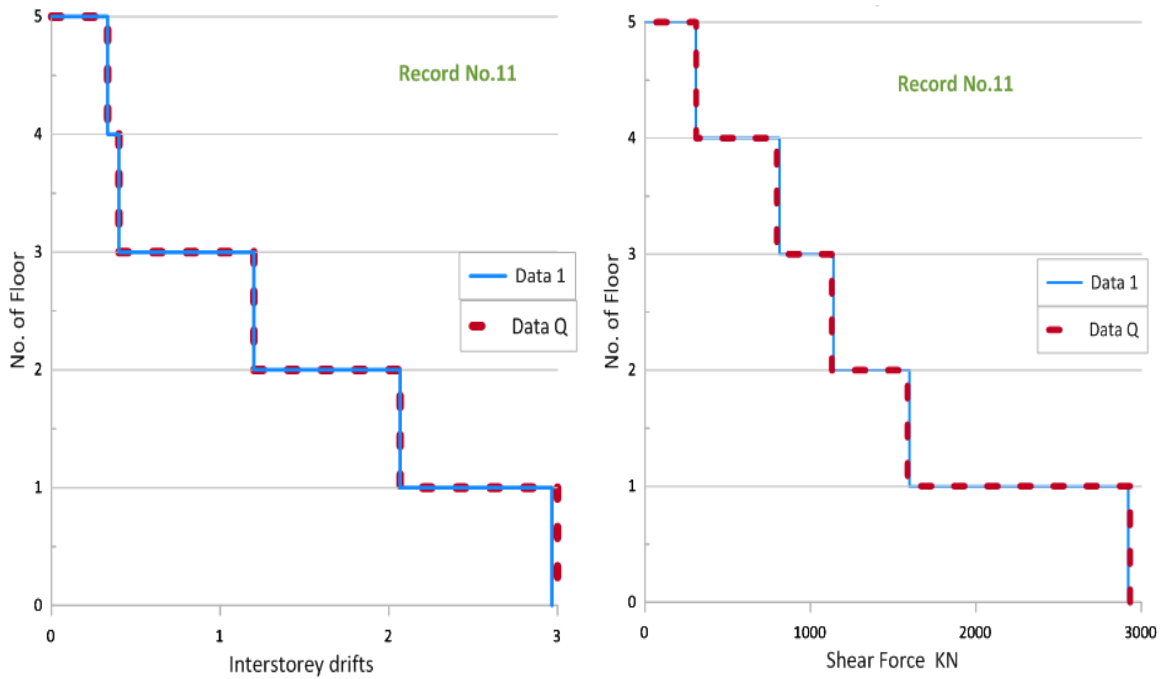


Figure 6.33. Profile of inter storey drifts and shear force for every floor Vs along of the height of Building.



Record 12

Record No.(12)	Data1	DataQ
Time (Sec.)	6.15	3.98
Displacement at the top of building (m)	0.123	0.123

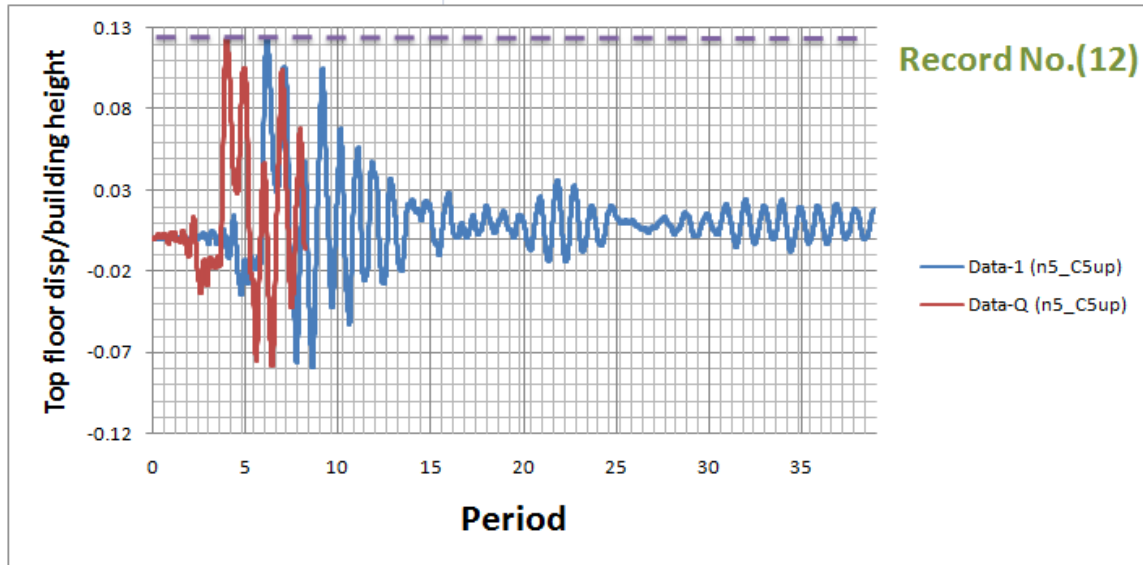


Figure 6.34. Maximum displacement of the original ground motions Data1 and the displacement of DataQ along height of the building.

Height of floor (m)	3				
Record No.(12)	Max. (Disp./height)	Drift (Disp./height)%			
Floor No.	Data1	DataQ	Data1	DataQ	
GF	0	0.000	0.000	0.000	0.000
1 st Floor	1	0.031	0.031	1.033	1.033
2 ^{sd} Floor	2	0.080	0.079	1.633	1.600
3 rd Floor	3	0.101	0.101	0.700	0.733
4 th Floor	4	0.113	0.112	0.400	0.367
5 th Floor	5	0.123	0.123	0.333	0.367

Record No.(12)	Shear Force (KN) for every floor		
Floor No.	Data1	DataQ	
GF	0	3140.454	3144.904
1 st Floor	1	3140.454	3144.904
2 ^{sd} Floor	2	2040.236	2043.974
3 rd Floor	3	1483.274	1457.286
4 th Floor	4	698.294	707.906
5 th Floor	5	332.326	351.194

Table 6.13. Table Maximum Displacement and inter storey drifts and shear force for every floor Vs along of the height of Building for recording Data1&DataQ.

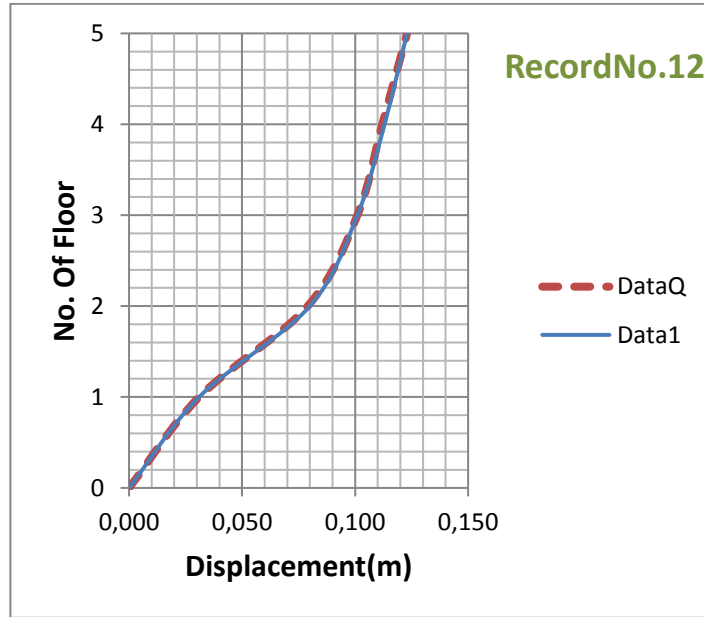


Figure 6.35. Profile of displacements for every floor along of the height of Building.

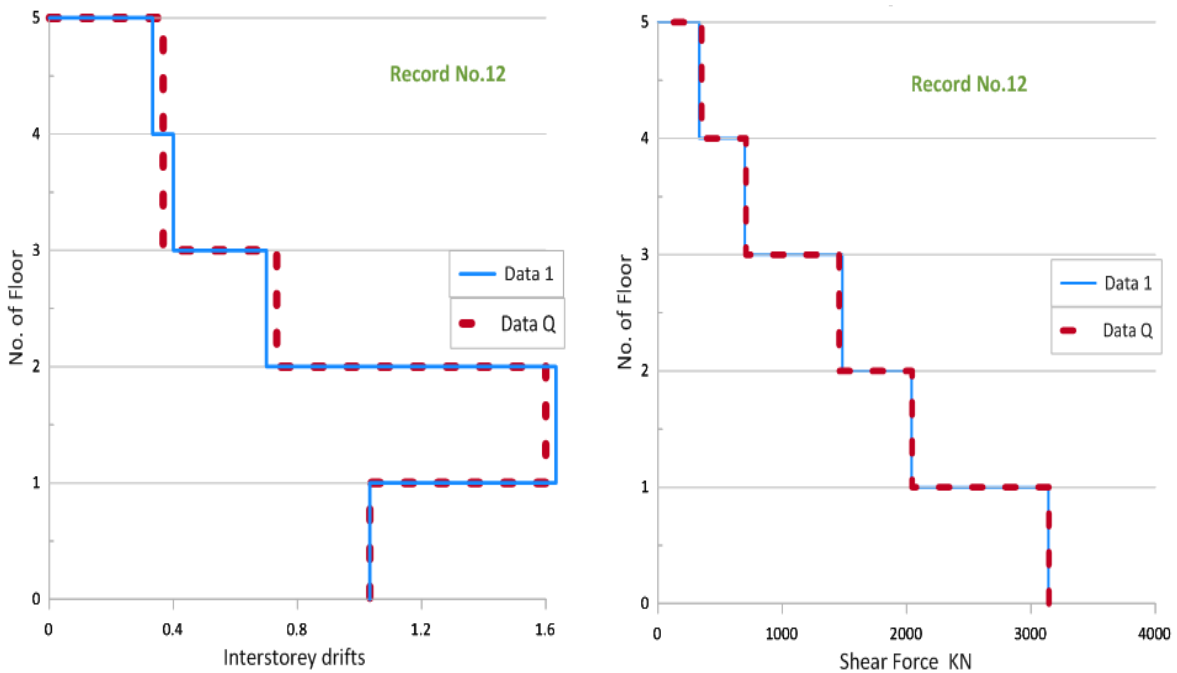


Figure 6.36. Profile of inter storey drifts and shear force for every floor Vs along of the height of Building.



Record 13

Record No.(13)	Data1	DataQ
Time (Sec.)	5.26	2.85
Displacement at the top of building (m)	-0.187	-0.188

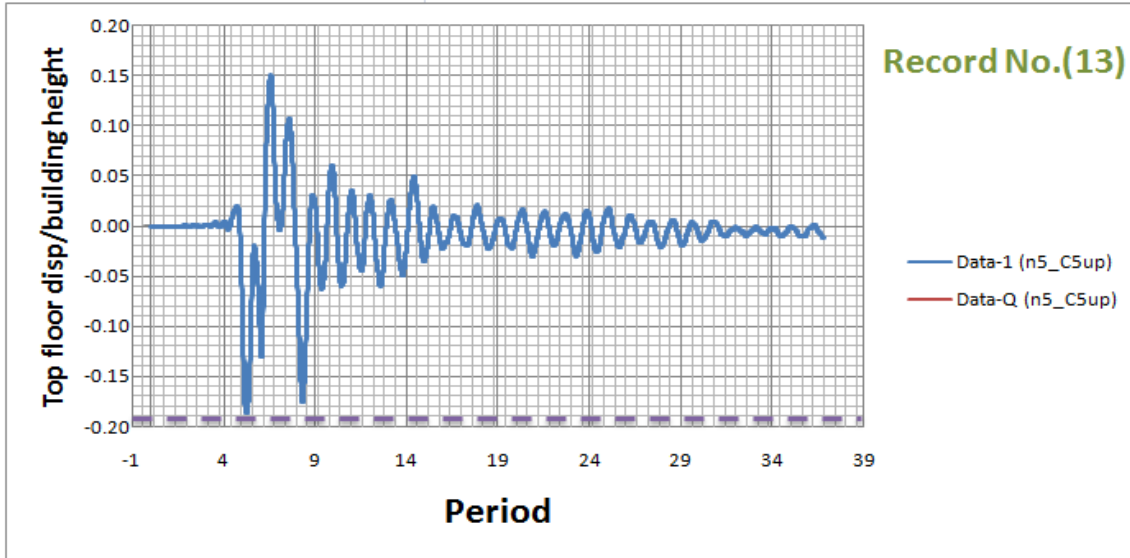


Figure 6.37. Maximum displacement of the original ground motions Data1 and the displacement of DataQ along height of the building.

Height of floor (m)		3			
Record No.(13)		Max. (Disp./height)		Drift(Disp./height)%	
Floor No.		Data1	DataQ	Data1	DataQ
GF	0	0.000	0.000	0.000	0.000
1 st Floor	1	0.072	0.072	2.400	2.400
2 ^{sd} Floor	2	0.148	0.149	2.533	2.567
3 rd Floor	3	0.171	0.172	0.767	0.767
4 th Floor	4	0.182	0.183	0.367	0.367
5 th Floor	5	0.187	0.188	0.167	0.167

Record No.(13)		Shear Force (KN) for every floor	
Floor No.		Data1	DataQ
GF	0	3197.948	3191.184
1 st Floor	1	3197.948	3191.184
2 ^{sd} Floor	2	2003.212	1995.914
3 rd Floor	3	1403.352	1385.908
4 th Floor	4	692.242	694.200
5 th Floor	5	90.602	88.288

Table 6.14. Table Maximum Displacement and inter storey drifts and shear force for every floor Vs along of the height of Building for recording Data1&DataQ.

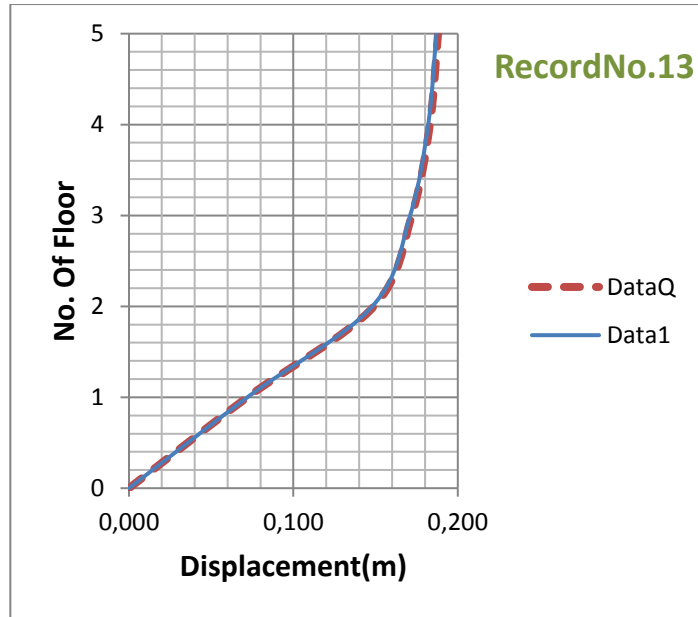


Figure 6.38. Profile of displacements for every floor along of the height of Building.

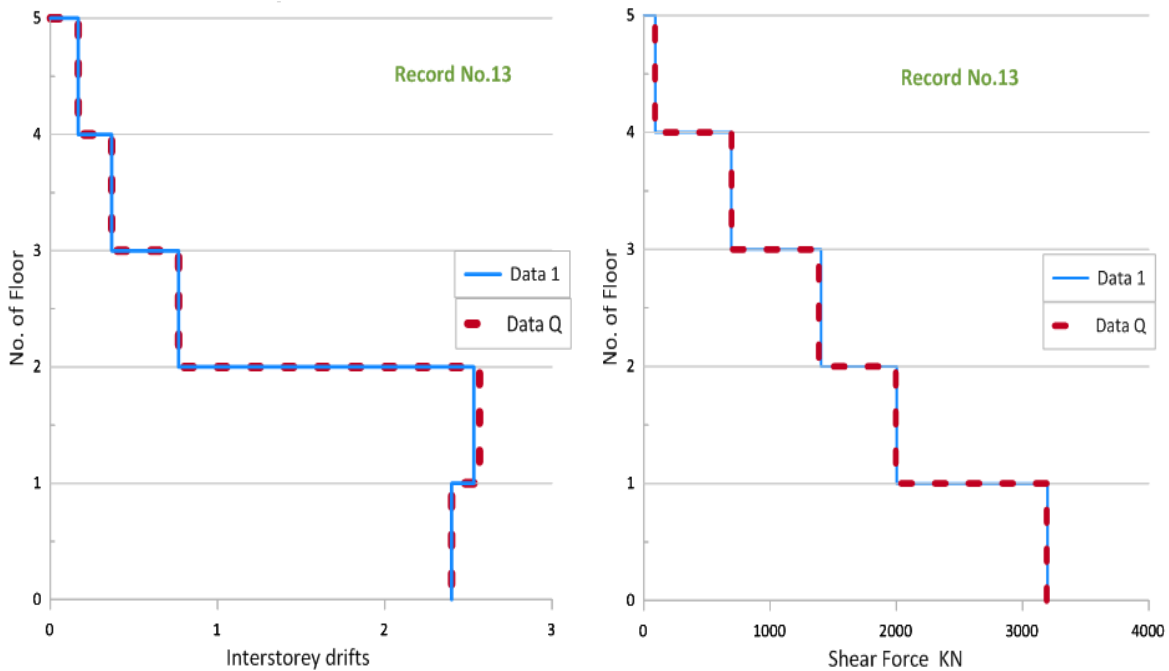


Figure 6.39. Profile of inter storey drifts and shear force for every floor Vs along of the height of Building.



Record 14

Record No.(14)	Data1	DataQ
Time (Sec.)	8.44	7.08
Displacement at the top of building (m)	-0.08	-0.079

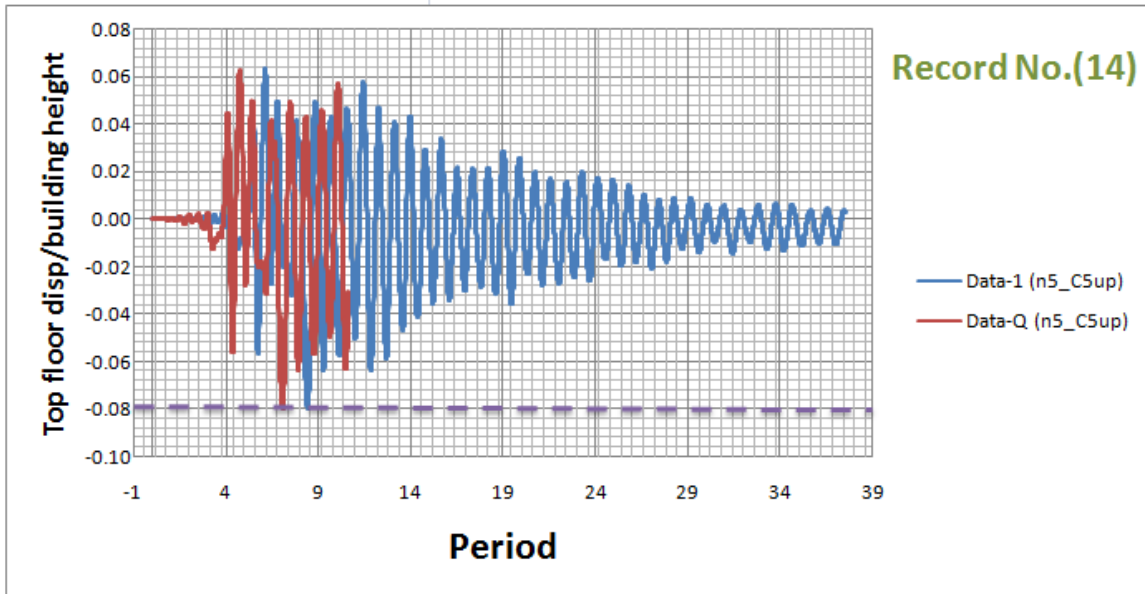


Figure 6.40. Maximum displacement of the original ground motions Data1 and the displacement of DataQ along height of the building.

Height of floor (m)		3			
Record No.(14)		Max. (Disp./height)		Drift (Disp./height)%	
Floor No.		Data1	DataQ	Data1	DataQ
GF	0	0.000	0.000	0.000	0.000
1 st Floor	1	0.022	0.022	0.733	0.733
2 ^{sd} Floor	2	0.050	0.050	0.933	0.933
3 rd Floor	3	0.066	0.066	0.533	0.533
4 th Floor	4	0.073	0.073	0.233	0.233
5 th Floor	5	0.080	0.079	0.233	0.200

Record No.(14)		Shear Force (Kn) for every floor	
Floor No.		Data1	DataQ
GF	0	2942.696	2944.120
1 st Floor	1	2942.696	2944.120
2 ^{sd} Floor	2	1891.784	1888.758
3 rd Floor	3	1331.618	1325.566
4 th Floor	4	458.706	458.884
5 th Floor	5	219.830	215.202

Table 6.15. Table Maximum Displacement and inter storey drifts and shear force for every floor Vs along of the height of Building for recording Data1&DataQ.

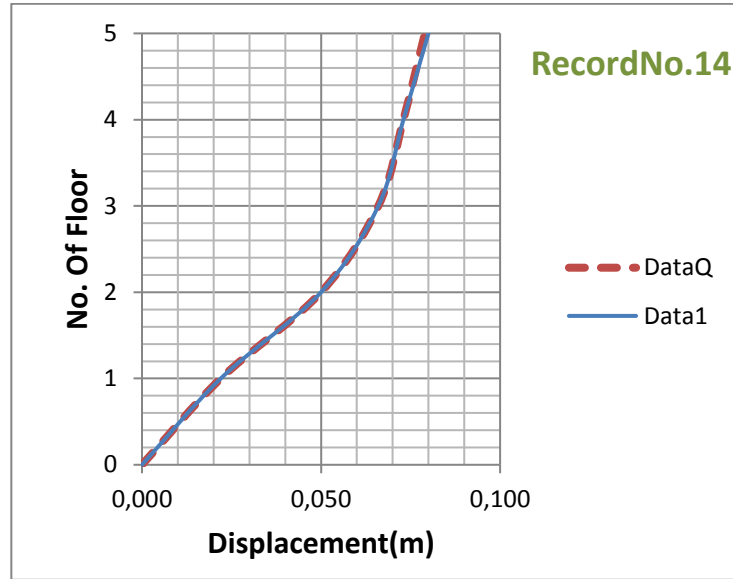


Figure 6.41. Profile of displacements for every floor along of the height of Building.

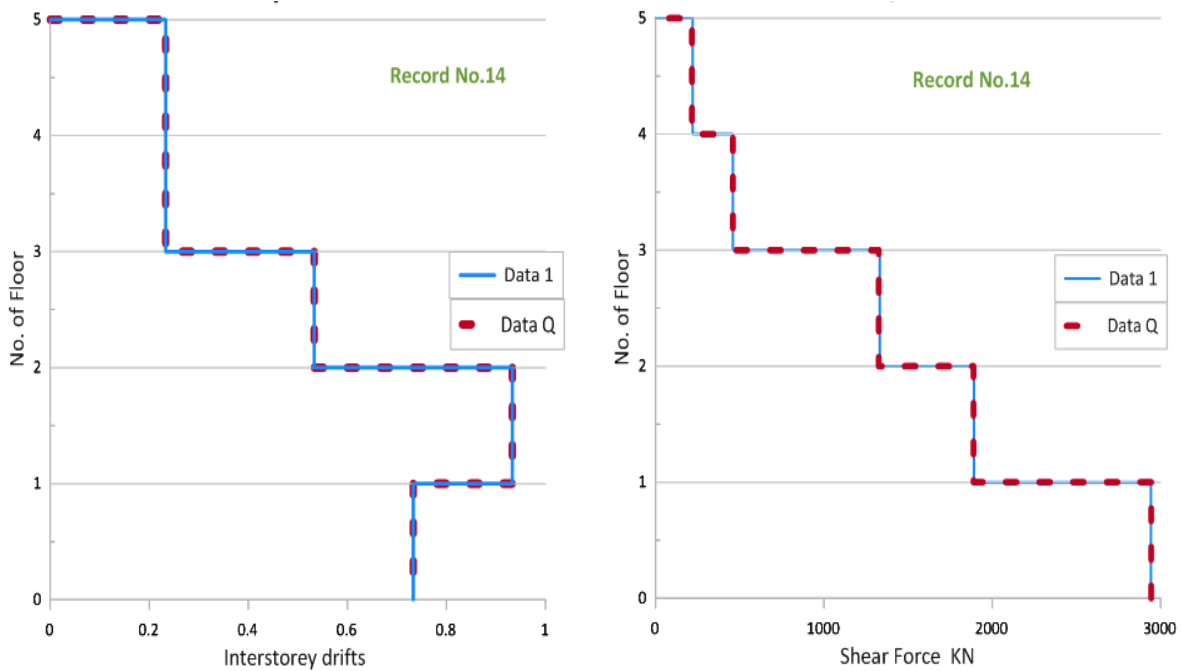


Figure 6.42. Profile of inter storey drifts and shear force for every floor Vs along of the height of Building.



Record 15

Record No.(15)	Data1	DataQ
Time (Sec.)	9.03	7.75
Displacement at the top of building (m)	-0.111	-0.111

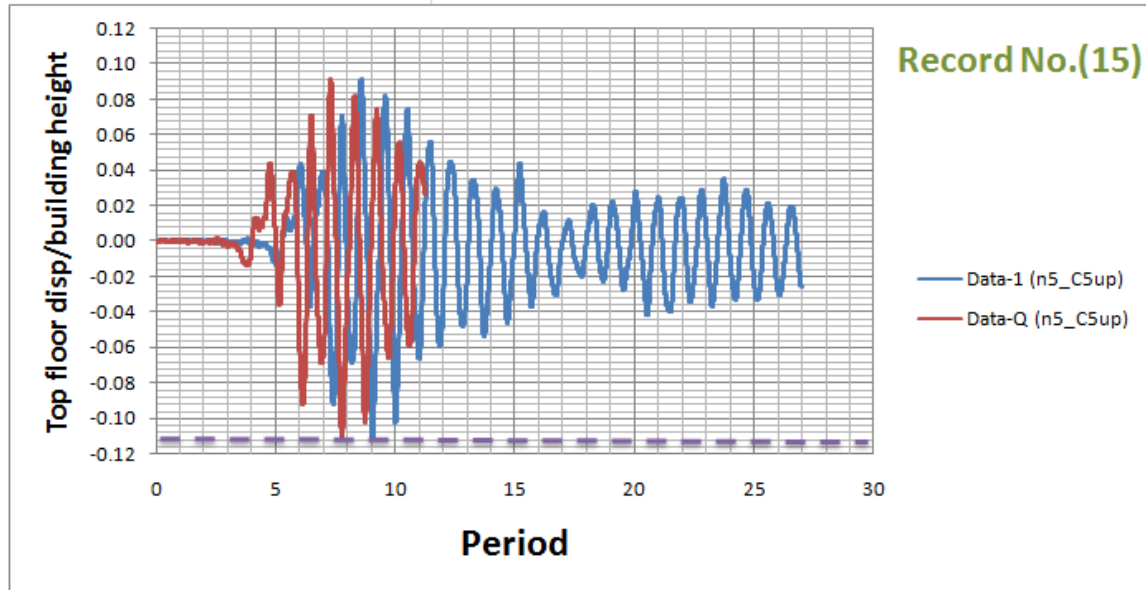


Figure 6.43. Maximum displacement of the original ground motions Data1 and the displacement of DataQ along height of the building.

Height of floor (m)		3			
Record No.(15)		Max. (Disp./height)		Drift (Disp./height)%	
Floor No.		Data1	DataQ	Data1	DataQ
GF	0	0.000	0.000	0.000	0.000
1 st Floor	1	0.018	0.018	0.600	0.600
2 ^{sd} Floor	2	0.051	0.051	1.100	1.100
3 rd Floor	3	0.074	0.074	0.767	0.767
4 th Floor	4	0.092	0.092	0.600	0.600
5 th Floor	5	0.111	0.111	0.633	0.633

Record No.(15)		Shear Force (Kn) for every floor	
Floor No.		Data1	DataQ
GF	0	2183.526	2182.280
1 st Floor	1	2183.526	2182.280
2 ^{sd} Floor	2	2069.250	2071.742
3 rd Floor	3	1748.672	1749.384
4 th Floor	4	1413.320	1412.608
5 th Floor	5	694.200	687.792

Table 6.16. Table Maximum Displacement and inter storey drifts and shear force for every floor Vs along of the height of Building for recording Data1&DataQ.

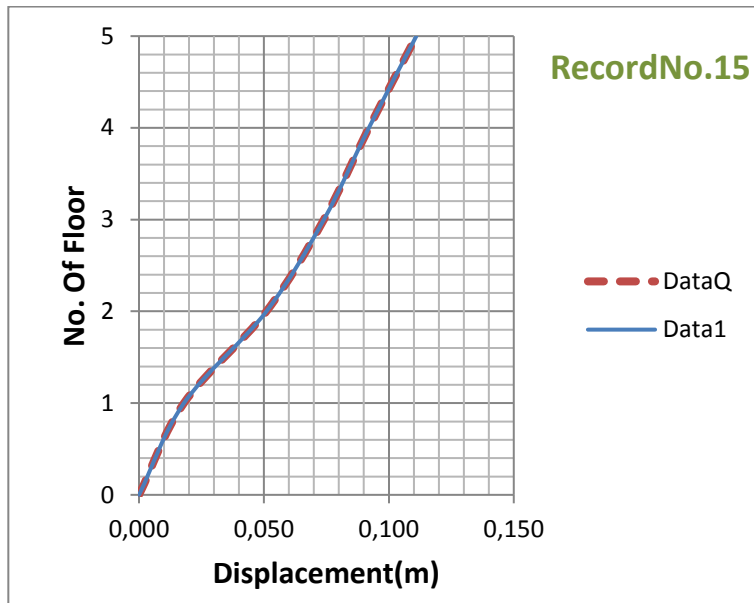


Figure 6.44. Profile of displacements for every floor along of the height of Building.

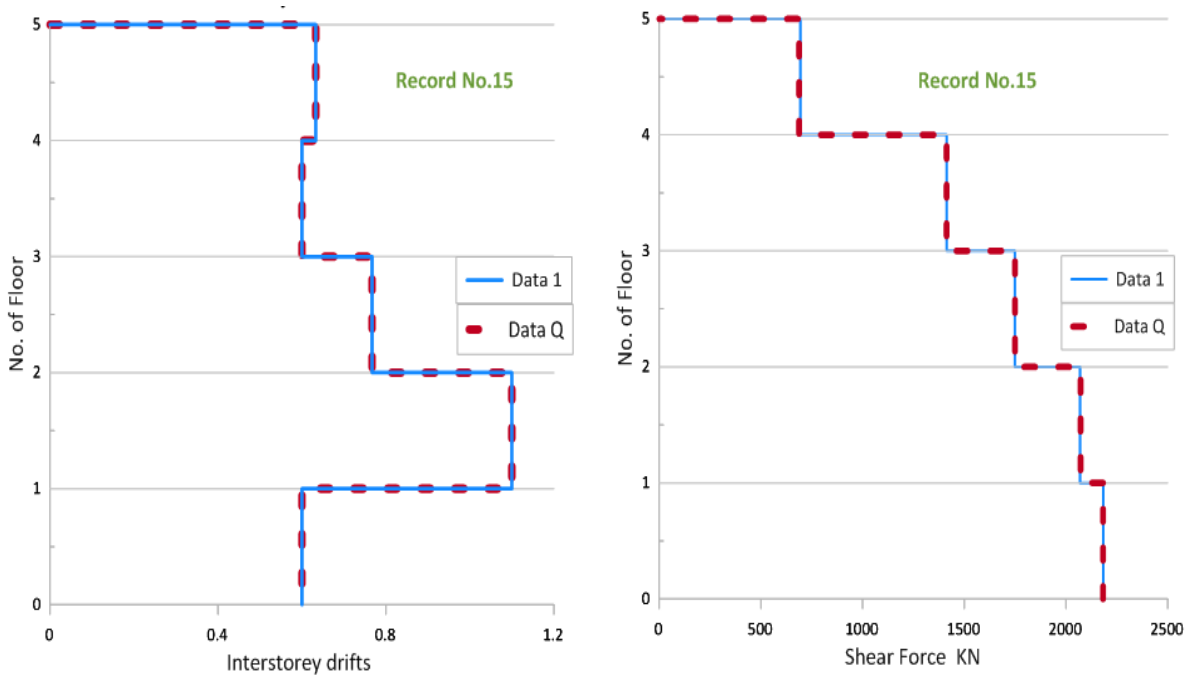


Figure 6.45. Profile of inter storey drifts and shear force for every floor Vs along of the height of Building.



Record 16

Record No.(16)	Data1	DataQ
Time (Sec.)	6.82	3.47
Displacement at the top of building (m)	0.09	0.092

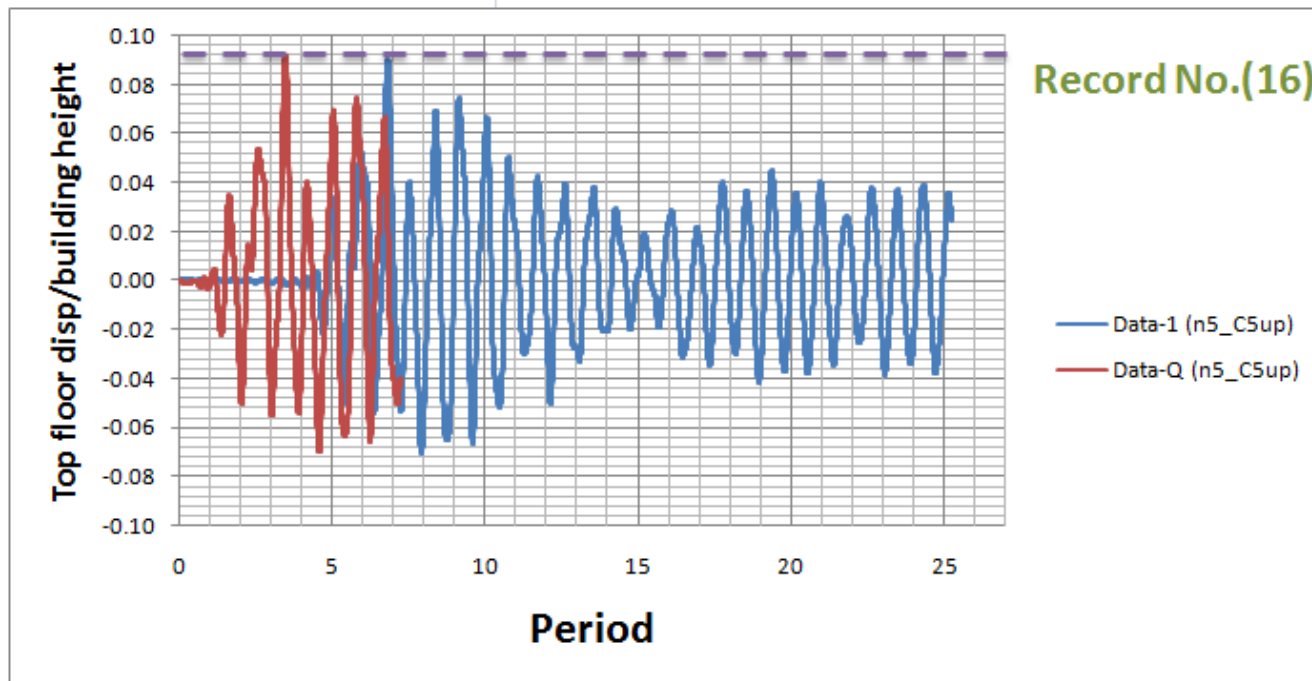


Figure 6.46. Maximum displacement of the original ground motions Data1 and the displacement of DataQ along height of the building.

Height of floor (m)		3			
Record No.(16)		Max. (Disp./height)		Drift (Disp./height)%	
Floor No.		Data1	DataQ	Data1	DataQ
GF	0	0.000	0.000	0.000	0.000
1 st Floor	1	0.012	0.013	0.400	0.433
2 ^{sd} Floor	2	0.029	0.029	0.567	0.533
3 rd Floor	3	0.048	0.048	0.633	0.633
4 th Floor	4	0.069	0.070	0.700	0.733
5 th Floor	5	0.090	0.092	0.700	0.733

Record No.(16)		Shear Force (Kn) for every floor	
Floor No.		Data1	DataQ
GF	0	1968.502	1995.202
1 st Floor	1	1968.502	1995.202
2 ^{sd} Floor	2	1647.746	1630.302
3 rd Floor	3	1624.428	1592.566
4 th Floor	4	1593.990	1641.694
5 th Floor	5	756.856	773.944

Table 6.17. Table Maximum Displacement and inter storey drifts and shear force for every floor Vs along of the height of Building for recording Data1&DataQ.

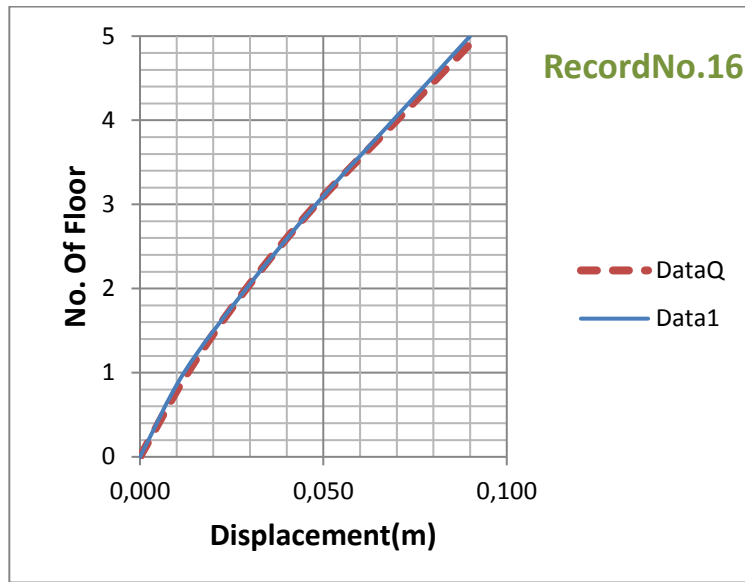


Figure 6.47. Profile of displacements for every floor along of the height of Building.

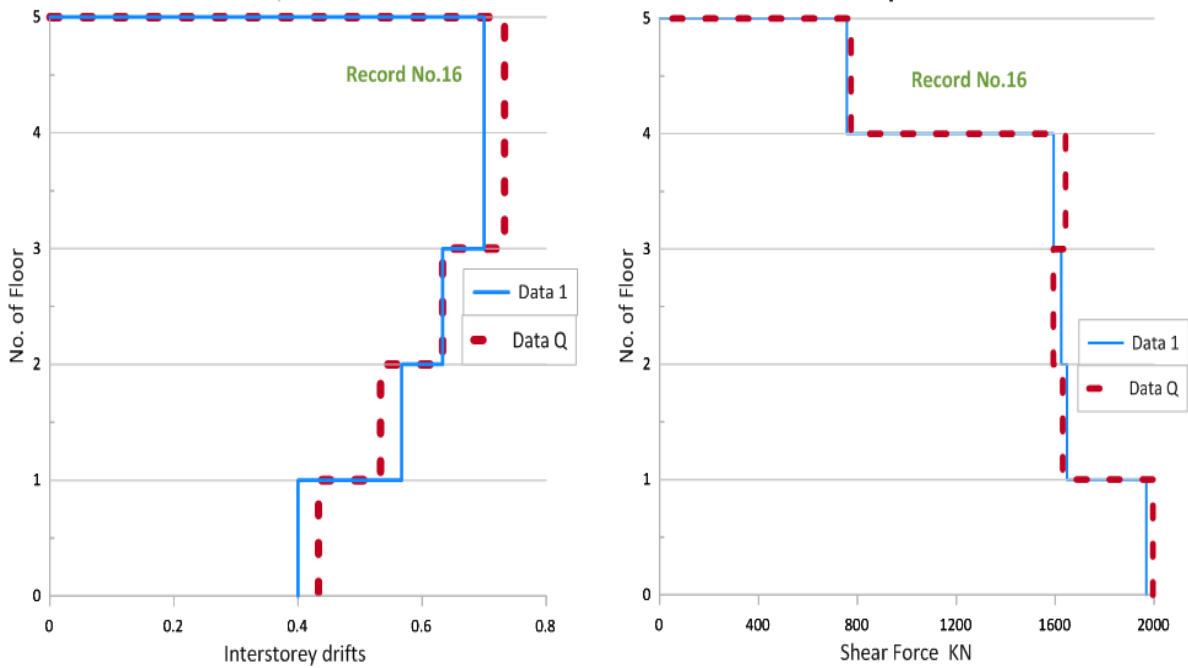


Figure 6.48. Profile of inter storey drifts and shear force for every floor Vs along of the height of Building.



Record 17

Record No.(17)	Data1	DataQ
Time (Sec.)	12.4	11.21
Displacement at the top of building (m)	-0.073	-0.073

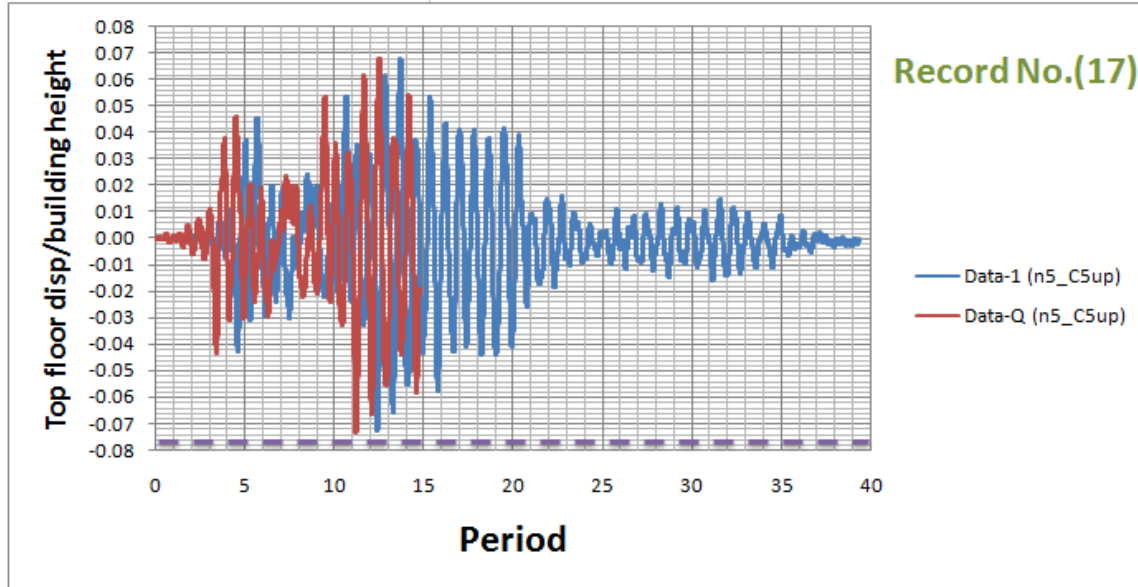


Figure 6.49. Maximum displacement of the original ground motions Data1 and the displacement of DataQ along height of the building.

Height of floor (m)		3			
Record No.(17)		Max. (Disp./height)		Drift (Disp./height)%	
Floor No.		Data1	DataQ	Data1	DataQ
GF	0	0.000	0.000	0.000	0.000
1 st Floor	1	0.012	0.012	0.400	0.400
2 ^{sd} Floor	2	0.028	0.028	0.533	0.533
3 rd Floor	3	0.040	0.040	0.400	0.400
4 th Floor	4	0.052	0.052	0.400	0.400
5 th Floor	5	0.073	0.073	0.700	0.700

Record No.(17)		Shear Force (Kn) for every floor	
Floor No.		Data1	DataQ
GF	0	2075.658	2074.768
1 st Floor	1	2075.658	2074.768
2 ^{sd} Floor	2	1569.604	1576.902
3 rd Floor	3	1081.706	1091.674
4 th Floor	4	990.570	994.308
5 th Floor	5	741.904	745.286

Table 6.18. Table Maximum Displacement and inter storey drifts and shear force for every floor Vs along of the height of Building for recording Data1&DataQ.

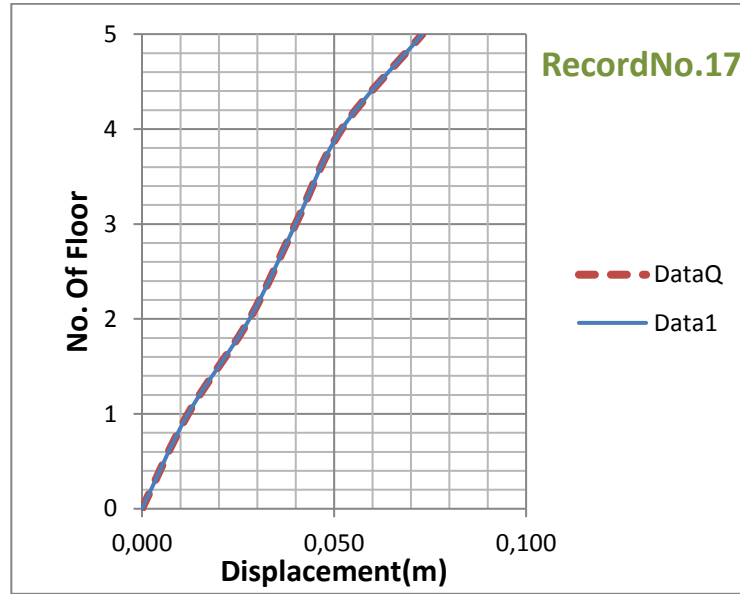


Figure 6.50. Profile of displacements for every floor along of the height of Building.

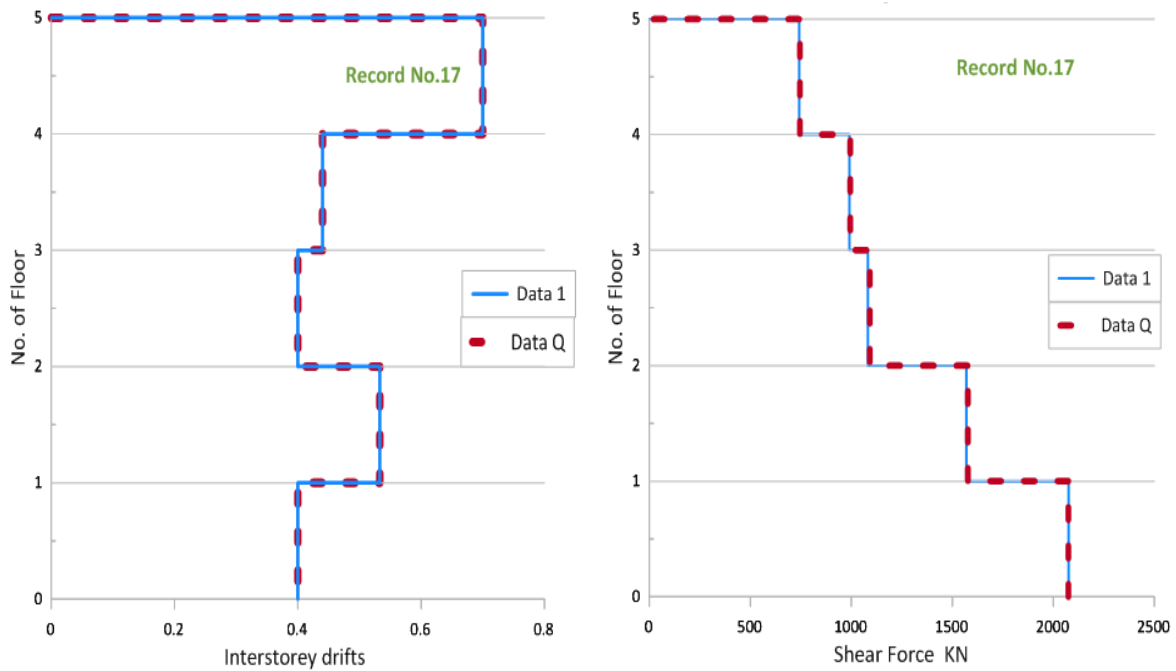


Figure 6.51. Profile of inter storey drifts and shear force for every floor Vs along of the height of Building.



Record 18

Record No.(18)	Data1	DataQ
Time (Sec.)	13.95	3.88
Displacement at the top of building (m)	0.078	0.073

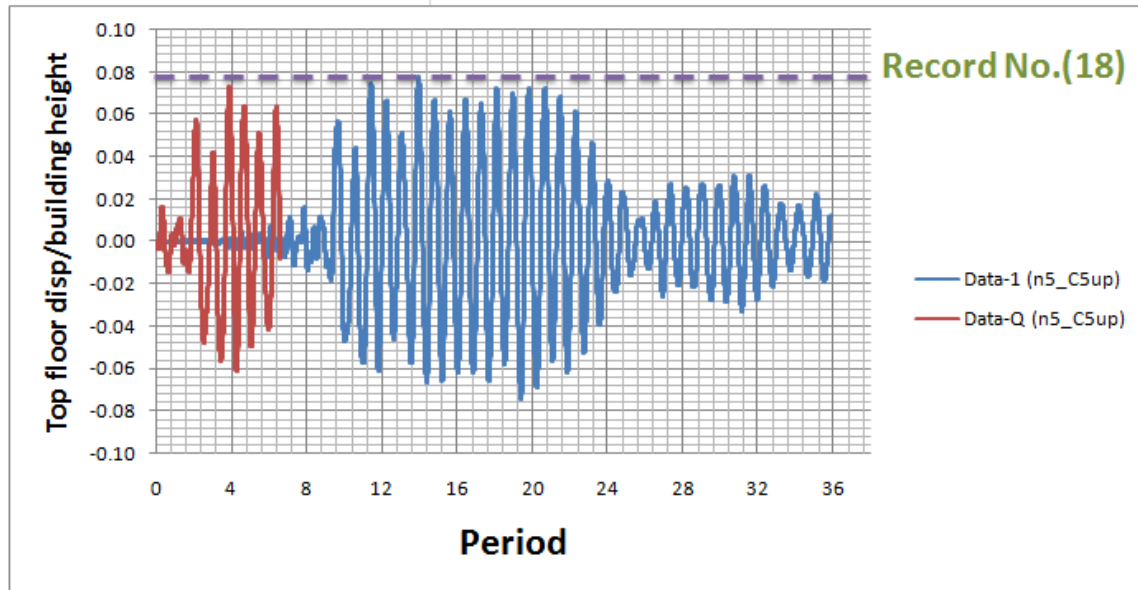


Figure 6.52. Maximum displacement of the original ground motions Data1 and the displacement of DataQ along height of the building.

Height of floor (m)		3			
Record No.(18)		Max.(Disp./height)		Drift(Disp./height)%	
Floor No.		Data1	DataQ	Data1	DataQ
GF	0	0.000	0.000	0.000	0.000
1 st Floor	1	0.015	0.014	0.500	0.467
2 nd Floor	2	0.036	0.034	0.700	0.667
3 rd Floor	3	0.053	0.049	0.567	0.500
4 th Floor	4	0.066	0.062	0.433	0.433
5 th Floor	5	0.078	0.073	0.400	0.367

Record No.(18)		Shear Force (Kn) for every floor	
Floor No.		Data1	DataQ
GF	0	2160.564	2310.974
1 st Floor	1	2160.564	2310.974
2 nd Floor	2	1777.330	1721.260
3 rd Floor	3	1361.878	1309.190
4 th Floor	4	968.854	943.578
5 th Floor	5	465.826	424.530

Table 6.19. Table Maximum Displacement and inter storey drifts and shear force for every floor Vs along of the height of Building for recording Data1&DataQ.

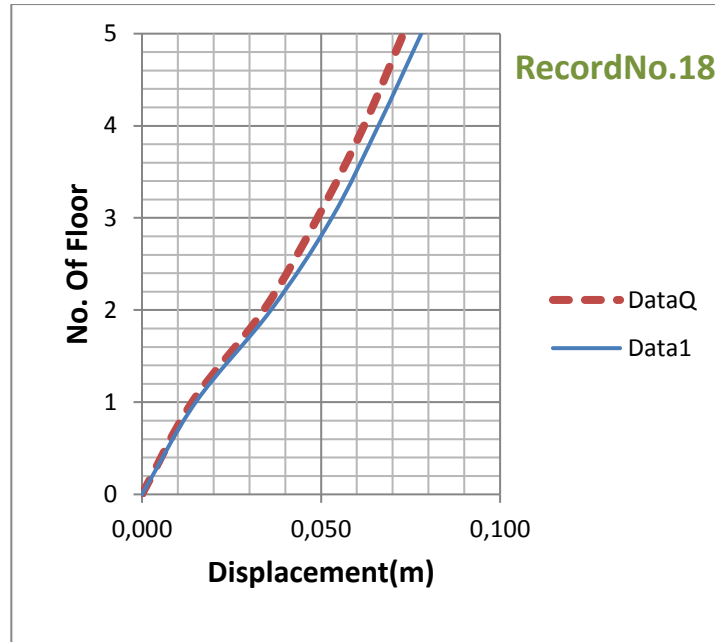


Figure 6.53. Profile of displacements for every floor along of the height of Building.

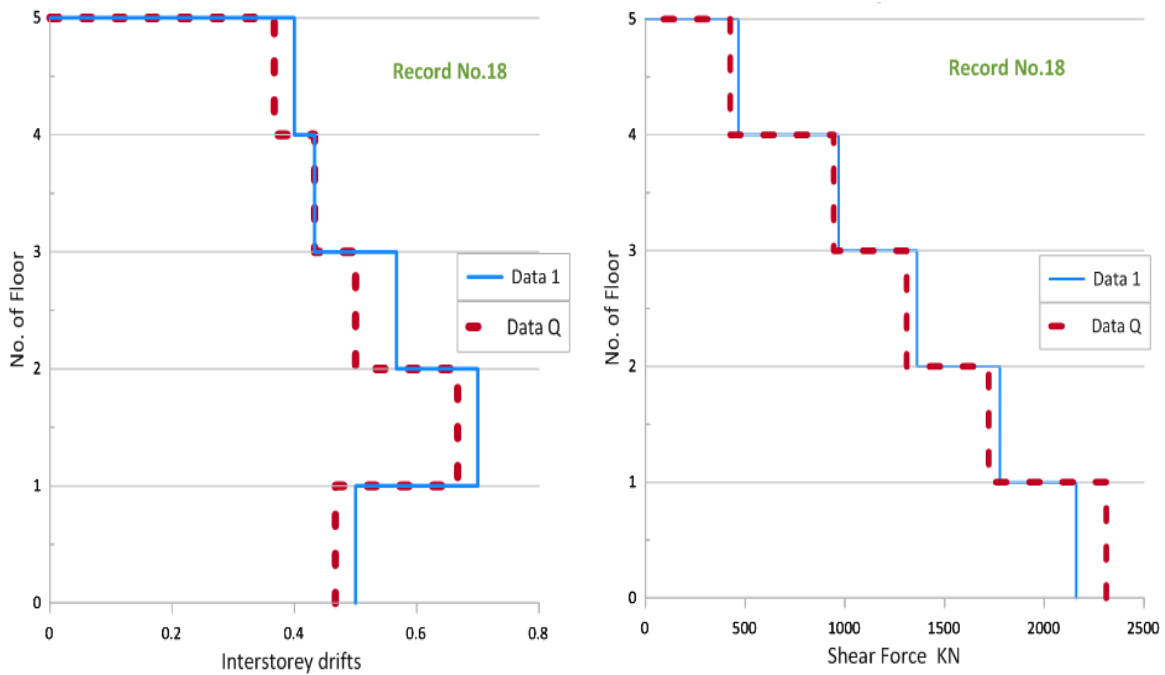


Figure 6.54. Profile of inter storey drifts and shear force for every floor Vs along of the height of Building.



Record 19

Record No.(19)	Data1	DataQ
Time (Sec.)	3.28	1.07
Displacement at the top of building (m)	-0.13	-0.142

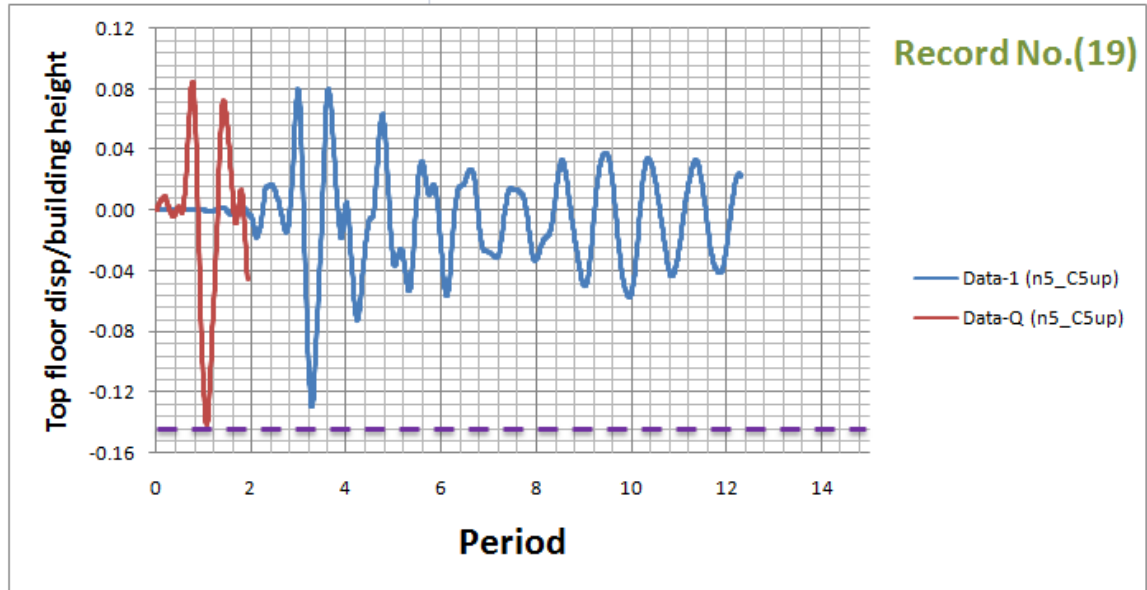


Figure 6.55. Maximum displacement of the original ground motions Data1 and the displacement of DataQ along height of the building.

Height of floor (m)	3				
Record No.(19)	Max. (Disp./height)		Drift (Disp./height)%		
Floor No.	Data1	DataQ	Data1	DataQ	
GF	0	0.000	0.000	0.000	
1 st Floor	1	0.019	0.021	0.633	0.703
2 ^{sd} Floor	2	0.050	0.056	1.033	1.163
3 rd Floor	3	0.071	0.083	0.700	0.900
4 th Floor	4	0.091	0.105	0.667	0.733
5 th Floor	5	0.130	0.142	1.300	1.233

Record No.(19)	Shear Force (Kn) for every floor		
Floor No.	Data1	DataQ	
GF	0	2775.732	2886.270
1 st Floor	1	2775.732	2886.270
2 ^{sd} Floor	2	2025.106	2073.344
3 rd Floor	3	1352.444	1743.154
4 th Floor	4	1155.576	1249.204
5 th Floor	5	881.100	836.422

Table 6.20. Table Maximum Displacement and inter storey drifts and shear force for every floor Vs along of the height of Building for recording Data1&DataQ.

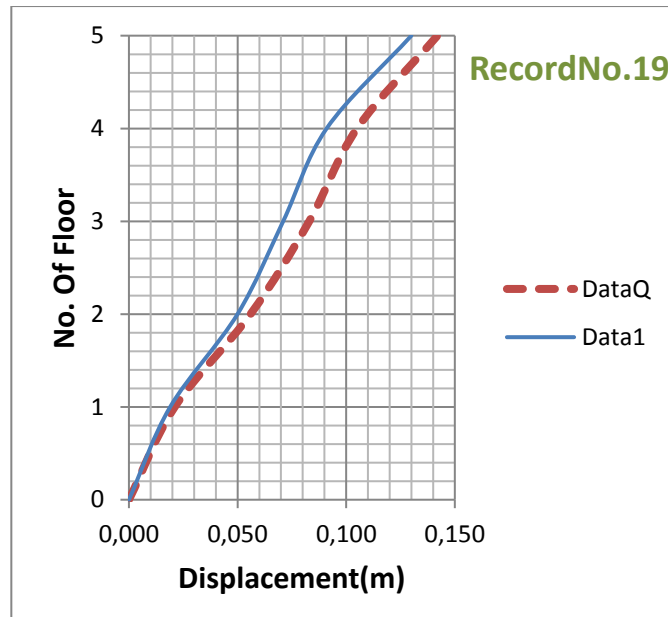


Figure 6.56. Profile of displacements for every floor along of the height of Building.

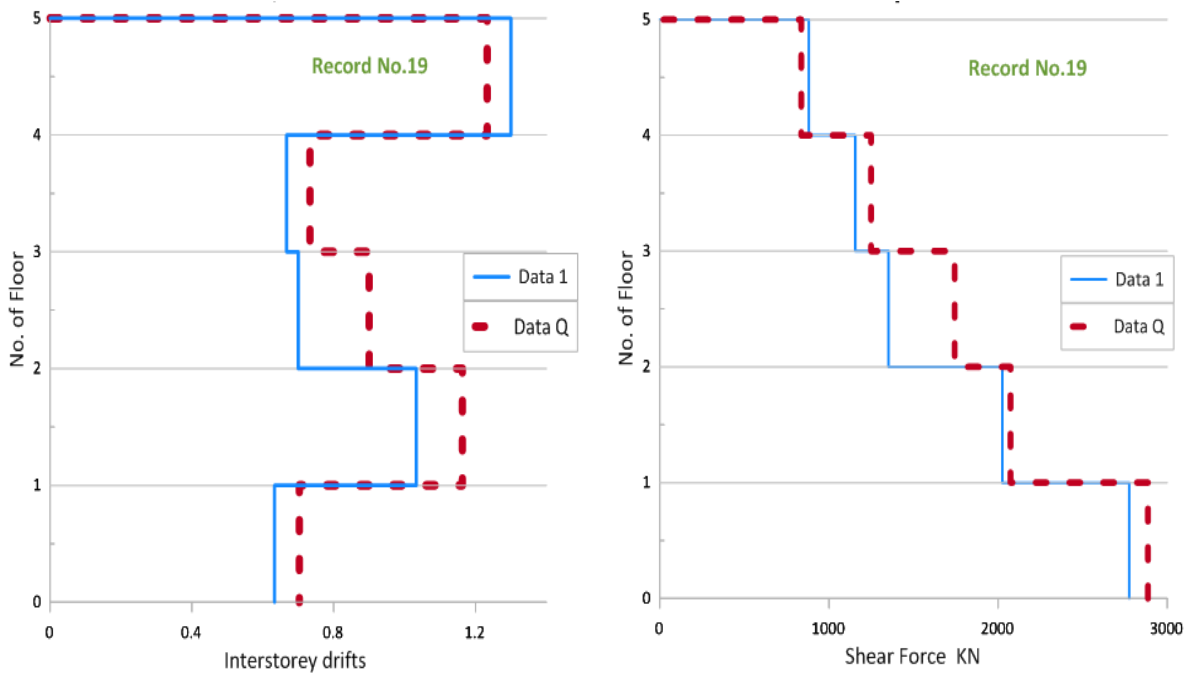


Figure 6.57. Profile of inter storey drifts and shear force for every floor Vs along of the height of Building.



Record 20

Record No.(20)	Data1	DataQ
Time (Sec.)	3.4	1.35
Displacement at the top of building (m)	-0.173	-0.183

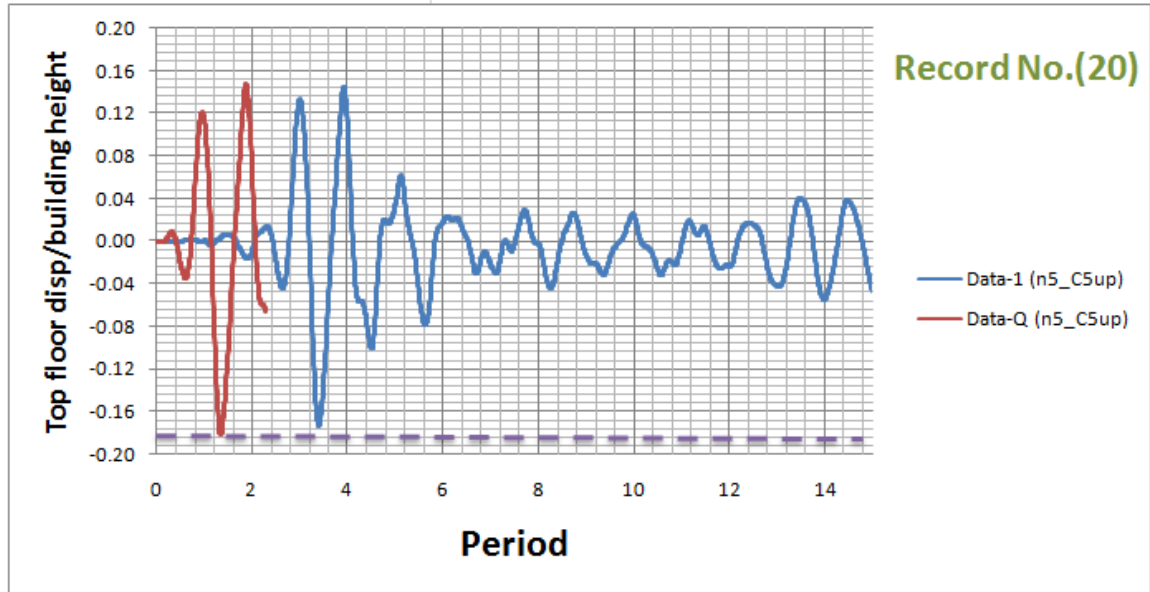


Figure 6.58. Maximum displacement of the original ground motions Data1 and the displacement of DataQ along height of the building.

Height of floor (m)		3			
Record No.(20)		Max. (Disp./height)		Drift (Disp./height)%	
Floor No.		Data1	DataQ	Data1	DataQ
GF	0	0.000	0.000	0.000	0.000
1 st Floor	1	0.028	0.033	0.933	1.100
2 ^{sd} Floor	2	0.090	0.098	2.067	2.167
3 rd Floor	3	0.136	0.144	1.533	1.533
4 th Floor	4	0.157	0.165	0.700	0.700
5 th Floor	5	0.173	0.182	0.533	0.567

Record No.(20)		Shear Force (Kn) for every floor	
Floor No.		Data1	DataQ
GF	0	2526.888	2930.948
1 st Floor	1	2526.888	2930.948
2 ^{sd} Floor	2	2155.758	2155.046
3 rd Floor	3	1954.796	1957.466
4 th Floor	4	1390.002	1406.200
5 th Floor	5	571.558	581.526

Table 6.21. Table Maximum Displacement and inter storey drifts and shear force for every floor Vs along of the height of Building for recording Data1&DataQ.

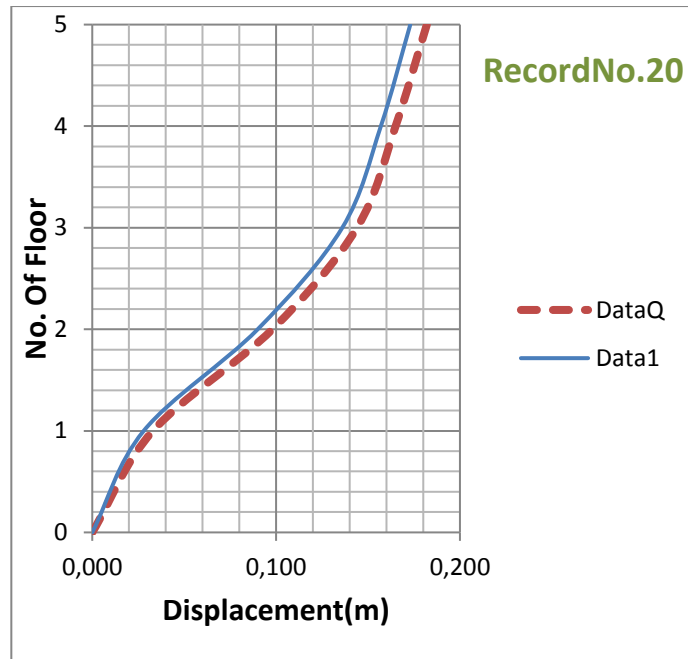


Figure 6.59. Profile of displacements for every floor along of the height of Building.

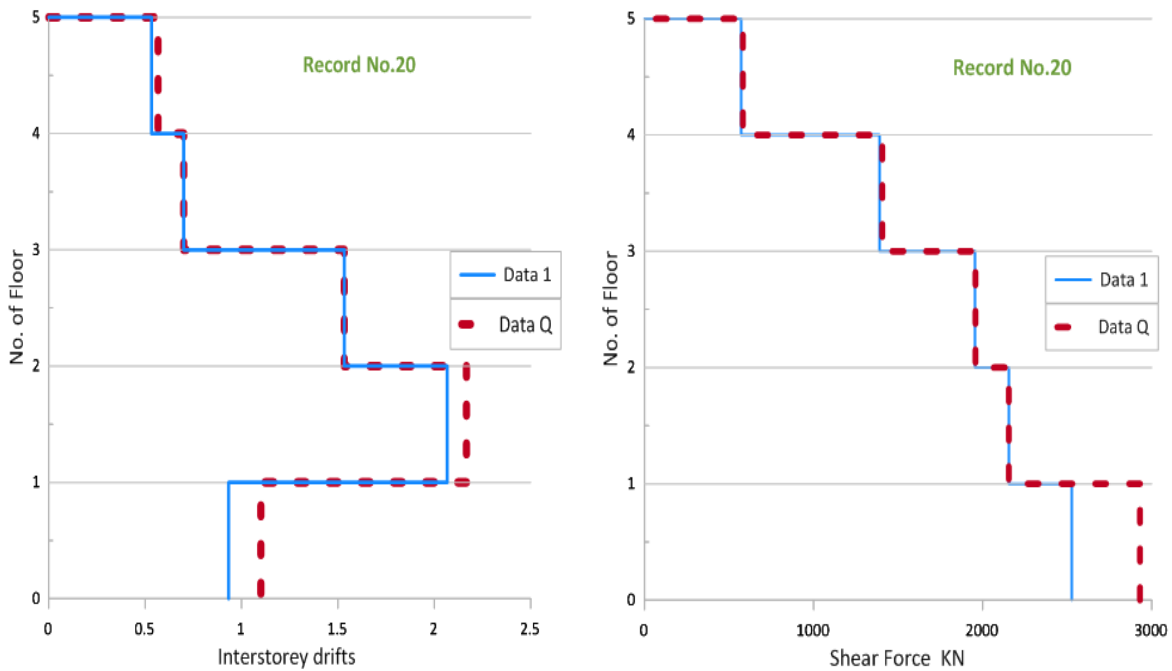


Figure 6.60. Profile of inter storey drifts and shear force for every floor Vs along of the height of Building.



Record 21

Record No.(21)	Data1	DataQ
Time (Sec.)	2.99	0.52
Displacement at the top of building (m)	0.101	0.099

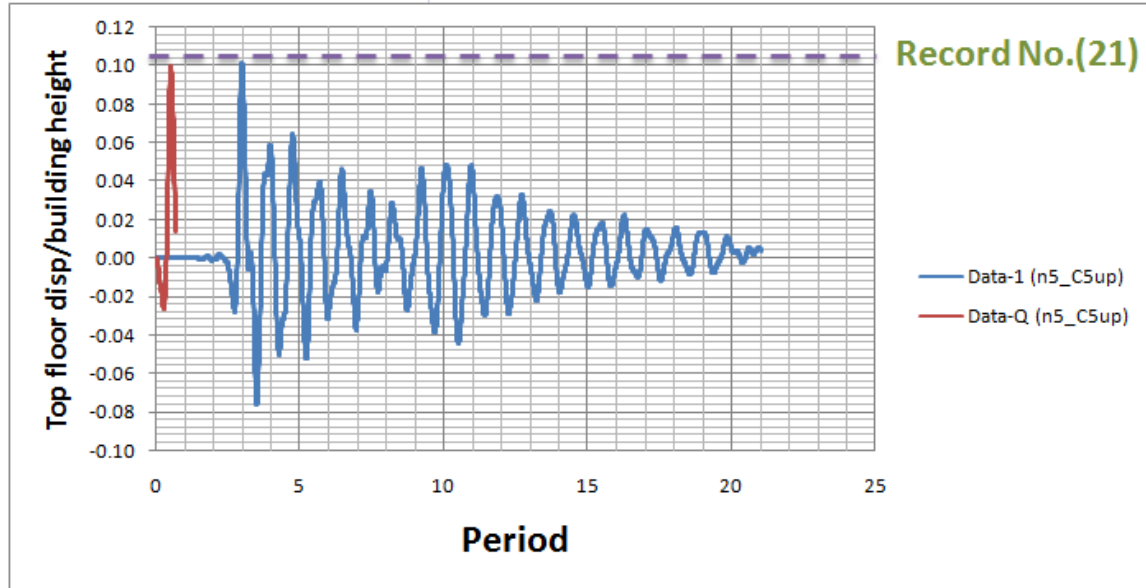


Figure 6.61. Maximum displacement of the original ground motions Data1 and the displacement of DataQ along height of the building.

Height of floor (m)		3			
Record No.(21)		Max.(Disp./height)		Drift(Disp./height)%	
Floor No.		Data1	DataQ	Data1	DataQ
GF	0	0.000	0.000	0.000	0.000
1 st Floor	1	0.006	0.006	0.200	0.200
2 ^{sd} Floor	2	0.032	0.030	0.867	0.800
3 rd Floor	3	0.056	0.054	0.800	0.800
4 th Floor	4	0.075	0.072	0.633	0.600
5 th Floor	5	0.101	0.099	0.867	0.900

Record No.(21)		Shear Force (Kn) for every floor	
Floor No.		Data1	DataQ
GF	0	1926.850	1926.850
1 st Floor	1	1931.300	1926.850
2 ^{sd} Floor	2	1898.192	1867.042
3 rd Floor	3	1812.930	1808.124
4 th Floor	4	1325.744	1320.048
5 th Floor	5	833.040	836.956

Table 6.22. Table Maximum Displacement and inter storey drifts and shear force for every floor Vs along of the height of Building for recording Data1&DataQ.

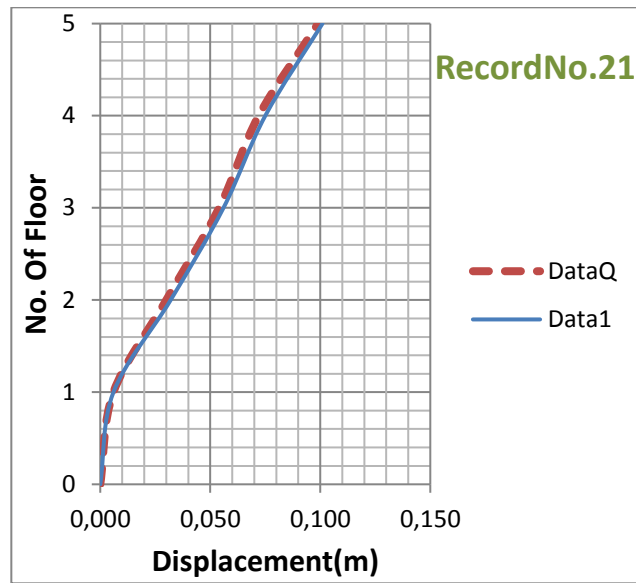


Figure 6.62. Profile of displacements for every floor along of the height of Building.

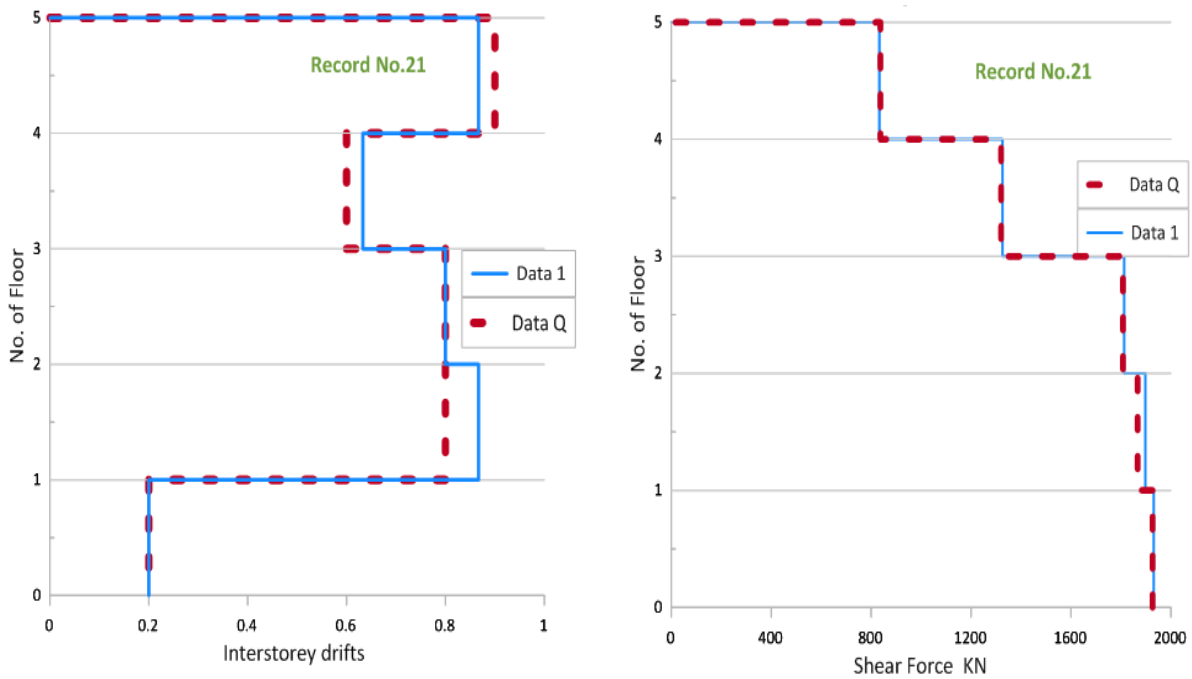


Figure 6.63. Profile of inter storey drifts and shear force for every floor Vs along of the height of Building.



Record 22

Record No.(22)	Data1	DataQ
Time (Sec.)	3.75	1.46
Displacement at the top of building (m)	0.199	0.198

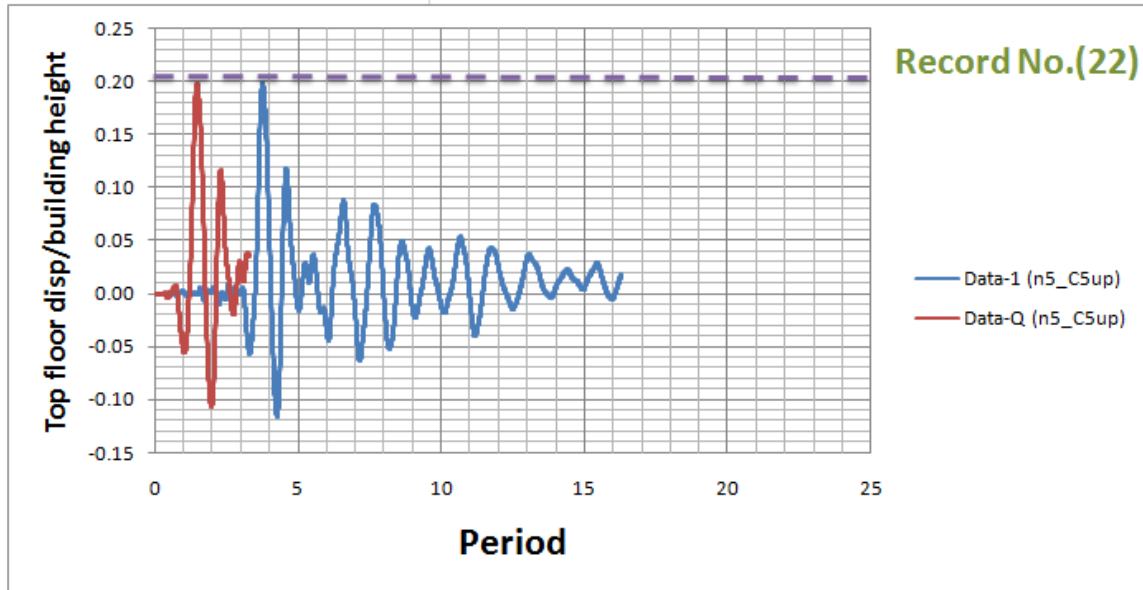


Figure 6.64. Maximum displacement of the original ground motions Data1 and the displacement of DataQ along height of the building.

Height of floor (m)		3			
Record No.(22)		Max. (Disp./height)		Drift(Disp./height)%	
Floor No.		Data1	DataQ	Data1	DataQ
GF	0	0.000	0.000	0.000	0.000
1 st Floor	1	0.065	0.067	2.167	2.233
2 ^{sd} Floor	2	0.144	0.149	2.633	2.733
3 rd Floor	3	0.171	0.175	0.900	0.867
4 th Floor	4	0.187	0.189	0.533	0.467
5 th Floor	5	0.200	0.198	0.433	0.300

Record No.(22)		Shear Force (Kn) for every floor	
Floor No.		Data1	DataQ
GF	0	2936.644	3054.658
1 st Floor	1	2936.644	3054.658
2 ^{sd} Floor	2	2051.272	2016.740
3 rd Floor	3	1765.760	1693.314
4 th Floor	4	962.624	767.358
5 th Floor	5	386.260	271.450

Table 6.23. Table Maximum Displacement and inter storey drifts and shear force for every floor Vs along of the height of Building for recording Data1&DataQ.

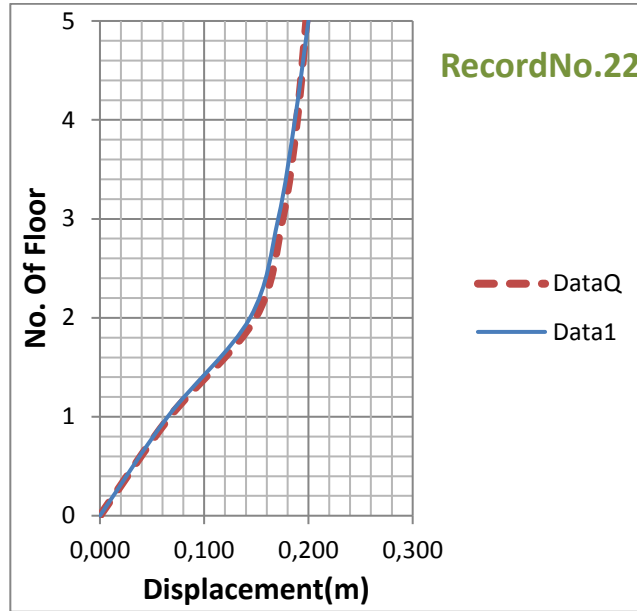


Figure 6.65. Profile of displacements for every floor along of the height of Building.

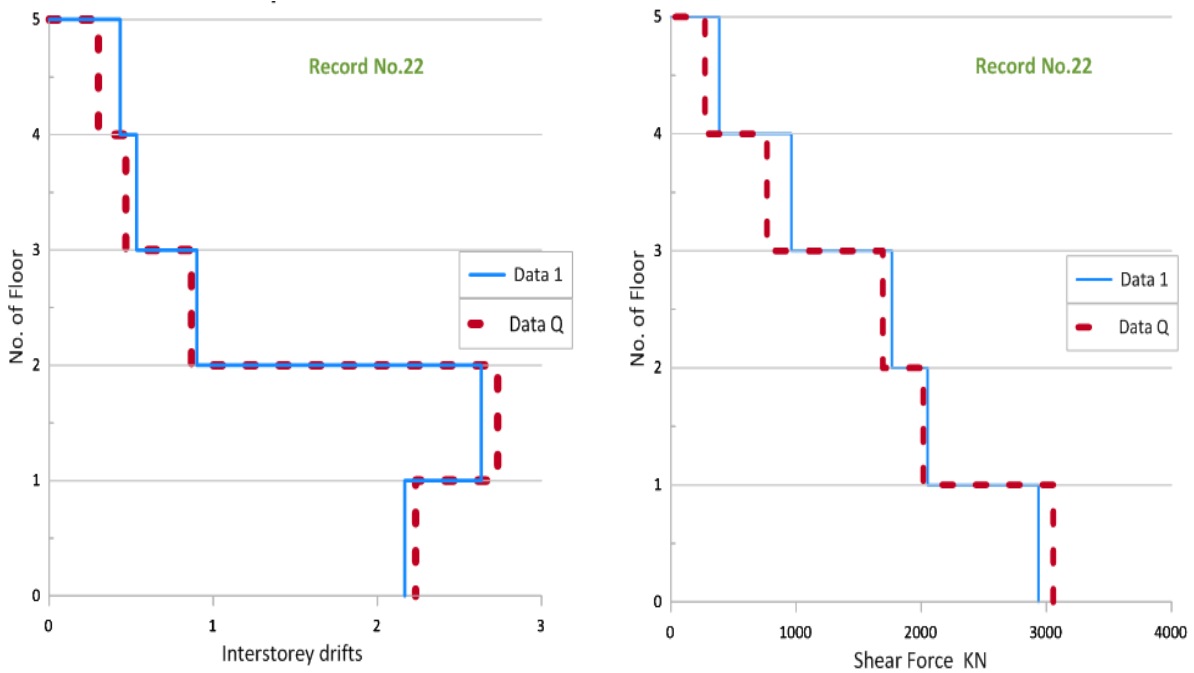


Figure 6.66. Profile of inter storey drifts and shear force for every floor Vs along of the height of Building.



Record 23

Record No.(23)	Data1	DataQ
Time (Sec.)	6.28	1.79
Displacement at the top of building (m)	-0.164	-0.144

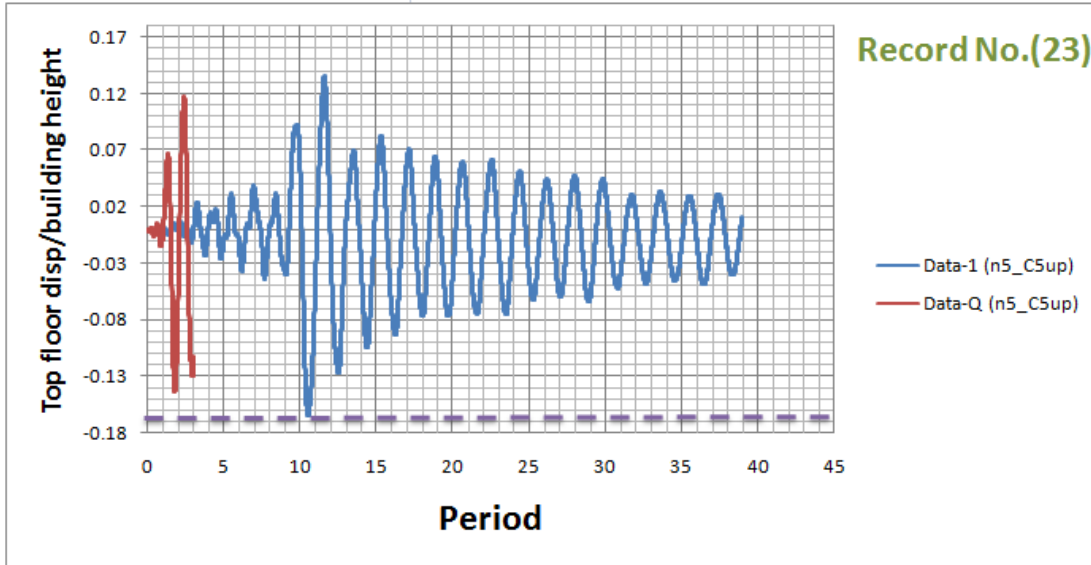


Figure 6.67. Maximum displacement of the original ground motions Data1 and the displacement of DataQ along height of the building.

Height of floor (m)		3			
Record No.(23)		Max. (Disp./height)		Drift(Disp./height)%	
Floor No.		Data1	DataQ	Data1	DataQ
GF	0	0.000	0.000	0.000	0.000
1 st Floor	1	0.040	0.038	1.333	1.267
2 ^{sd} Floor	2	0.102	0.093	2.067	1.833
3 rd Floor	3	0.136	0.117	1.133	0.800
4 th Floor	4	0.152	0.132	0.533	0.500
5 th Floor	5	0.164	0.144	0.400	0.400

Record No.(23)		Shear Force (Kn) for every floor	
Floor No.		Data1	DataQ
GF	0	3258.646	3273.598
1 st Floor	1	3258.646	3273.598
2 ^{sd} Floor	2	2071.742	2090.788
3 rd Floor	3	1819.160	1755.970
4 th Floor	4	1064.440	1069.246
5 th Floor	5	385.370	356.534

Table 6.24. Table Maximum Displacement and inter storey drifts and shear force for every floor Vs along of the height of Building for recording Data1&DataQ.

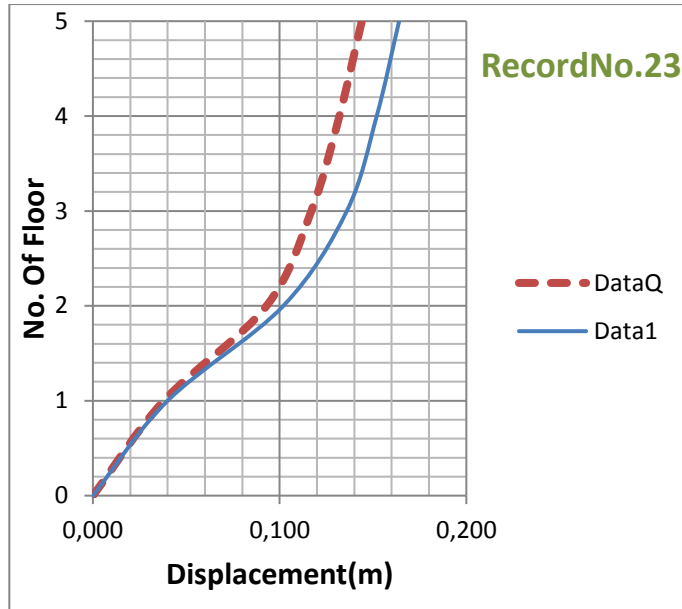


Figure 6.68. Profile of displacements for every floor along of the height of Building.

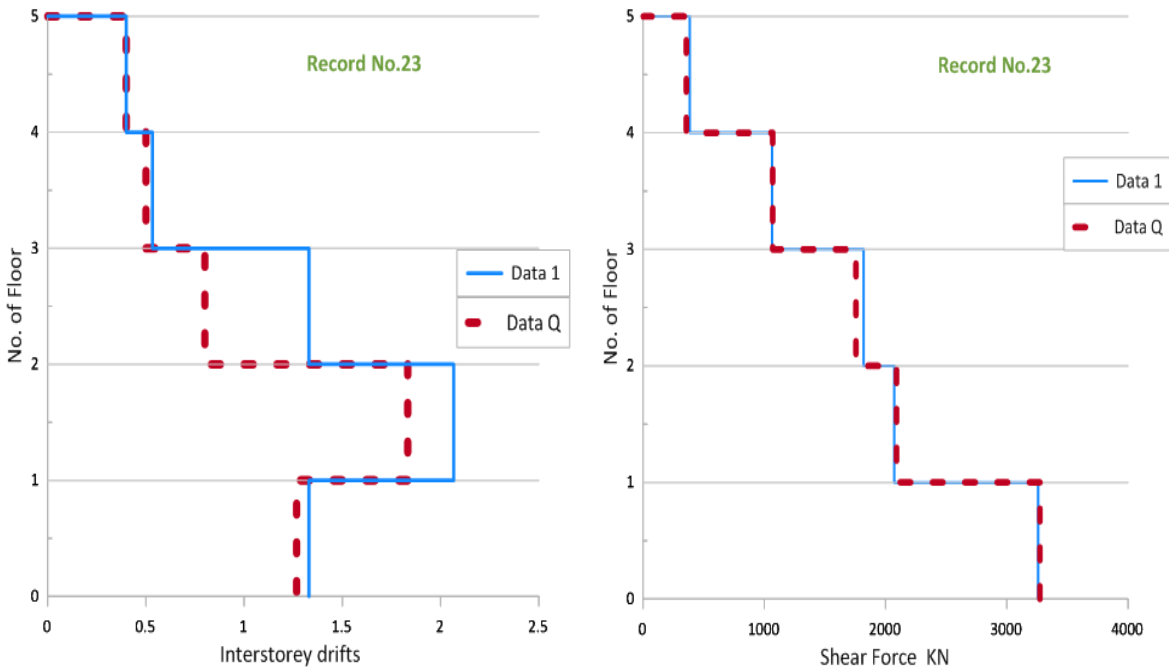


Figure 6.69 Profile of inter storey drifts and shear force for every floor Vs along of the height of Building.



Record 24

Record No.(24)	Data1	DataQ
Time (Sec.)	12.52	2.33
Displacement at the top of building (m)	0.077	0.078

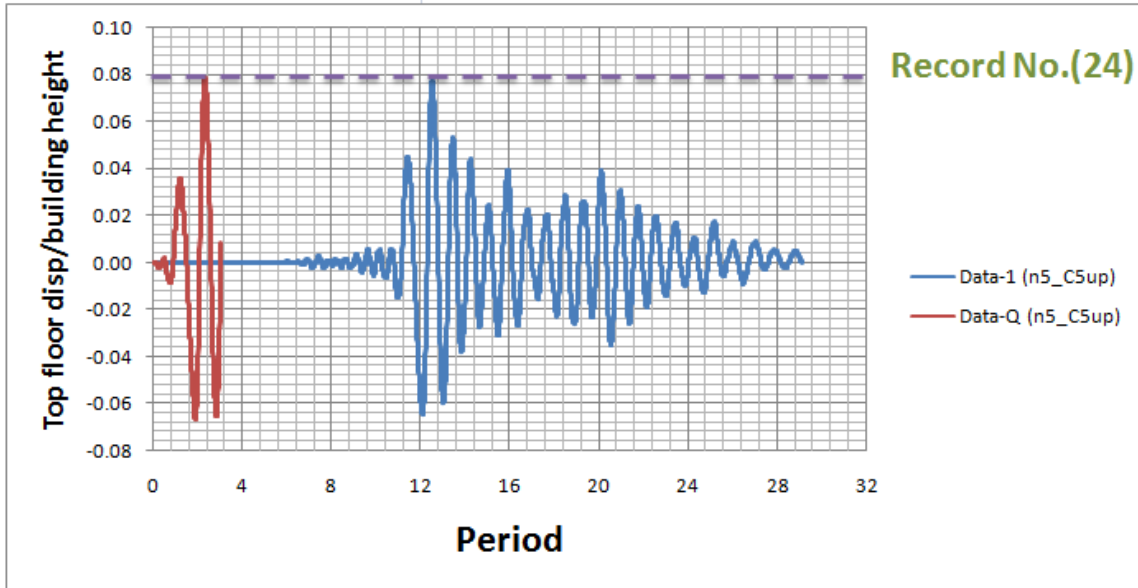


Figure 6.70. Maximum displacement of the original ground motions Data1 and the displacement of DataQ along height of the building.

Height of floor (m)	3				
Record No.(24)	Max. (Disp./height)		Drift(Disp./height)%		
Floor No.	Data1	DataQ	Data1	DataQ	
GF	0	0.000	0.000	0.000	
1 st Floor	1	0.017	0.019	0.567	0.633
2 ^{sd} Floor	2	0.040	0.044	0.767	0.833
3 rd Floor	3	0.056	0.059	0.533	0.500
4 th Floor	4	0.068	0.070	0.400	0.367
5 th Floor	5	0.077	0.078	0.300	0.267

Record No.(24)	Shear Force (Kn) for every floor		
Floor No.	Data1	DataQ	
GF	0	2610.904	2707.914
1 st Floor	1	2610.904	2707.914
2 ^{sd} Floor	2	1861.524	1890.716
3 rd Floor	3	1292.458	1258.282
4 th Floor	4	881.990	810.256
5 th Floor	5	333.216	297.972

Table 6.25. Table Maximum Displacement and inter storey drifts and shear force for every floor Vs along of the height of Building for recording Data1&DataQ.

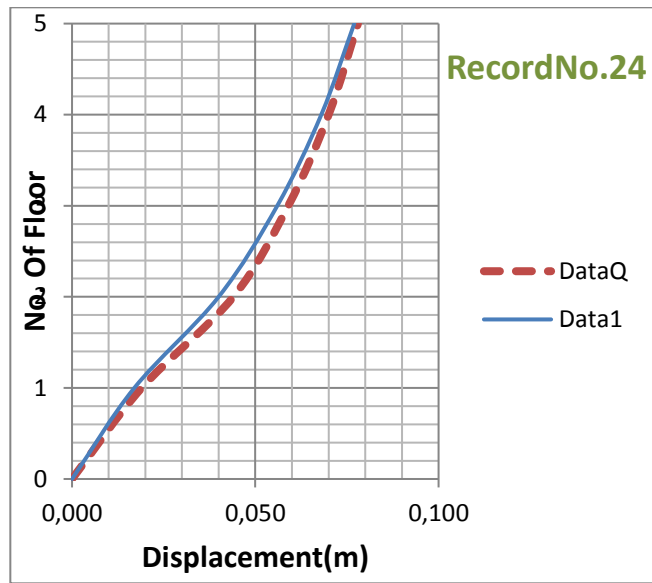


Figure 6.71. Profile of displacements for every floor along of the height of Building.

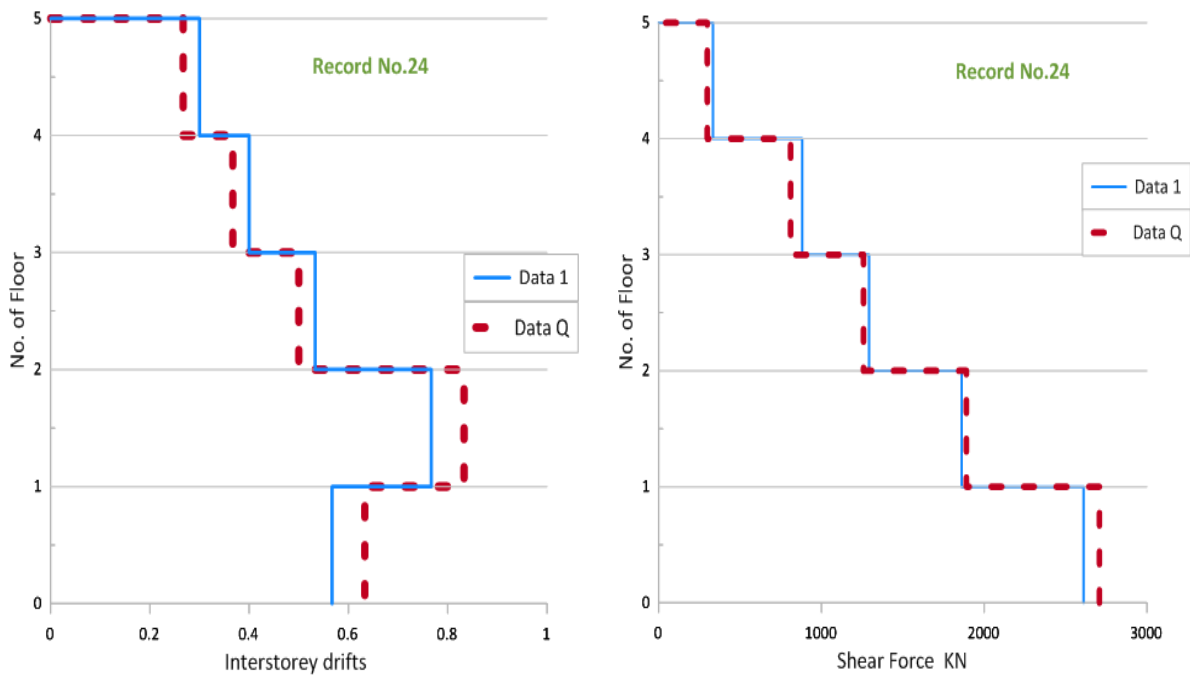


Figure 6.72 Profile of inter storey drifts and shear force for every floor Vs along of the height of Building.



Record 25

Record No.(25)	Data1	DataQ
Time (Sec.)	3.49	1.8
Displacement at the top of building (m)	0.212	0.209

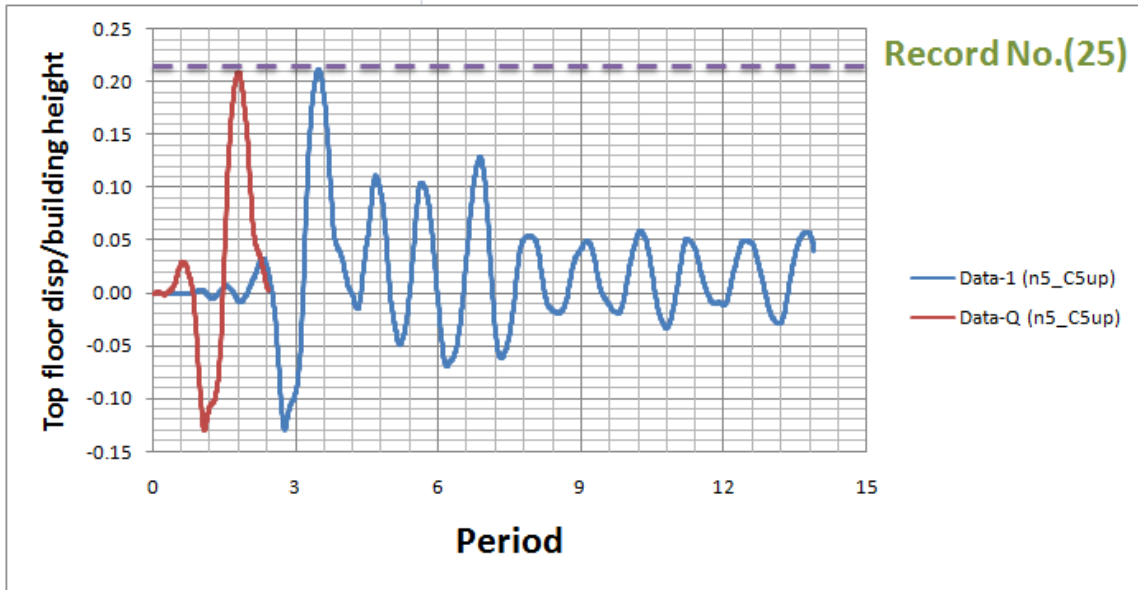


Figure 6.73. Maximum displacement of the original ground motions Data1 and the displacement of DataQ along height of the building.

Height of floor (m)		3			
Record No.(25)		Max. (Disp./height)		Drift(Disp./height)%	
Floor No.		Data1	DataQ	Data1	DataQ
GF	0	0.000	0.000	0.000	0.000
1 st Floor	1	0.070	0.069	2.333	2.300
2 ^{sd} Floor	2	0.160	0.158	3.000	2.967
3 rd Floor	3	0.192	0.190	1.067	1.067
4 th Floor	4	0.205	0.203	0.433	0.433
5 th Floor	5	0.212	0.209	0.233	0.200

Record No.(25)		Shear Force (Kn) for every floor	
Floor No.		Data1	DataQ
GF	0	3160.212	3147.574
1 st Floor	1	3160.212	3147.574
2 ^{sd} Floor	2	1913.322	1922.222
3 rd Floor	3	1190.108	1232.472
4 th Floor	4	531.686	556.962
5 th Floor	5	108.758	92.916

Table 6.26. Table Maximum Displacement and inter storey drifts and shear force for every floor Vs along of the height of Building for recording Data1&DataQ.

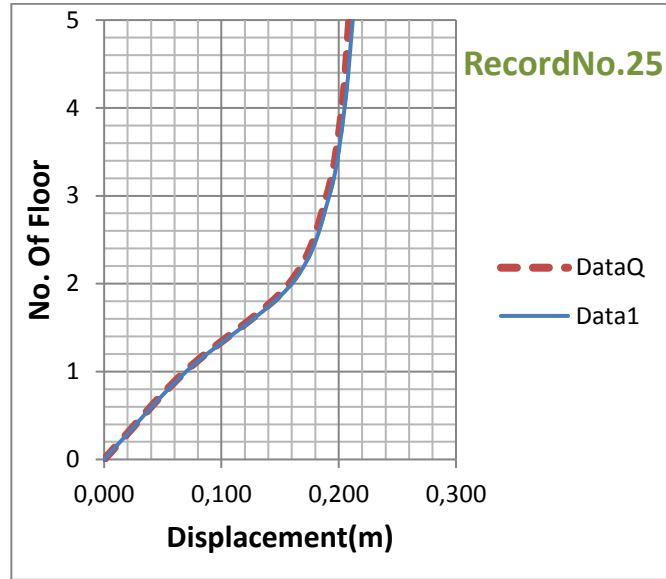


Figure 6.73. Profile of displacements for every floor along of the height of Building.

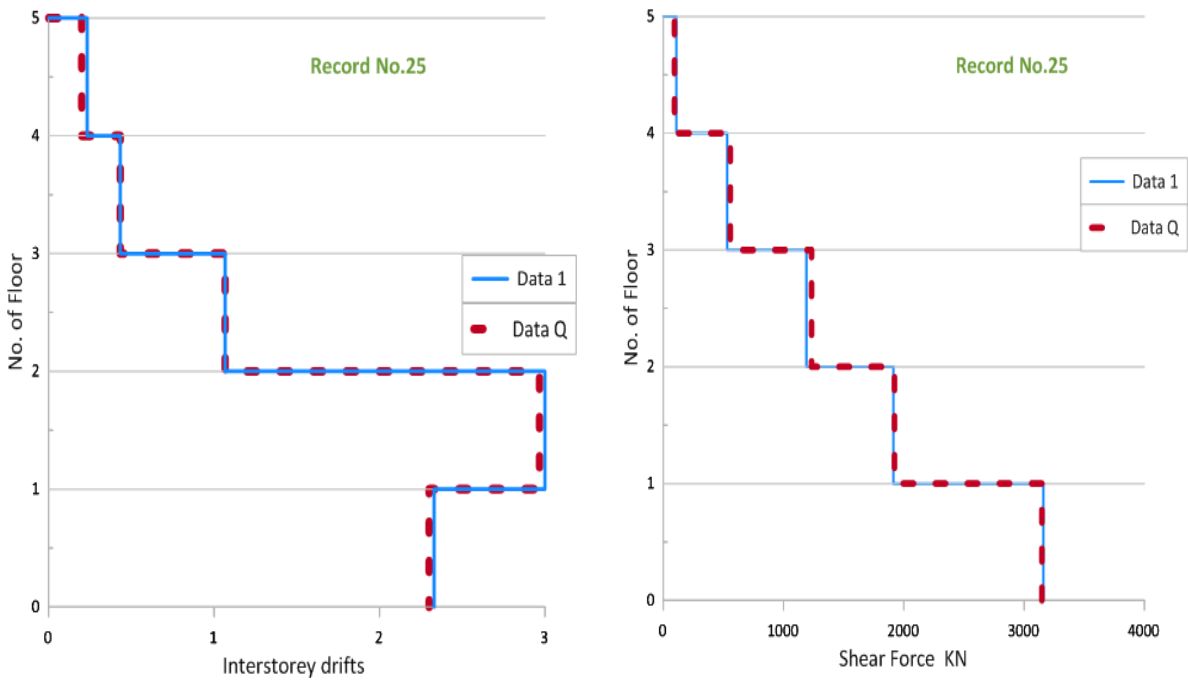


Figure 6.75 Profile of inter storey drifts and shear force for every floor Vs along of the height of Building.



Record 26

Record No.(29)	Data1	DataQ
Time (Sec.)	1.91	1.38
Displacement at the top of building (m)	-0.207	-0.205

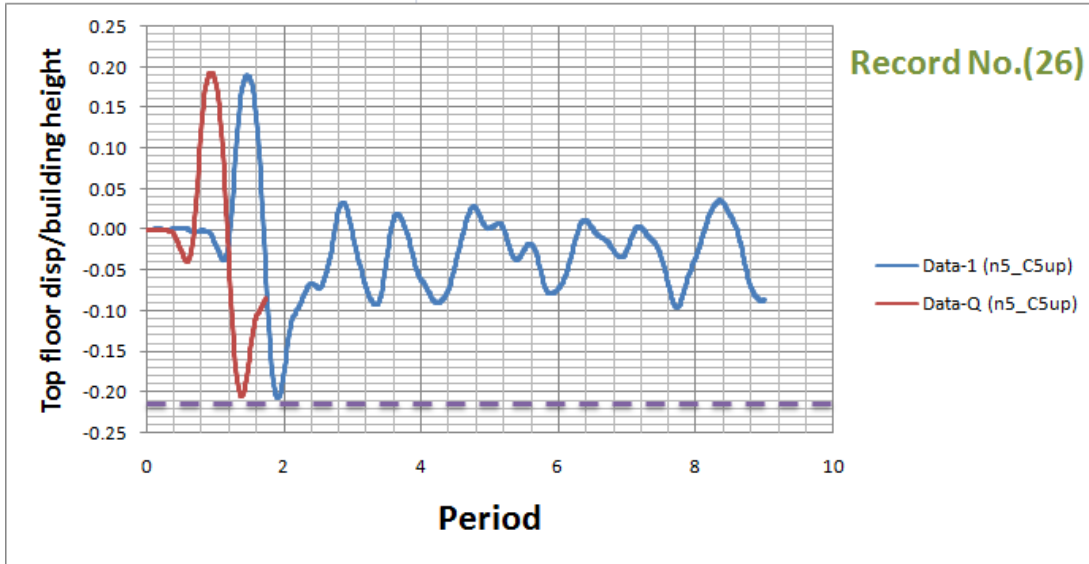


Figure 6.76. Maximum displacement of the original ground motions Data1 and the displacement of DataQ along height of the building.

Height of floor (m)		3			
Record No.(26)		Max. (Disp./height)		Drift(Disp./height)%	
Floor No.		Data1	DataQ	Data1	DataQ
GF	0	0.000	0.000	0.000	0.000
1 st Floor	1	0.021	0.021	0.700	0.700
2 nd Floor	2	0.083	0.082	2.067	2.033
3 rd Floor	3	0.148	0.146	2.167	2.133
4 th Floor	4	0.180	0.177	1.067	1.033
5 th Floor	5	0.207	0.205	0.900	0.933

Record No.(26)		Shear Force (Kn) for every floor	
Floor No.		Data1	DataQ
GF	0	2329.486	2324.146
1 st Floor	1	2329.486	2324.146
2 nd Floor	2	1275.548	1257.748
3 rd Floor	3	1964.052	1959.602
4 th Floor	4	1848.886	1844.792
5 th Floor	5	831.082	834.286

Table 6.27. Table Maximum Displacement and inter storey drifts and shear force for every floor Vs along of the height of Building for recording Data1&DataQ.

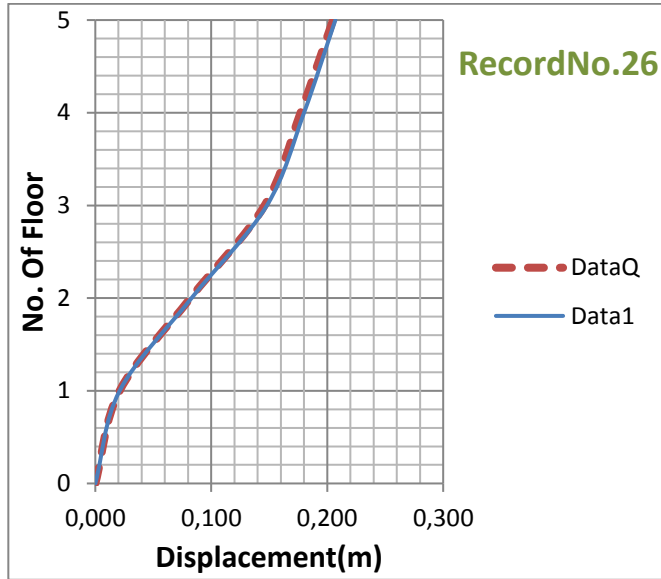


Figure 6.77. Profile of displacements for every floor along of the height of Building.

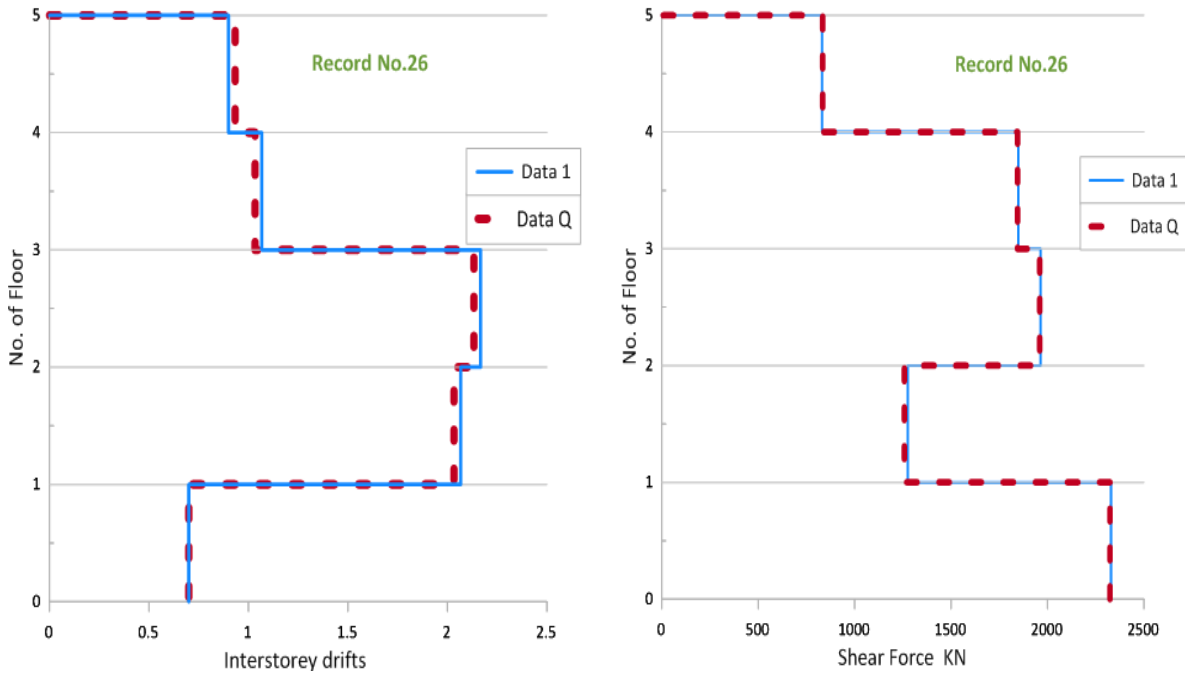


Figure 6.78. Profile of inter storey drifts and shear force for every floor Vs along of the height of Building.



Record 27

Record No.(27)	Data1	DataQ
Time (Sec.)	5.63	1.26
Displacement at the top of building (m)	-0.137	-0.123

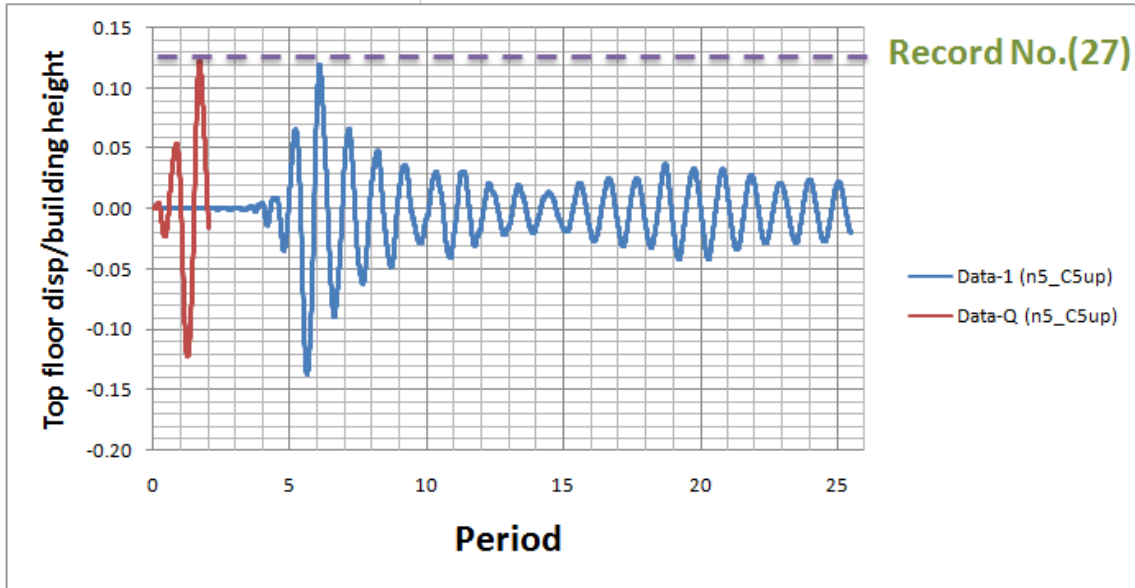


Figure 6.79. Maximum displacement of the original ground motions Data1 and the displacement of DataQ along height of the building.

Height of floor (m)		3			
Record No.(27)		Max. (Disp./height)		Drift(Disp./height)%	
Floor No.		Data1	DataQ	Data1	DataQ
GF	0	0.000	0.000	0.000	0.000
1 st Floor	1	0.032	0.028	1.067	0.933
2 ^{sd} Floor	2	0.080	0.070	1.600	1.400
3 rd Floor	3	0.106	0.094	0.867	0.800
4 th Floor	4	0.122	0.110	0.533	0.533
5 th Floor	5	0.137	0.123	0.500	0.433

Record No.(27)		Shear Force (Kn) for every floor	
Floor No.		Data1	DataQ
GF	0	3245.652	3197.948
1 st Floor	1	3245.652	3197.948
2 ^{sd} Floor	2	2108.054	2110.724
3 rd Floor	3	1801.182	1771.278
4 th Floor	4	1150.592	1137.598
5 th Floor	5	493.060	427.734

Table 6.28. Table Maximum Displacement and inter storey drifts and shear force for every floor Vs along of the height of Building for recording Data1&DataQ.

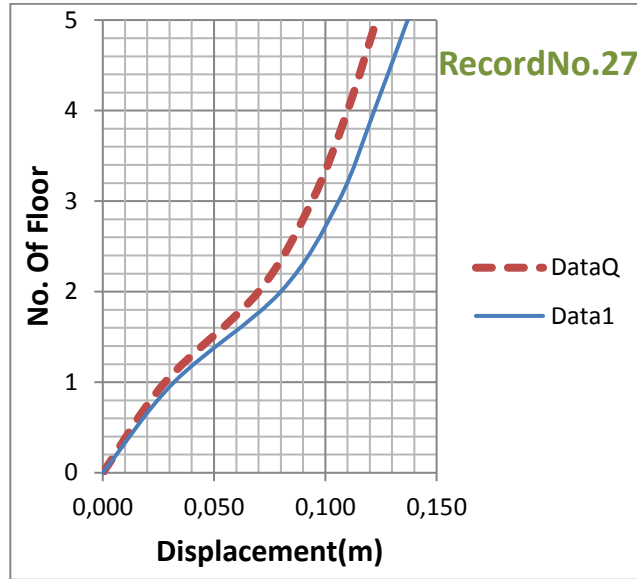


Figure 6.80. Profile of displacements for every floor along of the height of Building.

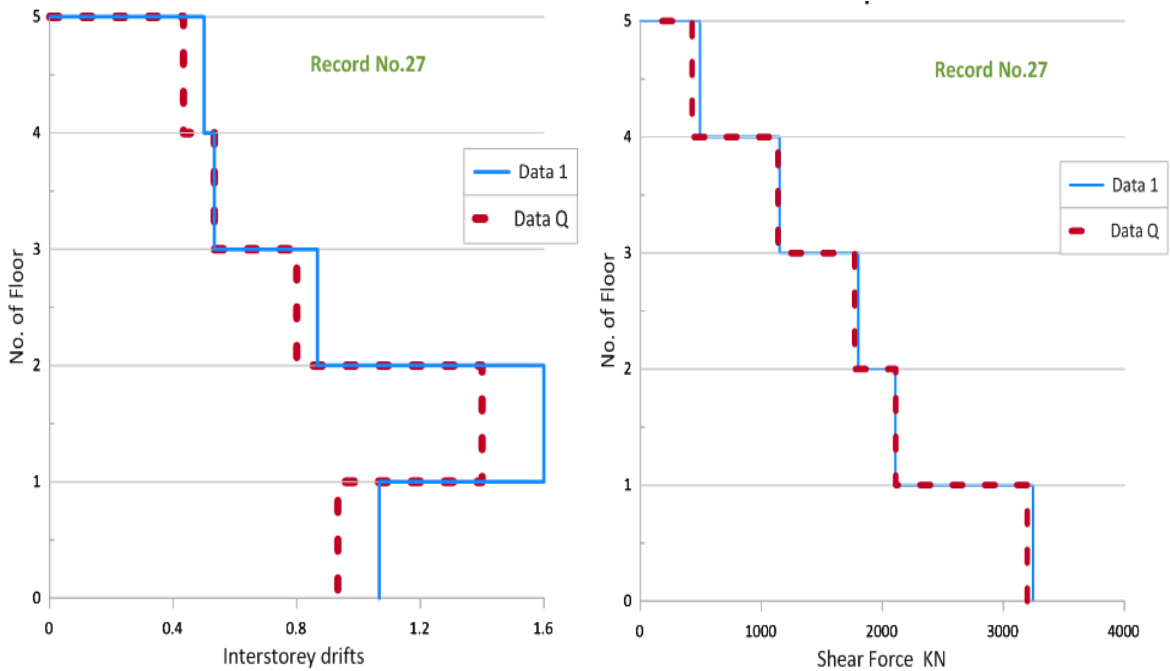


Figure 6.81. Profile of inter storey drifts and shear force for every floor Vs along of the height of Building.



Record 28

Record No.(28)	Data1	DataQ
Time (Sec.)	6.31	1.25
Displacement at the top of building (m)	-0.155	-0.146

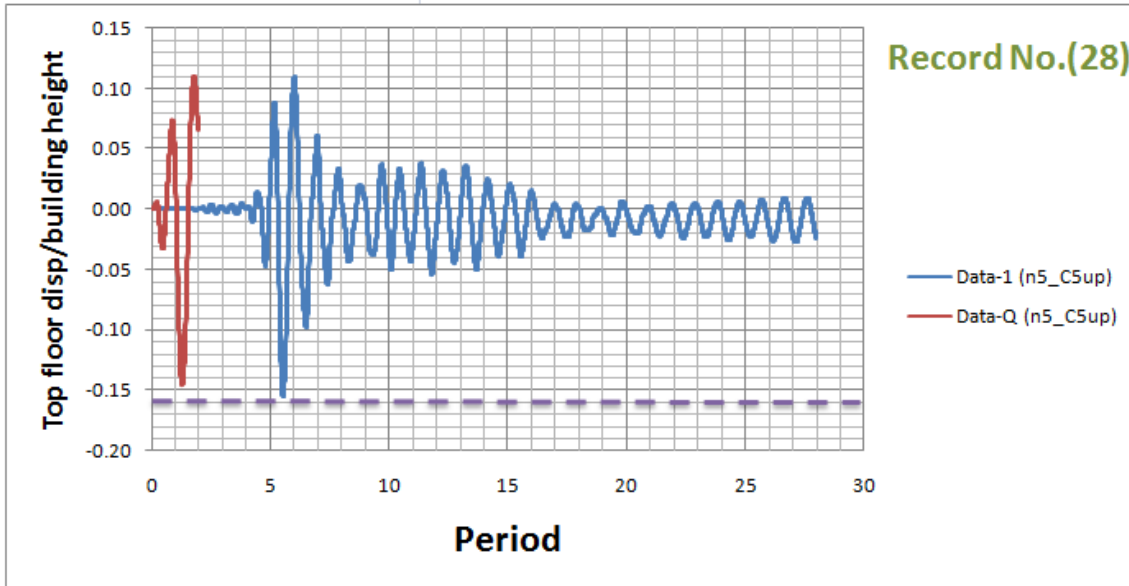


Figure 6.82. Maximum displacement of the original ground motions Data1 and the displacement of DataQ along height of the building.

Height of floor (m)		3			
Record No.(28)		Max. (Disp./height)		Drift(Disp./height)%	
Floor No.		Data1	DataQ	Data1	DataQ
GF	0	0.000	0.000	0.000	0.000
1 st Floor	1	0.040	0.035	1.333	1.167
2 ^{sd} Floor	2	0.099	0.090	1.967	1.833
3 rd Floor	3	0.126	0.118	0.900	0.933
4 th Floor	4	0.142	0.133	0.533	0.500
5 th Floor	5	0.155	0.146	0.433	0.433

Record No.(28)		Shear Force (Kn) for every floor	
Floor No.		Data1	DataQ
GF	0	1682.456	2278.222
1 st Floor	1	1682.456	2278.222
2 ^{sd} Floor	2	1097.726	2079.218
3 rd Floor	3	649.344	1609.298
4 th Floor	4	727.664	1134.572
5 th Floor	5	273.052	327.342

Table 6.29. Table Maximum Displacement and inter storey drifts and shear force for every floor Vs along of the height of Building for recording Data1&DataQ.

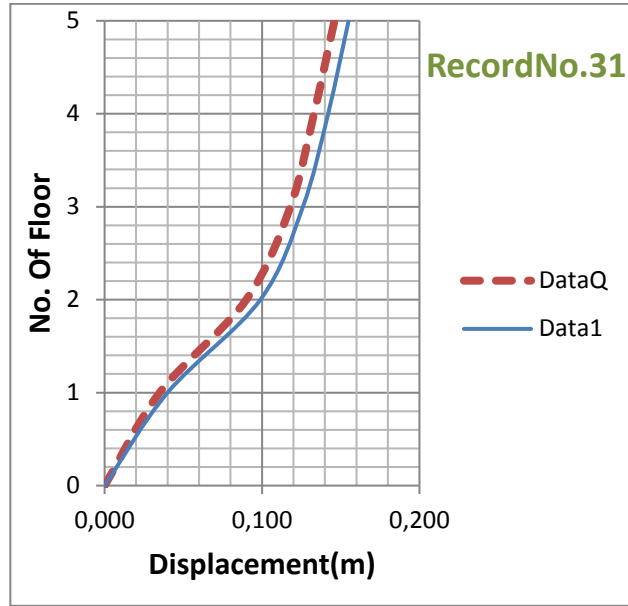


Figure 6.83. Profile of displacements for every floor along of the height of Building.

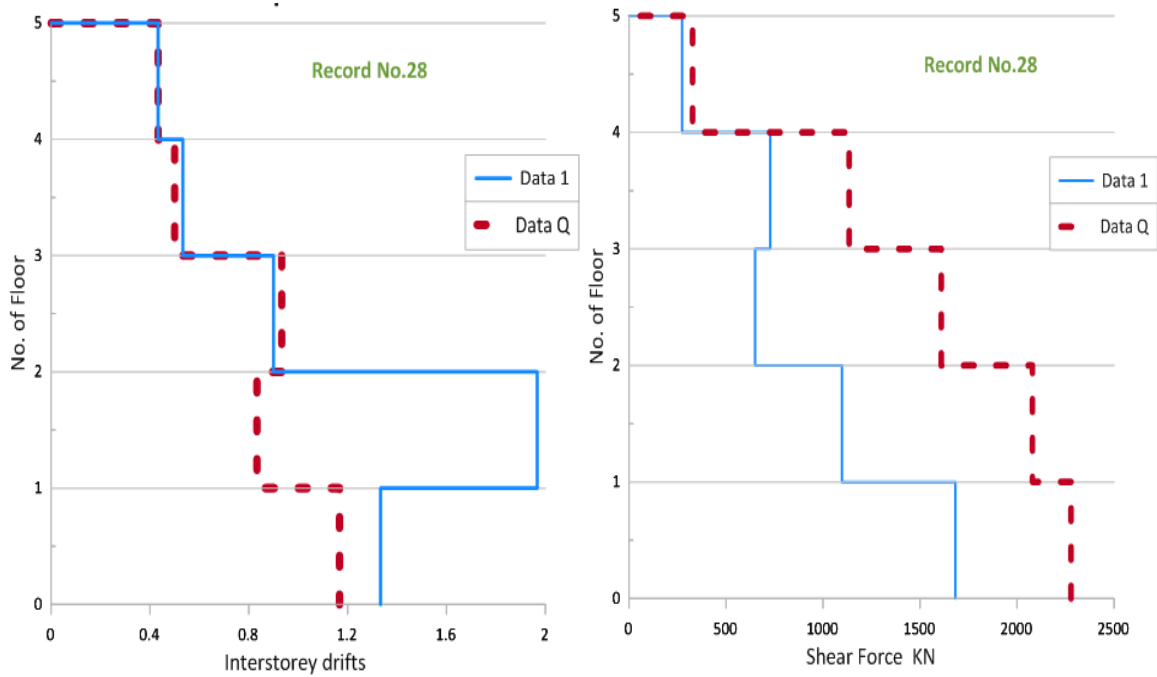


Figure 6.84. Profile of inter storey drifts and shear force for every floor Vs along of the height of Building.



Record 29

Record No.(29)	Data1	DataQ
Time (Sec.)	12.74	6.51
Displacement at the top of building (m)	0.065	0.069

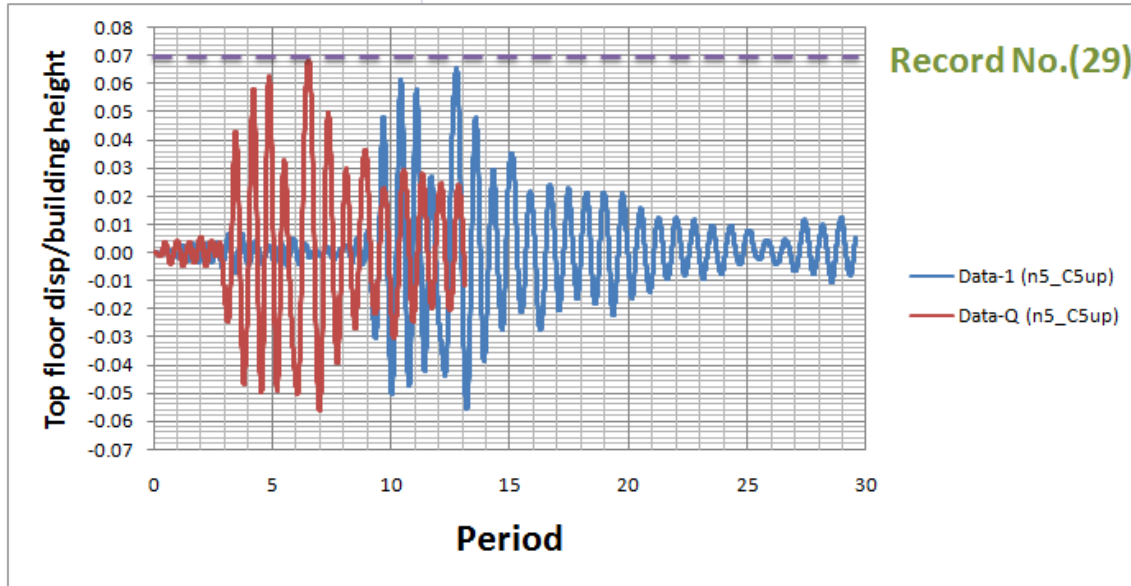


Figure 6.85. Maximum displacement of the original ground motions Data1 and the displacement of DataQ along height of the building.

Height of floor (m)		3			
Record No.(29)		Max.(Disp./height)		Drift(Disp./height)%	
Floor No.		Data1	DataQ	Data1	DataQ
GF	0	0.000	0.000	0.000	0.000
1 st Floor	1	0.016	0.018	0.533	0.600
2 ^{sd} Floor	2	0.034	0.037	0.600	0.633
3 rd Floor	3	0.047	0.051	0.433	0.467
4 th Floor	4	0.057	0.061	0.333	0.333
5 th Floor	5	0.065	0.069	0.267	0.267

Record No.(29)		Shear Force (Kn) for every floor	
Floor No.		Data1	DataQ
GF	0	2404.246	2665.372
1 st Floor	1	2404.246	2665.372
2 ^{sd} Floor	2	1599.686	1627.276
3 rd Floor	3	1150.770	1144.718
4 th Floor	4	715.560	718.586
5 th Floor	5	316.128	293.344

Table 6.30. Table Maximum Displacement and inter storey drifts and shear force for every floor Vs along of the height of Building for recording Data1&DataQ.

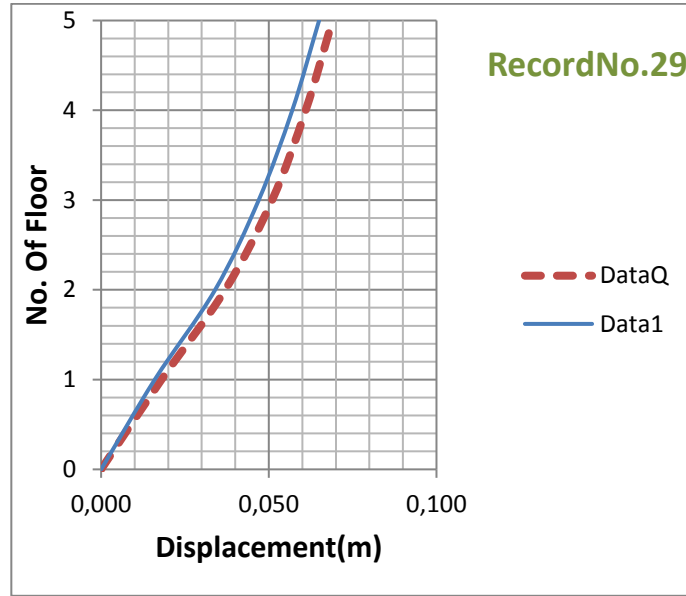


Figure 6.86. Profile of displacements for every floor along of the height of Building.

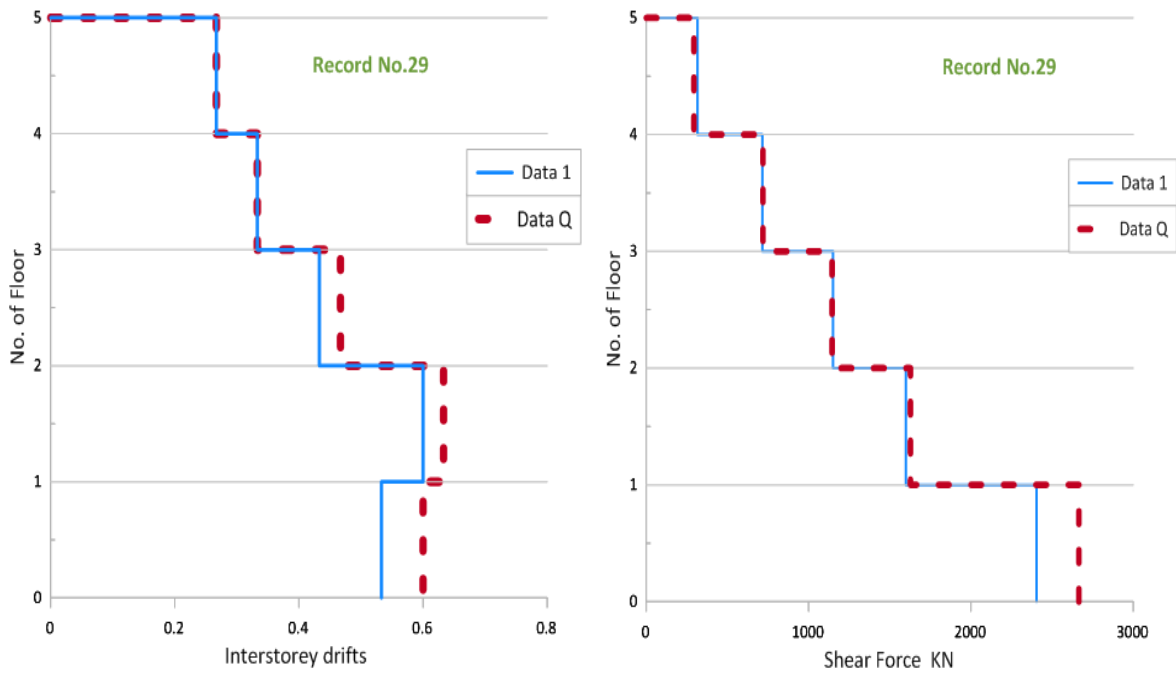


Figure 6.87. Profile of inter storey drifts and shear force for every floor Vs along of the height of Building.



Record 30

Record No.(30)	Data1	DataQ
Time (Sec.)	5.77	4.6
Displacement at the top of building (m)	0.117	0.117

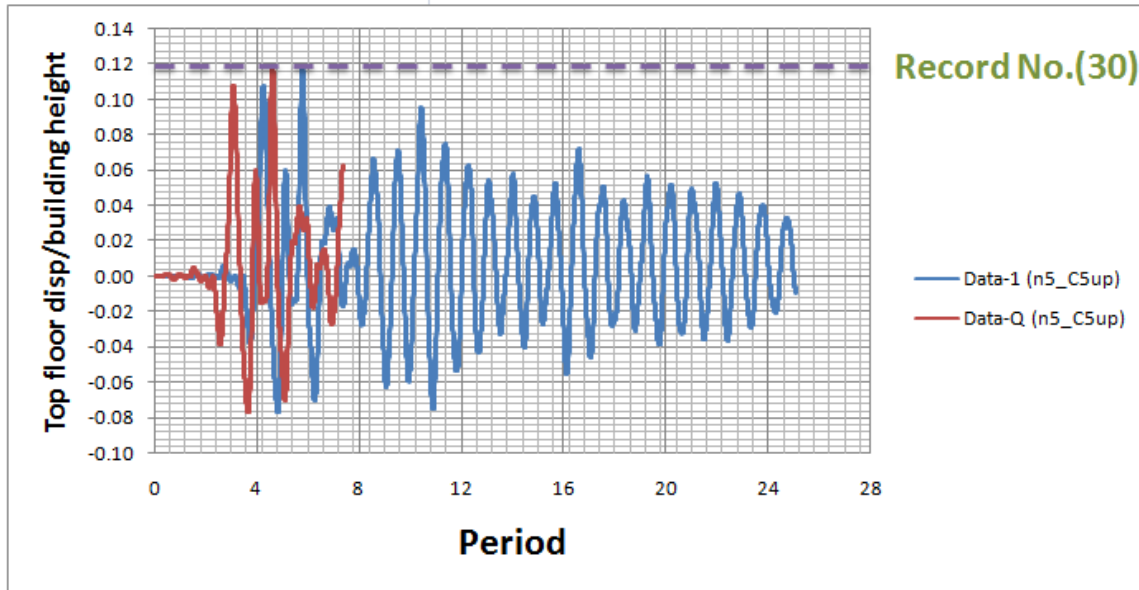


Figure 6.88. Maximum displacement of the original ground motions Data1 and the displacement of DataQ along height of the building.

Height of floor (m)		3			
Record No.(30)		Max. (Disp./height)		Drift(Disp./height)%	
Floor No.		Data1	DataQ	Data1	DataQ
GF	0	0.000	0.000	0.000	0.000
1 st Floor	1	0.012	0.012	0.400	0.400
2 nd Floor	2	0.038	0.038	0.867	0.867
3 rd Floor	3	0.064	0.064	0.867	0.867
4 th Floor	4	0.087	0.087	0.767	0.767
5 th Floor	5	0.117	0.117	1.000	1.000

Record No.(30)		Shear Force (KN) for every floor	
Floor No.		Data1	DataQ
GF	0	1924.002	1919.730
1 st Floor	1	1924.002	1919.730
2 nd Floor	2	1861.702	1855.828
3 rd Floor	3	1836.426	1839.808
4 th Floor	4	1647.390	1637.244
5 th Floor	5	848.170	848.170

Table 6.31. Table Maximum Displacement and inter storey drifts and shear force for every floor Vs along of the height of Building for recording Data1&DataQ.

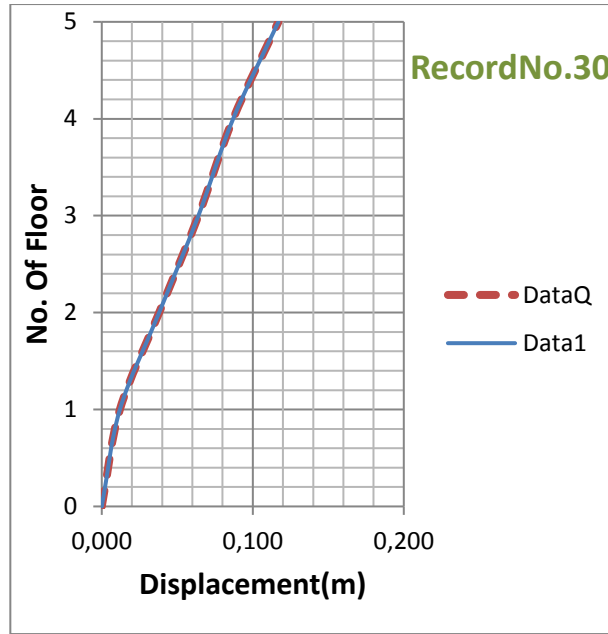


Figure 6.89. Profile of displacements for every floor along of the height of Building.

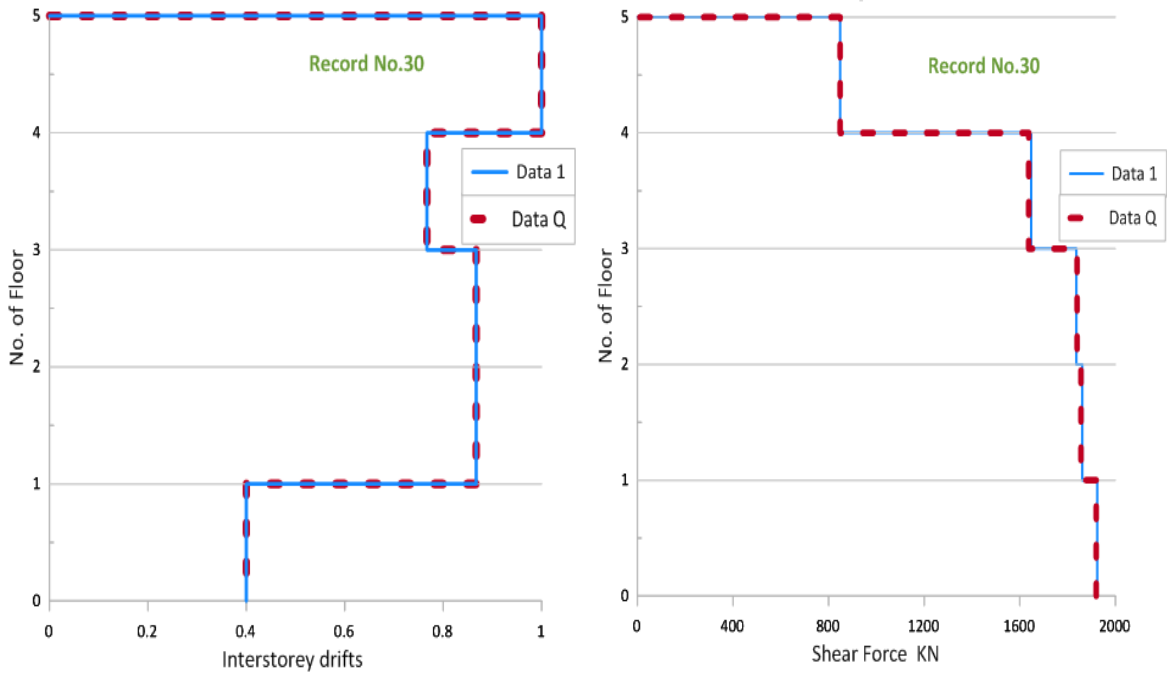


Figure 6.90. Profile of inter storey drifts and shear force for every floor Vs along of the height of Building.



Record 31

Record No.(31)	Data1	DataQ
Time (Sec.)	6.14	3.63
Displacement at the top of building (m)	0.116	0.116

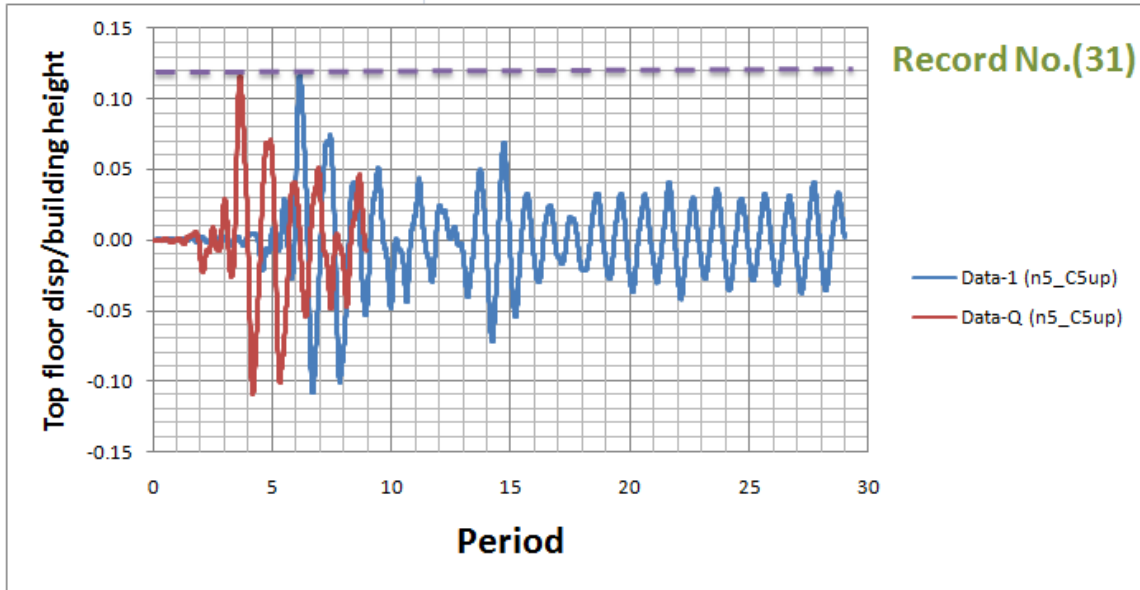


Figure 6.91 Maximum displacement of the original ground motions Data1 and the displacement of DataQ along height of the building.

Height of floor (m)		3			
Record No.(31)		Max.(Disp./height)		Drift(Disp./height)%	
Floor No.		Data1	DataQ	Data1	DataQ
GF	0	0.000	0.000	0.000	0.000
1 st Floor	1	0.020	0.019	0.667	0.633
2 ^{sd} Floor	2	0.059	0.057	1.300	1.267
3 rd Floor	3	0.087	0.086	0.933	0.967
4 th Floor	4	0.104	0.103	0.567	0.567
5 th Floor	5	0.116	0.116	0.400	0.433

Record No.(31)		Shear Force (KN) for every floor	
Floor No.		Data1	DataQ
GF	0	2561.064	2489.330
1 st Floor	1	2561.064	2489.330
2 ^{sd} Floor	2	2101.646	2103.248
3 rd Floor	3	1813.642	1822.898
4 th Floor	4	1134.928	1164.298
5 th Floor	5	425.064	447.136

Table 6.32. Table Maximum Displacement and inter storey drifts and shear force for every floor Vs along of the height of Building for recording Data1&DataQ.

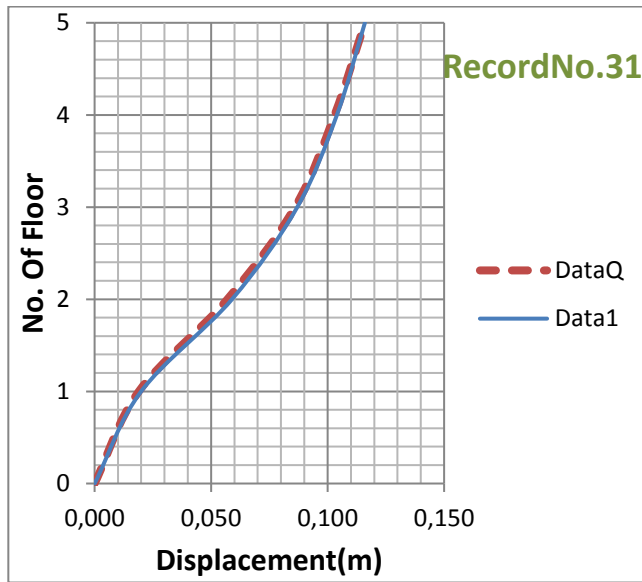


Figure 6.92. Profile of displacements for every floor along of the height of Building.

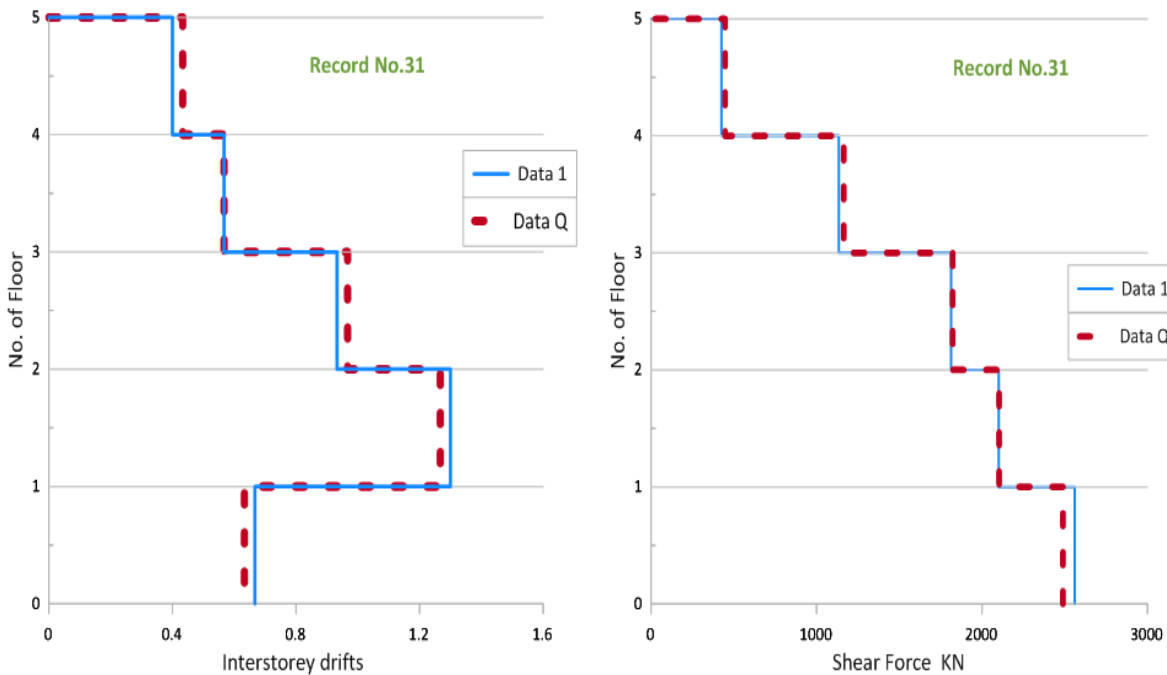


Figure 6.93. Profile of inter storey drifts and shear force for every floor Vs along of the height of Building.



Record 32

Record No.(32)	Data1	DataQ
Time (Sec.)	3.42	2.25
Displacement at the top of building (m)	-0.326	-0.316

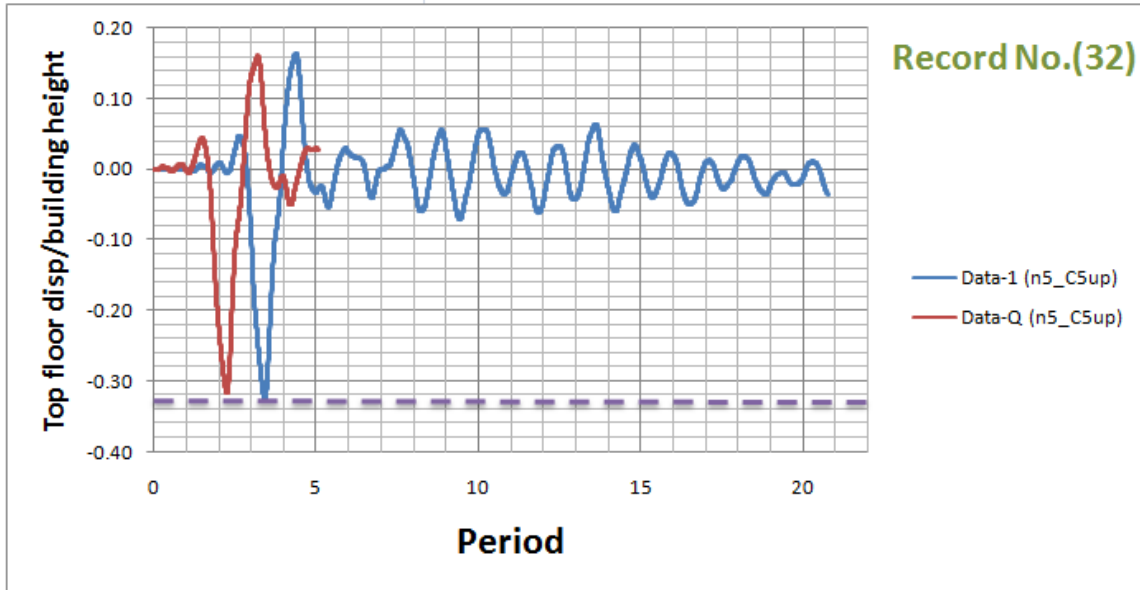


Figure 6.94 Maximum displacement of the original ground motions Data1 and the displacement of DataQ along height of the building.

Height of floor (m)		3			
Record No.(32)		Max.(Disp./height)		Drift(Disp./height)%	
Floor No.		Data1	DataQ	Data1	DataQ
GF	0	0.000	0.000	0.000	0.000
1 st Floor	1	0.150	0.143	5.000	4.767
2 ^{sd} Floor	2	0.274	0.266	4.133	4.100
3 rd Floor	3	0.299	0.289	0.833	0.767
4 th Floor	4	0.313	0.304	0.467	0.500
5 th Floor	5	0.326	0.316	0.433	0.400

Record No.(32)		Shear Force (KN) for every floor	
Floor No.		Data1	DataQ
GF	0	2246.182	2205.598
1 st Floor	1	2246.182	2205.598
2 ^{sd} Floor	2	1966.722	1973.130
3 rd Floor	3	1606.628	1614.104
4 th Floor	4	937.882	946.426
5 th Floor	5	426.844	401.390

Table 6.33. Table Maximum Displacement and inter storey drifts and shear force for every floor Vs along of the height of Building for recording Data1&DataQ.

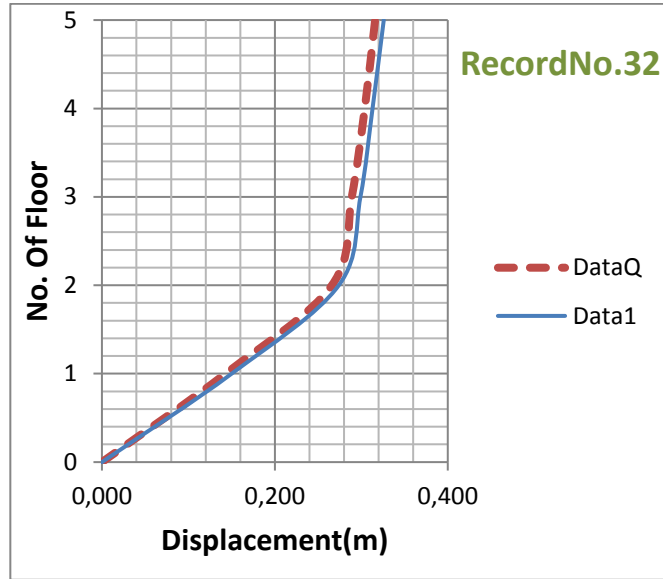


Figure 6.95. Profile of displacements for every floor along of the height of Building.

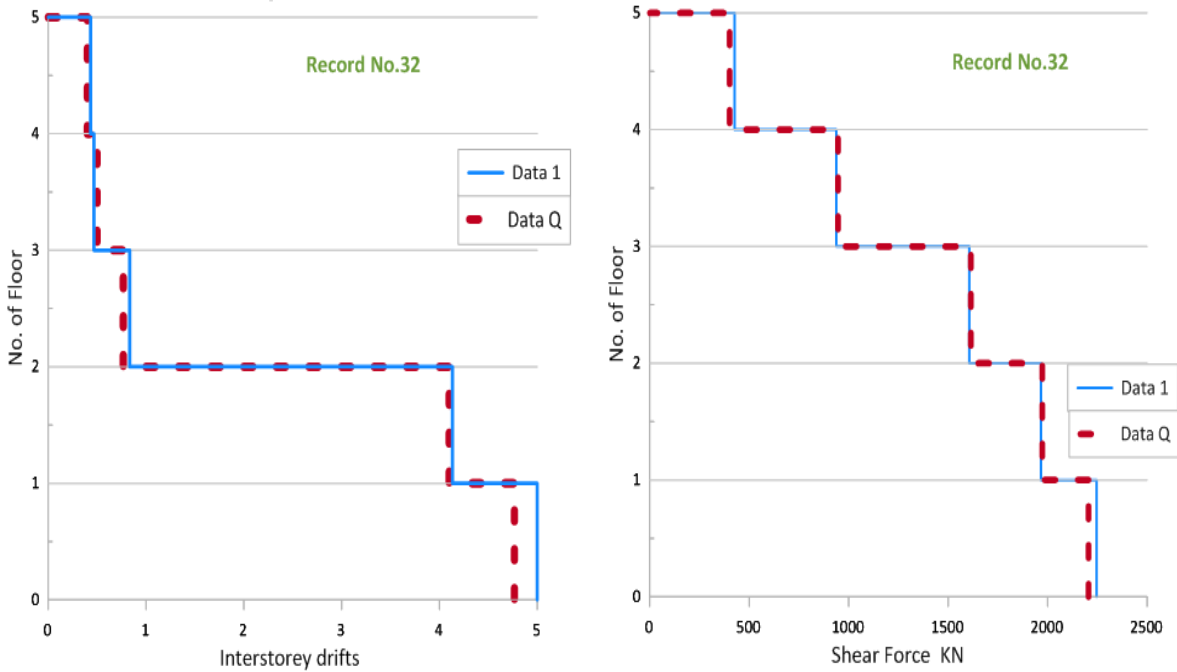


Figure 6.96. Profile of inter storey drifts and shear force for every floor Vs along of the height of Building.



Record 33

Record No.(33)	Data1	DataQ
Time (Sec.)	3.6	2.69
Displacement at the top of building (m)	0.205	0.226

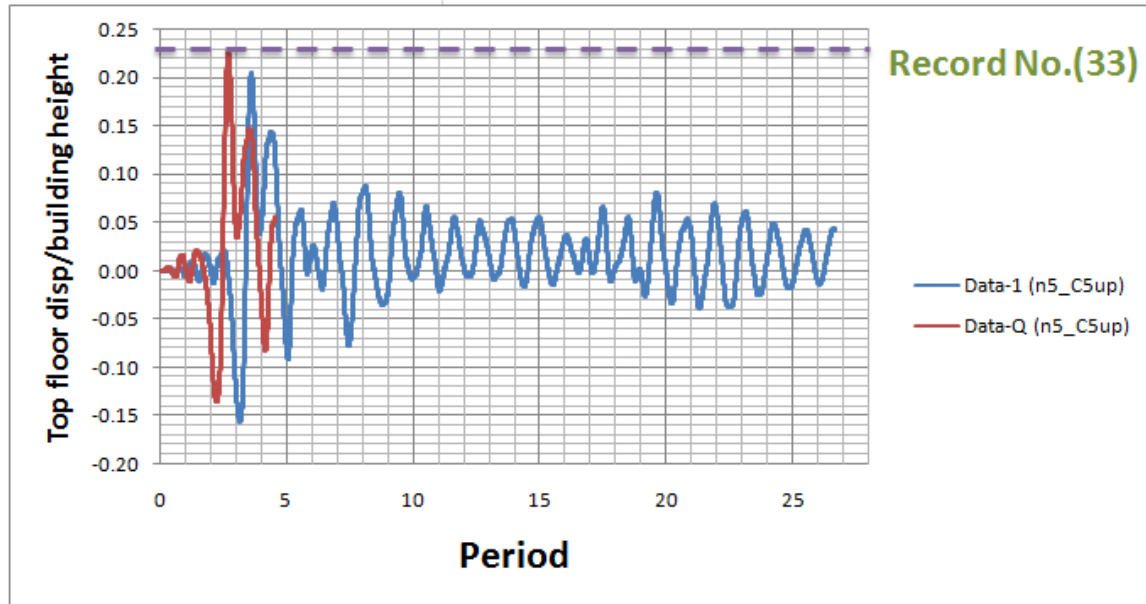


Figure 6.97 Maximum displacement of the original ground motions Data1 and the displacement of DataQ along height of the building.

Height of floor (m)		3			
Record No.(33)		Max.(Disp./height)		Drift(Disp./height)%	
Floor No.		Data1	DataQ	Data1	DataQ
GF	0	0.000	0.000	0.000	0.000
1 st Floor	1	0.046	0.049	1.533	1.633
2 ^{sd} Floor	2	0.133	0.138	2.900	2.967
3 rd Floor	3	0.176	0.191	1.433	1.767
4 th Floor	4	0.193	0.211	0.567	0.667
5 th Floor	5	0.205	0.226	0.400	0.500

Record No.(33)		Shear Force (Kn) for every floor	
Floor No.		Data1	DataQ
GF	0	2572.634	2775.910
1 st Floor	1	2572.634	2775.910
2 ^{sd} Floor	2	2074.234	2066.580
3 rd Floor	3	1901.574	1919.730
4 th Floor	4	1003.030	1248.314
5 th Floor	5	354.932	444.288

Table 6.34. Table Maximum Displacement and inter storey drifts and shear force for every floor Vs along of the height of Building for recording Data1&DataQ.

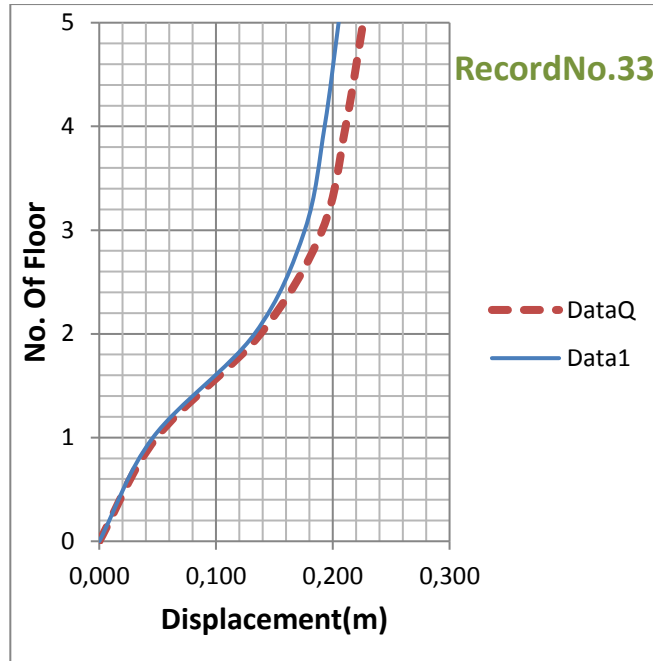


Figure 6.98. Profile of displacements for every floor along of the height of Building.

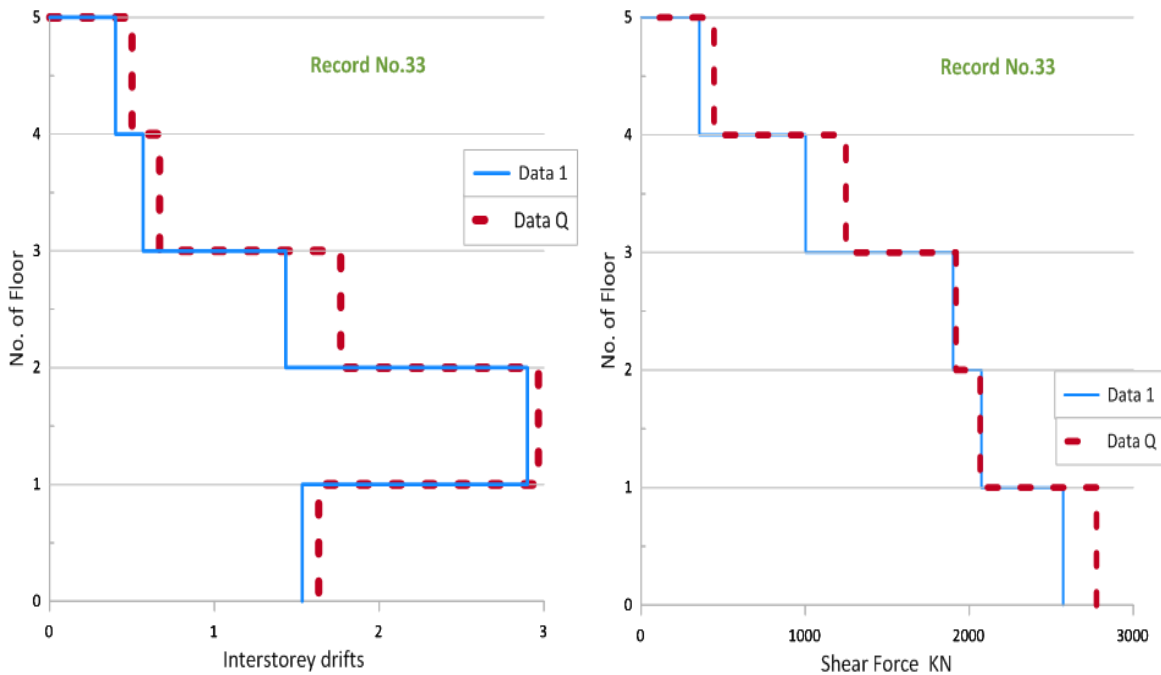


Figure 6.99. Profile of inter storey drifts and shear force for every floor Vs along of the height of Building.



Record 34

Record No.(34)	Data1	DataQ
Time (Sec.)	17.46	7.11
Displacement at the top of building (m)	0.09	0.091

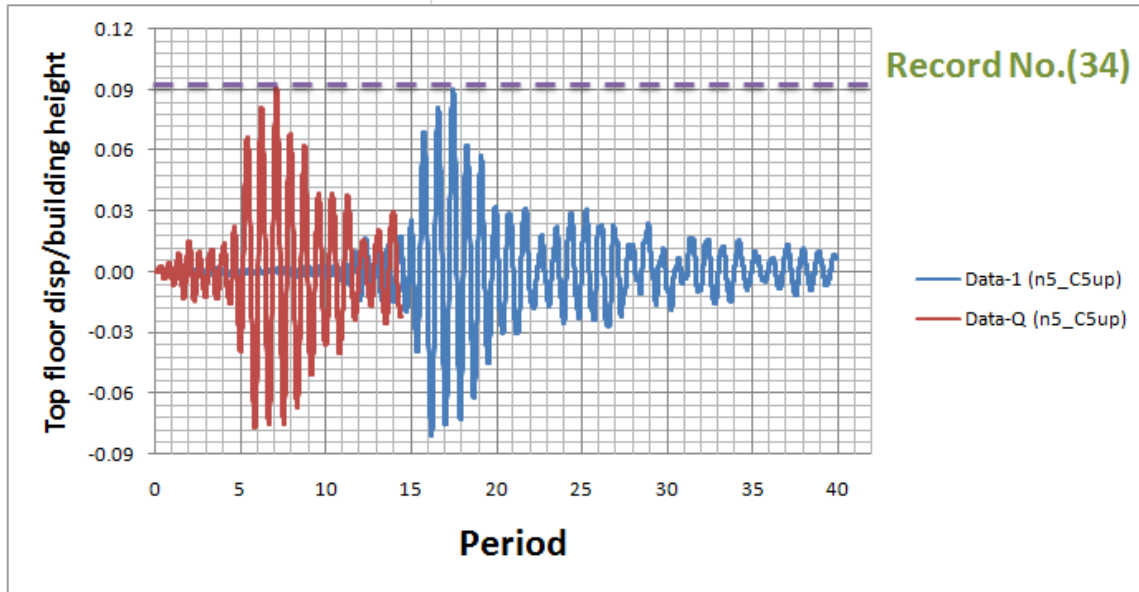


Figure 6.100. Maximum displacement of the original ground motions Data1 and the displacement of DataQ along height of the building.

Height of floor (m)		3			
Record No.(34)		Max. (Disp./height)		Drift (Disp./height)%	
Floor No.		Data1	DataQ	Data1	DataQ
GF	0	0.000	0.000	0.000	0.000
1 st Floor	1	0.018	0.018	0.600	0.600
2 ^{sd} Floor	2	0.045	0.044	0.900	0.867
3 rd Floor	3	0.064	0.064	0.633	0.667
4 th Floor	4	0.077	0.078	0.433	0.467
5 th Floor	5	0.090	0.091	0.433	0.433

Record No.(34)		Shear Force (Kn) for every floor	
Floor No.		Data1	DataQ
GF	0	2620.516	2578.508
1 st Floor	1	2620.516	2578.508
2 ^{sd} Floor	2	1927.384	1946.608
3 rd Floor	3	1553.228	1547.888
4 th Floor	4	945.358	1009.972
5 th Floor	5	456.392	486.830

Table 6.35. Table Maximum Displacement and inter storey drifts and shear force for every floor Vs along of the height of Building for recording Data1&DataQ.

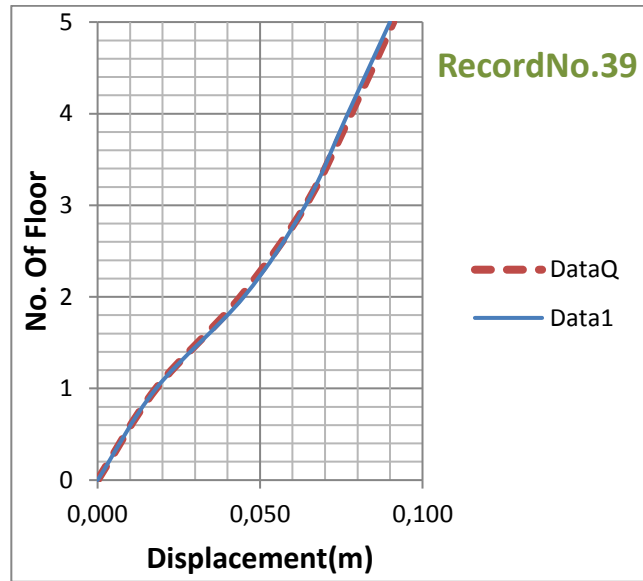


Figure 6.101. Profile of displacements for every floor along of the height of Building.

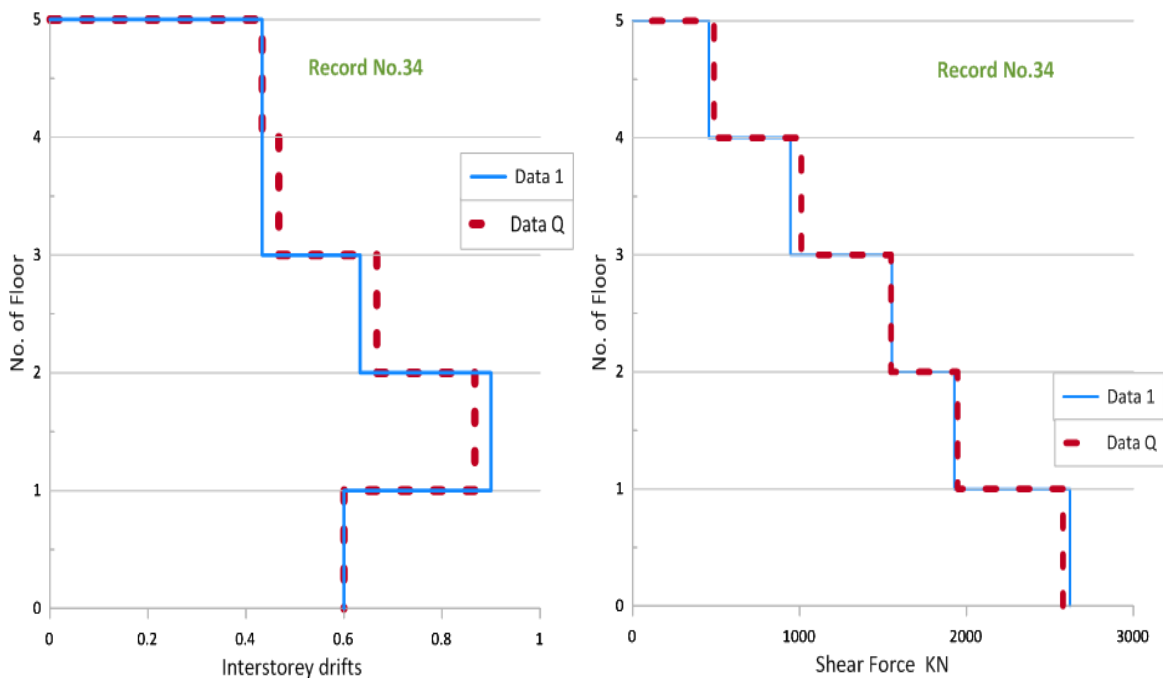


Figure 6.102. Profile of inter storey drifts and shear force for every floor Vs along of the height of Building.



Record 35

Record No.(35)	Data1	DataQ
Time (Sec.)	10.87	3.86
Displacement at the top of building (m)	0.171	0.167

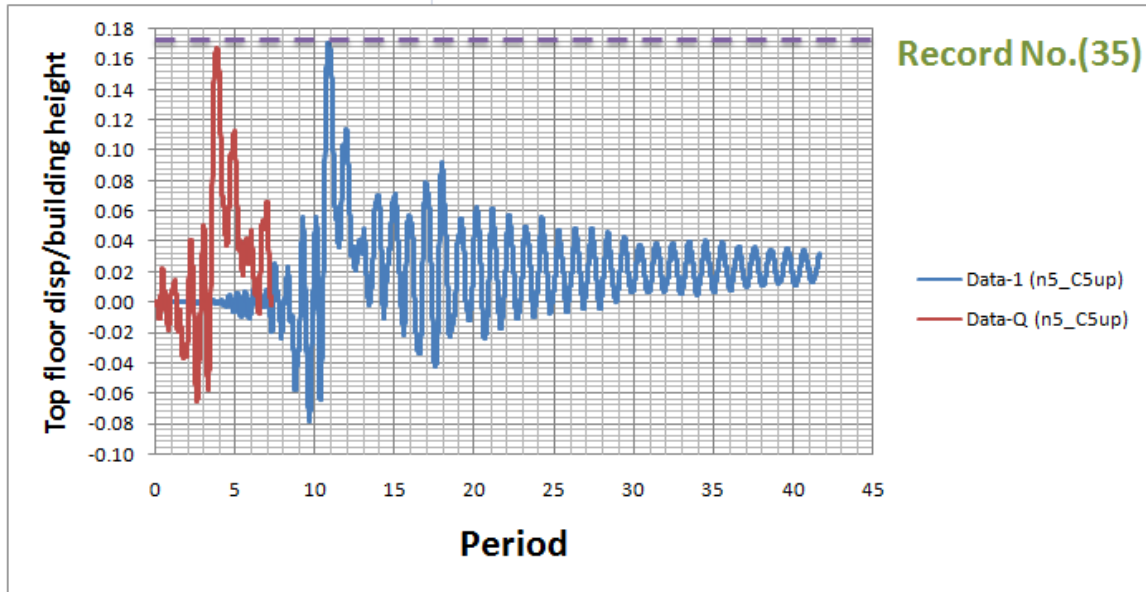


Figure 6.103. Maximum displacement of the original ground motions Data1 and the displacement of DataQ along height of the building.

Height of floor (m)		3			
Record No.(35)		Max.(Disp./height)		Drift(Disp./height)%	
Floor No.		Data1	DataQ	Data1	DataQ
GF	0	0.000	0.000	0.000	0.000
1 st Floor	1	0.063	0.068	2.100	2.267
2 ^{sd} Floor	2	0.130	0.132	2.233	2.133
3 rd Floor	3	0.151	0.148	0.700	0.533
4 th Floor	4	0.160	0.157	0.300	0.300
5 th Floor	5	0.171	0.167	0.367	0.333

Record No.(35)		Shear Force (Kn) for every floor	
Floor No.		Data1	DataQ
GF	0	3196.346	3152.380
1 st Floor	1	3196.346	3152.380
2 ^{sd} Floor	2	2001.966	1844.970
3 rd Floor	3	1259.350	1042.902
4 th Floor	4	465.648	480.778
5 th Floor	5	242.792	269.136

Table 6.36. Table Maximum Displacement and inter storey drifts and shear force for every floor Vs along of the height of Building for recording Data1&DataQ.

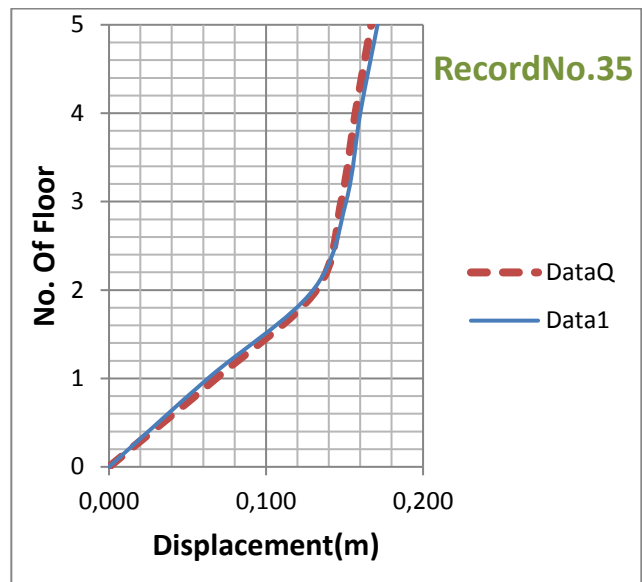


Figure 6.104. Profile of displacements for every floor along of the height of Building.

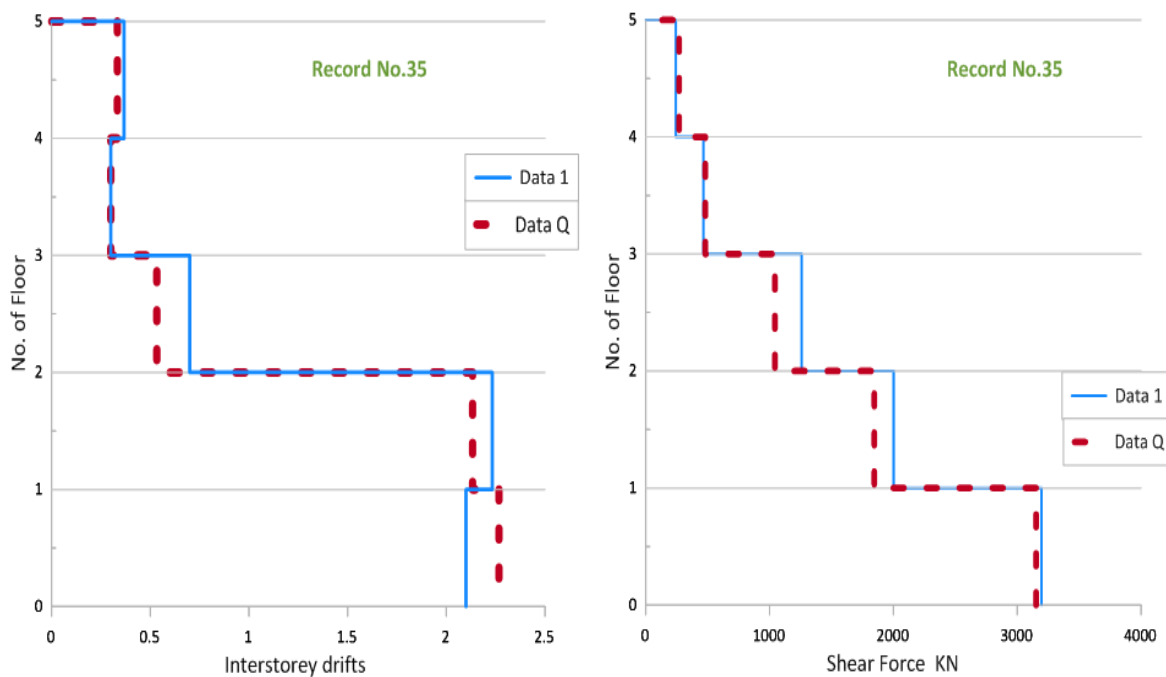


Figure 6.105. Profile of inter storey drifts and shear force for every floor Vs along of the height of Building.



Record 36

Record No.(36)	Data1	DataQ
Time (Sec.)	19.69	8.75
Displacement at the top of building (m)	-0.12	-0.117

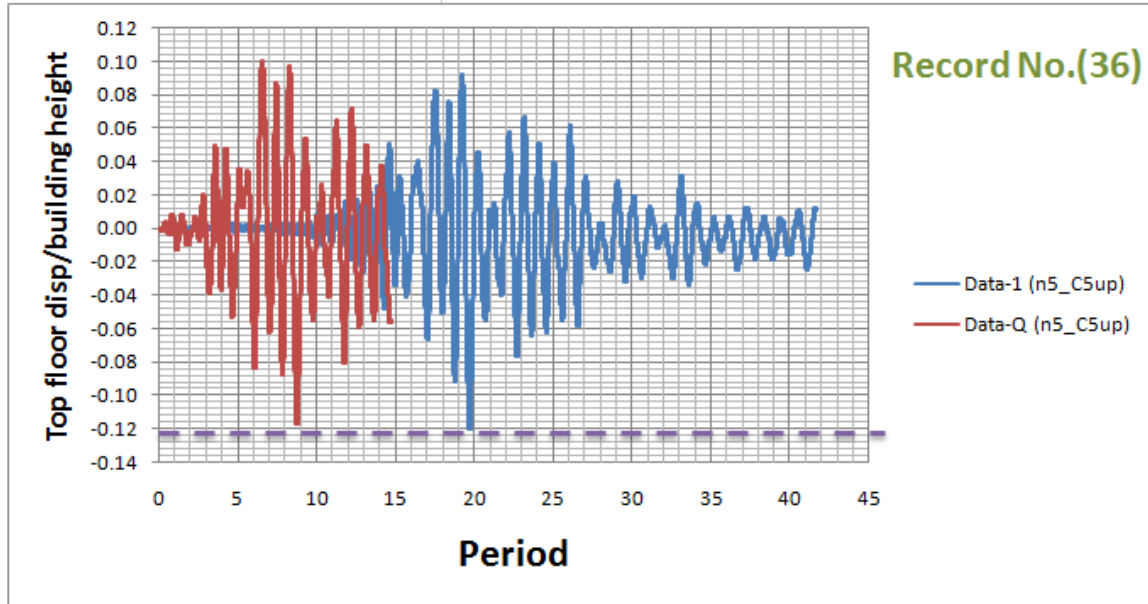


Figure 6.106. Maximum displacement of the original ground motions Data1 and the displacement of DataQ along height of the building.

Height of floor (m)		3			
Record No.(36)		Max. (Disp./height)		Drift(Disp./height)%	
Floor No.		Data1	DataQ	Data1	DataQ
GF	0	0.000	0.000	0.000	0.000
1 st Floor	1	0.030	0.030	1.000	1.000
2 ^{sd} Floor	2	0.071	0.066	1.367	1.200
3 rd Floor	3	0.091	0.088	0.667	0.733
4 th Floor	4	0.105	0.101	0.467	0.433
5 th Floor	5	0.120	0.117	0.500	0.533

Record No.(36)		Shear Force (Kn) for every floor	
Floor No.		Data1	DataQ
GF	0	3220.020	3208.628
1 st Floor	1	3220.020	3208.628
2 ^{sd} Floor	2	2058.748	2029.912
3 rd Floor	3	1499.828	1467.076
4 th Floor	4	1070.314	976.330
5 th Floor	5	519.048	590.782

Table 6.37. Table Maximum Displacement and inter storey drifts and shear force for every floor Vs along of the height of Building for recording Data1&DataQ.

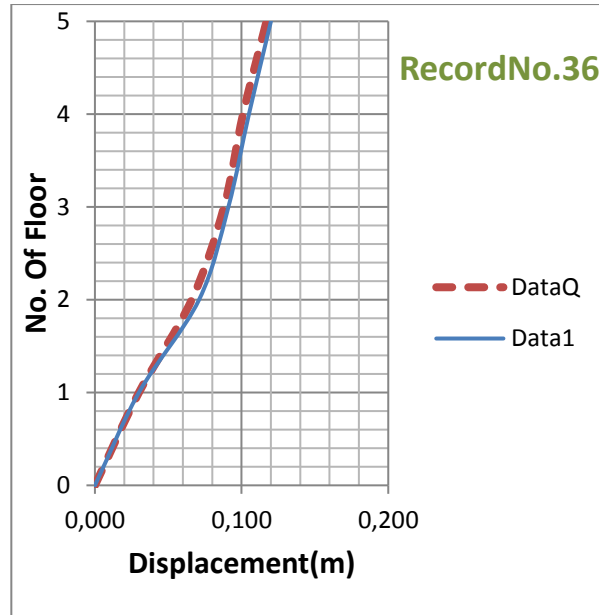


Figure 6.107. Profile of displacements for every floor along of the height of Building.

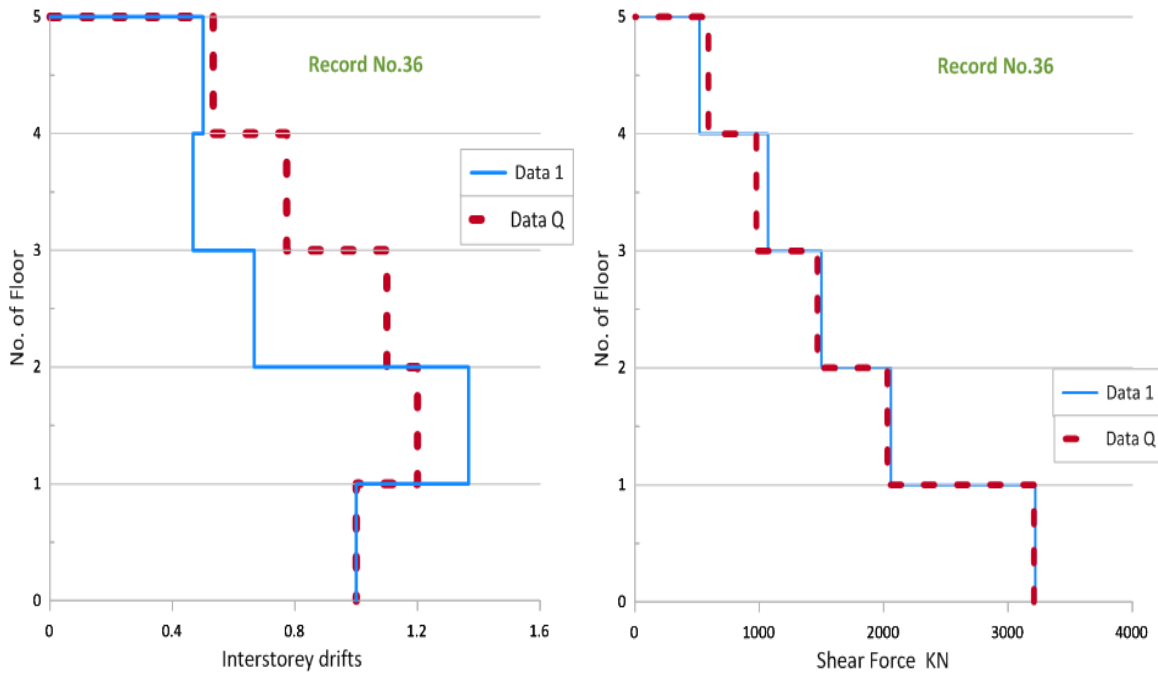


Figure 6.108. Profile of inter storey drifts and shear force for every floor Vs along of the height of Building.



Record 37

Record No.(37)	Data1	DataQ
Time (Sec.)	7.44	7.43
Displacement at the top of building (m)	-0.12	-0.12

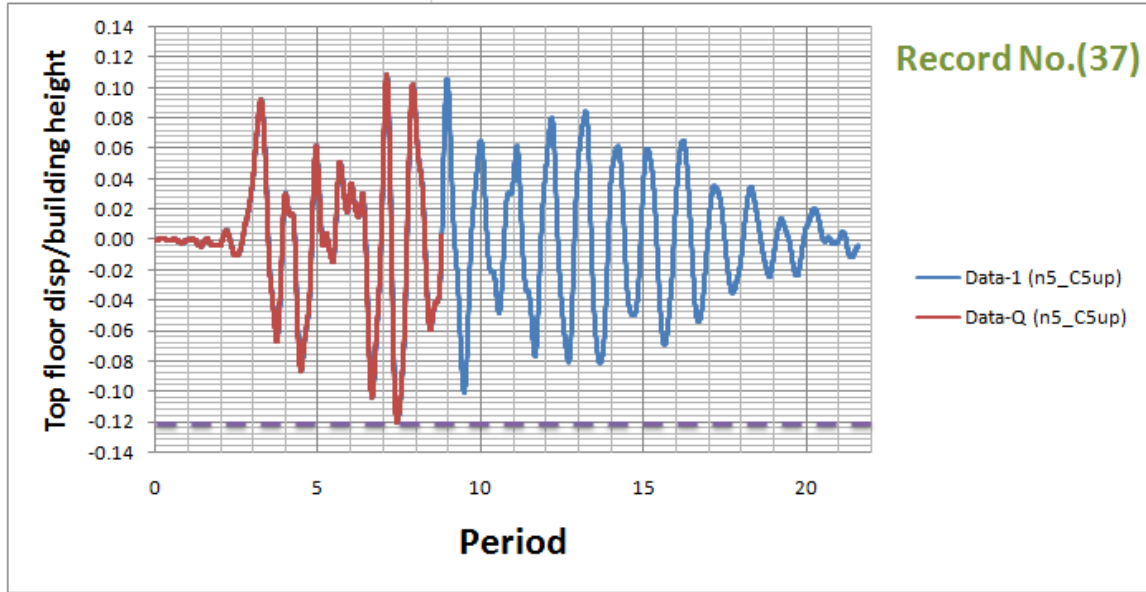


Figure 6.109. Maximum displacement of the original ground motions Data1 and the displacement of DataQ along height of the building.

Height of floor (m)		3			
Record No.(37)		Max. (Disp./height)		Drift(Disp./height)%	
Floor No.		Data1	DataQ	Data1	DataQ
GF	0	0.000	0.000	0.000	0.000
1 st Floor	1	0.028	0.028	0.933	0.933
2 nd Floor	2	0.059	0.059	1.033	1.033
3 rd Floor	3	0.082	0.082	0.767	0.767
4 th Floor	4	0.099	0.099	0.567	0.567
5 th Floor	5	0.120	0.120	0.700	0.700

Record No.(37)		Shear Force (Kn) for every floor	
Floor No.		Data1	DataQ
GF	0	3153.626	3155.050
1 st Floor	1	3153.626	3155.050
2 nd Floor	2	1994.846	1993.422
3 rd Floor	3	1643.830	1644.542
4 th Floor	4	1184.590	1181.030
5 th Floor	5	445.712	444.110

Table 6.38. Table Maximum Displacement and inter storey drifts and shear force for every floor Vs along of the height of Building for recording Data1&DataQ.

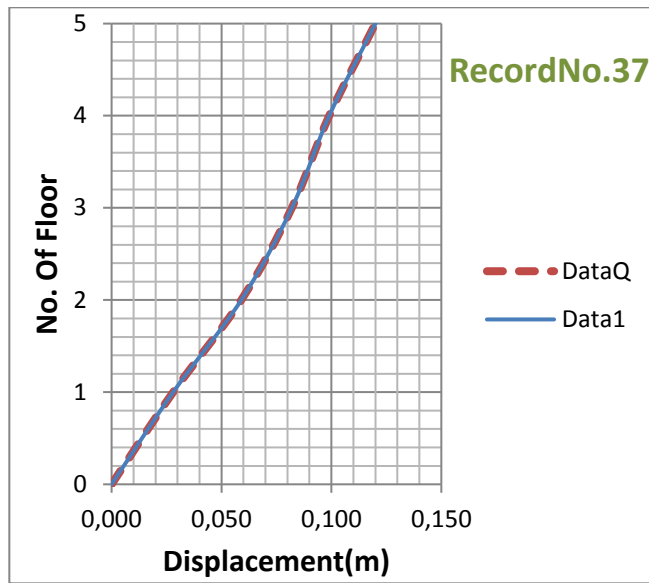


Figure 6.110. Profile of displacements for every floor along of the height of Building.

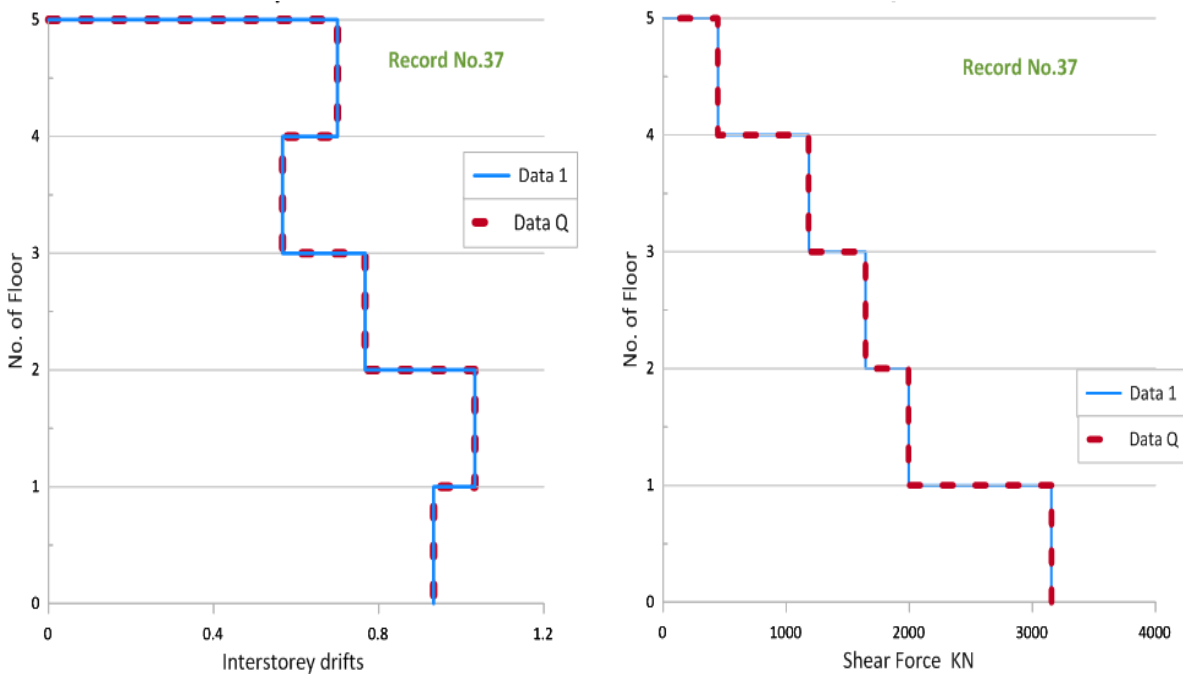


Figure 6.111. Profile of inter storey drifts and shear force for every floor Vs along of the height of Building.



Record 38

Record No.(38)	Data1	DataQ
Time (Sec.)	7.44	7.42
Displacement at the top of building (m)	-0.12	-0.12

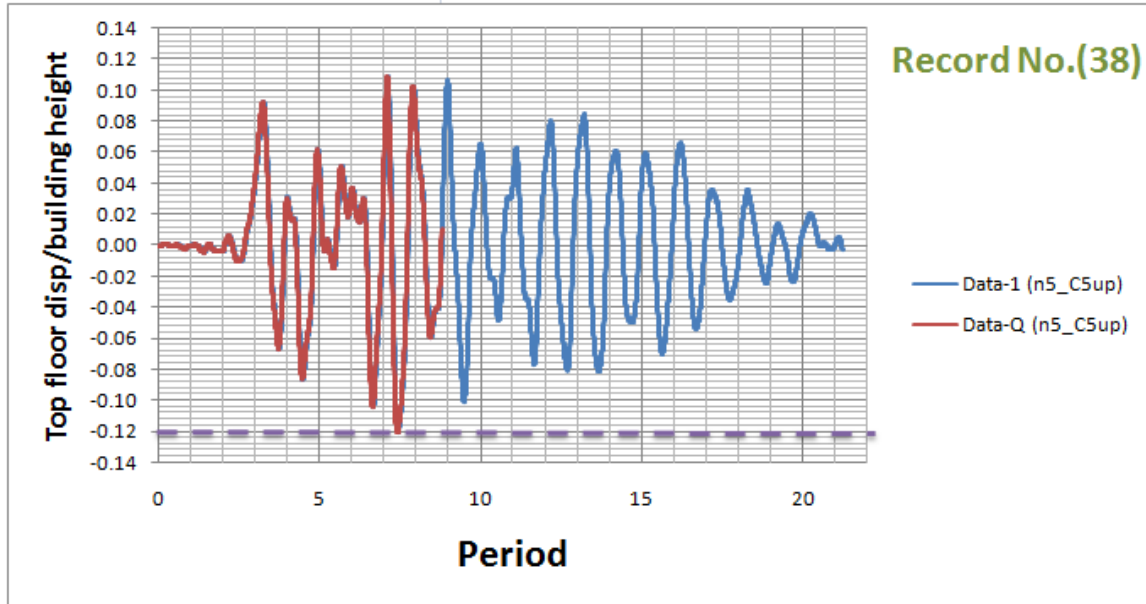


Figure 6.112. Maximum displacement of the original ground motions Data1 and the displacement of DataQ along height of the building.

Height of floor (m)		3			
Record No.(38)		Max.(Disp./height)		Drift(Disp./height)%	
Floor No.		Data1	DataQ	Data1	DataQ
GF	0	0.000	0.000	0.000	0.000
1 st Floor	1	0.028	0.028	0.933	0.933
2 ^{sd} Floor	2	0.059	0.059	1.033	1.033
3 rd Floor	3	0.082	0.082	0.767	0.767
4 th Floor	4	0.099	0.099	0.567	0.567
5 th Floor	5	0.120	0.120	0.700	0.700

Record No.(38)		Shear Force (Kn) for every floor	
Floor No.		Data1	DataQ
GF	0	3146.328	3148.286
1 st Floor	1	3146.328	3148.286
2 ^{sd} Floor	2	1993.778	1993.778
3 rd Floor	3	1644.008	1643.474
4 th Floor	4	1182.276	1183.522
5 th Floor	5	446.246	446.602

Table 6.39. Table Maximum Displacement and inter storey drifts and shear force for every floor Vs along of the height of Building for recording Data1&DataQ.

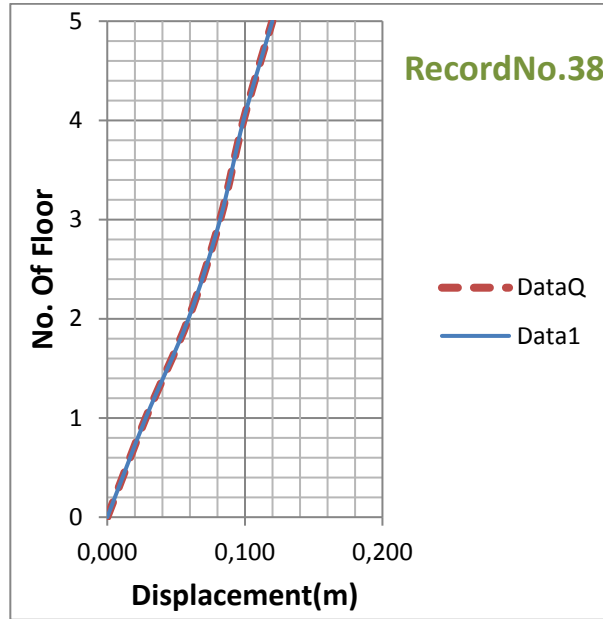


Figure 6.113. Profile of displacements for every floor along of the height of Building.

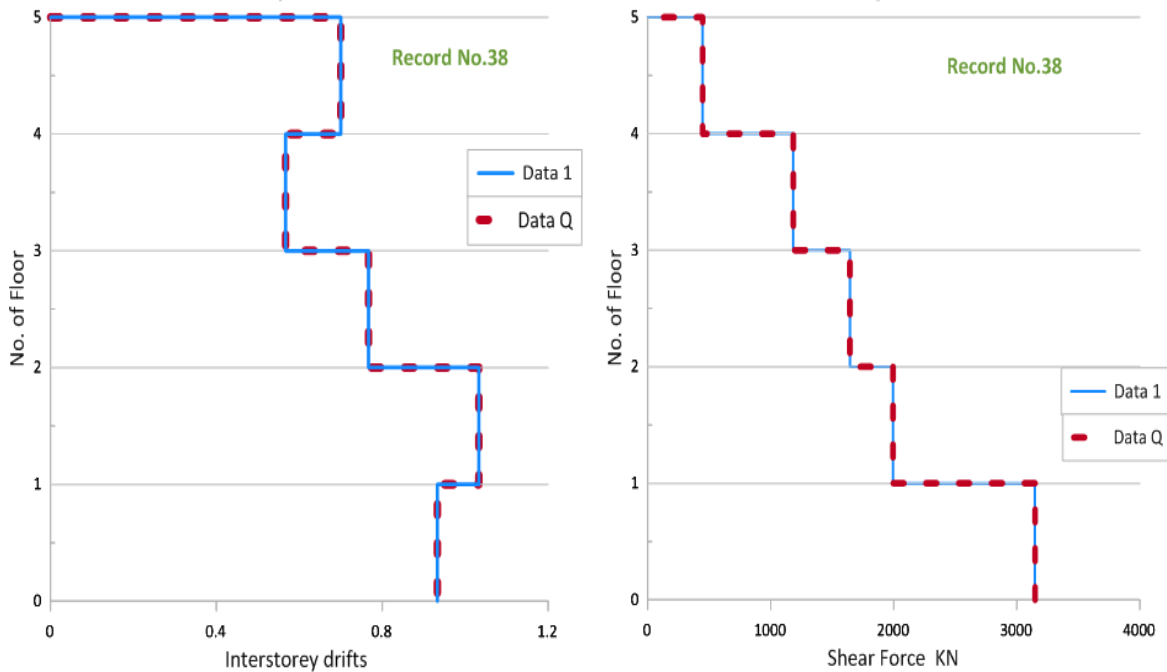


Figure 6.114. Profile of inter storey drifts and shear force for every floor Vs along of the height of Building.



Record 39

Record No.(39)	Data1	DataQ
Time (Sec.)	10.48	3.43
Displacement at the top of building (m)	0.08	0.071

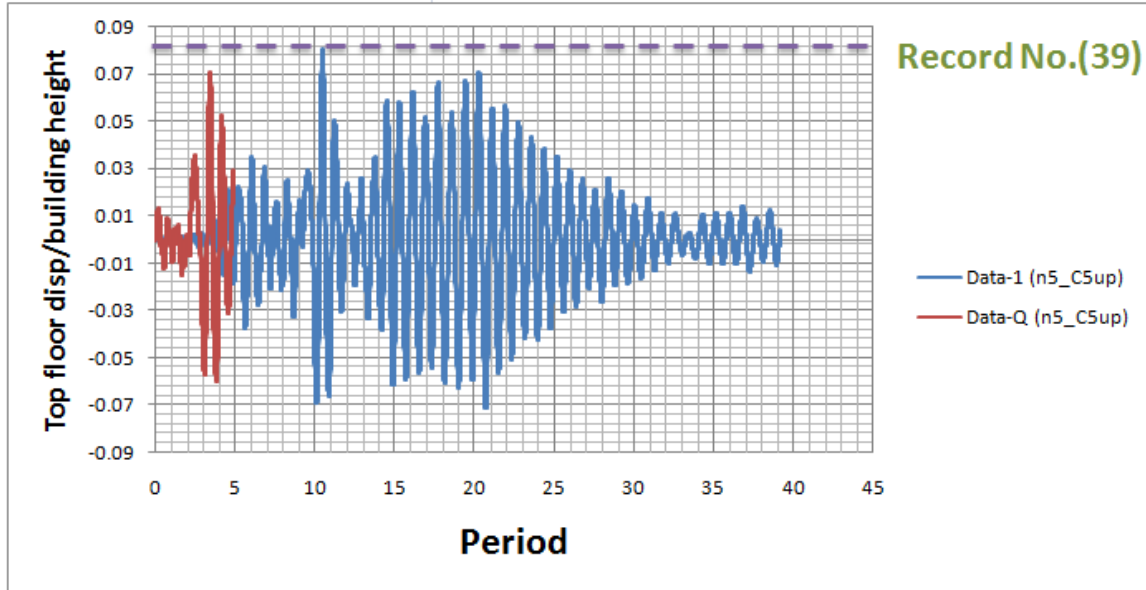


Figure 6.115. Maximum displacement of the original ground motions Data1 and the displacement of DataQ along height of the building.

Height of floor (m)		3			
Record No.(39)		Max.(Disp./height)		Drift(Disp./height)%	
Floor No.		Data1	DataQ	Data1	DataQ
GF	0	0.000	0.000	0.000	0.000
1 st Floor	1	0.013	0.011	0.433	0.367
2 ^{sd} Floor	2	0.032	0.029	0.633	0.600
3 rd Floor	3	0.048	0.043	0.533	0.467
4 th Floor	4	0.063	0.057	0.500	0.467
5 th Floor	5	0.080	0.071	0.567	0.467

Record No.(39)		Shear Force (Kn) for every floor	
Floor No.		Data1	DataQ
GF	0	2120.158	1752.410
1 st Floor	1	2120.158	1752.410
2 ^{sd} Floor	2	1695.094	1687.618
3 rd Floor	3	1352.800	1281.778
4 th Floor	4	1119.086	1028.128
5 th Floor	5	688.148	554.114

Table 6.40. Table Maximum Displacement and inter storey drifts and shear force for every floor Vs along of the height of Building for recording Data1&DataQ.

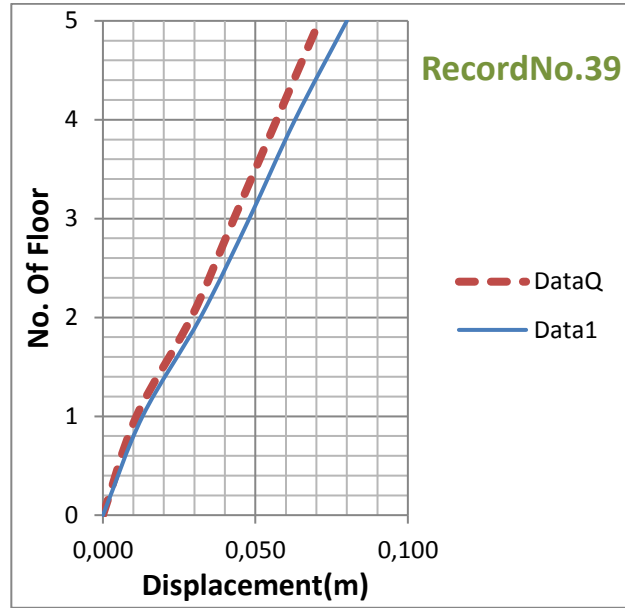


Figure 6.116. Profile of displacements for every floor along of the height of Building.

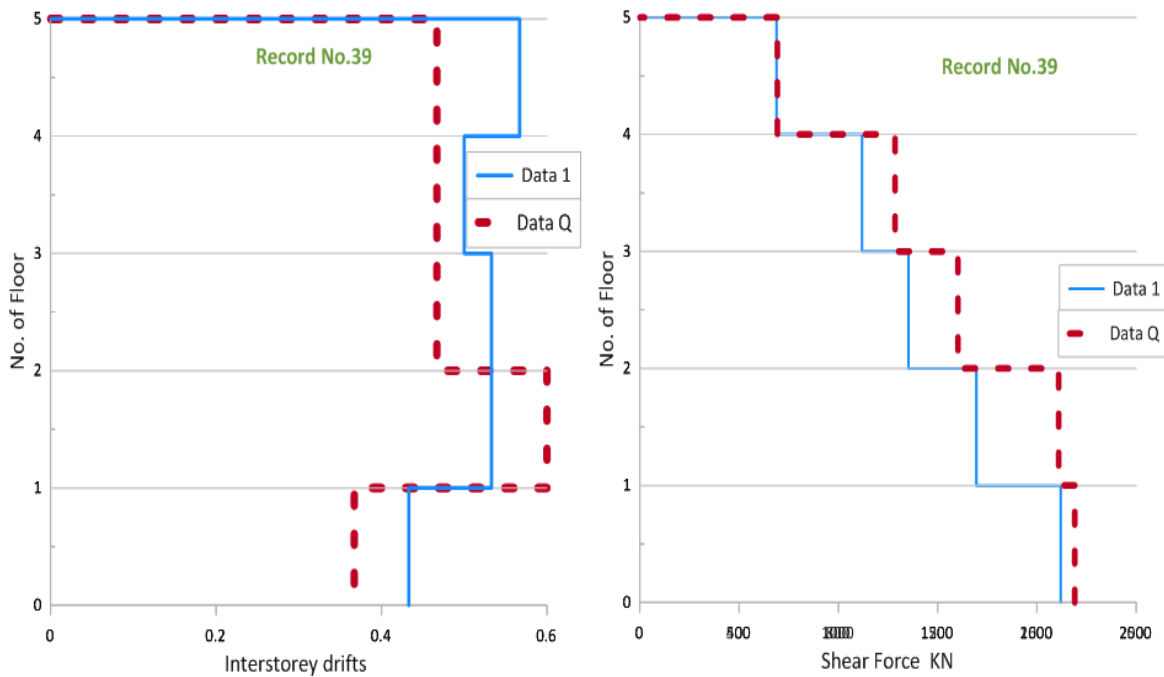


Figure 6.117. Profile of inter storey drifts and shear force for every floor Vs along of the height of Building.



Record 40

Record No.(40)	Data1	DataQ
Time (Sec.)	3.52	2.25
Displacement at the top of building (m)	-0.297	-0.3

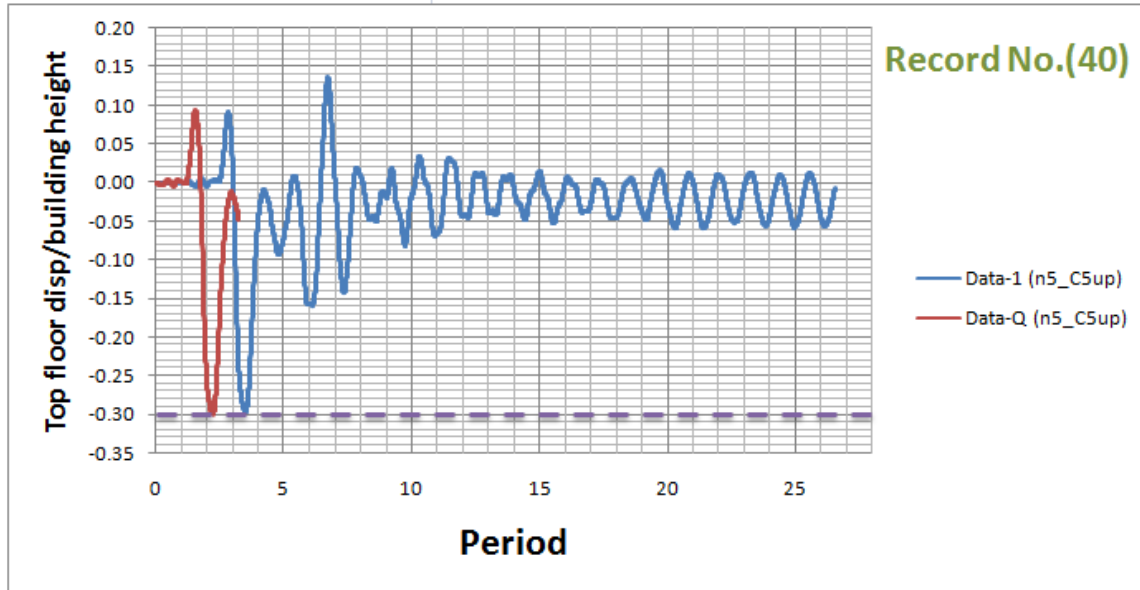


Figure 6.118. Maximum displacement of the original ground motions Data1 and the displacement of DataQ along height of the building.

Height of floor (m)		3			
Record No.(40)		Max.(Disp./height)		Drift(Disp./height)%	
Floor No.		Data1	DataQ	Data1	DataQ
GF	0	0.000	0.000	0.000	0.000
1 st Floor	1	0.123	0.124	4.100	4.133
2 ^{sd} Floor	2	0.238	0.240	3.833	3.867
3 rd Floor	3	0.271	0.273	1.100	1.100
4 th Floor	4	0.283	0.285	0.400	0.400
5 th Floor	5	0.297	0.300	0.467	0.500

Record No.(40)		Shear Force (Kn) for every floor	
Floor No.		Data1	DataQ
GF	0	2341.234	2131.906
1 st Floor	1	2341.234	2131.906
2 ^{sd} Floor	2	1476.866	1560.526
3 rd Floor	3	1038.986	1029.374
4 th Floor	4	803.848	795.482
5 th Floor	5	288.004	329.122

Table 6.41. Table Maximum Displacement and inter storey drifts and shear force for every floor Vs along of the height of Building for recording Data1&DataQ.

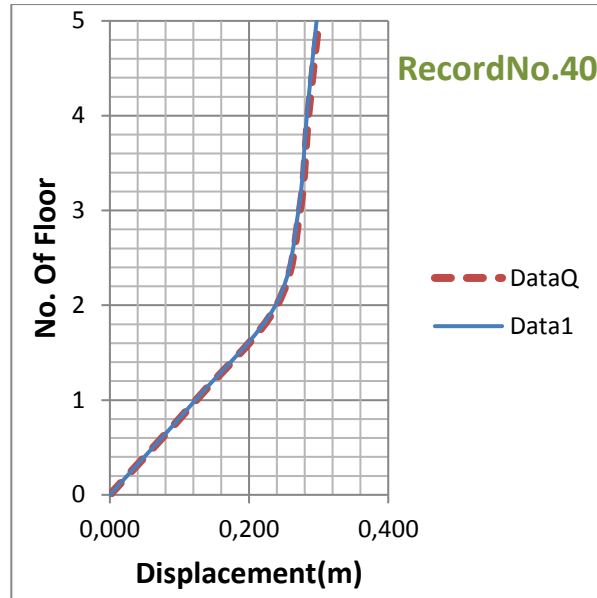


Figure 6.119. Profile of displacements for every floor along of the height of Building.

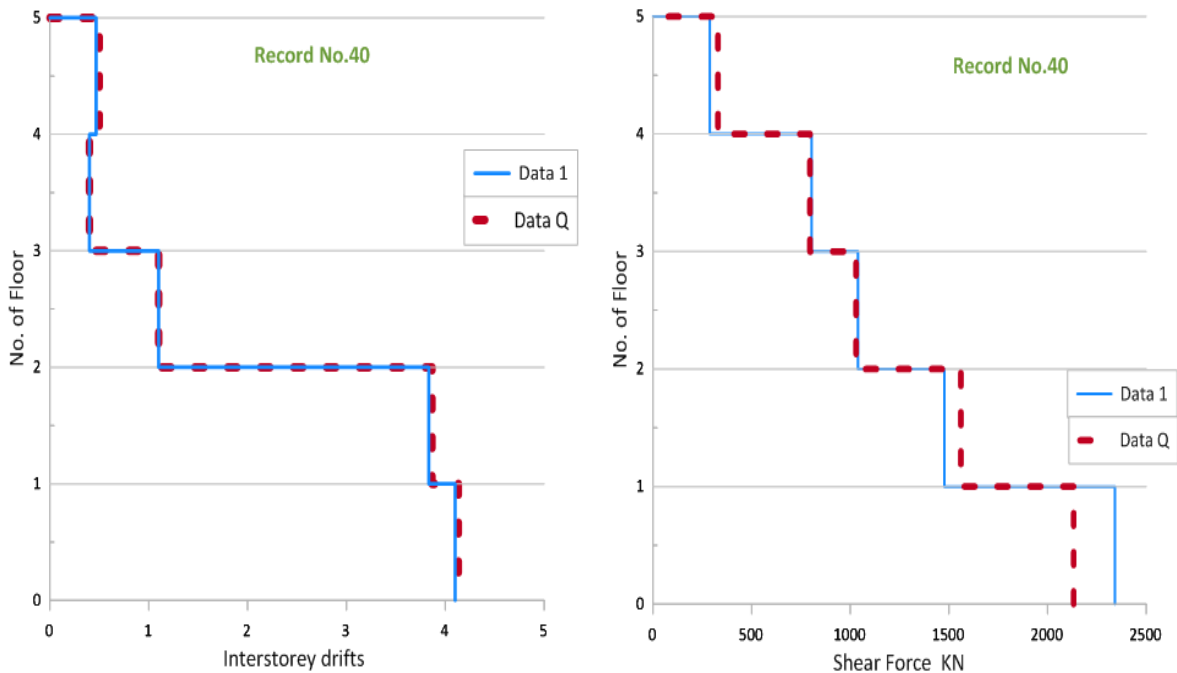


Figure 6.120. Profile of inter storey drifts and shear force for every floor Vs along of the height of Building.



Record 41

Record No.(41)	Data1	DataQ
Time (Sec.)	5.58	2.13
Displacement at the top of building (m)	-0.399	-0.326

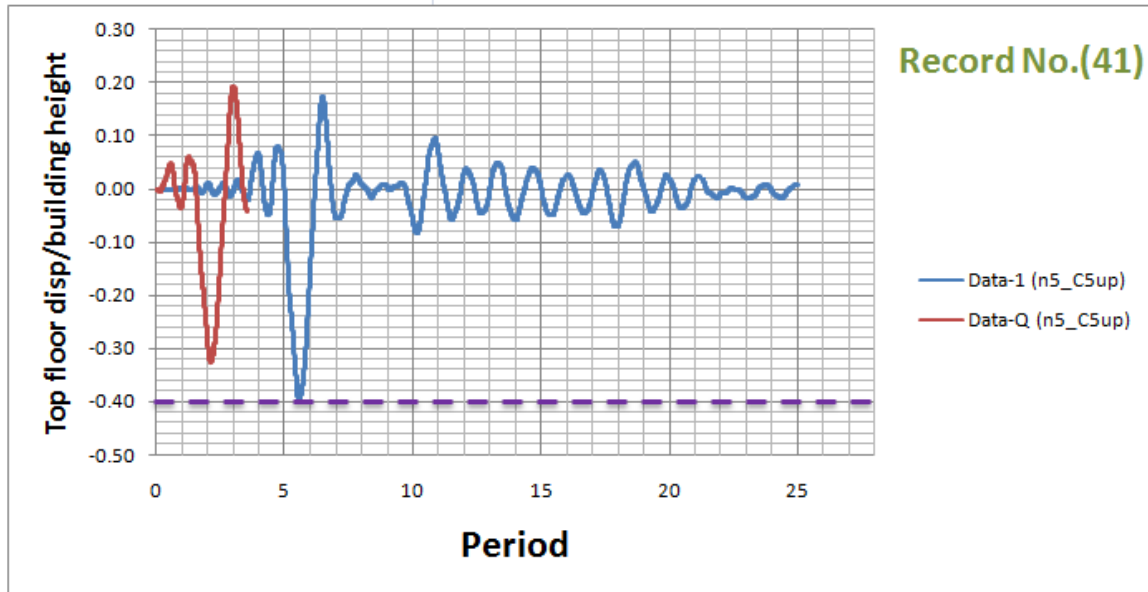


Figure 6.121. Maximum displacement of the original ground motions Data1 and the displacement of DataQ along height of the building.

Height of floor (m)	3			
Record No.(41)	Max. (Disp./height)		Drift(Disp./height)%	
Floor No.	Data1	DataQ	Data1	DataQ
GF	0	0.000	0.000	0.000
1 st Floor	1	0.200	6.667	5.700
2 ^{sd} Floor	2	0.330	4.333	3.233
3 rd Floor	3	0.362	1.067	0.867
4 th Floor	4	0.379	0.567	0.500
5 th Floor	5	0.399	0.667	0.567

Record No.(41)	Shear Force (Kn) for every floor		
Floor No.	Data1	DataQ	
GF	0	2838.388	2926.676
1 st Floor	1	2838.388	2926.676
2 ^{sd} Floor	2	1937.886	2008.196
3 rd Floor	3	1385.552	1359.030
4 th Floor	4	1034.714	1041.300
5 th Floor	5	521.896	454.078

Table 6.42. Table Maximum Displacement and inter storey drifts and shear force for every floor Vs along of the height of Building for recording Data1&DataQ.

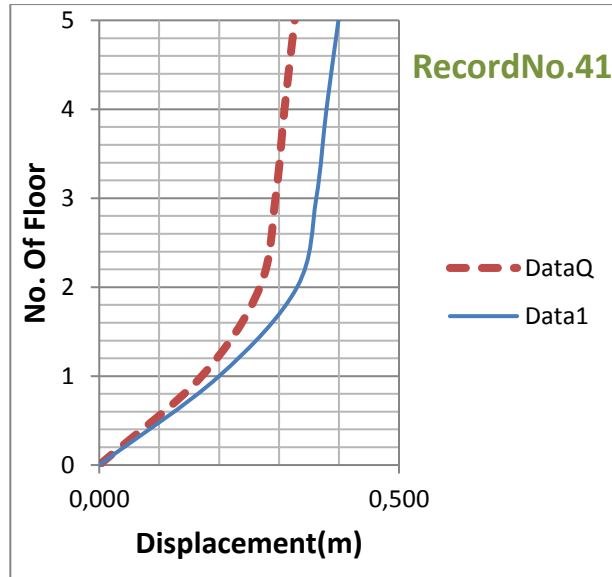


Figure 6.122. Profile of displacements for every floor along of the height of Building.

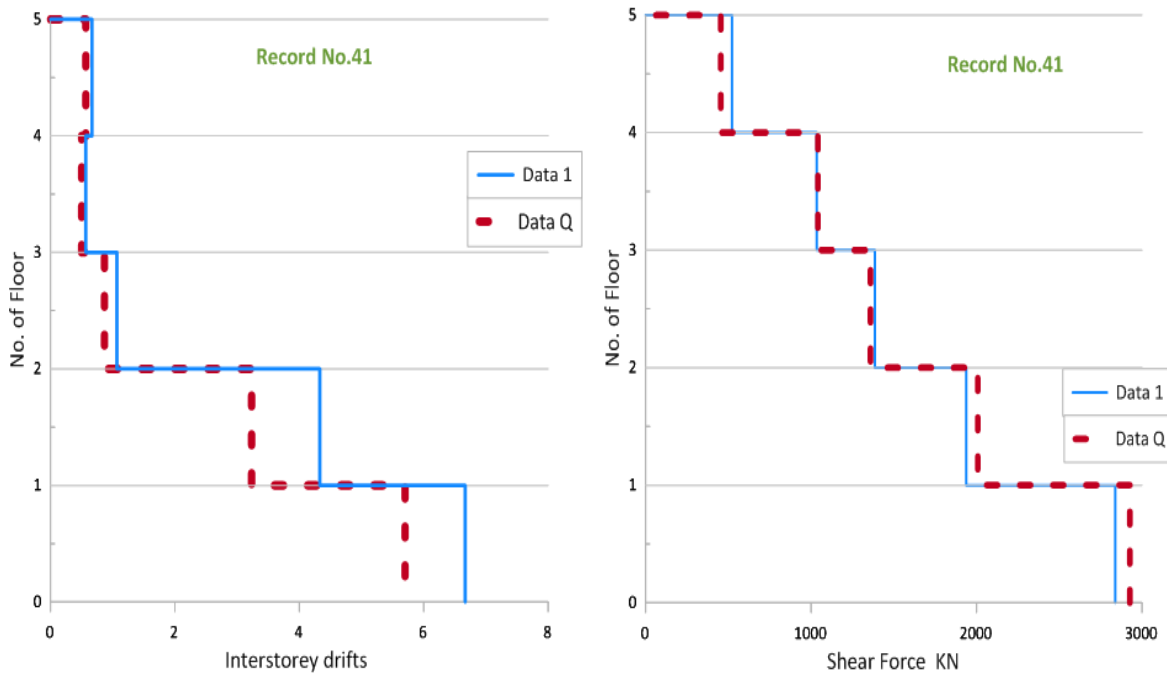


Figure 6.123. Profile of inter storey drifts and shear force for every floor Vs along of the height of Building.



Record 42

Record No.(42)	Data1	DataQ
Time (Sec.)	3.77	3.75
Displacement at the top of building (m)	-0.115	-0.115

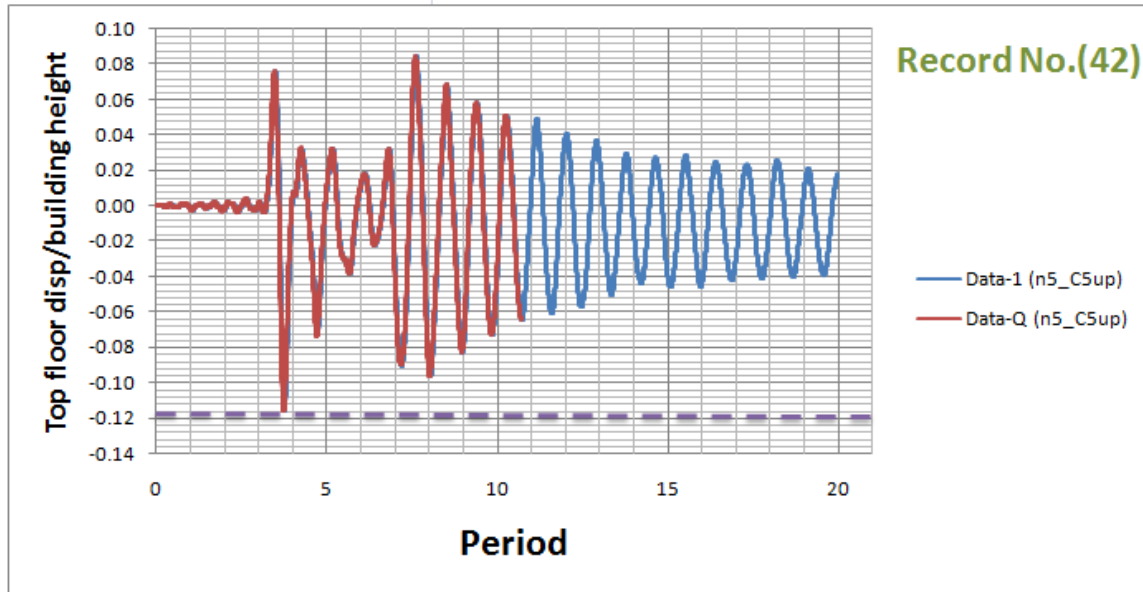


Figure 6.124. Maximum displacement of the original ground motions Data1 and the displacement of DataQ along height of the building.

Height of floor (m)	3			
Record No.(42)	Max. (Disp./height)		Drift(Disp./height)%	
Floor No.	Data1	DataQ	Data1	DataQ
GF	0	0.000	0.000	0.000
1 st Floor	1	0.008	0.267	0.267
2 ^{sd} Floor	2	0.027	0.633	0.633
3 rd Floor	3	0.053	0.867	0.867
4 th Floor	4	0.079	0.867	0.867
5 th Floor	5	0.115	1.200	1.200

Record No.(42)	Shear Force (Kn) for every floor		
Floor No.	Data1	DataQ	
GF	0	1962.272	1960.314
1 st Floor	1	1962.272	1960.314
2 ^{sd} Floor	2	1922.222	1919.730
3 rd Floor	3	1877.544	1877.366
4 th Floor	4	1808.658	1808.658
5 th Floor	5	886.440	886.440

Table 6.43. Table Maximum Displacement and inter storey drifts and shear force for every floor Vs along of the height of Building for recording Data1&DataQ.

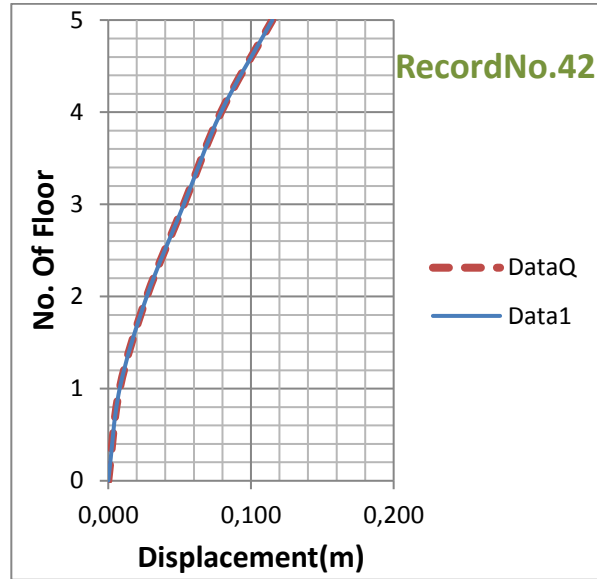


Figure 6.125. Profile of displacements for every floor along of the height of Building.

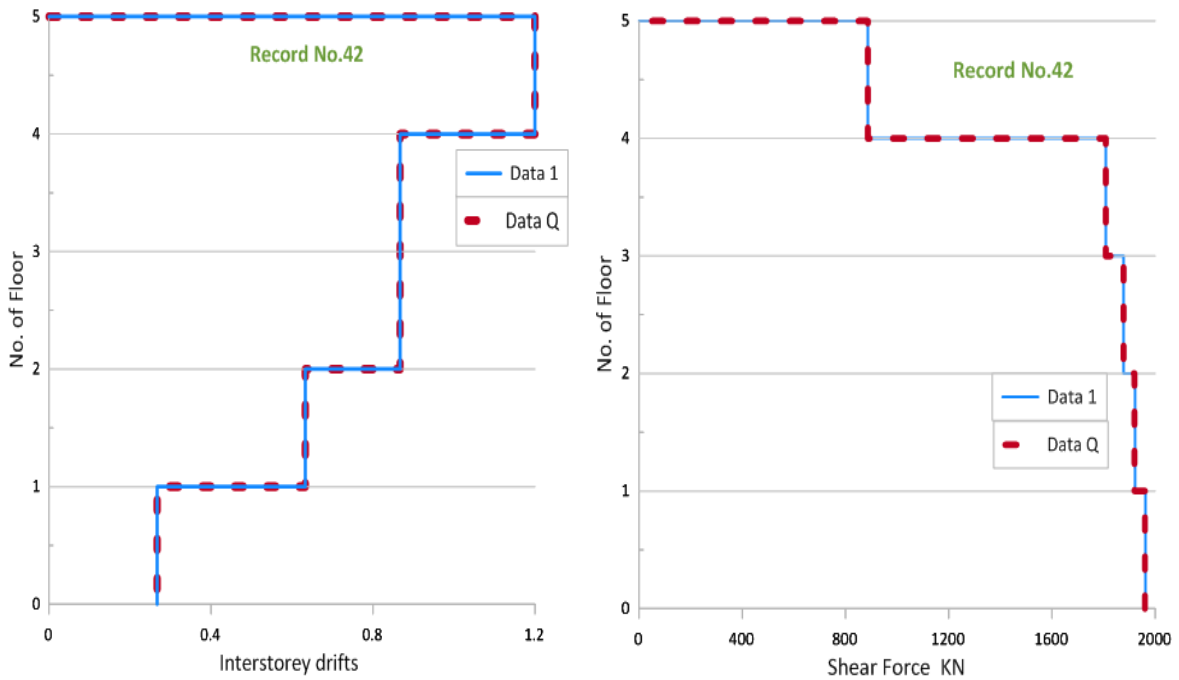


Figure 6.126. Profile of inter storey drifts and shear force for every floor Vs along of the height of Building.



Record 43

Record No.(43)	Data1	DataQ
Time (Sec.)	4.44	1.18
Displacement at the top of building (m)	-0.318	-0.336

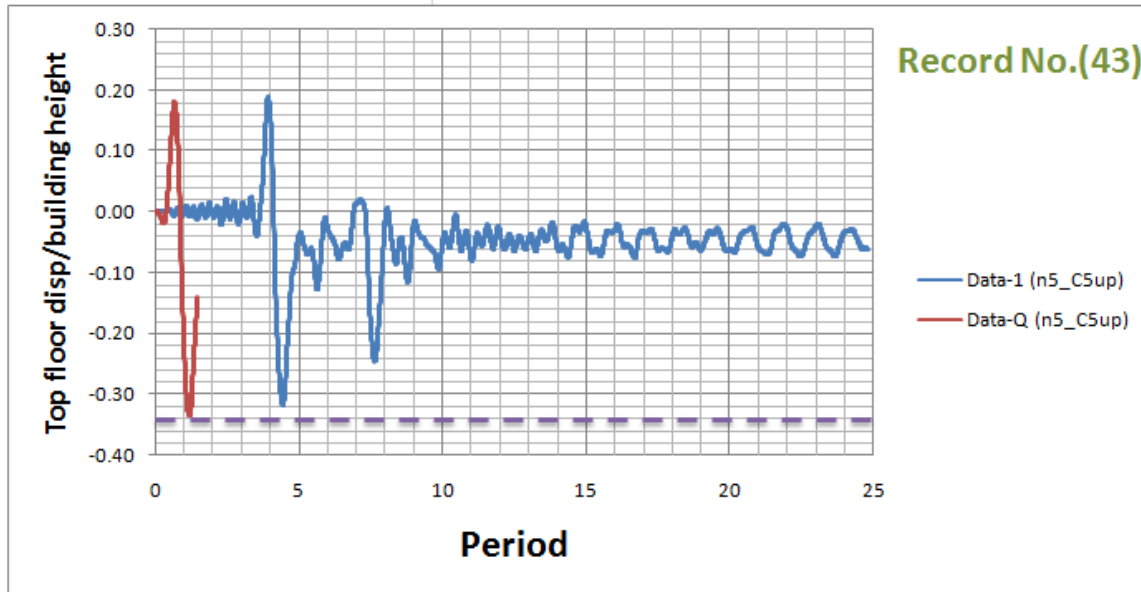


Figure 6.127. Maximum displacement of the original ground motions Data1 and the displacement of DataQ along height of the building.

Height of floor (m)	3	Max. (Disp./height)		Drift (Disp./height)%	
Record No.(43)		Data1	DataQ	Data1	DataQ
Floor No.		Data1	DataQ	Data1	DataQ
GF	0	0.000	0.000	0.000	0.000
1 st Floor	1	0.106	0.109	3.533	3.633
2 ^{sd} Floor	2	0.253	0.264	4.900	5.167
3 rd Floor	3	0.287	0.309	1.133	1.500
4 th Floor	4	0.299	0.325	0.400	0.533
5 th Floor	5	0.318	0.336	0.633	0.367

Record No.(43)	Shear Force (Kn) for every floor		
Floor No.	Data1	DataQ	
GF	0	3054.124	3050.386
1 st Floor	1	3054.124	3050.386
2 ^{sd} Floor	2	1846.928	1834.290
3 rd Floor	3	1029.552	1068.000
4 th Floor	4	1008.726	811.858
5 th Floor	5	173.728	217.160

Table 6.44. Table Maximum Displacement and inter storey drifts and shear force for every floor Vs along of the height of Building for recording Data1&DataQ.

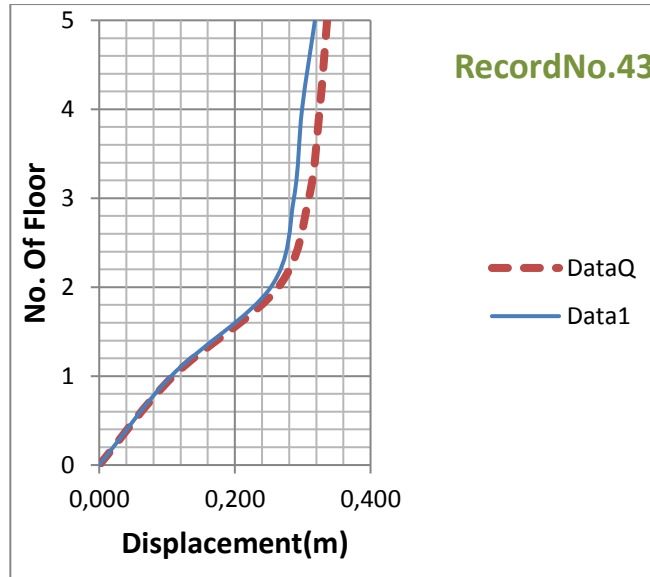


Figure 6.128. Profile of displacements for every floor along of the height of Building.

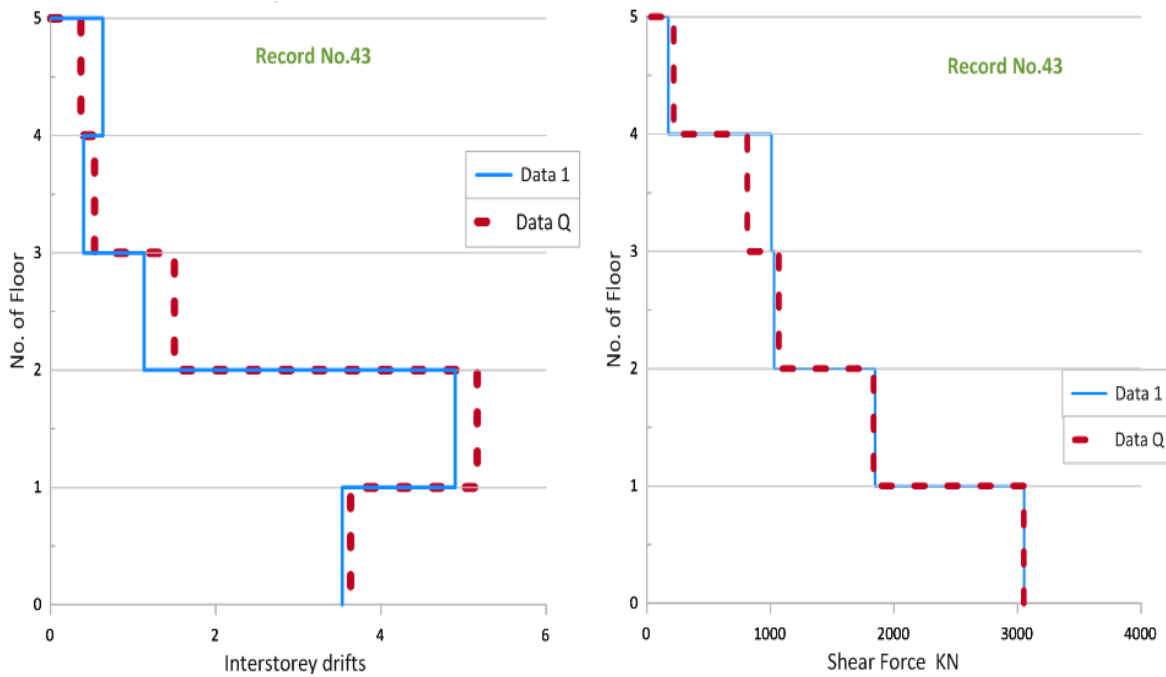


Figure 6.129. Profile of inter storey drifts and shear force for every floor Vs along of the height of Building.



Record 44

Record No.(44)	Data1	DataQ
Time (Sec.)	3.24	1.71
Displacement at the top of building (m)	-0.687	-0.638

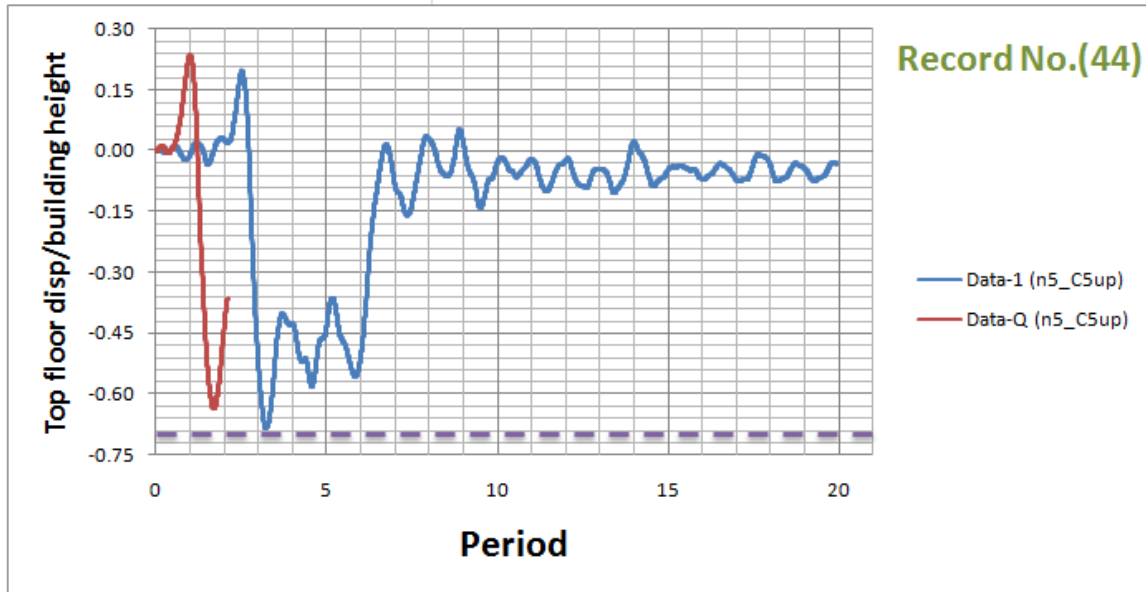


Figure 6.130. Maximum displacement of the original ground motions Data1 and the displacement of DataQ along height of the building.

Height of floor (m)	3				
Record No.(44)	Max.(Disp./height)		Drift(Disp./height)%		
Floor No.	Data1	DataQ	Data1	DataQ	
GF	0	0.000	0.000	0.000	
1 st Floor	1	0.273	0.312	9.100	10.400
2 ^{sd} Floor	2	0.570	0.615	9.900	10.100
3 rd Floor	3	0.604	0.649	1.133	1.133
4 th Floor	4	0.616	0.665	0.400	0.533
5 th Floor	5	0.638	0.687	0.733	0.733

Record No.(44)		Shear Force (Kn) for every floor	
Floor No.	Data1	DataQ	
GF	0	1797.800	2127.456
1 st Floor	1	1797.800	2127.456
2 ^{sd} Floor	2	954.436	901.392
3 rd Floor	3	794.592	957.640
4 th Floor	4	643.648	561.590
5 th Floor	5	420.792	431.294

Table 6.45. Table Maximum Displacement and inter storey drifts and shear force for every floor Vs along of the height of Building for recording Data1&DataQ.

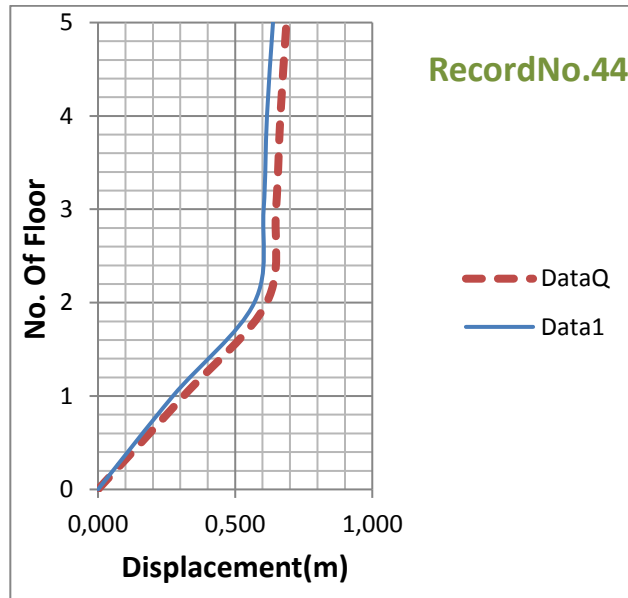


Figure 6.131. Profile of displacements for every floor along of the height of Building.

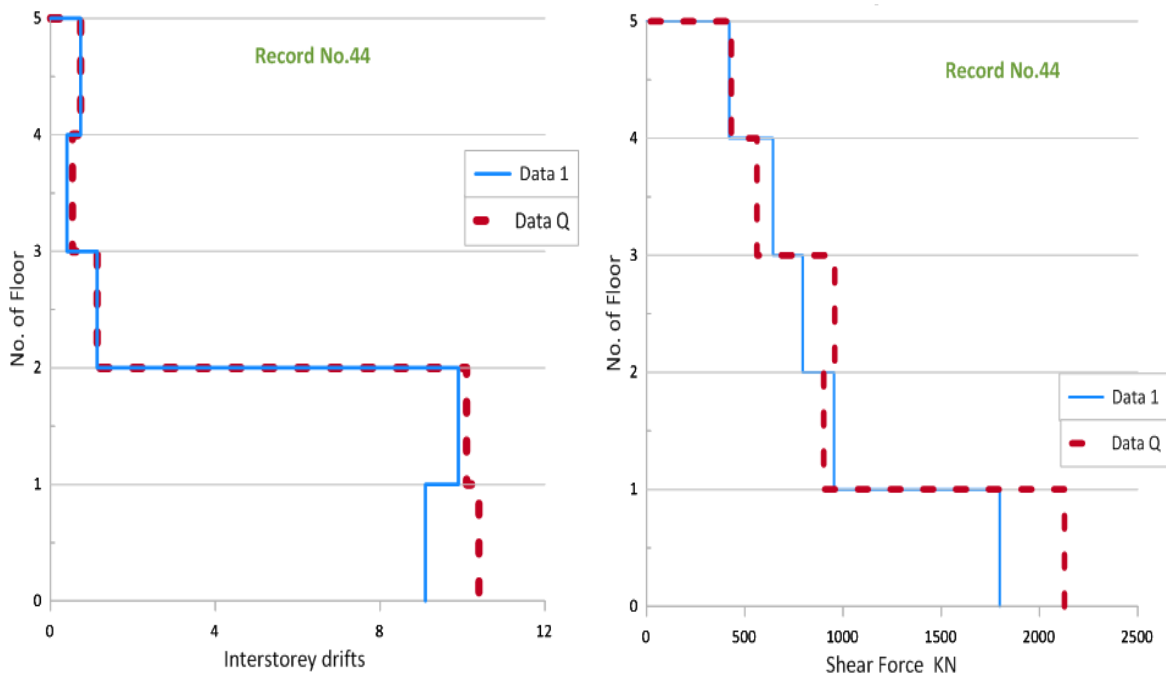


Figure 6.132. Profile of inter storey drifts and shear force for every floor Vs along of the height of Building.



Record 45

Record No.(45)	Data1	DataQ
Time (Sec.)	7.63	7.62
Displacement at the top of building (m)	-0.459	-0.457

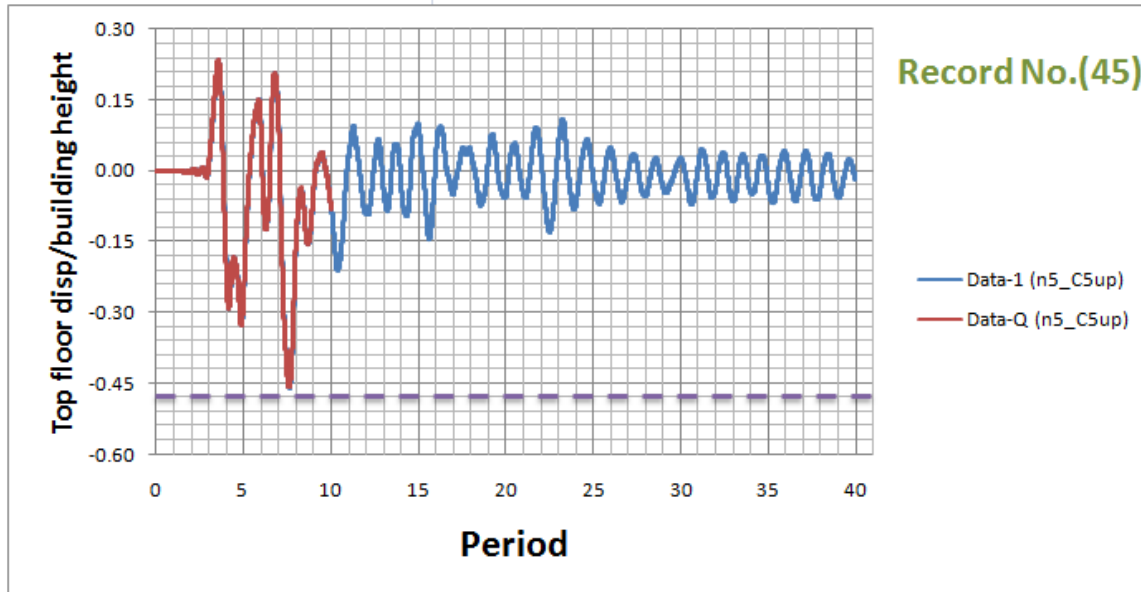


Figure 6.133. Maximum displacement of the original ground motions Data1 and the displacement of DataQ along height of the building.

Height of floor (m)	3	Max. (Disp./height)		Drift (Disp./height)%	
Record No.(45)		Data1	DataQ	Data1	DataQ
Floor No.		Data1	DataQ	Data1	DataQ
GF	0	0.000	0.000	0.000	0.000
1 st Floor	1	0.214	0.213	7.133	7.100
2 ^{sd} Floor	2	0.400	0.399	6.200	6.200
3 rd Floor	3	0.429	0.428	0.967	0.967
4 th Floor	4	0.444	0.443	0.500	0.500
5 th Floor	5	0.459	0.458	0.500	0.500

Record No.(45)	Shear Force (Kn) for every floor		
Floor No.	Data1	DataQ	
GF	0	2734.614	2738.352
1 st Floor	1	2734.614	2738.352
2 ^{sd} Floor	2	1748.316	1750.630
3 rd Floor	3	1229.446	1215.562
4 th Floor	4	978.110	975.796
5 th Floor	5	354.576	356.000

Table 6.46. Table Maximum Displacement and inter storey drifts and shear force for every floor Vs along of the height of Building for recording Data1&DataQ.

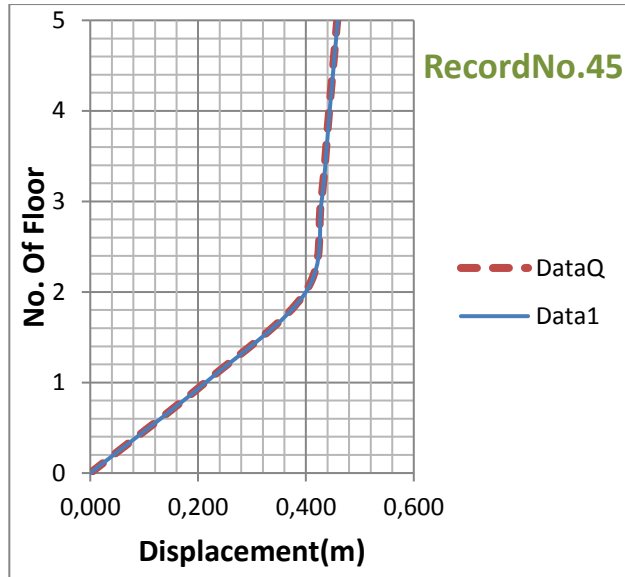


Figure 6.134. Profile of displacements for every floor along of the height of Building.

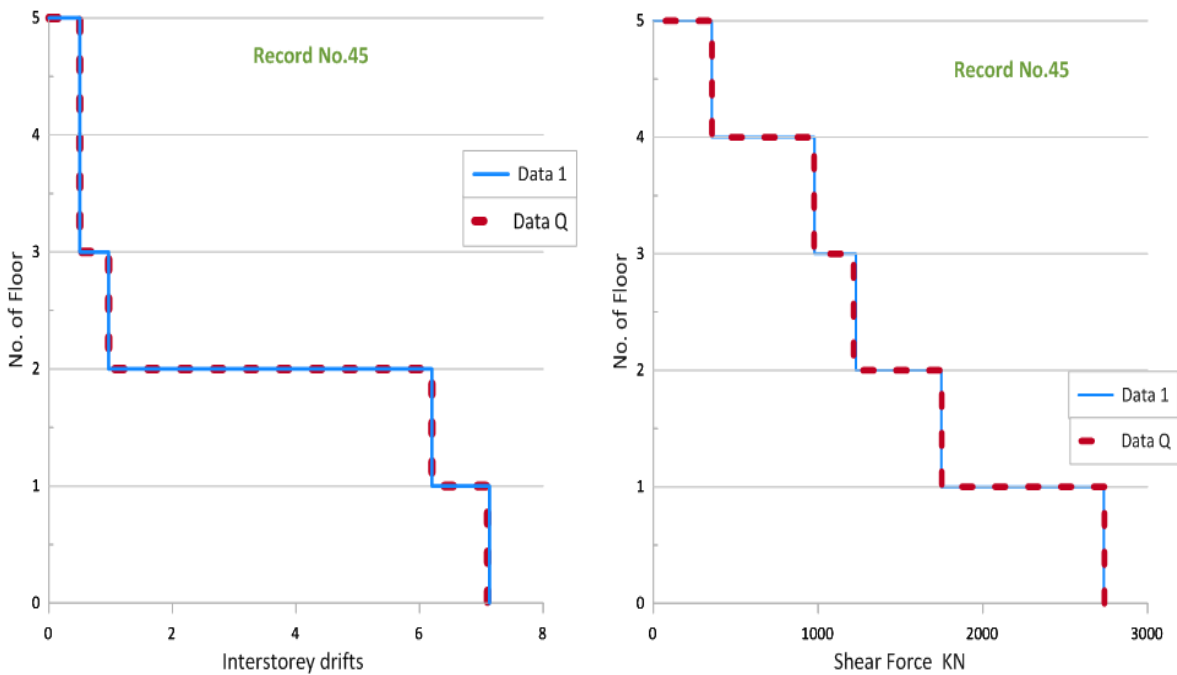


Figure 6.135. Profile of inter storey drifts and shear force for every floor Vs along of the height of Building.



Record 46

Record No.(46)	Data1	DataQ
Time (Sec.)	7.21	2.83
Displacement at the top of building (m)	-0.23	-0.194

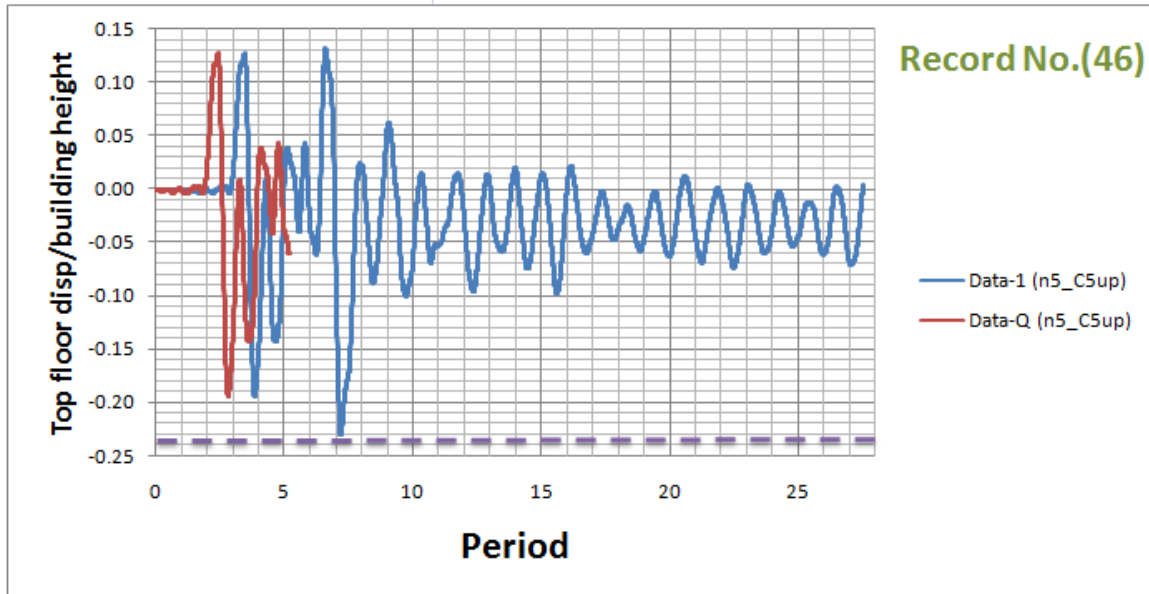


Figure 6.136. Maximum displacement of the original ground motions Data1 and the displacement of DataQ along height of the building.

Height of floor (m)	3				
Record No.(46)	Max.(Disp./height)		Drif.(Disp./height)%		
Floor No.	Data1	DataQ	Data1	DataQ	
GF	0	0.000	0.000	0.000	
1 st Floor	1	0.037	0.040	1.233	1.333
2 ^{sd} Floor	2	0.109	0.101	2.400	2.033
3 rd Floor	3	0.168	0.142	1.967	1.367
4 th Floor	4	0.198	0.167	1.000	0.833
5 th Floor	5	0.230	0.195	1.067	0.933

Record No.(46)	Shear Force (Kn) for every floor		
Floor No.	Data1	DataQ	
GF	0	2921.336	3258.824
1 st Floor	1	2921.336	3258.824
2 ^{sd} Floor	2	2050.204	2108.054
3 rd Floor	3	1979.894	1902.820
4 th Floor	4	1438.418	1385.552
5 th Floor	5	775.724	552.868

Table 6.47. Table Maximum Displacement and inter storey drifts and shear force for every floor Vs along of the height of Building for recording Data1&DataQ.

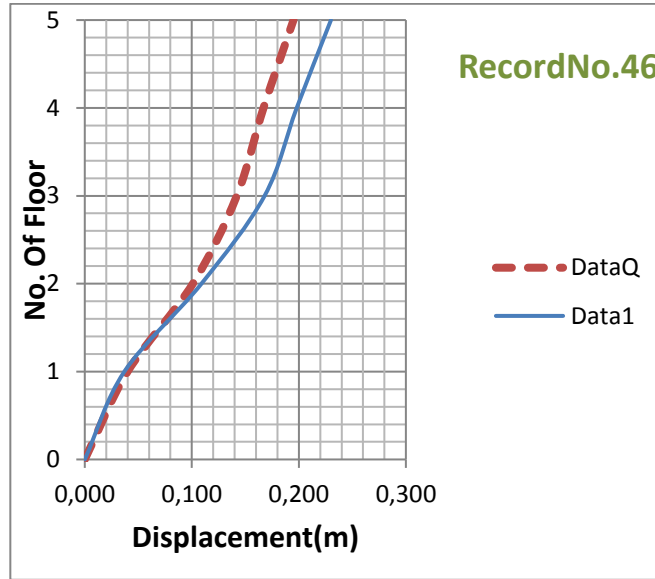


Figure 6.137. Profile of displacements for every floor along of the height of Building.

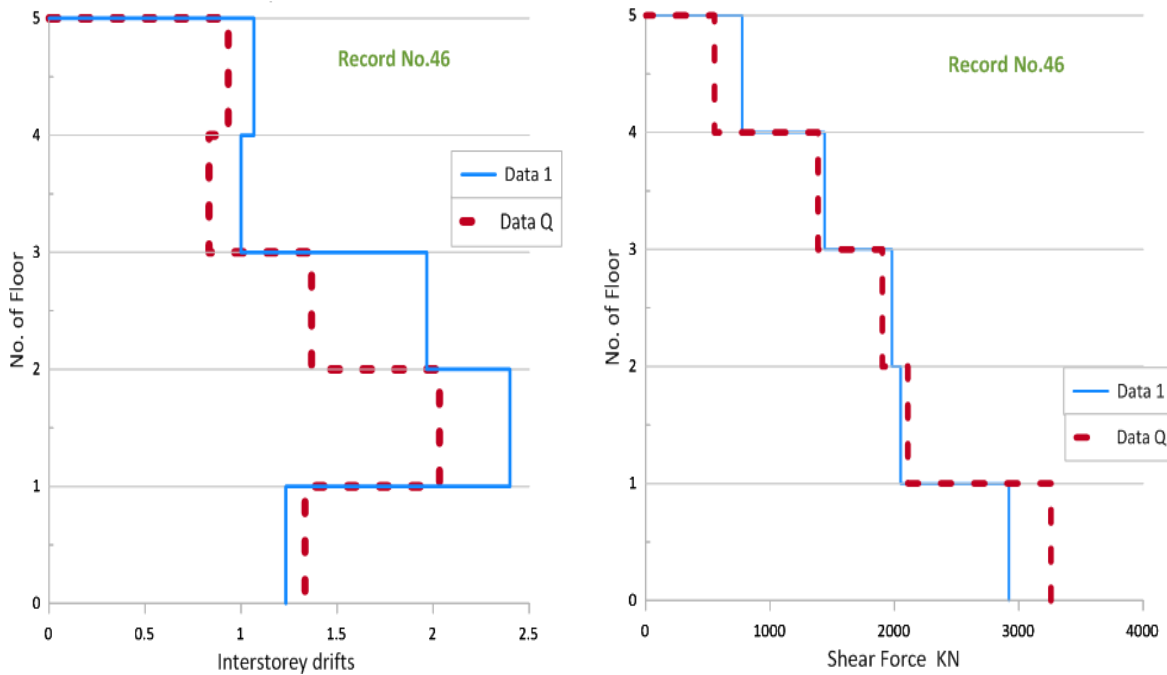


Figure 6.138. Profile of inter storey drifts and shear force for every floor Vs along of the height of Building.



Record 47

Record No.(47)	Data1	DataQ
Time (Sec.)	4.54	4.06
Displacement at the top of buliding (m)	-0.317	-0.315

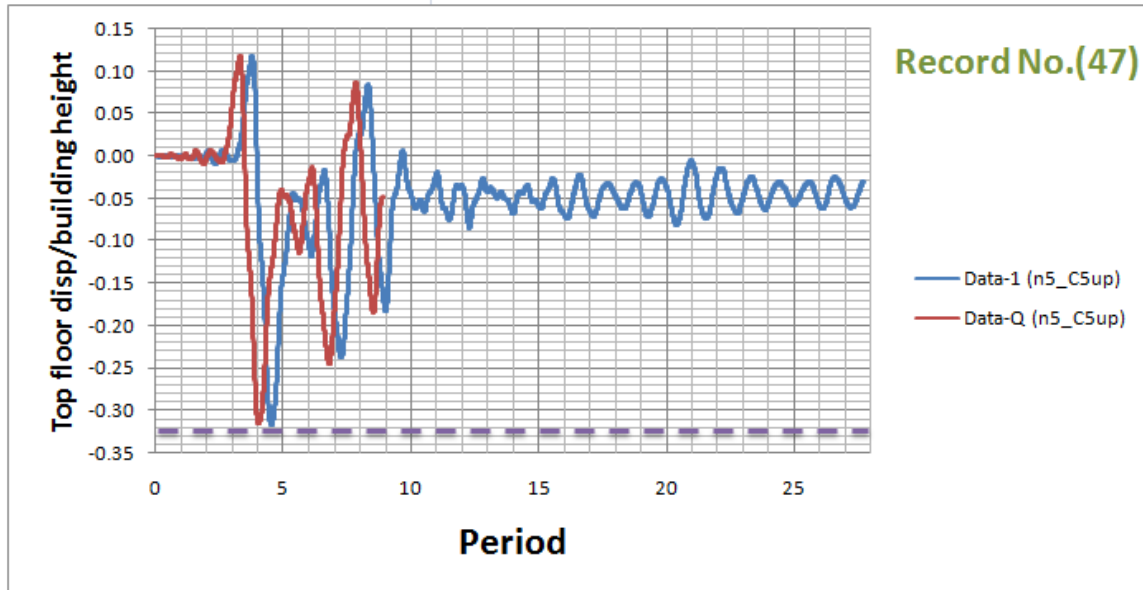


Figure 6.139.Maximum displacement of the original ground motions Data1 and the displacement of DataQ along height of the building.

Height of floor (m)		3			
Record No.(47)		Max. (Disp./height)		Drift(Disp./height)%	
Floor No.		Data1	DataQ	Data1	DataQ
GF	0	0.000	0.000	0.000	0.000
1 st Floor	1	0.181	0.180	6.033	6.000
2 ^{sd} Floor	2	0.265	0.262	2.800	2.733
3 rd Floor	3	0.289	0.287	0.800	0.833
4 th Floor	4	0.304	0.302	0.500	0.500
5 th Floor	5	0.317	0.315	0.433	0.433

Record No.(47)		Shear Force (Kn) for every floor	
Floor No.		Data1	DataQ
GF	0	2889.118	2889.474
1 st Floor	1	2889.118	2889.474
2 ^{sd} Floor	2	2019.944	2019.232
3 rd Floor	3	1582.064	1571.384
4 th Floor	4	879.854	875.226
5 th Floor	5	257.388	260.770

Table 6.48.Table Maximum Displacement and inter storey drifts and shear force for every floor Vs along of the height of Building for recording Data1&DataQ.

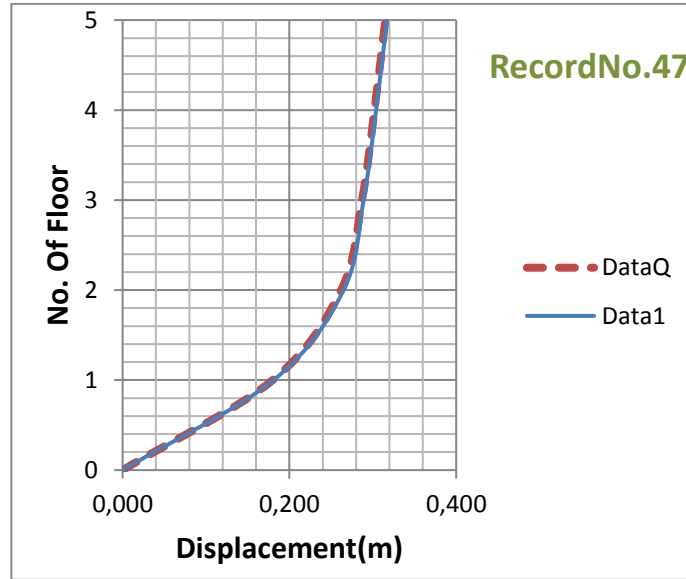


Figure 6.140. Profile of displacements for every floor along of the height of Building.

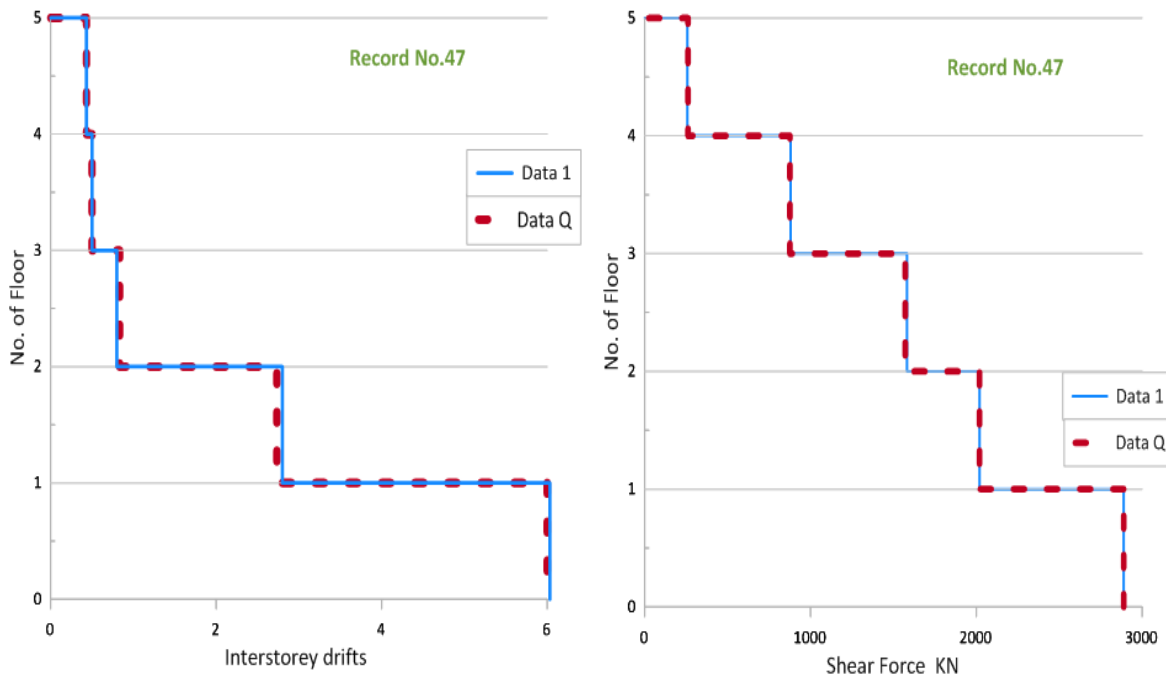


Figure 6.141. Profile of inter storey drifts and shear force for every floor Vs along of the height of Building.



Record 48

Record No.(48)	Data1	DataQ
	5.38	2.32
Displacement at the top of building (m)	0.261	-0.262

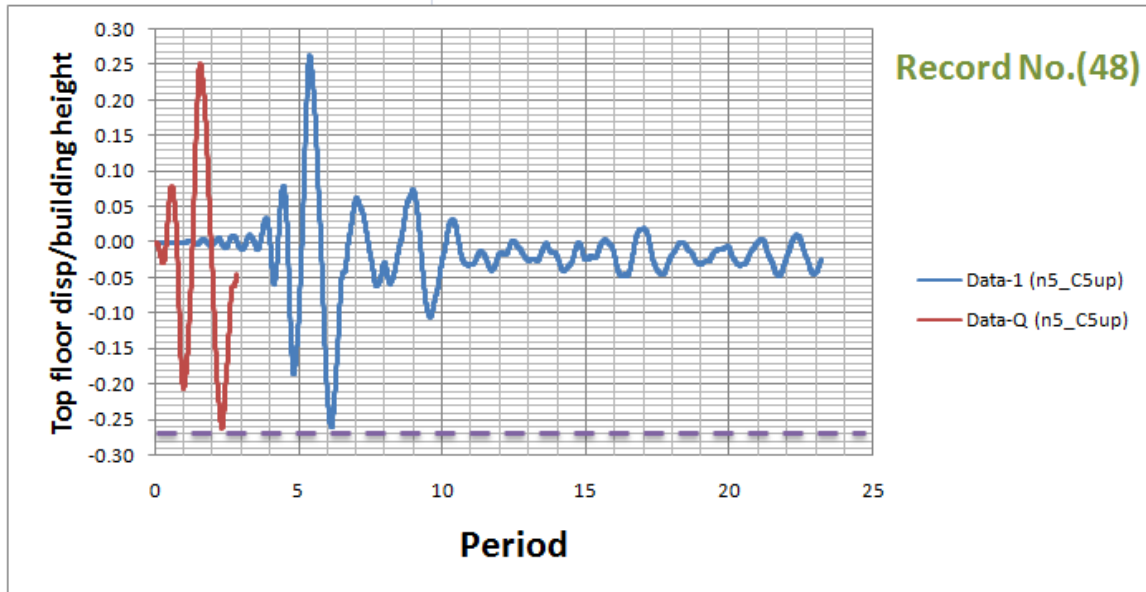


Figure 6.142. Maximum displacement of the original ground motions Data1 and the displacement of DataQ along height of the building.

Height of floor (m)	3				
Record No.(48)	Max. (Disp./height)	Drift(Disp./height)%			
Floor No.	Data1	DataQ	Data1	DataQ	
GF	0	0.000	0.000	0.000	0.000
1 st Floor	1	0.066	0.102	2.200	3.400
2 ^{sd} Floor	2	0.159	0.198	3.100	3.200
3 rd Floor	3	0.210	0.234	1.700	1.200
4 th Floor	4	0.233	0.247	0.767	0.433
5 th Floor	5	0.263	0.262	1.000	0.500

Record No.(48)	Shear Force (Kn) for every floor		
Floor No.	Data1	DataQ	
GF	0	2921.692	3134.936
1 st Floor	1	2921.692	3134.936
2 ^{sd} Floor	2	2080.998	1977.224
3 rd Floor	3	1939.310	1545.218
4 th Floor	4	1341.052	754.898
5 th Floor	5	706.126	326.986

Table 6.49. Table Maximum Displacement and inter storey drifts and shear force for every floor Vs along of the height of Building for recording Data1&DataQ.

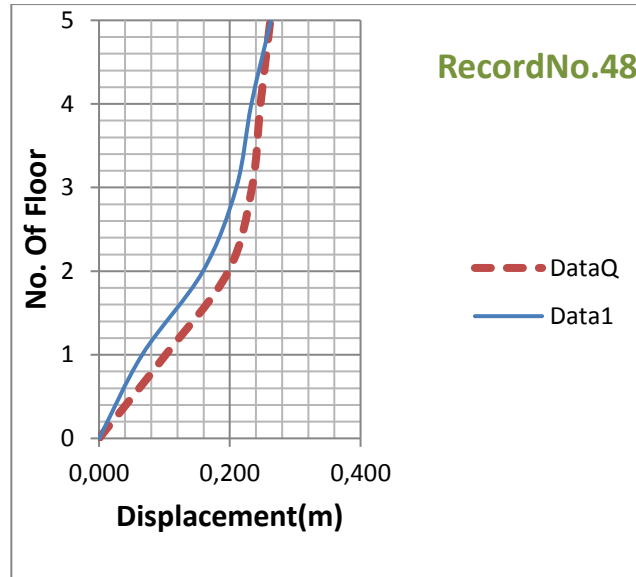


Figure 6.143. Profile of displacements for every floor along of the height of Building.

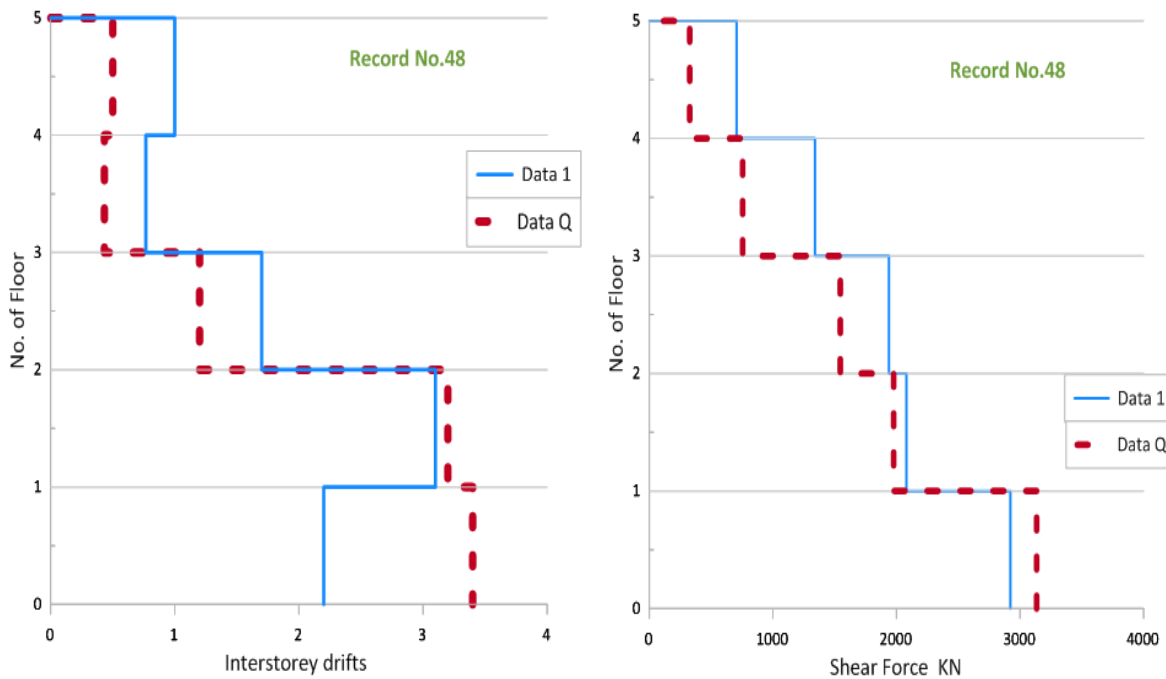


Figure 6.144. Profile of inter storey drifts and shear force for every floor Vs along of the height of Building.



Record 49

Record No.(49)	Data1	DataQ
Time (Sec.)	8.95	5.51
Displacement at the top of building (m)	-0.052	-0.053

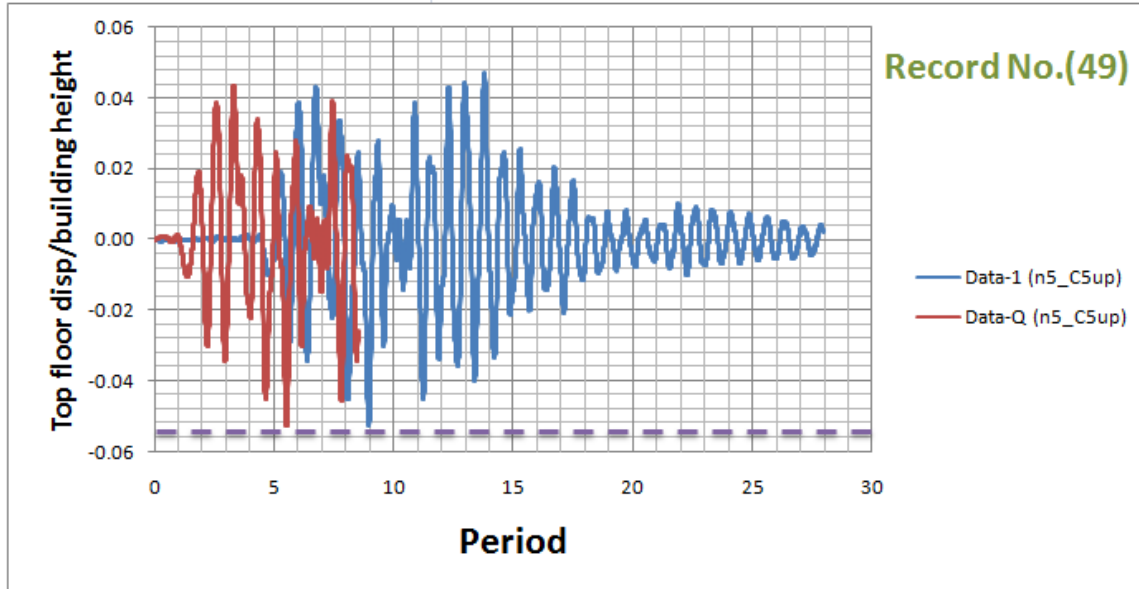


Figure 6.145. Maximum displacement of the original ground motions Data1 and the displacement of DataQ along height of the building.

Height of floor (m)		3			
Record No.(49)		Max.(Disp./height)		Drift(Disp./height)%	
Floor No.		Data1	DataQ	Data1	DataQ
GF	0	0.000	0.000	0.000	0.000
1 st Floor	1	0.006	0.006	0.200	0.200
2 ^{sd} Floor	2	0.015	0.015	0.300	0.300
3 rd Floor	3	0.025	0.026	0.333	0.367
4 th Floor	4	0.040	0.040	0.500	0.467
5 th Floor	5	0.052	0.053	0.400	0.433

Record No.(49)		Shear Force (Kn) for every floor	
Floor No.		Data1	DataQ
GF	0	2921.692	3134.936
1 st Floor	1	2921.692	3134.936
2 ^{sd} Floor	2	2080.998	1977.224
3 rd Floor	3	1939.310	1545.218
4 th Floor	4	1341.052	754.898
5 th Floor	5	706.126	326.986

Table 6.50. Table Maximum Displacement and inter storey drifts and shear force for every floor Vs along of the height of Building for recording Data1&DataQ.

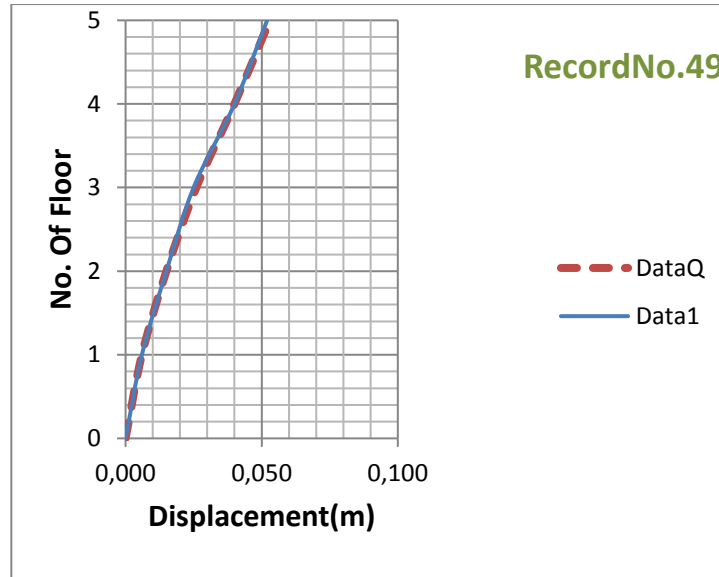


Figure 6.146. Profile of displacements for every floor along of the height of Building.

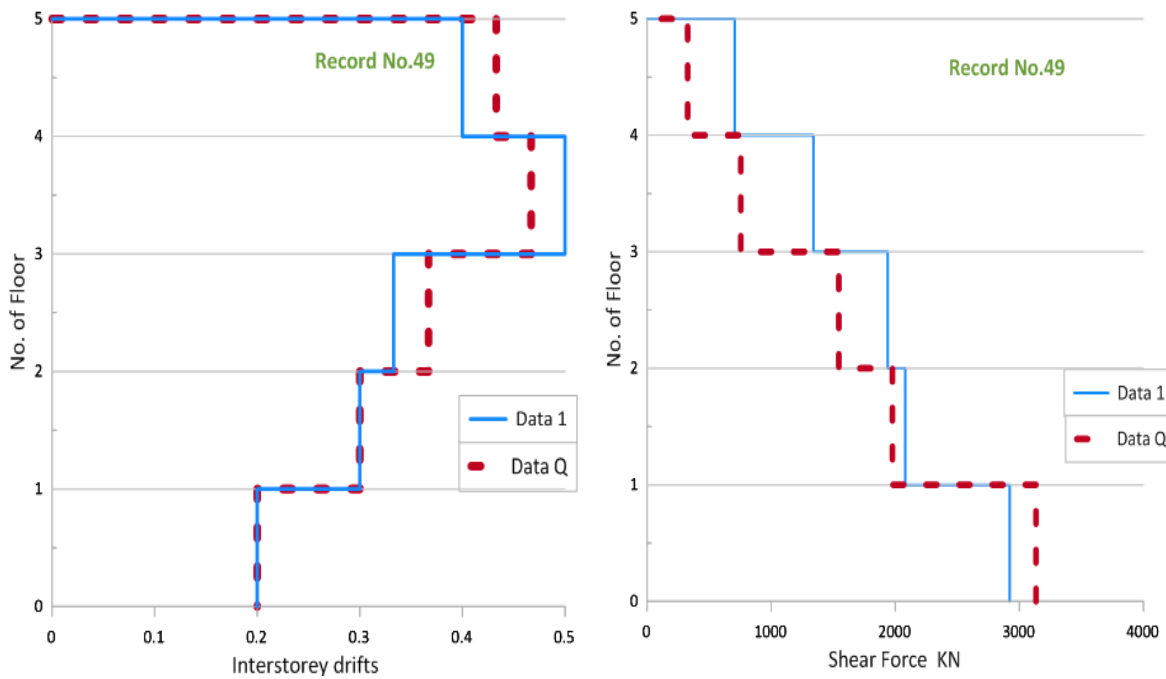


Figure 6.147. Profile of inter storey drifts and shear force for every floor Vs along of the height of Building.



CHAPTER 7 CONCLUSIONS

Since the identification of pulse like records in the near field region the need for a new significant duration concept has emerged.

This new concept should be compatible with the velocity time history and its energy flux integral.

A first approach shows that the energy flux content is usually associated with the inherent predominant pulse duration.

Furthermore, the use of the M&P wavelet for the simulation of the predominant pulse, with its bell shaped envelope creates a tapered region at both ends of the pulse duration attenuating possible baseline effects of the truncated time history coinciding with the time interval of the pulse.

A reiterative procedure using the residual time history of each cycle for the estimation of consecutive wavelets has shown that the significant pulses, affecting elastic and inelastic displacement spectra, are those coupled in duration with the predominant pulse.

This has permitted the evaluation of a new concept of significant duration of pulse like records coinciding with the truncated time history of the pulse duration.

Furthermore, the inelastic displacement spectra of the original and the truncated significant time history are found to be almost identical.

As a case study for the use of the new concept of significant duration a particular of typical reinforced concrete buildings were subjected to a sample of pulse like time histories.

From the results shown it appears that the displacement at the top, the storey drifts and shear forces are very close between those produced for the original time history and the significant duration.

The correlation coefficients are close to 99%. The main effect of the new concept is that it is not simply a new index for the significant duration but it also permits the substitution of the original time history with the truncated one for inelastic time history analyses of structures.

The gain is a reduced computation time by 70% with almost the same accuracy in computations.



REFERENCES

1. Bernal D. Viscous damping in inelastic structural response. *ASCE Journal of Structural Engineering* April 1994; 120(4):1240–1254.
2. Carr AJ. Damping models for inelastic analysis. *Proceedings Asia-Pacific Vibration Conference*, Kyonju, Korea, 1997, pp. 42
3. Mavroeidis, G.P. and Papageorgiou, A.S. A Mathematical Representation of Near-Fault Ground Motions. *Bulletin of the Seismological Society of America* 2003; 93(3):1099-1131.
4. Baker, J.W. Quantitative classification of near-fault ground motions using wavelet analysis. *Bulletin of the Seismological Society of America* 2007; 97:1486-1501.
5. Mimoglou, P., Psycharis, I. N., & Taflampas, I. M. (2014). Explicit determination of the pulse inherent in pulse-like ground motions. *Earthquake Engineering & Structural Dynamics*, 43(15), 2261-2281.
6. Taflampas, I. M., Maniatakis, C. A., & Spyrakos, C. C. (2008). Estimation of Input Seismic Energy by Means of a New Definition of Strong Motion Duration. In *14th World Conference on Earthquake Engineering*, Beijing, China Report No. S10-065: 12 (Vol. 17).
7. PEER – Pacific Earthquake Engineering Research Center. Strong motion database. Available from: http://peer.berkeley.edu/peer_ground_motion_database [July 2013].
8. Chrisp D. Damping Models for Inelastic Structures. Master's Thesis, University of Canterbury, Christchurch, New Zealand, 1980.
9. Tassiou, N., “Development of Inelastic Model for Infill Walls and Analytical Study of their Influence to the Behavior of Existing RC Buildings,” MSc Dissertation Thesis (in Greek), National Technical University of Athens, Athens, Greece, 2003.
10. Zarnic, R. and Gostic, S., “Masonry infilled frames as an effective structural sub-assembly,” in *Seismic Design Methodologies for the Next Generation of Codes*, P. Fajfar and H. Krawinkler eds., Balkema, Rotterdam, 1997.
11. Paulay, T. and Priestley, M. N. J., *Seismic Design of Reinforced Concrete and Masonry Buildings*, John Wiley & Sons, Inc., New York, 1992.
12. Repapis C., Vintzileou E., Zeris C., “Evaluation of the Seismic Behaviour of Existing RC Buildings: I. Suggested Methodology”, *Journal of Earthquake Engineering*, Imperial College Press, Vol. 10, No. 2, 2006, pp. 265-287.
13. EN 1992-1-1, Eurocode 2: Design of concrete structures. Part 1: General rules and rules for buildings. 2004.
14. Somerville, P.G., Smith, N. F., Graves, R.W. and Abrahamson, N. A. “Modification of empirical strong ground motion attenuation relations to include the amplitude and duration effects of rupture directivity”. *Seismological Research Letters* 1997, 68(1): 199-222.